Tobias David Reinhardt

Adsorptive Removal of Phosphonates and Orthophosphate From Membrane Concentrate Using Granular Ferric Hydroxide

Stuttgarter Berichte zur Siedlungswasserwirtschaft Band 250

FORSCHUNGS- UND ENTWICKLUNGSINSTITUT FÜR
INDUSTRIE- UND SIEDLUNGSWASSERWIRTSCHAFT SOWIE
ABFALLWIRTSCHAFT E.V. (FEI)

Tobias David Reinhardt

Adsorptive Removal of Phosphonates and Orthophosphate From Membrane Concentrate Using Granular Ferric Hydroxide

D 93

IMPRESSUM

Bibliographische Information der Deutschen Bibliothek
Die Deutsche Bibliothek verzeichnet die Publikation in der Deutschen Nationalbibliographie; detaillierte bibliographische Daten sind im Internet über http://dnb.ddb.de abrufbar

Tobias David Reinhardt
Adsorptive Removal of Phosphonates and Orthophosphate From Membrane Concentrate Using Granular Ferric Hydroxide

Forschungs- und Entwicklungsinstitut für Industrie- und Siedlungswasserwirtschaft sowie Abfallwirtschaft e.V. (FEI)

Stuttgarter Berichte zur Siedlungswasserwirtschaft, Band 250

Layout:
Institut für Siedlungswasserbau, Wassergüte- und Abfallwirtschaft
der Universität Stuttgart ISWA
Bandtäle 2, 70569 Stuttgart

Druck:
e.kurz + co. druck und medientechnik gmbh
Kernerstr. 5, 70182 Stuttgart

Printed in Germany

Adsorptive Removal of Phosphonates and Orthophosphate From Membrane Concentrate Using Granular Ferric Hydroxide

Von der Fakultät für Bau- und Umweltingenieurwissenschaften der Universität Stuttgart zur Erlangung der Würde eines Doktor-Ingenieurs (Dr.-Ing.) genehmigte Abhandlung

Vorgelegt von
Tobias David Reinhardt
aus Stuttgart

Hauptberichter: PD Dr.-Ing. habil. Harald Schönberger
Mitberichterin: Prof. Dr.-Ing. Heidrun Steinmetz

Tag der mündlichen Prüfung: 25. März 2022

Institut für Siedlungswasserbau, Wassergüte- und Abfallwirtschaft
der Universität Stuttgart

2022

Acknowledgement

This thesis was written during my employment as a research assistant at the Institute for Sanitary Engineering, Water Quality and Solid Waste Management at the University of Stuttgart. I acknowledge gratefully the Willy-Hager-Stiftung, Stuttgart, for funding the research project from which this thesis originated.

I would like to thank PD Dr.-Ing. habil. Harald Schönberger for his suggestions and constructive criticism, which contributed to the success of my work. I further express my gratitude to Prof. Dr.-Ing. Heidrun Steinmetz for being the co-supervisor of this thesis, for recognizing my potential, and giving me the opportunity to work as a research assistant. Without her, this work would probably not exist, as it was her who first got me fascinated by wastewater treatment.

Dr.-Ing. Eduard Rott, thank you for sharing your scientific experience with me, for your continuous encouragement, and for motivating me to publish the findings of my research. I would like to thank Carsten Meyer for his trust and for giving me the chance to grow and develop as a research engineer. I would also like to thank Dr.-Ing. Werner Maier, a partner in many projects, from whom I have learned a lot, both on a professional and human level. Thanks to Dr. Phil Schneider for introducing me to the world of research and for being a great mentor.

A particularly huge thank you goes to the many students who assisted me in conducting the laboratory experiments. Thank you very much for your great effort and the good knowledge exchange. I am delighted every time I see one of you again.

I would like to thank my colleagues, who always supported me, critically discussed my results with me, and provided the perfect basis for this thesis with a good and friendly atmosphere. I would also like to thank the laboratory staff, who always provided me with valuable tips and patiently answered my questions.

My sincere thanks go to my family, who accompanied me on this path for many years. I would like to particularly mention my wife Sabine, who has supported me on this path almost to the point of self-sacrifice. Thank you for all the patience and your understanding. David and Finn, you cannot read yet, but daddy loves you and now has more time for you again – finally!

Publications

Parts of the results from experiments performed for this thesis have been published in advance:

Rott, E., Reinhardt, T., Wasielewski, S., Raith-Bausch, E. and Minke, R. 2018 Optimized Procedure for Determining the Adsorption of Phosphonates onto Granular Ferric Hydroxide using a Miniaturized Phosphorus Determination Method. *Journal of Visualized Experiments* (135).

Rott, E., Reinhardt, T. and Minke, R. 2019 *Untersuchungen zur Elimination von Phosphonaten und ortho-Phosphat aus Abwasser mithilfe metallhaltiger Filtermaterialien: Abschlussbericht an die Willy-Hager-Stiftung*.

Reinhardt, T., Gómez Elordi, M., Minke, R., Schönberger, H. and Rott, E. 2020. Batch Studies of Phosphonate Adsorption on Granular Ferric Hydroxides. *Water Sci. Technol.*, **81**(1), 10–20.

Reinhardt, T., Veizaga Campero, A. N., Minke, R., Schönberger, H. and Rott, E. 2020. Batch Studies of Phosphonate and Phosphate Adsorption on Granular Ferric Hydroxide (GFH) with Membrane Concentrate and Its Synthetic Replicas. *Molecules*, **25**(21).

Reinhardt, T., Rott, E., Schneider, P. A., Minke, R. and Schönberger, H. 2021 Fixed-Bed Column Studies of Phosphonate and Phosphate Adsorption on Granular Ferric Hydroxide (GFH). *Process Safety and Environmental Protection*, **153**, 301–310.

Cumulative Structure

The present thesis combines three scientific papers published in peer-reviewed journals into one doctoral thesis according to the guideline for cumulative dissertations of Faculty 2 at the University of Stuttgart, adopted on 22 January 2020, and the doctoral regulations of the University of Stuttgart (PromO), adopted on 01 March 2019. Editorial modifications were made to the three publications to make the spelling in this thesis consistent.

The cumulative dissertation is divided into five Chapters:

- **General Introduction (Chapter 1)**
- **Publication I (Chapter 2)**

  Reinhardt, T., Gómez Elordi, M., Minke, R., Schönberger, H. and Rott, E. 2020. Batch studies of phosphonate adsorption on granular ferric hydroxides. *Water Sci. Technol.*, **81**(1), 10–20. https://doi.org/10.2166/wst.2020.055.

- **Publication II (Chapter 3)**

  Reinhardt, T., Veizaga Campero, A. N., Minke, R., Schönberger, H. and Rott, E. 2020. Batch Studies of Phosphonate and Phosphate Adsorption on Granular Ferric Hydroxide (GFH) with Membrane Concentrate and Its Synthetic Replicas. *Molecules*, **25**(21). https://doi.org/10.3390/molecules25215202.

- **Publication III (Chapter 4)**

  Reinhardt, T., Rott, E., Schneider, P. A., Minke, R. and Schönberger, H. 2021 Fixed-bed column studies of phosphonate and phosphate adsorption on granular ferric hydroxide (GFH). *Process Safety and Environmental Protection*, **153**, 301–310. https://doi.org/10.1016/j.psep.2021.07.027.

- **General Discussion (Chapter 5)**

Abstract

Phosphonates are used as complexing agents in various industries, in cooling water systems and in drinking water treatment. They are additives with a threshold effect, i.e. they efficiently prevent or at least delay the formation of precipitates already in the sub-stoichiometric range. They are highly water soluble, but also stable over a wide pH and temperature range. Their C–P bond makes them relatively persistent to chemical and biological degradation compared to molecules with N–P, S–P or O–P bonds. Consumption phosphonates used as complexing agents has increased significantly worldwide in recent decades; in the period from 1998 to 2012, for example, by almost 70% from 56,000 t to 94,000 t.

Usually, phosphonates are released into wastewater streams after use. A load balance for the year 2012 showed that in Europe about 7,800–13,700 tons of phosphonates used in industry were discharged to water bodies by direct dischargers. About 65%–90% of this was accounted for by cooling waters and membrane concentrates, for which on-site wastewater treatment prior to discharge is often uncommon. In Germany, the discharge of membrane concentrates from drinking water treatment, which often have concentrations > 1 mg/L P, is approvable, whereas the requirements for phosphorus removal in municipal wastewater treatment plants are steadily increasing.

Phosphonates are suspected of contributing to the eutrophication of water bodies, as they can be partially degraded to orthophosphate in the aquatic environment by catalytic oxidation, photolysis, hydrolysis, and by microbial processes in the long-term. In addition, phosphonates have a high adsorption affinity, which leads to a strong accumulation of phosphonates in aquatic sediments. Reaching the adsorption capacity of sediments could lead to a significant increase in phosphonate concentrations in water bodies in the future. As a result, ecotoxic effects with unknown environmental impacts are to be expected, such as the redissolution of heavy metals. Therefore, in order to achieve the objectives of the European Water Framework Directive, treatment processes for the group of phosphonates should be developed and investigated in addition to processes for the removal of orthophosphate.

One approach to treating the membrane concentrate from drinking water treatment is adsorption onto suitable filter materials sauch as iron (hydr)oxide that utilize the high adsorption affinity of phosphonates. Published studies on the adsorption of phosphonates on granular ferric hydroxide (GFH) lack, among other things, investigations of material stability, regeneration capability, and application to real wastewater in fixed-bed columns. In addition, the ions present in the (wastewater) matrix can have a major

influence on the adsorption of phosphorus compounds. In some studies on the adsorption of phosphate as well as the phosphonate nitrilotrimethylphosphonic acid (NTMP) on GFH, the influence of individual ions was investigated, but in real wastewater different ions are present simultaneously and may interact. The published studies on fixed-bed adsorption are limited to synthetic solutions with the phosphonate NTMP and consider a maximum of three adsorption/desorption cycles, so that a prediction on the long-term applicability of GFH is uncertain.

The objective of this work was to investigate the adsorption of orthophosphate and in particular phosphonates on GFH. This was to serve the overarching goal of understanding the adsorption process in more detail in order to apply it to the treatment of membrane concentrate containing orthophosphate and DTPMP and thus help to reduce phosphorus discharge to water bodies. For this purpose, batch experiments with phosphonate-spiked pure water were first conducted to investigate the adsorption process in detail and to pave the way for further experiments in fixed bed columns with the membrane concentrate of a drinking water treatment plant. In the batch experiments, the most important phosphonates in terms of quantity 2-phosphonobutane-1,2,4-tricarboxylic acid (PBTC), 1-hydroxyethylidene-(1,1-diphosphonic acid) (HEDP), NTMP, ethylenediaminetetra(methylene phosphonic acid) (EDTMP), and diethylenetriaminepenta(methylene phosphonic acid) (DTPMP) as well as 2-hydroxy phosphonoacetic acid (HPAA) were investigated.

In this thesis, four different GFH were applied in batch experiments in a first step to compare their adsorption capacities. The maximum loading in experiments with an initial concentration of 1 mg/L NTMP-P and a contact time of 7 d at room temperature (20 °C) was ~12 mg P/g GFH. Increasing the initial concentration to 5 mg/L NTMP-P resulted in a maximum loading of ~18 mg P/g. Using the GFH with the largest adsorption capacity, further experiments were then conducted on the influence of temperature, pH, and phosphonate properties on adsorption capacity and on subsequent regeneration. It was found that the maximum loading at an initial concentration of 1 mg/L NTMP-P and at a temperature of 5 °C dropped by > 40% compared to the loading at 20 °C to only ~7 mg P/g. Cold wastewater temperatures should therefore be avoided for phosphonate adsorption on GFH. For all six phosphonates studied, adsorption capacity decreased with increasing pH (e.g., 80% NTMP removal at pH 4 and 25% at pH 12). For the polyphosphonates investigated, the adsorption capacity decreased with increasing molecular size and number of phosphonate groups. Furthermore, five adsorption/desorption cycles demonstrated that regeneration of GFH with 1 M sodium hydroxide solution (NaOH) is possible.

In further batch experiments, the influence of other ions on the removal of phosphonates and orthophosphate was investigated in the presence and absence of GFH. The focus herein was particularly on calcium (Ca^{II}) and the possible precipitation of calcium compounds. In experiments with different calcium-phosphonate ratios (0:1 to 60:1), it was found that the calcium fraction in the GFH itself plays an essential role in the adsorption process, as it can redissolve and thus increase the calcium-phosphonate ratio. At pH > 8, removal of phosphonates occurred even in the absence of GFH when certain calcium-phosphonate ratios were exceeded. This removal is due to precipitation of Ca-phosphonate complexes. Further experiments with DTPMP-containing membrane concentrate and its synthetic replicas showed that the influence of nitrate and sulfate ions on the adsorption process was negligible, but (hydrogen-) carbonate ions competed with the adsorption of phosphonates and orthophosphate. The presence of Ca^{II} had a positive effect on the adsorption of phosphonates and orthophosphate up to pH 8, probably through the formation of ternary complexes. In the presence of Ca^{II} at pH > 8 and of Mg^{II} at pH > 10, precipitation occurred. Software-based modeling (PHREEQC Interactive 3) to calculate speciation and solution equilibria showed that, in addition to Ca-DTPMP complexes, the observed precipitation could consist of inorganic precipitates of calcium, magnesium, and phosphate. In the additional presence of (hydrogen-)carbonate, precipitation of calcium carbonate and/or dolomite ($CaMg(CO_3)_2$) may occur. All these precipitates can decrease the phosphonate and orthophosphate concentrations either by direct precipitation or by their adsorption onto the precipitates. It can be assumed that the membrane concentrate from drinking water treatment plants is suitable for adsorption to GEH due to its high content of Ca^{II} and Mg^{II}, provided that potential precipitates do not interfere with the adsorption/desorption process.

Experiments with fixed-bed columns were then conducted to investigate the applicability of GEH for treating membrane concentrate from drinking water treatment for up to 24 cycles. For this purpose, column experiments were first carried out with phosphonate-spiked pure water, before the influence of the pH value and various regeneration methods were investigated in further experiments with membrane concentrate. Experiments with a synthetic solution consisting of pure water, DTPMP and a buffer showed that the GFH can be successfully regenerated almost completely with 1 M NaOH. Although using fresh NaOH in each cycle showed a slightly better regeneration efficiency in each cycle, the reuse of NaOH is recommended due to its vast economic and environmental advantages. In experiments with membrane concentrate at its original pH (pH ≅ 8), the adsorption efficiency decreased significantly from ≥ 92% in the first two adsorption/desorption cycles to 29% in the eighth cycle. This can be attributed to surface precipitation of calcium compounds, which interfere with the

adsorption/desorption processes. To avoid these interferences, the precipitates should either be avoided or subsequently removed. To avoid precipitation, the pH of the membrane concentrate was decreased to pH 6. Although this allowed an adsorption efficiency of ≥ 90% per cycle to be steadily achieved over 20 cycles, due to the high buffer capacity of the membrane concentrate, such a strong pH reduction is not recommended. Experiments without pH reduction, but with an additional acidic regeneration step to remove precipitates, showed a cumulative adsorption efficiency of > 95% over 20 adsorption/desorption cycles. The hydrochloric acid could be reused over the entire period when its pH value was kept stable at pH 2.5 by a control system. The sodium hydroxide solution of the alkaline regeneration step could also be reused throughout all cycles. However, replacement of the caustic soda could increase the desorption efficiency, and the electrical conductivity could serve as a parameter for the time of its replacement. While calcium was removed only during the acidic regeneration, DTPMP and orthophosphate were found almost exclusively in the alkaline regeneration solution. Consequently, the precipitates are not phosphorus-containing calcium compounds, but calcium carbonate. The dissolution of iron from the GFH during acidic and alkaline regeneration was negligible.

The results of this thesis show that GFH is a suitable adsorbent for the removal of phosphonates and orthophosphate from membrane concentrate from drinking water treatment. The systematic treatment of membrane concentrate can reduce the phosphonate discharge into water bodies and thus contribute to environmental protection and the achievement of the objectives of the European Water Framework Directive. A rough cost comparison shows that adsorption on GFH can compete with precipitation/flocculation processes in terms of cost, while better removal efficiencies can be achieved with the adsorption process.

Keywords: Adsorption, antiscalant, fixed-bed columns, GFH, membrane concentrate, regeneration.

Kurzfassung

Phosphonate werden als Komplexbildner in diversen Industriezweigen, in Kühlwassersystemen und auch in der Trinkwasseraufbereitung eingesetzt. Sie sind Additive mit Thresholdeffekt, d. h. bereits im unterstöchiometrischen Bereich verhindern sie effizient die Bildung von Ausfällungen oder verzögern diese zumindest. Sie sind gut wasserlöslich, aber auch über einen weiten pH- und Temperaturbereich stabil. Durch ihre C–P Bindung sind sie im Vergleich zu Molekülen mit N–P, S–P oder O–P Bindung relativ persistent gegenüber chemischem und biologischem Abbau. Der Verbrauch der als Komplexbildner eingesetzten Phosphonate stieg in den letzten Jahrzehnten weltweit deutlich an; im Zeitraum von 1998 bis 2012 beispielsweise um fast 70 % von 56.000 t auf 94.000 t.

In der Regel werden Phosphonate über den Abwasserstrom entsorgt. Eine Bilanzierung für das Jahr 2012 zeigte, dass in Europa etwa 7.800–13.700 Tonnen der in der Industrie eingesetzten Phosphonate durch Direkteinleiter in Gewässer eingetragen wurden. Davon entfielen etwa 65 %–90 % auf Kühlwässer und Membrankonzentrate, für die eine innerbetriebliche Abwasserbehandlung vor der Einleitung oft unüblich ist. In Deutschland ist die Einleitung von Membrankonzentraten aus der Trinkwasseraufbereitung, die häufig Konzentrationen > 1 mg/L P aufweisen, genehmigungsfähig, wohingegen die Anforderungen an die Phosphorelimination in kommunalen Kläranlagen stetig steigen.

Phosphonate stehen im Verdacht zur Eutrophierung von Gewässern beizutragen, da sie teilweise in der aquatischen Umwelt durch katalytische Oxidation, Photolyse, Hydrolyse sowie mikrobielle Prozesse langfristig zu ortho-Phosphat abgebaut werden können. Darüber hinaus haben Phosphonate eine hohe Adsorptionsaffinität, welche zu einer starken Akkumulation der Phosphonate in den Gewässersedimenten führt. Das Erreichen der Adsorptionskapazität der Sedimente könnte zukünftig zu einem deutlichen Anstieg der Phosphonatkonzentrationen in Gewässern führen. Infolgedessen sind ökotoxische Effekte mit unbekannten Umweltwirkungen zu erwarten, wie zum Beispiel die Rücklösung von Schwermetallen. Um die Ziele der Europäischen Wasserrahmenrichtlinie zu erreichen, sollten daher neben Verfahren zur Elimination von ortho-Phosphat auch Behandlungsverfahren für die Gruppe der Phosphonate entwickelt und untersucht werden.

Eine Möglichkeit zur Behandlung des Membrankonzentrats aus der Trinkwasseraufbereitung stellt die Adsorption an geeignete Filtermaterialien wie beispielsweise, Eisen(hydr)oxid dar, welche die hohe Adsorptionsaffinität der Phosphonate nutzen. In den publizierten Studien zur Adsorption von Phosphonaten an granuliertem Eisen-

hydroxid (GEH) fehlen u. a. Untersuchungen der Materialstabilität, der Regenerierbarkeit und der Anwendung auf reale Abwässer in Festbettsäulen. Außerdem können die in der (Abwasser-)Matrix vorhandenen Ionen einen großen Einfluss auf die Adsorption von Phosphorverbindungen haben. In einigen Studien zur Adsorption von Phosphat sowie dem Phosphonat Nitrilotris(methylenphosphonsäure) (NTMP) an GEH wurde zwar der Einfluss einzelner Ionen untersucht, in realen Abwässern liegen jedoch verschiedene Ionen zugleich vor und können interagieren. Die publizierten Studien zur Festbettadsorption beschränken sich auf synthetische Lösungen mit dem Phosphonat NTMP und betrachten maximal drei Adsorptions-/Desorptionszyklen, so dass eine Vorhersage über die langfristige Anwendbarkeit von GEH unsicher ist.

Ziel dieser Arbeit war es, die Adsorption von ortho-Phosphat und insbesondere Phosphonaten an GEH zu untersuchen. Dies sollte dem übergeordneten Ziel dienen, den Adsorptionsprozess näher zu verstehen, um diesen auf die Behandlung von ortho-Phosphat- und DTPMP-haltigem Membrankonzentrat anzuwenden und somit dazu beizutragen, den Phosphor-Eintrag in die Gewässer zu vermindern. Hierfür wurden zunächst Batchversuche mit Phosphonat-aufgestocktem Reinstwasser durchgeführt, um den Adsorptionsprozess detailliert zu untersuchen und weitergehende Experimente in Festbettsäulen mit dem Membrankonzentrat einer Trinkwasseraufbereitungsanlage vorzubereiten. In den Batchversuchen kamen die hinsichtlich ihrer Verwendungsmenge relevantesten Phosphonate 2-Phosphonobutan-1,2,4-tricarbonsäure (PBTC), 1-Hydroxyethan-(1,1-diphosphonsäure) (HEDP), NTMP, Ethylendiamintetra(methylenphosphonsäure) (EDTMP) und Diethylentriaminpenta(methylenphosphonsäure) (DTPMP) sowie Hydroxy(phosphono)essigsäure (HPAA) zum Einsatz.

In dieser Arbeit wurden dazu in einem ersten Schritt vier verschiedene GEH in Batchversuchen eingesetzt, um deren Adsorptionskapazitäten miteinander zu vergleichen. Die maximale Beladung bei einer Ausgangskonzentration von 1 mg/L NTMP-P, einer Kontaktzeit von 7 d und bei Raumtemperatur (20 °C) betrug ~12 mg P/g GEH. Eine Erhöhung der Ausgangskonzentration auf 5 mg/L NTMP-P resultierte in einer maximalen Beladung von ~18 mg P/g. Mit dem GEH mit der größten Adsorptionskapazität wurden daraufhin weitere Untersuchungen zum Einfluss der Temperatur, des pH-Wertes sowie der Phosphonateigenschaften auf die Adsorptionskapazität und zu einer anschließenden Regeneration durchgeführt. Es zeigte sich, dass die maximale Beladung bei einer Ausgangskonzentration von 1 mg/L NTMP-P und bei einer Temperatur von 5 °C im Vergleich zur Beladung bei 20 °C um > 40 % auf lediglich ~7 mg P/g abfiel. Niedrige Abwassertemperaturen sollten daher bei einem Einsatz von GEH zur Phosphonat-Adsorption vermieden werden. Die Adsorptionskapazität des GEH ließ bei allen sechs untersuchten Phosphonaten mit steigendem pH-Wert nach (z. B. 80 % NTMP Elimination bei pH 4 und 25 % bei pH 12). Mit steigender Molekülgröße und

Anzahl an Phosphonatgruppen der untersuchten Polyphosphonate sank die Adsorptionskapazität des GEH. In fünf Adsorptions-/Desorptionszyklen konnte nachgewiesen werden, dass eine Regeneration des GEH mit 1 M Natronlauge (NaOH) möglich ist.

In weiteren Batchversuchen wurde der Einfluss zusätzlich anwesender Ionen in An- und Abwesenheit von GEH auf die Elimination von Phosphonaten und ortho-Phosphat untersucht. Hierbei lag der Fokus insbesondere auf Calcium (Ca^{II}) und der möglichen Ausfällung von Calciumverbindungen. In Untersuchungen mit verschiedenen Calcium-Phosphonat-Verhältnissen (0:1 bis 60:1) wurde festgestellt, dass der Calciumanteil im GEH eine wesentliche Rolle im Adsorptionsprozess einnimmt, da sich dieser rücklösen und dadurch das Calcium-Phosphonat-Verhältnis erhöhen kann. Bei pH > 8 kam es auch in Abwesenheit von GEH zur Elimination von Phosphonaten, wenn bestimmte Calcium-Phosphonat-Verhältnisse überschritten wurden. Dies ist auf die Ausfällung von Calcium-Phosphonat-Komplexen zurückzuführen. Weitere Untersuchungen mit DTPMP-haltigem Membrankonzentrat und dessen synthetischen Replikas zeigten, dass der Einfluss von Nitrat- und Sulfationen auf die Adsorptionsvorgänge vernachlässigbar war, (Hydrogen-)Carbonationen jedoch in Konkurrenz zur Adsorption von Phosphonaten und des ortho-Phosphats standen. Die Gegenwart von Ca^{II} hatte bis pH 8 einen positiven Einfluss auf die Adsorption der Phosphonate und ortho-Phosphat, wahrscheinlich durch die Bildung ternärer Komplexe. Unter Anwesenheit von Ca^{II} bei pH > 8 und von Mg^{II} bei pH > 10 kam es zu Ausfällungen. Die softwaregestützte Modellierung (PHREEQC Interactive 3) zur Berechnung von Speziation und Lösungsgleichgewichten zeigte, dass es sich dabei neben Calcium-DTPMP-Komplexen auch um anorganische Ausfällungen von Calcium, Magnesium und Phosphat handeln kann. Bei zusätzlicher Anwesenheit von (Hydrogen-)Carbonat kann es zu Ausfällungen von Calciumcarbonat und/oder Dolomit ($CaMg(CO_3)_2$) kommen. All diese Ausfällungen können die Phosphonat- sowie ortho-Phosphatkonzentrationen entweder durch direkte Fällung oder durch deren Adsorption an den Ausfällungen vermindern. Es ist davon auszugehen, dass sich das Membrankonzentrat aus Trinkwasseraufbereitungsanlagen durch seinen hohen Gehalt an Ca^{II} und Mg^{II} für die Adsorption an GEH anbietet, sofern potenzielle Ausfällungen den Adsorptions-/Desorptionsprozess nicht stören.

In Experimenten mit Festbettsäulen wurde anschließend die Anwendbarkeit des GEH zur Behandlung von Membrankonzentrat aus der Trinkwasseraufbereitung über bis zu 24 Zyklen hinweg untersucht. Hierfür wurden zunächst Untersuchungen mit Phosphonat-aufgestocktem Reinstwasser durchgeführt, bevor in weiteren Experimenten mit Membrankonzentrat der Einfluss des pH-Wertes sowie verschiedener Regenerationsmethoden untersucht wurde. Experimente mit einer synthetischen Lösung bestehend aus Reinstwasser, DTPMP und einem Puffer zeigten, dass das GEH erfolgreich

mit 1 M NaOH nahezu vollständig regeneriert werden konnte. Obwohl die Verwendung frischer NaOH in jedem Zyklus eine geringfügig bessere Regenerationseffizienz zeigte, wird aufgrund wirtschaftlicher und ökonomischer Vorteile die Wiederverwendung der NaOH empfohlen. Bei Untersuchungen mit Membrankonzentrat mit seinem Ausgangs-pH-Wert (pH ≅ 8) sank die Adsorptionseffizienz von ≥ 92 % in den ersten beiden Adsorptions-/Desorptionszyklen auf 29 % im achten Zyklus deutlich ab. Dies ist auf Ausfällungen von Calciumverbindungen an der Oberfläche des GEH zurückzuführen, die die Adsorptions-/Desorptionsprozesse stören. Um diese Störungen zu vermeiden, sollten die Ausfällungen entweder vermieden oder wieder entfernt werden. Um die Ausfällungen zu vermeiden, wurde der pH-Wert des Membrankonzentrats auf pH 6 abgesenkt. Hierdurch konnte zwar über 20 Zyklen hinweg stabil eine Adsorptionseffizienz von ≥ 90 % pro Zyklus erreicht werden, aufgrund der hohen Pufferkapazität des Membrankonzentrats ist jedoch von einer derart starken pH-Absenkung abzuraten. Experimente ohne pH-Absenkung, aber mit einem zusätzlichen sauren Regenerationsschritt zur Entfernung von Ausfällungen, zeigten eine kumulative Adsorptionseffizienz von > 95 % über 20 Adsorptions-/Desorptionszyklen. Die verwendete Salzsäure konnte dabei über den gesamten Zeitraum wiederverwendet werden, wenn deren pH-Wert durch eine Regelung stabil bei pH 2,5 gehalten wurde. Die Natronlauge des alkalischen Regenerationsschrittes konnte ebenfalls über alle Zyklen hinweg verwendet werden. Ein Austausch der Natronlauge konnte die Desorptionseffizienz jedoch erhöhen, die elektrische Leitfähigkeit konnte als Parameter für den Zeitpunkt ihres Austausches dienen. Während Calcium nur durch die saure Regeneration entfernt wurde, fanden sich DTPMP und ortho-Phosphat nahezu ausschließlich in der alkalischen Regenerationslösung. Demzufolge handelte es sich bei den Ausfällungen nicht um phosphorhaltige Calciumverbindungen, sondern um Calciumcarbonat. Die Rücklösung von Eisen aus dem GEH während der sauren und alkalischen Regeneration war vernachlässigbar.

Die Ergebnisse dieser Arbeit zeigen, dass GEH ein geeignetes Adsorbens zur Elimination von Phosphonaten und ortho-Phosphat aus Membrankonzentrat aus der Trinkwasseraufbereitung ist. Durch die gezielte Behandlung von Membrankonzentrat kann der Phosphonateintrag in die Gewässer reduziert werden und somit ein Beitrag zum Umweltschutz und zum Erreichen der Ziele der Europäischen Wasserrahmenrichtlinie geleistet werden. Ein überschlägiger Kostenvergleich zeigt, dass die Adsorption an GEH in Bezug auf Kosten mit Fällung-/Flockungsprozessen konkurrenzfähig ist, obwohl beim Adsorptionsprozess eine bessere Eliminationsseffizienz erreicht werden kann.

Schlagwörter: Adsorption, Antiscalant, DTPMP, Festbettsäulen, GEH, Membrankonzentrat, Regeneration.

Table of Contents

List of Figures

List of Tables

List of Abbreviations

$	US-Dollar
%	Percent
€	Euro
°C	Degree Celsius
2-AEP	2-aminoethylphosphonic acid
A^-	Monovalent anion
A^{2-}	Bivalent anion
AbwV	Abwasserverordnung (German Wastewater Ordinance)
AcOH	Acetic acid
Al^{III}	Trivalent aluminum
AMPA	Aminomethylphosphonic acid
atm	Standard atmosphere
ATP	Adenosine triphosphate
BES	*N*,*N*-bis(2-hydroxy-ethyl)-2-aminoethane-sulfonic acid
BTC	Breakthrough curve
BV	Bed volume
c (c_0)	Concentration (c_0: Initial concentration)
c/c_0	Ratio of concentration to initial concentration
c_a, c_{ads}	Concentration of an adsorbed substance in a solution
Ca_{end}	Calcium concentration after contact time
Ca^{II}	Bivalent calcium
CAPS	3-(cyclohexylamino)-1-propanesulfonic acid
CAPSO	3-(cyclohexylamino)-2-hydroxy-1-propanesulfonic acid
CAS-No.	Chemical Abstracts Service Number
Ca_{start}	Calcium concentration before contact time
Ca_{target}	Target calcium concentration for Ca_{start}
CMI	Carboxymethyl inulin
COD	Chemical oxygen demand
COD_{max}	Maximum chemical oxygen demand
Cu^{II}	Bivalent copper
d	Day
DIN	Deutsche Industrienorm (German industrial standard)

DNA	Deoxyribonucleic acid
DOC	Dissolved organic carbon
DTPMP	Diethylenetriaminepenta(methylene phosphonic acid)
DUP	Dissolved unreactive P
EBCT	Empty bed contact time
EDS	Energy-dispersive X-ray spectroscopy
EDTA	Ethylenediaminetetraacetic acid
EDTMP	Ethylenediaminetetra(methylene phosphonic acid)
Eff_{ads}	Adsorption efficiency
Eff_{des}	Desorption efficiency
EN	European Standard
EPA	European Phosphonate Association
EPPS	4-(2-hydroxyethyl)-1-piperazinepropanesulfonic acid
Eq.	Equation
EU	European Union
Fe^{II}	Bivalent iron
Fe^{III}	Trivalent iron
FIDMP	N-formyl iminodi(methylene)-phosphonate
Fig.	Figure
FTIR	Fourier-transform infrared spectroscopy
g, kg, mg, µg	Gram, kilogram, milligram, microgram
GAC	Granular activated carbon
GEH	Granuliertes Eisenhydroxid (granular ferric hydroxiode)
GFH	Granular ferric hydroxiode
h	Hour
HCl	Hydrochloric acid solution
HEDP	1-hydroxyethylidene-(1,1-diphosphonic acid)
HEPES	4-(2-hydroxyethyl)-1-piperazineethanesulfonic acid
HERA	Human & Environmental Risk Assessment Initiative
HPAA	2-hydroxy phosphonoacetic acid
IDMP	Iminodi(methylene)phosphonate
IKW	Industrieverband Körperpflege- und Waschmittel e. V. (German Cosmetic, Toiletry, Perfumery and Detergent Association)

IOCS	Iron oxide coated sand
IR	Infrared
ISO	International Organization for Standardization
ISO_{mini}	Miniaturized form of the ISO 6878 method
K	Kelvin
k_1	Pseudo-first order rate constant
k_2	Pseudo-second order rate constant
K_d	Dimensionless form of the Freundlich constant
K_F	Freundlich constant
K_{Henry}	Henry's law constant
kJ	Kilojoule
K_L	Langmuir constant
kWh	Kilowatt hours
L, mL	Liter, milliliter
LC_0	Lethal concentration 0: concentration resulting in the death of 0% of the test population
LC_{50}	Lethal concentration 50: concentration resulting in the death of 50% of the test population
ln	Natural logarithm
log K_{OW}	Decadic logarithm of the Octanol-water partition coefficient
LPRO	Low pressure reverse osmosis
m, cm, mm, µm, nm	Meter, centimeter, millimeter, micrometer, nanometer
M, mM, µM	Molarity (mol/L, mmol/L, µmol/L)
m_A	Adsorbent mass
Me^{2+}	Bivalent metal ion
MES	2-(N-morpholino)ethanesulfonic acid
Mg^{II}	Bivalent magnesium
min	Minute
Mn^{II}	Bivalent manganese
MO	Missouri
mol, mmol, µmol	Mole, millimole, micromole
MOPS	3-(*N*-morpholino)propanesulfonic acid
$m_{P,ads,i}$	Total P load adsorbed in cycle i
$m_{P,des,i}$	Total P load desorbed in cycle i

$m_{P,in,i}$	Total P load fed into the column with the influent in cycle i
mS/cm	Millisiemens per centimeter (unit of electrical conductivity)
N	Number of observations
n	Quantitiy or heterogeneity factor in Freundlich model
NaOH	Sodium hydroxide (solution)
NaOH-Sol	Alkaline regeneration solution
nFe-GAC	nano iron coated granular activated carbon
No	Number
NOEC	No observed effect concentration
NOM	Natural organic matter
NPDES	National Pollution Discharge Elimination System
NTMP	Nitrilotrimethylphosphonic acid
NTU	Nephelometric turbidity unit
OECD	Organisation for Economic Co-operation and Development
o-PO4	orthophosphate
o-PO4-P	orthophosphate-phosphorus
OS	Original sample
P	Phosphorus
p	p-value (probability that the results from sample data occurred by chance)
p. a.	pro analysi (for analysis)
p/p_0	Relative pressure
PASP	Poly(aspartic acid)
PBTC	2-phosphonobutane-1,2,4-tricarboxylic acid
pc.	Piece
PE	Population equivalents
PESA	Polyepoxysuccinic acid (PESA)
PG	Phosphonate group
pH	Negative decadic logarithm of hydrogen ion activity
Ph. Eur.	Pharmacopoea Europaea (European Pharmacopoeia)
pH_{end}	pH after contact time
pH_{PZC}	Point of zero charge
pH_{start}	pH before contact time
pH_{target}	Target pH for pH_{end}

pK	Negative decadic logarithm of the acid dissociation constant
PLC	Programmable Logic Controller
PO_4	Phosphate
PO_4-P	Phosphate-phosphorus
PP	Particulate Phosphorus
ppm	Parts per million (equals mg/L)
$\bar{q}_i$	Mean value of experimentally determined loadings
q	Loading
q(t)	Loading at time t
q_e	Loading at equilibrium
q_i	Experimentally determined loading
q_m	Determined loading using the model function
q_{max}	Maximum loading
R	Universal gas constant
r^2	Coefficient of determination
rpm	Revolutions per minute
RSSCT	Rapid small-scale column tests
s	Second or sample standard deviation
Sb^{III}	Trivalent Antimony
SDD	Silicon drift detector
SIDS	Screening Information Dataset
Synth-Sol	Synthetic solution
T	Temperature
t	time or metric ton (1,000 kg)
Tab.	Table
TAPS	(2-hydroxy-1,1-bis(hydroxymethyl)ethyl)amino-1-propanesulfonic acid
t_c	Contact time
TDP	Total dissolved P
TP	Total Phosphorus
u	Unified atomic mass unit
US EPA	United States Environmental Protection Agency
USA	United States of America

UV	Ultraviolet
UV/VIS	UV–visible
w/o	without
WHO	World Health Organization
WWTP	Wastewater treatment plant
$\bar{x}$	Mean value of the observations
x_i	Observed sample value
XPS	X-ray photoelectron spectroscopy
yr	Year
Zn^{II}	Bivalent Zinc
β-value	Molar ratio of metal to phosphorus
ΔG^0	Change in free Gibbs energy
ΔH^0	Change in enthalpy
ΔS^0	Change in entropy
λ_{max}	absorption maximum

1 General Introduction

1.1 Introduction

1.1.1 Motivation

The implementation of the European Water Framework Directive requires considerable efforts to reduce nutrient emissions to surface waters (EU 2000). This requires a more detailed assessment of phosphorus emissions, as this is the only way to achieve water quality objectives with the greatest possible efficiency. In addition to phosphates, the group of phosphonates is relevant in terms of quantity (see section 5.2). They are used in various industries such as in the textile and paper industries as bleach stabilizers, in drinking water treatment as antiscalants, in cooling water systems as corrosion and hardness stabilizers, in detergents as a combination of scale inhibitors and bleach stabilizers, and in personal care products. Phosphonates are stable over a wide pH range and relatively persistent to chemical and biological decomposition (Steber and Wierich 1986, 1987; Schowanek and Verstraete 1990b; Gledhill and Feijtel 1992; Nowack 1998).

Phosphonates are suspected of contributing to the eutrophication of water bodies in the long term (Grohmann and Horstmann 1989; Studnik *et al.* 2015; Rott *et al.* 2018c). For example, UV radiation from sunlight as well as the presence of Mn^{II} and dissolved oxygen have the potential for steady breakdown to microbiologically available phosphates (Matthijs *et al.* 1989; Nowack and Stone 2000; Kuhn *et al.* 2017; Kuhn *et al.* 2018). The oversupply of phosphate is a major characteristic of ecologically disequilibrated water bodies and thus an important target substance with regard to the sustainable improvement of the ecological status of water bodies.

Phosphonates can be removed from wastewater by precipitation/flocculation when iron or aluminum salts are added (Rott *et al.* 2017b). The principle behind this is the conversion of the metal into poorly soluble metal hydroxides. These polar flocs with a relatively large specific surface area then act as adsorbents for the negatively charged phosphonates. The flocculation process can have two main disadvantages. Depending on the wastewater, sludge volumes of up to 30% of the sample volume can occur. This sludge must be separated in a further sedimentation or filtration stage, treated further and discharged. Furthermore, phosphonates present in the wastewater can complex

the added flocculant and thus prevent flocculation. This problem can be compensated by increasing the dosage of flocculants, but the additional consumption will lead to an increase in costs.

Metal-containing filter materials represent a possible alternative that utilizes the relatively high adsorption affinity of phosphonates on metal-containing surfaces (Nowack and Stone 1999a; Boels *et al.* 2010; Boels *et al.* 2012). Such adsorbents can consist of pure metal oxides, which are often available as fine powders or as supensions with hydroxide flocs. However, these fine powders are not suitable for application in filter columns (Jianbo *et al.* 2009). Therefore, processes have been developed to coat materials such as sand and activated carbon with iron (Jianbo *et al.* 2009; Dongmei *et al.* 2011; Zach-Maor *et al.* 2011b). Furthermore, there are granulated substances such as granular ferric hydroxides, which are used in the treatment of wastewater and raw water in filter columns (Genz *et al.* 2008; Sperlich 2010; Boels *et al.* 2012; Chen *et al.* 2017).

This thesis aimed to investigate the adsorption of orthophosphate and, in particular, phosphonates on granular ferric hydroxide, and the possible use of it to treat membrane concentrate from drinking water treatment containing orthophosphate and diethylenetriaminepenta(methylene phosphonic acid) (DTPMP) before its discharge. In addition to orthophosphate, the five most important phosphonates in terms of quantity used as complexing agents 2-phosphonobutane-1,2,4-tricarboxylic acid (PBTC), 1-hydroxyethylidene-(1,1-diphosphonic acid) (HEDP), nitrilotrimethylphosphonic acid (NTMP), ethylenediaminetetra(methylene phosphonic acid) (EDTMP), and diethylenetriaminepenta(methylene phosphonic acid) (DTPMP), as well as 2-hydroxy phosphonoacetic acid (HPAA) were investigated.

1.1.2 Research Questions

The following research questions were to be investigated as part of this thesis:

- Is GFH suitable for adsorption of phosphonates?
- How do the parameters temperature, pH, and the phosphonate structure (molecular size and weight, number of phosphonate groups) influence adsorption?
- Is regeneration possible and can GFH be reused in multiple adsorption-desorption cycles?

- How does the presence of other ions, particularly calcium, affect adsorption?
- Does the Ca^{II} present in GFH also have an effect?
- Do precipitates affect the adsorption/desorption process?
- Is NaOH as regeneration solution reusable over many cycles?
- Can precipitation be prevented by lowering the pH of the membrane concentrate?
- Can the precipitates be removed subsequently with a novel regeneration method using HCl?

The aim of this thesis was to find a suitable adsorbent for the removal of phosphonates and orthophosphate, which is also present in the investigated membrane concentrate. In batch experiments, an understanding of the adsorption process was to be gained in order to subsequently apply it to real wastewater (membrane concentrate from drinking water treatment) in fixed-bed column experiments. The adsorbent in these column experiments should be able to be reused over multiple cycles and be regenerated in an efficient manner.

1.2 Phosphorus

1.2.1 Natural Occurrence

Phosphorus (P) is an element with the atomic number 15 and an atomic weight of 30.97376 u, which was discovered in 1669 by Henning Brandt. It is widely distributed on the Earth and is the 11^{th} most abundant element in the Earth's crustal rock. It can be found not only in rocks, soils and waters, but is also essential in all living organisms as a component of DNA and its important role in energy metabolism. At the same time, phosphorus compounds are also among the known most toxic compounds and are also used as pesticides and even chemical warfare weapons. There are more than 100,000 known phosphorus compounds, but in nature phosphorus is found almost exclusively as phosphate (Bryant 2004).

In nature, phosphorus undergoes three different, party overlapping, cycles. The exogenous part of the inorganic phosphorus cycle describes its movement on the Earth's surface. It begins with the release of phosphorus from phosphate minerals, followed by cycling in soils and release and transport to surface waters. It ends with the burial

of phosphorus in sedimentary sequences. The phosphorus bound in sediments subsequently enters the endogenous part of the inorganic phosphorus cycle and is converted by global tectonic processes and geologic pressure to so-called sedimentary rocks, closing the inorganic cycle. The duration of the inorganic phosphorus cycle is several million years (Valsami-Jones 2004; Cornel and Schaum 2009; Liu and Chen 2014).

In addition, there are two organic phosphorus cycles that describe the movement of phosphorus as part of the food chain through living organisms. The land-based organic phosphorus cycle describes the path of phosphorus from the soil, through plants, to animals and humans, and back to the soil. The water-based organic cycle, on the other hand, describes the circulation of phosphorus in surface waters. While the water-based P cycle takes only a few weeks, the land-based P cycle takes an average of one year (Cornel and Schaum 2009; Liu and Chen 2014). Humans intervene significantly in the global P cycle through agriculture and industry, and therefore, phosphorus flux has significantly increased in the last centuries and is expected to increase further in the coming decades due to the increasing world population. Fig. 1.1 shows a schematic representation of the inorganic and land-based organic P cycle including anthropogenic impacts.

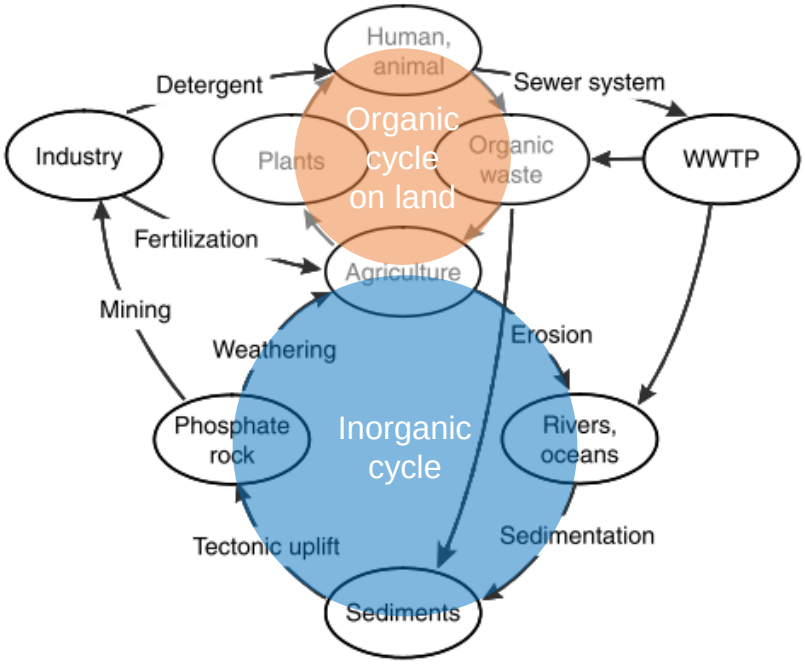

Fig. 1.1: Inorganic and land-based organic phosphorus cycles (Cornel and Schaum (2009), modified). Water-based organic phosphorus cycle not included.

1.2.2 Phosphorus Fractions and Analysis

In water bodies, phosphorus compounds can be classified into different fractions based on the analytical methods involved. The total P (TP) fraction includes the particulate P (PP) and total dissolved P (TDP) fractions. Particulate and dissolved phosphorus are separated by filtration using a 0.45 µm membrane filter (ISO 6878). The TDP fraction can be further subdivided into reactive orthophosphate and dissolved unreactive P (DUP), as shown in Eq. 1.1. It is common to equate the DUP fraction with organic phosphorus (Denison *et al.* 1998; Neft *et al.* 2010).

$$c(TP) = c(PP) + c(TDP) = c(PP) + c(DUP) + c(o\text{-}PO_4\text{-}P) \quad (1.1)$$

Therefore, after measurement of TDP and orthophosphate in the filtered sample, the DUP fraction can be calculated in accordance with Eq. 1.2.

$$c(DUP) = c(TDP) - c(o\text{-}PO_4\text{-}P) \quad (1.2)$$

Orthophosphate analysis is mostly conducted with the method introduced by Murphy and Riley (1962). Their proposed method uses ascorbic acid and Sb^{III} as reducing agents to form an intensely blue-colored phosphomolybdenum complex in the presence of acidified molybdate and phosphate, which can then be measured spectrophotometrically. The formed $[PSb_2Mo_{12}O_{40}]^-$ complex has its absorption maximum λ_{max} at 880 nm (Nagul *et al.* 2015). More details on the molybdenum blue reaction can be found in the review paper of Nagul *et al.* (2015).

To determine the total phosphorus in the unfiltered (TP) or filtered (TDP) sample, the phosphorus-containing compounds must be converted to molybdate-reactive orthophosphate. This conversion process, in which the P–O–P, C–O–P and C–P bonds are broken, is called digestion (Worsfold *et al.* 2016). Peroxydisulfate is usually used as the oxidizing agent, as first proposed by Menzel and Corwin (1965). Subsequently, Gales *et al.* (1966) reported a method using peroxydisulfate in an acidic milieu, the procedure of which was further simplified by Eisenreich *et al.* (1975) (Worsfold *et al.* 2016). Today, there is a well accepted description of the International Organization for Standardization, which systematically describes the methodology for the analysis of orthophosphate and total phosphorus in all water types (ISO 6878). Fig. 1.2 provides a synoptic overview of the P fractions and their analytics.

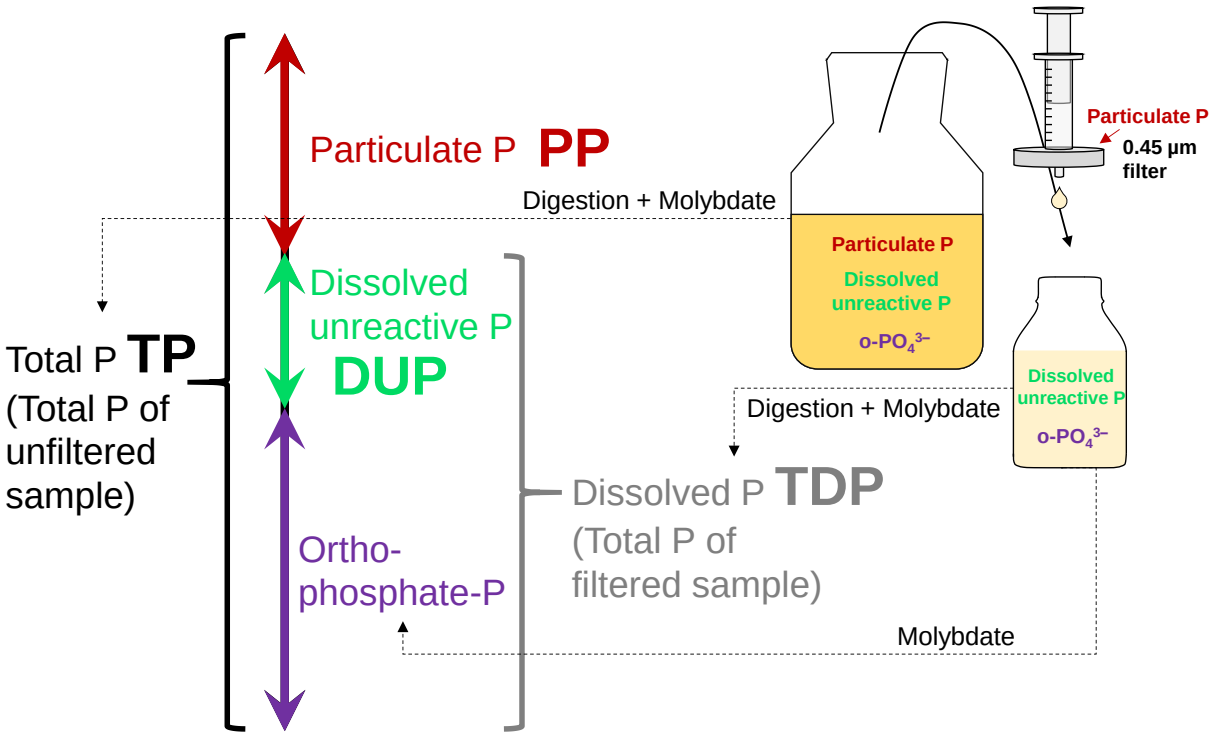

Fig. 1.2: Phosphorus fractions and analysis.

1.2.3 Phosphorus Discharge Limits

Phosphorus discharges into surface waters originate from two different sources. While diffuse sources such as agricultural runoff are difficult to monitor, point sources such as wastewater discharges are easy to regulate and are responsible for more than 50% of the discharged phosphorus in Europe (White and Hammond 2009; Sperlich 2010; Hendriks and Langeveld 2017). There is no agreement yet on a phosphorus limit that is acceptable to prevent eutrophication, but many studies suggest total phosphorus threshold concentrations between 20 and 100 µg P/L (Dodds *et al.* 1998; Schindler *et al.* 2016; Kumar *et al.* 2019; Chorus *et al.* 2020; Vuorio *et al.* 2020).

This has led to increasingly stringent phosphorus limits for wastewater discharges. In the USA, the National Pollution Discharge Elimination System (NPDES), for example, often limits municipal wastewater treatment plants (WWTP) to phosphorus effluent values between 0.1 and 0.5 mg P/L (US EPA 2007). However, less than 30% of major municipal WWTPs in the USA have any P limits to comply with (US EPA 2016).

In the Eurpean Union, the Water Framework Directive established an ecosystem approach to the management and protection of water resources and defined objectives (EU 2000). To achive a better quality of water bodies, P limits for effluent of municipal

WWTPs can be found in the Urban Wastewater Treatment Directive, namely 2 mg P/L for WWTPs with a size of 10,000 - 100,000 population equivalents (PE) and 1 mg P/L for plants > 100,000 PE in sensitive areas (EU 1991, 1998). In many countries, however, even stricter limits apply depending on the receiving waters. For instance, Sweden has an effluent limit of 0.5 mg P/L for WWTPs > 2,000 PE and Denmark of 0.4 mg P/L for all WWTPs in sensitive areas (Preisner *et al.* 2020). In sensitive areas in Germany such as Lake Constance, the effluent limit is 0.3 mg P/L, the target in Berlin is even as low as 0.05 mg P/L (Schaum 2018).

In the future, however, stricter effluent limits of about 0.1 mg P/L are expected in many countries (Zheng *et al.* 2011; Ashekuzzaman and Jiang 2017). Therefore, the DUP fraction is increasingly coming into focus in the context of these increasing demands. At a total P effluent value of 0.5 mg/l, the DUP fraction in municipal WWTPs can be as high as 0.05–0.1 mg P/l (Voigt *et al.* 2013; Rott *et al.* 2020a).

The limits for direct discharge of industrial wastewater vary greatly depending on the country and sector. Concentrates from drinking water treatment in Germany, for example, often contain 0.8–1.3 mg P/L and are permitted to be discharged into water bodies (Müller and Sacher 2016; Reinhardt *et al.* 2020a).

1.2.4 Phosphorus Compounds

1.2.4.1 Overview

More than 100,000 different phosphorus compounds are known, and most of them contain bonds to oxygen, carbon, nitrogen, or metals. The majority of naturally occurring phosphorus exists in the pentavalent form as phosphates with P–O and P═O bonds, such as orthophosphate, pyrophosphate and polyphosphates. Organophosphates, also called organic phosphate esters, have P–O–C bonds (Jenkins *et al.* 1971; Correll 1999; Bryant 2004). Phosphonates, on the other hand, contain phosphorus in a trivalent form and have a chemically stable direct C–P bond (Correll 1999; Bisson *et al.* 2017; Stasi *et al.* 2019). The aforementioned phosphorus compounds can be found in the aquatic environment in both dissolved and particulate forms (Jenkins *et al.* 1971; Correll 1999). In addition, there are many other organophosphorus compounds, such as various pesticides, some of which are classified as extremely hazardous by the

World Health Organization, or even chemical weapons such as Tabun (Bryant 2004; WHO 2020).

In the aquatic environment, particulate phosphorus can settle in the sediment (Correll 1999). Due to their strong adsorption affinity to aluminum and iron compounds, dissolved phosphorus compounds can also adsorb to materials in the sediment (Correll 1999; Loganathan *et al.* 2014; Boyd 2015). Sediments therefore often act as a sink for phosphorus. Since the phosphorus compounds in the sediment are in equilibrium with the dissolved phosphorus compounds, phosphorus can also redissolve from the sediment (Loganathan *et al.* 2014; Boyd 2015). This mechanism is also known as the phosphate buffer mechanism (Froelich 1988).

Furthermore, polyphosphates and organophosphorus compounds can be converted to orthophosphate by hydrolysis, photolysis, or microbial degradation (Zhou *et al.* 2011; Loganathan *et al.* 2014; Kuhn *et al.* 2018). Therefore, particulate and dissolved unreactive phosphorus fractions in aquatic systems should not be considered inert, as these forms of phosphorus may be converted to dissolved orthophosphate under appropriate conditions (Correll 1999). An in-depth overview on the chemistry of phosphorus is provided by Corbridge (2013).

1.2.4.2 Phosphates and Their Environmental Relevance

All life on earth is based on phosphorus. Organic phosphate esters are not only an important component of DNA, which is required for the storage of genetic information, but are also key components of the cellular energy storage adenosine triphosphate (ATP) (Bryant 2004; McGrath *et al.* 2013). Orthophosphate, however, is the only form of phosphorus which can be directly used by autotrophs to incorporate it into biomass (Correll 1999; Loganathan *et al.* 2014). However, there are bacteria that can also metabolize reduced phosphorus compounds (Quinn *et al.* 2007; White and Metcalf 2007; Stone and White 2012; Villarreal-Chiu *et al.* 2012; McGrath *et al.* 2013; Karl 2014; Horsman and Zechel 2017).

Apatites, which are orthophosphate minerals, are the most abundant, naturally found form of phosphorus (Valsami-Jones 2004). One kind of it, hydroxyapatite, also constitutes about 60% by weight of animal bones and even 70% of teeth (Bryant 2004).

Phosphoric adic and orthophosphate are used in industrial processes, such as phosphate conversion coating to treat metal surfaces. Phosphates are also used as ingredients in toothpastes, detergents, flame retardants, and food additives. Sodium triphosphate, for example, is a key ingredient in many synthetic detergents owing to its ability to soften water by sequestering calcium and magnesium ions (Halliwell *et al.* 2001; Bryant 2004). All of the above compounds, along with phosphorus from human excreta, can enter surface waters through wastewater discharge.

Therefore, the high global consumption of phosphates is also related to the problem of eutrophication of water bodies, i. e. their over-enrichment with mineral nutrients, with phosphorus usually being the limiting factor (Bryant 2004; Loganathan *et al.* 2014; Le Moal *et al.* 2019). Eutrophication leads to excessive production of autotrophs such as algae and cyanobacteria in particular. With advanced eutrophication, this leads to oxygen depletion especially at the bottom of the water bodies when the algae decay, caused by their subsequent aerobic decomposition. The formation of an anoxic zone near the sediment can release phosphorus bound to the sediment, which reinforces eutrophication (Correll 1999; Ludwig 2000; Loganathan *et al.* 2014). In addition to the oxygen depletion that can lead to death of aquatic life, some cyanobacteria can produce toxins that can be harmful to both aquatic species and other organisms along the food chain including humans (US EPA 2009; Catherine *et al.* 2013; Kumar 2018; Metcalf and Souza 2019).

Besides the negative impact on the environment, algal blooms also entail economic damage, among others on tourism, waterfront real estate, drinking water, and the fishing industry (Dodds *et al.* 2009; Kumar 2018; Le Moal *et al.* 2019). For instance, calculations by Dodds *et al.* (2009) show costs of roughly $2.2 billion annually resulting from eutrophication in freshwaters in the USA.

1.2.4.3 Phosphonates and Their Environmental Relevance Properties

Phosphonates are the salts of phosphonic acids, which were firstly synthetically prepared in 1897 (Baeyer and Hofmann 1897). A naturally occurring phosphonic acid, 2-aminoethylphosphonic acid (2-AEP) extracted from rumen protozoa, was only discovered many decades later (Horiguchi and Kandatsu 1959). The characteristic C–P bond of phosphonic acids is considered a relic from times of the primitive earth, where a

reducing atmosphere still prevailed due to low oxygen concentrations (McGrath *et al.* 2013).

Due to the C–P bond in the characteristic phosphonate groups ($C–PO(OH)_2$), phosphonates are chemically stable and, compared to molecules with the more reactive bonds N–P, S–P, or O–P, they are more resistant to processes such as thermal decomposition, chemical hydrolysis, enzymatic degradation and photolysis (Gledhill and Feijtel 1992; McGrath *et al.* 2013).

Tab. 1.1 gives an overview of physicochemical properties of the five quantitatively most important phosphonates used as complexing agents 2-phosphonobutane-1,2,4-tricarboxylic acid (PBTC), 1-hydroxyethylidene-(1,1-diphosphonic acid) (HEDP), nitrilotrimethylphosphonic acid (NTMP), ethylenediaminetetra(methylene phosphonic acid) (EDTMP), diethylenetriaminepenta(methylene phosphonic acid) (DTPMP), and additionally 2-hydroxy phosphonoacetic acid (HPAA). HPAA was also considered in this thesis as it was added to a cooling water that was studied as part of the project from which this thesis originated (Section 1.3.6).

Tab. 1.1: Physicochemical properties of phosphonates. K_{Henry} and log K_{ow} for HPAA from (US EPA 2017), all others from Rott et al. (2018c) and sources cited therein.

	HPAA	PBTC	HEDP	NTMP	EDTMP	DTPMP
CAS-No.	23783 -26-8	37971 -36-1	2809 -21-4	6419 -19-8	1429 -50-1	15827 -60-8
molecular formula	$C_2H_5O_6P$	$C_7H_{11}O_9P$	$C_2H_8O_7P_2$	$C_3H_{12}NO_9P_3$	$C_6H_{20}N_2O_{12}P_4$	$C_9H_{28}N_3O_{15}P_5$
molar mass	156.03	270.13	206.03	299.05	436.12	573.20
phosphorus content (%)	19.8	11.5	30.1	31.1	28.4	27.0
phosphonate groups	1	1	2	3	4	5
amine groups	0	0	0	1	2	3
water solubility (g/L)	> 100	> 100	> 100	> 100	21	> 100
K_{Henry} ($atm \cdot m^3/mol$)	$6.18 \cdot 10^{-15}$	$3.3 \cdot 10^{-17}$	$5.2 \cdot 10^{-17}$	$8.1 \cdot 10^{-18}$	$1.2 \cdot 10^{-17}$	$7.3 \cdot 10^{-18}$
log K_{ow}	-1.47	-1.36	-3.49	-3.53	-4.10	-3.40

In Tab. 1.1, HPAA, PBTC, and HEDP are three nitrogen-free phosphonates that also contain characteristic carboxyl and hydroxyl groups, and NTMP, EDTMP, and DTPMP are three aminophosphonates with three to five phosphonate groups. Phosphonates are highly soluble in water, poorly soluble in organic solvents (low log K_{OW}), and non-volatile (low K_{Henry}) (Jaworska *et al.* 2002; Rott *et al.* 2018c). Their chemical structures are depicted in Fig. 1.3.

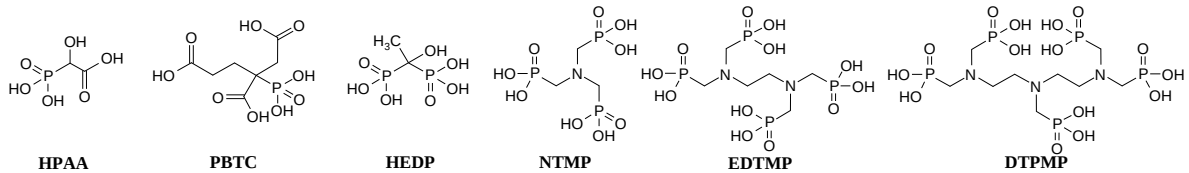

HPAA 2-Hydroxy phosphonoacetic acid | **PBTC** 2-Phosphonobutane-1,2,4-tricarboxylic acid | **HEDP** 1-Hydroxyethylidene-(1,1-diphosphonic acid) | **NTMP** Nitrilotrimethyl-phosphonic acid | **EDTMP** Ethylenediaminetetra(methylene phosphonic acid) | **DTPMP** Diethylenetriaminepenta(methylene phosphonic acid)

Fig. 1.3: Chemical structures of considered phosphonates.

Phosphonates belong to the substances with a so-called threshold effect, which describes two properties: they are already effective in substoichiometric concentrations and delay or change the precipitation of minerals by reducing their wall adhesion and firmness so that no incrustations form (Maise 1984). This scale inhibition is explained by the incorporation of phosphonates into the crystal lattice leading to prevention of

crystal growth, or by the adsorption of phosphonates onto the active growth sites of the crystals (Maise 1984; Jonasson *et al.* 1996; Yang *et al.* 2001; Tang *et al.* 2008; Jarrahian *et al.* 2020). All substances with threshold effect also act as chelating agents when applied in higher concentrations (Maise 1984). Chelate formation is strictly stoichiometric and results in water-soluble chelate complexes in which a multidentate ligand with more than one free pair of electrons occupies at least two coordination sites of the central atom, usually a metal ion. These chelate complexes prevent the central atoms from participating in further reactions and can thus prevent the precipitation of minerals (Maise 1984; Nowack 2003; Pilgrim 2018). Depending on the applied concentration, phosphonates can therefore act both as chelating agents and as scale inhibitors with threshold effect. Between the threshold and the stoichiometric regions there is a so-called turbidity region in which calcium phosphonates can precipitate in the presence of high calcium concentrations (Italmatch Chemicals 2015).

Due to their physicochemical properties described above, phosphonates are used in various industries, such as in the textile industry as bleach stabilizers, in cooling water systems as corrosion and scale inhibitors, in domestic and industrial detergents as a combination of scale inhibitor and bleach stabilizer, as stabilizers in personal care products, and also as antiscalants in drinking water treatment (Nowack and Stone 1999a; Nowack 2003; Boels *et al.* 2012; Kuhn *et al.* 2019).

Consumption

Phosphonate consumption has strongly increased in recent years. Fig. 1.4 gives a graphical overview of the development of phosphonate consumption in Europe and worldwide, as well as of consumption in detergents, cleaning and maintenance products in Germany. The estimated production volume of polyphosphonates in 1990 was 11,820 t in Europe and 9,545 t in the USA, making a total of 21,365 t (Gledhill and Feijtel 1992; HERA 2004). For the year 1998, Davenport *et al.* (2000) already indicated a worldwide phosphonate consumption of 56,000 t, distributed among 40,000 t in the USA, 15,000 t in Europe, and less than 800 t in Japan. In 1999, the phosphonate consumption in Europe was estimated to be 16,000 t (Knepper and Weil 2001). Since then, phosphonate consumption in Europe has increased sharply, with an estimated consumption of approximately 30,000 t in 2003 (HERA 2004), 40,000 t in 2008 (Groß *et al.* 2012), and 49,000 t in 2012 (EPA 2013). For 2012, the worldwide phosphonate

consumption was estimated at 94,000 t (EPA 2013). Thus, from 1998 to 2012, phosphonate consumption in Europe increased by almost 230%, while global consumption increased by almost 70%. The above figures only take phosphonates used as complexing agents into account; substances such as glyphosate used as herbicides are not included.

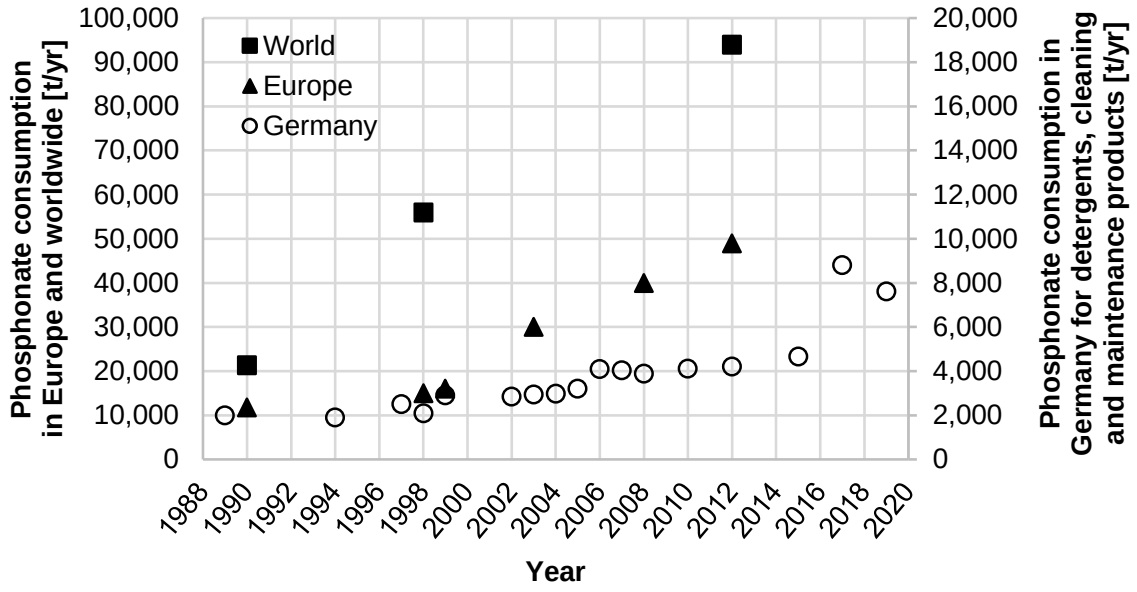

Fig. 1.4: Phosphonate consumption (Gledhill and Feijtel 1992; Davenport et al. 2000; Knepper and Weil 2001; UBA 2003; HERA 2004; IKW 2007, 2011; Groß et al. 2012; EPA 2013; IKW 2017, 2021).

Unfortunately, more recent, reliable estimates are not available. However, due to a change in European legislation, it can be assumed that phosphonate consumption is even higher today. Since 2017, EU Regulation No 648/2004 has limited the use of phosphorus to a maximum of 0.3 g per standard dose in consumer automatic washing detergents. This limit is so low that in practice phosphates are hardly ever used anymore, but have been replaced by the more efficient phosphonates. In Germany, for example, phosphonate use in detergents, cleaning and maintenance products therefore increased by over 60% from 4,673 t in 2015 to 7,613 t in 2019 (IKW 2021).

There are also other chelating agents with similar applications such as aminopolycarboxylic acids (APCAs). For comparison, the worldwide consumptions of APCAs NTA, EDTA, and DTPA was around 200.000 t/yr, split into about 50% EDTA and 25% NTA and DTPA each (Jäger and Schul 2001, Schmidt et al. 2004). However, unlike phosphonates, APCAs have a very low adsorption affinity. In WWTPs, therefore, they are

almost exclusively degraded microbially. While NTA is readily biodegradable, DTPA is only moderately degradable and EDTA is hardly degradable at all (Bucheli-Witschel and Egli 2001, MUNLV 2004). For instance, at WWTP Düsseldorf-Süd in Germany, a monitoring found removal rates of 91.9% for NTA, 23.4% for DTPA and 6.4% for EDTA (MUNLV 2004). EDTA has been under critical scrutiny since many decades and ended up on first list of priority substances as foreseen under Council Regulation (EEC) No 793/93 in the early 1990s (Means and Alexander 1981, EU 1993, 1994). In Germany, for instance, a voluntary joint declaration was therefore concluded in 1991 between the Federal Environment Agency and the industry with the aim of reducing EDTA discharge into water bodies by 50% within five years (BfG 2021a). This led to a sharp drop in EDTA consumption in Germany, for example in detergents, cleaning agents and maintenance products from about 435 t in 1999 to about 40 t in 2008 (Groß et al. 2012). A possible substitute for EDTA are phosphonates (Groß et al. 2012, IKSR 2012). Overall, EDTA consumption in Germany was about 3,000 t/yr in 2008. However, this also includes the agricultural sector, which was not included in the phosphonate consumption figures above (Groß et al. 2012).

Fate in Waters

Due to the usage of phosphonates in above mentioned applications, they usually are released into wastewater streams. Many studies show that phosphonates are comparatively well removed in municipal wastewater treatment plants. These can be divided into studies that spiked the influent of WWTPs with phosphonates and studies that measured ambient concentrations of phosphonates in WWTPs (Nowack 2004). For example, the former show removal rates for DTPMP of 90% (Hoelger *et al.* 2008) and 95% (Nowack 2002a), and for HEDP 90%–> 97.5% (Müller *et al.* 1984). The latter show removal rates for NTMP of ≥ 93% (Nowack 2002a) and for NTMP ≥ 80%, EDTMP ≥ 70%, and DTPMP 85% (Nowack 1998). For the removal rates indicated with a ≥ sign, the concentrations in the effluent of the WWTPs were below the limit of determination and therefore indicate minimum removals. Only recently, two methods have been developed for wastewater analysis which have limits of quantification in a range that they can be well applied to environmental samples (Wang, Shu *et al.* 2019; Armbruster *et al.* 2020). Both methods were used to analyze phosphonates in WWTP influents and effluents and removal rates of > 95% (Wang, Shu *et al.* 2019) and > 88% (median value) (Rott *et al.* 2020a) were observed.

A load balance by Rott *et al.* (2018c) estimates that about 24,600 t phosphonates of the 49,000 t used in Europe in 2012 entered wastewater treatment plants (Fig. 1.5). Assuming a removal rate of 80%–95%, they assume a load of 1,200–4,900 t discharged into receiving waters. However, for industrial direct dischargers, there is currently no state of the art for selective phosphonate removal (Rott *et al.* 2018c). The German wastewater ordinance, for instance, prohibits the use of organic complexing agents for some industries that do not attain a DOC degradation of 80 % after 28 days according to DIN EN ISO 9888, which includes phosphonates (ISO 9888). However, phosphonates are explicitly excluded from this for wastewaters from textile manufacturing and finishing, laundries, as well as water treatment, cooling systems, and steam generation (AbwV 2004). Rott *et al.* (2018c) estimate that roughly 7,800 to 13,700 tons of phosphonates are discharged directly from industry into water bodies, of which approximately 65%–90% is probably attributed to membrane concentrates and cooling waters, for which treatment is not common in many cases (Gartiser and Urich 2002; Müller and Sacher 2016). Accordingly, industrial direct dischargers account for a significantly larger share of the phosphonate load in water bodies than municipal WWTPs.

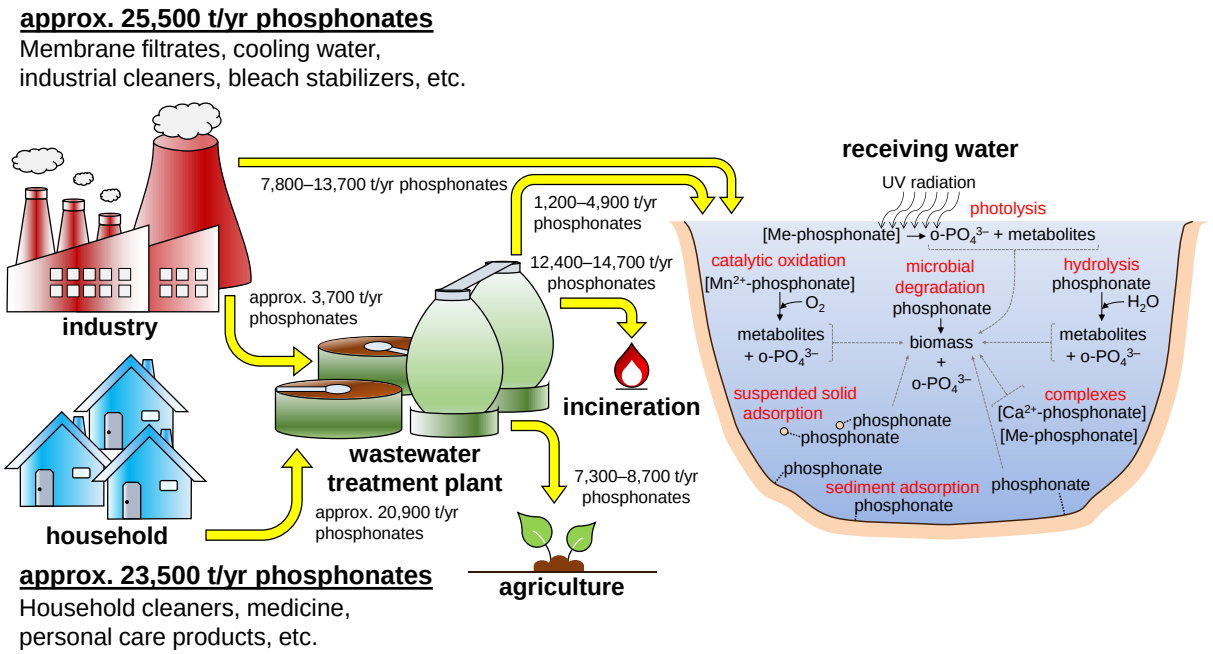

Fig. 1.5: Phosphonate loads in Europe and fate in receiving waters, modified from Rott et al. (2018c) and Rott (2018).

In total, 9,000 to 18,600 tons of phosphonates were thus discharged into water bodies in Europe in 2012. Due to the aforementioned lack of analytical methods for phosphonates in low concentrations, there have been few studies so far on the actual phosphonate content in water bodies resulting from this discharge. Schmidt *et al.* (2014) found concentrations of 0.3–1.6 µg/L HEDP and 0.1–1.3 µg/L DTPMP in four German rivers. Müller and Sacher (2016) found an increase in NTMP from < 0.5 to 6.7 µg/L and DTPMP from < 0.5–2 µg/L to up to 70 µg/L in two German creeks, respectively, due to the discharge of membrane concentrate from drinking water treatment. In a river in China, concentrations of 0.094 µg/L PBTC and 0.088 µg/L HEDP were observed (Wang, Shu *et al.* 2019). Rott *et al.* (2020b) investigated the influence of wastewater treatment plant effluent on phosphonate concentrations in two German rivers and their sediments. While the phosphonate concentration increased only slightly from 2.4–5.8 µg/L before to 2.5–6.6 µg/L after effluent discharge in the first river, it increased significantly from < 0.1–1.6 µg/L to 19–39 µg/L in the second river. This was caused by the flow volume of the second river being dominated by the WWTP effluent. In the sediments, a concentration increase from 6.7–29.4 mg/kg to 17.8–53.5 mg/kg in river 1 and from 1.8–5.0 mg/kg to 18.1–51.4 mg/kg in river 2 was observed. Thus, the sediment represents a phosphonate sink and there is a huge accumulation of phosphonates in sediments (factor 1000 between µg/L and mg/kg).

Ecotoxicity

Various studies on the ecotoxicity of phosphonates indicate significantly higher concentrations as critical. For example, phosphonates often show a toxic effect on fish only at concentrations > 100 mg/L, usually measured as LC_0/NOEC (highest concentration tested with no effect) after 48 or 96 hours or LC_{50} (concentration resulting in the death of 50% of the test population) (Huber 1975; Metzner and Nägerl 1982; Kästner and Gode 1983; Schöberl and Huber 1988; Gledhill and Feijtel 1992; Knepper and Weil 2001; Jaworska *et al.* 2002; Connect Chemicals 2018), and the bioconcentration factor for fish is also low (Steber and Wierich 1986, 1987). Similarly, no toxicity was observed in tests with daphnia at concentrations < 100 mg/L (Kästner and Gode 1983; Schöberl and Huber 1988; Grohmann and Horstmann 1989; Gledhill and Feijtel 1992; Knepper and Weil 2001; Jaworska *et al.* 2002; Connect Chemicals 2018). Experiments with oral administration of phosphonates to rats showed low to moderate toxicity with LC_{50} values ranging from 0.94 g/kg to 26.1 g/kg body weight (Metzner and Nägerl

1982; Kästner and Gode 1983; Maise 1984; HERA 2004; Connect Chemicals 2018). Assuming that the results of these laboratory experiments can be transferred to real ecosystems, phosphonate concentrations currently present in water bodies are therefore well below toxic levels. However, none of the above studies have examined long-term effects of phosphonates on aquatic life.

Degradation Pathways

In aquatic environments, phosphonates can be degraded by catalytic oxidation, photolysis, hydrolysis, or microbially, as well as removed by adsorption to suspended particles or to sediment (Fig. 1.5). The latter is described in Section 1.3.3.

Catalytic Oxidation

Aminophosphonates can be calatytically oxidized in the simultaneous presence of Mn^{II} and oxygen or of manganite (MnOOH) alone. However, this does not apply to the degradation products iminodi(methylene)phosphonate (IDMP) and N-formyl iminodi(methylene)-phosphonate (FIDMP) as well as to the nitrogen-free HEDP (Nowack 2002b; Nowack and Stone 2002, 2003). Nowack (2002b) indicates that manganese catalyzed oxidation could be an important degradation pathway in waste and natural waters.

Photolysis

Phosphonates can also be degraded by photolysis (Steber and Wierich 1986; Grohmann and Horstmann 1989; Matthijs *et al.* 1989; Gledhill and Feijtel 1992; Sabin *et al.* 1992; Fischer 1993; Nowack and Baumann 1998; Lesueur *et al.* 2005; Chen *et al.* 2007; Kuhn *et al.* 2017; Kuhn *et al.* 2018; Kuhn *et al.* 2020). This degradation pathway is considered relevant in water bodies and occurs mainly near the water surface, depending on turbidity and coloration (Steber and Wierich 1986; Grohmann and Horstmann 1989; Jaworska *et al.* 2002; Nowack 2004; Rott *et al.* 2018c; Kuhn *et al.* 2019). Metal-phosphonate complexes, especially iron-phosphonate complexes which are likely to be found in the environment, are photolytically degraded significantly faster than uncomplexed phosphonates (Fischer 1993; Jaworska *et al.* 2002; Lesueur *et al.* 2005; Kuhn *et al.* 2018). For instance, in laboratory experiments, ferric EDTMP complexes showed a half-life of about 26 h in central European waters, while it was about 100 h for uncomplexed HEDP (Matthijs *et al.* 1989; Fischer 1993), although nitrogen-

free phosphonates are more readily photodegradable (Grohmann and Horstmann 1989). However, the experiments were carried out under different boundary conditions, so that a direct comparison is not possible. Ferric HEDP complexes, on the other hand, were > 98% degraded after 40 h (Fischer 1993). While photolytic degradation of HEDP yields phosphate and acetate, degradation of aminophosphates also results in other by-products as well (Steber and Wierich 1986; Lesueur *et al.* 2005; Kuhn *et al.* 2017; Kuhn *et al.* 2018). For example, photolysis of NTMP, EDTMP, and DTPMP also produces IDMP and aminomethylphosphonic acid (AMPA) (Lesueur *et al.* 2005; Kuhn *et al.* 2017; Kuhn *et al.* 2018). Thus, AMPA is not a specific degradation product of glyphosate, for which it has been used as a tracer for a long time (Botta *et al.* 2009; Hanke *et al.* 2010). A more recent study showed that ferrous DTPMP complexes degrade four times faster than uncomplexed DTPMP. However, this only applies to DTPMP and not to its degradation products (Kuhn *et al.* 2018).

Hydrolysis

Another possible route for the degradation of nitrogen-containing polyphosphonates is hydrolysis (Steber and Wierich 1987; Tschäbunin *et al.* 1989; Schowanek and Verstraete 1990b; Schowanek and Verstraete 1991). For example, Schowanek and Verstraete (1991) found light-independent degradation rates of up to 1% per day for EDTMP in the presence of bivalent metal ions. The degradation rate in the absence of bivalent metal ions is significantly lower (Schowanek and Verstraete 1990b; Schowanek and Verstraete 1991). Although Schowanek and Verstraete (1991) referred to hydrolysis, redox reactions presumably play a role as well, since the degradation rate is considerably lower under anaerobic conditions (Nowack 2004). Compared to the degradation rates of photolysis, those of hydrolysis are relatively low. However, hydrolysis may be a significant degradation pathway of phosphonates in soils and sediments (Grohmann and Horstmann 1989; Jaworska *et al.* 2002).

Microbial Degradation

Due to naturally occurring phosphonates in the environment, bacteria have developed the ability to cleave the C–P bond and use phosphonates as a P source (Nowack 2003). Microbial degradation can occur in both water bodies and sediments (Steber and Wierich 1987). The enzymes involved in this process were described by Kononova

and Nesmeyanova (2002) and McGrath *et al.* (2013). There are many studies on microbial degradation of naturally occurring phosphonates such as 2-AEP or other less complex phosphonates such as glyphosate (Zeleznick *et al.* 1963; Rosenberg and La Nauze 1967; Kittredge and Roberts 1969; La Nauze *et al.* 1970; Cook *et al.* 1978; Daughton *et al.* 1979; Moore *et al.* 1983; Pipke *et al.* 1987; Lerbs *et al.* 1990; G.Ternan *et al.* 1998; Kononova and Nesmeyanova 2002; Fox and Mendz 2006; Martinez *et al.* 2010; Kamat and Raushel 2013). Cook *et al.* (1978), for instance, found that the naturally occurring 2-AEP was the only one of 14 phosphonates studied that also served as a C source for some bacterial strains. One strain, *Pseudomonas putida*, was capable of using 2-AEP as the sole source of C, N, and P. Other bacteria are known for being capable of using phosphonates as their sole carbon and/or nitrogen source (McMullan *et al.* 1992; McMullan and Quinn 1993; McGrath *et al.* 1998; Obojska *et al.* 1999). Since some cyanobacteria and eukaryotic microalgae can utilize phosphonates as their P source, they can thereby contribute directly to eutrophication without prior degradation (Studnik *et al.* 2015).

However, there are only few studies on the phosphonates considered in this work, namely HPAA, PBTC, HEDP, NTMP, EDTMP, and DTPMP. These phosphonates differ significantly from naturally occurring phosphonates as they have more complex structures, are larger molecules, often have a strong negative charge, and are commonly present in complexed form (Nowack 2003; Rott *et al.* 2018c). Schowanek and Verstraete (1990b) and Raschke *et al.* (1994) investigated the degradation of these synthetic phosphonates with pure bacterial strains.

Schowanek and Verstraete (1990b) investigated 13 different bacterial strains to determine whether they could use natural and synthetic phosphonates as P sources when no other P source was offered. While 9 of these could utilize 2-AEP, there was only one strain, *Arthrobacter* sp. strain GLP-1, that could utilize the phosphonates HEDP, NTMP, EDTMP, and DTPMP. Bacteria capable of using phosphonates were also detected in seven environmental samples, with the proportion of those capable of processing 2-AEP being significantly higher than for the four aminophosphonates. To those strains, DTPMP was less accessible than the other aminophosphonates. Raschke *et al.* (1994) enriched aerobic bacterial strains from eight environmental samples to test whether they could use PBTC as their sole P source. All bacterial strains were able to degrade > 90% PBTC in 200 h with the formation of orthophosphate. They

were also able to prove PBTC degradation under anaerobic conditions, although this was significantly slower.

Both Schowanek and Verstraete (1990b) and Raschke *et al.* (1994) concluded that bacteria capable of metabolizing phosphonates are ubiquitous in the environment, although they are found only at low proportions. Phosphonates are considered to be preferentially degraded in phosphate-free waters, although it has already been demonstrated that phosphonates are also degraded in the presence of phosphate if the enzymes have been previously induced (Schowanek and Verstraete 1990a; Raschke *et al.* 1994; Rott *et al.* 2018c).

The biodegradability of individual substances is typically assessed using standardized tests. OECD tests 301 A–F can be used to test the ready biodegradability. Substances that are readily biodegradable are assumed to undergo rapid degradation in the environment (OECD 2006). OECD tests 301 B (ISO 9439), 301 D (ISO 10707), and 301 F (ISO 9408) showed only low degradation of phosphonates (Huber 1975; BADSR 1976; Metzner and Nägerl 1982; Steber and Wierich 1986, 1987; Schöberl and Huber 1988). The phosphonate HPAA showed a biodegradability of ~50% in an OECD 301 D test (Connect Chemicals 2018). OECD tests 302 A–C are designed to test the inherent biodegradability. These tests are conducted under favorable conditions in order to assess the potential of a substance to be biodegraded under aerobic conditions (OECD 2006). In experiments using the Zahn-Wellens test, OECD 302 B (ISO 9888), with DOC as the analytical parameter, there was no inherent biodegradation despite the measured removal of PBTC (≤ 17%), HEDP (≤ 33%), NTMP (≤ 45%), EDTMP (≤ 20%), and DTPMP (≤ 50%), as the removal was attributed to adsorption on the inoculum (Steber and Wierich 1986, 1987; BADSR 1989; Held 1989; Cegarra *et al.* 1994; OECD SIDS 1996; Reichert 1996; Bachus 2003; HERA 2004). OECD 302 A (ISO 9887) showed degradation ≤ 6.7% of HEDP, NTMP, and DTPMP when CO_2 was measured (Saeger *et al;* HERA 2004). OECD 301 E (ISO 7827) showed < 3% degradation of HEDP and 20% degradation of NTMP when CO_2 was measured and no degradation of PBTC, HEDP, NTMP, EDTMP, and DTPMP when DOC was analyzed (AAW 1984; Steber and Wierich 1986, 1987; Horstmann and Grohmann 1988; OECD SIDS 1996). In experiments under anaerobic conditions, little to no degradation was observed as well (Steber and Wierich 1986, 1987; OECD SIDS 1996; Nowack 1998).

It should be mentioned, however, that biodegradability is rather dependent on the system conditions than a property of a substance (Schönberger 1991).

Although bacteria capable of metabolizing phosphonates are ubiquitous in the environment, the phosphonates considered in this work are mostly stable to microbial degradation. Therefore, no degradation of phosphonates is expected in wastewater treatment plants, which is why adsorption onto activated sludge may be the main pathway for phosphonate removal in WWTPs (Gledhill and Feijtel 1992; Fischer 1993; Jaworska *et al.* 2002). However, phosphonates can contribute to the eutrophication of water bodies not only through their direct microbial degradation, but also through their breakdown products, in particular through their abiotic degradation by photolysis (Rott *et al.* 2018c). Further studies on the biodegradation of phosphonates in the aquatic environment are needed to assess their environmental risks more accurately.

Redissolution of Heavy Metals

Due to their complexing property, phosphonates can also potentially redissolve heavy metals adsorbed on the sediment. There are several studies on the remobilization of metals, the results of which, however, differ considerably depending on the boundary conditions (Müller *et al.* 1984; Günther *et al.* 1987; Gledhill and Feijtel 1992; Bordas and Bourg 1998; Knepper and Weil 2001). However, the experiments showed that remobilization of iron, chromium, and zinc occurs only at phosphonate concentrations > 50 µg/L and of the toxic heavy metals mercury, cadmium, and lead only at > 1 mg/L (Rott *et al.* 2018c). Since this is above the usually measured phosphonate concentrations in water bodies, remobilization is presumably of no concern at present. However, this could change as soon as the adsorption capacities of the river sediments are depleted, leading to an increase in their concentrations in water bodies.

Summary

Phosphonates, the salts of phosphonic acids, with their characteristic phosphonate groups (C–$PO(OH)_2$), are efficient chelating agents and belong to the substances with a threshold effect. They are used in various industries, with a strongly increasing consumption in recent years. Typically, after use, they are released into wastewater streams. A load balance by Rott *et al.* (2018c) estimates that in total, 9,000 to 18,600 tons of phosphonates were discharged into water bodies in Europe in 2012. In

aquatic environments, phosphonates can be degraded by catalytic oxidation, photolysis, hydrolysis, or microbially, as well as removed by adsorption to suspended particles or to sediment. The resulting phosphonate concentrations in rivers are currently < 100 µg/L. Concentrations at which ecotoxic phenomena and remobilization of toxic heavy metals can occur are above these concentrations detected in river samples at present. In river sediments, however, concentrations of about 50 mg/kg were found. Thus, there is a huge accumulation of phosphonates in sediments, the future effects of which is uncertain. If the adsorption capacity of the sediments is reached one day, the phosphonate concentration in rivers can increase dramatically and thus be in the range of environmental effects.

1.3 Adsorption

1.3.1 Adsorption Process

1.3.1.1 Basics of Adsorption

The process of adsorption is generally considered to be the accumulation of substances (atoms, molecules, ions, etc.) at an interface. In the field of (waste)water treatment, this usually involves the adsorption of water constituents (adsorptives) onto the surface of solids (adsorbents) (Fig. 1.6). The figure also names the main variables influencing adsorption according to Cornel (1991). In order to practically apply adsorption in (waste)water treatment, it is necessary to know how various characteristic process parameters influence the adsorption of the substances to be removed, such as the temperature, pH, concentration of adsorptives in the aqueous solution, and contact time.

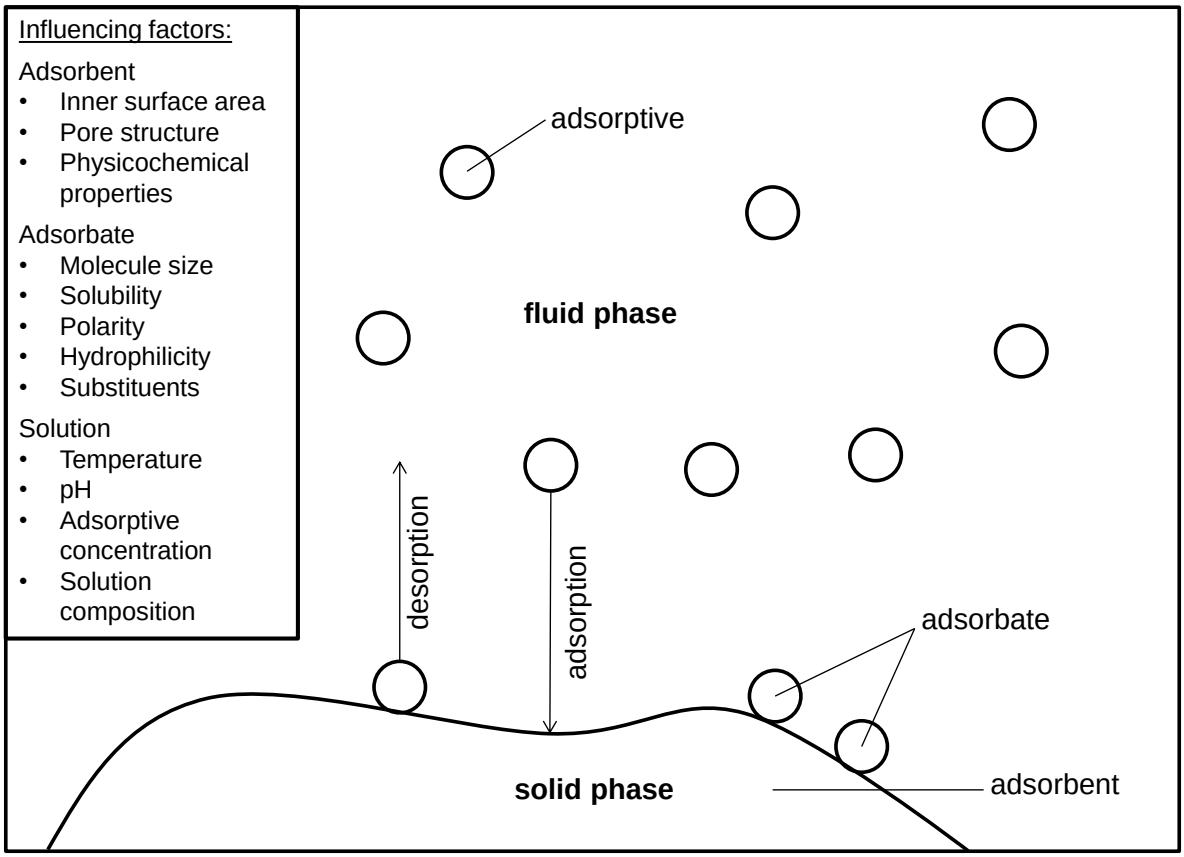

Fig. 1.6: Model and terms of adsorption. Influencing factors adapted from Cornel (1991).

When a solution containing an adsorptive is brought into contact with a suitable absorbent, adsorption begins until an equilibrium is reached. At this point, net adsorption no longer occurs, and the residual concentration of the adsorptive in the solution and the amount of adsorbate adsorbed on the adsorbent remain constant over time. To describe the amount of substance adsorbed onto an adsorbent material, the term loading (q) is often used. This is basically the quotient of the adsorbed amount of a substance (n_a) and the adsorbent mass (m_A) (Eq. 1.3).

$$q = \frac{n_a}{m_A} \tag{1.3}$$

For simplicity, the effect of temperature (T) is usually not taken into account by determining the loading under constant temperature conditions. The adsorption isotherm curves, i.e. the loading q plotted versus the adsorptive concentration c in the solution, can be described mathematically using various equations, with the Freundlich and Langmuir models being widely used in particular.

The Freundlich model is shown in Eq. 1.4.

$$q = K_F c^{1/n} \tag{1.4}$$

The parameter K_F is the Freundlich constant and n is the heterogeneity factor. The Freundlich model is a sort of standard equation for the characterization of adsorption processes in water treatment (Worch 2012). It is applied for heterogeneous adsorbent surfaces and assumes that the adsorption sites are not identical and multilayer adsorption occurs (Bonilla-Petriciolet *et al.* 2017). The model is valid only for a certain data range, because mathematically no saturation loading of the adsorbent is reached by the power function (Genz 2005).

The model by Langmuir is shown in Eq. 1.5**.**

$$q = q_{max} \frac{K_L c}{1 + K_L c} \tag{1.5}$$

The parameter q_{max} is the maximum loading, c is the adsorptive concentration in the solution, and K_L is the Langmuir constant. The Langmuir model assumes a homogeneous surface of the adsorbent, negligible interactions among adjacent adsorbed molecules, and considers monolayer adsorption (Bonilla-Petriciolet *et al.* 2017).

The corresponding parameters of both models can be determined either by non-linear regression or by converting the equations into their linear form followed by linear regression (Ho *et al.* 2002).

Adsorption kinetics is of importance to understand the time dependence of the adsorption process and the time to reach the equilibrium state. An adsorption kinetics curve shows the gradual decrease in the adsorptive concentration in the solution over time, or the gradual increase in adsorption loading. Adsorption kinetics can be modeled using the pseudo-first order model (Eq. 1.6) first presented by Lagergren (1898) or the pseudo-second order model (Eq. 1.7), which became known in particular through Ho and Mckay (1999).

$$q(t) = q_e(1 - e^{-k_1 t}) \tag{1.6}$$

$$q(t) = \frac{q_e^2 k_2 t}{1+q_e k_2 t} \tag{1.7}$$

The coefficient of determination r^2 of all model functions can be determined according to Eq. 1.8 (Ho 2006). Here, q_i is the experimentally determined data, $\bar{q}_i$ is the mean value of these data, and q_m is the data determined using the model function.

$$r^2 = \frac{\sum (q_m - \bar{q}_i)^2}{\sum (q_m - \bar{q}_i)^2 + \sum (q_m - q_i)^2} \tag{1.8}$$

1.3.1.2 Adsorption Mechanisms

Adsorption can be categorized by the nature of the intermolecular attraction between the adsorptive and the adsorbent. A distinction is made between physical adsorption, ion exchange and chemical adsorption (Xing and Pignatello 2005). For simplicity, the term adsorption is used in this thesis to refer to all sorption processes described in the following, with a focus on those that play a role in the adsorption of phosphorus compounds. Moreover, different categorizations are sometimes found in the literature. For example, ion exchange is not always classified as an adsorption process, and surface precipitation is sometimes considered to be structural incorporation (Song *et al.* 2021). Thus, the categorizations as used in this thesis are listed below.

In physisorption and ion exchange, relatively weak intermolecular interactions are involved, which are usually reversible. In physisorption, also called nonspecific adsorption, the electronic orbitals of the adsorbate and the adsorbent are not disrupted, instead attraction takes place through physical forces such as van der Waals, electrostatic, and hydrophobic interactions as well as hydrogen bonding and diffusion (Xing and Pignatello 2005; Ray *et al.* 2020). The process is considered as ion exchange if a stoichiometrically equivalent amount of ionic species is desorbed simultaneously during the adsorption process of ionic species to preserve the electro-neutrality of the ion exchanger (Dąbrowski 2001; Loganathan *et al.* 2014). A hydrogen bond is a particularly strong dipole-dipole attraction force and it is formed between a strong electropositive H atom in the adsorbent and a highly electronegative atom like oxygen in the adsorbate or vice versa (Weiner 2013). Hydrogen bonding is stronger than ion exchange, but not as strong as ligand exchange (Loganathan *et al.* 2014).

With regard to diffusion, the adsorption process can be described by four successive steps. In the first step, the adsorptive is transported from the bulk liquid phase to the film which surrounds the adsorbent, also called hydrodynamic boundary layer. This is followed by diffusion of the adsorptive through this film to the adsorbent's external surface (film diffusion). In a third step, the adsorptive is transported into the pores of the adsorbent, called intraparticle diffusion. This occurs either by diffusion across the liquid in the pores (pore diffusion) and/or by diffusion along the internal surface (surface diffusion). The final step is the interaction, by which the adsorptive is attached to the final adsorption site (surface reaction). The adsorption rate is often limited by film diffusion or intraparticle diffusion (Worch 2012; Tan and Hameed 2017; Song *et al.* 2021). For adsorbents with many micropores, adsorption rate is often limited by intraparticle diffusion. Often, a pseudo-equilibrium occurs first (within minutes to hours), followed by the much slower intraparticle diffusion (days to months) (Loganathan *et al.* 2014; Kumar *et al.* 2018). Adsorbate in micropores is often irreversibly adsorbed and can therefore no longer be completely desorbed (Cabrera *et al.* 1981).

In contrast to physisorption, chemisorption processes refer to chemical interactions between adsorbate and adsorbent involving valence forces and electronic orbitals. Chemisorption describes processes such as surface complexation, surface precipitation and redox reactions (Ray *et al.* 2020). Chemisorption is referred to as specific adsorption because the adsorbate is bound directly to the surface of the adsorbent without an intermediate water molecule (Goldberg and Sposito 1985; McGrath *et al.* 2014). Chemisorption can be confirmed by analytical methods such as Fourier-transform infrared spectroscopy (FTIR), Raman spectroscopy, X-ray photoelectron spectroscopy (XPS) and magnetic susceptibility (Ray *et al.* 2020).

One type of surface complexation is formed by ligand exchange and the resulting complexes with ligand-metal coordination bonds are quite stable (Goldberg and Sposito 1985; Xing and Pignatello 2005). In adsorption on metal (hydr)oxides by ligand exchange, an anion binds to a metallic cation via a covalent bond. This leads to the release of another anion such as OH^- that was previously bound to the surface of the adsorbent (Loganathan *et al.* 2014; Li *et al.* 2016). Ligand exchange is thus similar to ion exchange except that in conventional ion exchange the counterions are replaced,

whereas in ligand exchange the ligands are exchanged with the counterion remaining in the adsorbent (Helfferich 1962).

Due to the interactions of the adsorbent with the ions in the aqueous solution, a higher concentration can be expected close to the adsorbent surface than in the bulk solution (Ford 2006; Antelo *et al.* 2015). If this results in a supersaturated solution near the adsorbent surface and thus in exceeding the solubility product of a precipitate, surface precipitation can occur. Particularly in the presence of calcium, Ca-P precipitates can form in the alkaline range (Klimeski *et al.* 2012). Surface precipitation is reported as a rapid and hardly reversible adsorption mechanism (Loganathan *et al.* 2014).

The differentiation between physical adsorption and chemical adsorption is somewhat arbitrary with fluid boundaries (Worch 2012). Therefore, differing data on the binding energies can be found in the literature. The adsorption enthalpies mentioned for chemisorption range from > 50 kJ/mol (Worch 2012) through 80 to 200 kJ/mol (Liu and Liu 2008) to 80 to 450 kJ/mol (Song *et al.* 2021). For physisorption, bond strengths of < 50 kJ/mol (Worch 2012) and < 20 kJ/mol can be found, with electrostatic interactions reported as 20 to 80 kJ/mol (Song *et al.* 2021).

1.3.1.3 Adsorption on Granular Ferric Hydroxide

Currently, there is a variety of materials that are used for adsorption applications in (waste)water treatment. These materials can be of natural origin, such as clay minerals, natural zeolites, oxides or biopolymers, or they can be produced industrially as so-called engineered adsorbents, which can be subdivided into carbonaceous adsorbents (e.g. activated carbon), polymeric adsorbents (e.g. resins), oxidic adsorbents, and zeolite molecular sieves (Worch 2012). Compared to natural adsorbents, engineered adsorbents often have significantly better performance, higher adsorption capacities and almost constant properties due to strict quality control during production. Their disadvantage compared to natural adsorbents, however, is their high cost (Worch 2012).

Among the engineered adsorbents, oxidic materials show particularly good performance with respect to adsorption of polar, especially ionic compounds, such as orthophosphate and phosphonates. Oxidic adsorbents include solid hydroxides, oxides and hydrated oxides. The partially dehydrated granular ferric hydroxide (GFH) adsorbents are thermodynamically metastable and thus have a characteristically large surface

area which typically consists largely of micropores (pore size < 2 nm) (Worch 2012; Kumar *et al.* 2019). They usually have a large number of functional surface OH groups, which make the surface of the materials polar and also provide the possibility of protonation and deprotonation of the hydrogen atoms depending on the pH of the aqueous solution (Worch 2012). The surface OH groups of GFH show amphoteric behavior in the aqueous solution (Eq. 1.9). The symbol ≡ shows that the Fe is bound to the solid lattice of the adsorbent and OH represents a surface OH group. This schematic representation refers to "a" surface OH group, but various configurations are possible, such as  ,  , and  .

$$\equiv FeOH_2^+ \rightleftharpoons \equiv FeOH + H^+ \rightleftharpoons \equiv FeO^- + 2H^+ \qquad (1.9)$$

The reactions shown in Eq. 1.9 result in a surface charge that depends on the pH of the solution. This results in electrostatic interactions with the adjacent aqueous solution, which can attract counterions and allows them to concentrate near the surface (Genz 2005; Brezonik and Arnold 2011). The deprotonation sequence in Eq. 1.9 shows that the expected net surface charge is negative at high pH and positive at low pH. In between, there is a point where the net surface charge is zero, the so-called point of zero charge pH_{PZC}. Therefore, for example, at $pH<pH_{PZC}$, adsorption of anions is favored due to the electrostatic attraction. This behavior, on the other hand, can also be utilized for desorption. It should be emphasized, however, that the surface at pH_{PZC} is not uncharged, but that the sum of the positively and negatively charged sites is zero (Brezonik and Arnold 2011).

The functional surface OH groups at the interface of GFH with an aqueous solution can lead to coordinate bond formation betweeen positively charged central atoms and negatively charged species (Stumm 1995; Black 2016). It is often thought that this formation of coordinate bonds results from ligand exchange (Yates and Healy 1975). To describe these processes, the surface complexation model was developed (Stumm *et al.* 1987). In contrast to the assumption in the electric double layer model that the surface of the adsorbent interacts with the aqueous solution solely through its electric charge, the basis of the surface complexation model are the functional groups on the surface. Since the donor atoms of the functional groups are also found in the functional groups of the adsorptives, ligand exchange can occur, since deprotonated surface OH groups ($\equiv FeO^-$) can act as Lewis bases and the central ion ($\equiv Fe$) can act as a Lewis

acid (Stumm *et al.* 1987; Stumm 1995). Surface complexation models distinguish between inner-sphere and outer-sphere complexes. Inner-sphere complexes form a covalent bond which makes them more stable than outer-sphere complexes, which have at least one water molecule between the adsorbent and the adsorbate (Stumm 1995; Worch 2012).

Adsorption of anions leads to an exchange of surface OH groups with the ligands, as shown in Eq. 1.10 & 1.11 for a bivalent anion A^{2-}.

$$\equiv FeOH + A^{2-} \rightleftharpoons \equiv FeA^{-} + OH^{-} \tag{1.10}$$

$$2\equiv FeOH + A^{2-} \rightleftharpoons (\equiv Fe)_2A + 2OH^{-} \tag{1.11}$$

The protons of the surface OH groups can be replaced by cations, as shown in Eq. 1.12 and 1.13 for a bivalent metal ion Me^{2+}. Eq. 1.12 represents a mononuclear and Eq. 1.13 shows a binuclear surface complex.

$$\equiv FeOH + Me^{2+} \rightleftharpoons \equiv FeOMe^{+} + H^{+} \tag{1.12}$$

$$2\equiv FeOH + Me^{2+} \rightleftharpoons (\equiv FeO)_2Me + 2H^{+} \tag{1.13}$$

Adsorption of anions and cations can also lead to the formation of so-called ternary surface complexes. Eq. 1.14 & 1.15 show this for a monovalent anion A^{-} and a bivalent metal ion Me^{2+}, exemplarily. The formation of these ternary surface complexes is comprehensively described by Schindler (1990).

$$\equiv FeOH + A^{-} + Me^{2+} \rightleftharpoons \equiv FeAMe^{2+} + OH^{-} \tag{1.14}$$

$$\equiv FeOH + A^{-} + Me^{2+} \rightleftharpoons FeOMeA + H^{+} \tag{1.15}$$

The above equilibrium reactions show that with increasing pH the adsorption of cations increases, while with decreasing pH anions adsorb more effectively. This is also consistent with the behavior of the surface charge at pH values greater or less than pH_{PZC} described above. It is also evident from the reaction equations that neutral or charged surface complexes can be formed depending on the valence of the ions and the number of adsorption sites involved (Stumm 1995; Worch 2012). Since the inner-sphere

complexes are directly bound to the surface of the adsorbent, they also contribute directly to the surface charge. Thus, the pH_{PZC} can be shifted by the adsorbed species. If the adsorptive is a weak acid, it must be considered that it can at least partly deprotonate (Sigg and Stumm 1981; Worch 2012; Loganathan *et al.* 2014).

1.3.1.4 Regeneration of Adsorbents

During adsorption, several compounds present in the water are bound to the surface of the adsorbent material. After a certain time, however, the capacity of the adsorbent is exhausted and it can no longer be used effectively to remove the compounds present in the (waste)water. This gains importance in (waste)water treatment practice, where the period during which an adsorbent can be used depends on its capacity and its degree of saturation. When the capacity of the adsorbent is exhausted, it must either be replaced by a fresh material or undergo a regeneration process in which the compounds bound to the absorbent's surface are removed again, allowing the same material to be reused.

During regeneration, the adsorptives bound reversibly to the adsorbent surface are desorbed and transferred to the regeneration solution. In order to achieve a strong desorption of a certain compound, the opposite conditions that led to the adsorption can be used. Through contact of the loaded adsorbent with a solution that has a pH at which adsorption is significantly weaker than in the original solution in which the adsorption took place, the adsorbent strives to reach a new equilibrium state with the regeneration solution. This leads to a strong desorption of the adsorptive into the regeneration solution, and thus, to a lower adsorbent loading. The desorption rate can be driven by either equilibrium or kinetic effects. Equilibrium limitations depend in particular on the pH and temperature of the solution, while kinetic limitations include diffusional mass transfer and the rate of desorption reaction (Worch 2012; Chen *et al.* 2017).

For the regeneration of oxidic adsorbents, desorption by pH variation is an effective process. The pH has a strong influence on the desorption performance, since pH affects the speciation of adsorptives and the protonation and deprotonation of surface OH groups on the adsorbent. Therefore, oxidic adsorbents that have been used to remove anions such as orthophosphate and phosphonates can be regenerated with

strong bases such as NaOH. At high pH values, both the surface of the oxidic adsorbents and the phosphonates and the orthophosphate are strongly negatively charged, so that electrostatic repulsion takes place. Due to the high concentration of OH^- ions at high pH, there is also competition for the adsorption sites (Boels *et al.* 2012; Worch 2012; Loganathan *et al.* 2014).

1.3.2 Adsorption of Phosphate on Iron (Hydr)Oxides

Iron (hydr)oxides are commonly used in studies as adsorbents due to their wide distribution in nature as well as their ease of synthesis in the laboratory. Most of these studies use phosphate as an inorganic anion (Sperlich 2010). Accordingly, there is a large number of studies on the adsorption of phosphate on GFH (Genz *et al.* 2004; Sperlich *et al.* 2005; Ernst *et al.* 2007; Sperlich *et al.* 2008; Saha *et al.* 2010; Sperlich *et al.* 2010; Kanematsu *et al.* 2011; Kunaschk *et al.* 2015; Zhao *et al.* 2015; Hilbrandt *et al.* 2018; Kumar *et al.* 2018; Hilbrandt *et al.* 2019b; Hilbrandt *et al.* 2019a; Yousefi *et al.* 2019; Martí *et al.* 2021). Several review articles provide an overview of the studies conducted to date, a selection of which is presented below (Kumar *et al.* 2014; Li *et al.* 2016; Liu *et al.* 2018; Kumar *et al.* 2019).

Genz *et al.* (2004) studied the adsorption of phosphate on an activated alumina and on GFH (pH 5.5 and 8.2 (buffers: Na_2HPO_4 and KH_2PO_4, respectively, no pH adjustment), 20 °C, 96 h contact time, 10–1,000 mg GFH in 250 mL membrane bioreactor filtrate (spiked to 4 mg/L PO_4-P), stirrer, P determination from membrane-filtered sample (0.45 µm)). For maximum loading, the GFH performed about 1.4 times better than the activated alumina at pH 8.2 and 1.7 times better at pH 5.5. With equilibrium P concentrations > 2 mg/L, they oberved precipitation of calcium phosphate compounds.

Sperlich (2010) studied three different GFH with synthetic solutions (pH 6–8 (buffers: 2 mM 2-(*N*-morpholino)ethanesulfonic acid (MES), *N*,*N*-bis(2-hydroxy-ethyl)-2-aminoethane-sulfonic acid (BES), or (2-hydroxy-1,1-bis(hydroxymethyl)ethyl)amino-1-propanesulfonic acid (TAPS), no pH adjustment), 20±1 °C, 96 h contact time, 10 mM ionic strength (NaCl), 10–83 mg GFH in 250 mL synthetic solutions with deionized or drinking water (0.5–4.0 mg/L PO_4-P), shaker, P determination from membrane-filtered sample (0.45 µm)). They observed that the adsorption capacity increases with decreasing pH with loadings of ~23 mg P/g GFH at pH 6 and ~12 mg/g at pH 8. Experiments with deionized water at pH 7, which was spiked with calcium, showed an approximately

50% higher loading than experiments without calcium. Experiments with drinking water, which contained significantly more Ca^{II}, showed a slightly lower loading, which they attributed to the additional presence of other competing ions. They described that the adsorption of Ca^{II} increases the pH_{PZC} which enhances the adsorption of the negatively charged phosphate ions, faciliates double-layer adsorption of PO_4, or leads to ternary surface complex formation.

Genz *et al.* (2004) conducted breakthrough experiments on filter columns (pH 7.9–8.7 (no buffer, no pH adjustment), 18–25 °C, membrane bioreactor filtrate (0.1–0.3 mg/L PO_4-P), column with 25 mm inner diameter filled with GFH, downstream mode, 3–36 min EBCT, P determination from membrane-filtered sample (0.45 µm)). At a PO_4-P influent concentration of 0.3 mg/L, the 50 µg/L limit in the effluent was exceeded after 8,000 bed volumes (BV). At an influent concentration of 0.1 mg/L PO_4-P, this limit was never reached in three months. Desorption experiments with 0.6 M NaOH were successful, but the low adsorbent mass resulted in an NaOH:BV ratio of 100:1, whereas this ratio is typically 2:1 to 4:1 for adsorption filters.

Sperlich (2010) studied the adsorption of phosphate on GFH in laboratory-scale columns (pH 7–8 (no buffer, no pH adjustment), 20±1 °C, synthetic solutions with deionized or drinking water (2 mg/L PO_4-P), column with 25 mm inner diameter filled with 45.6–53.9 g GFH, 3.0–3.3 min EBCT, P determination from membrane-filtered sample (0.45 µm)). Again, they found lower capacity with deionized water than with drinking water. In additional rapid small-scale column tests (RSSCT), they found that downscaling with constant diffusivity scaling is more suitable than the proportional diffusivity approach. The RSSCT also showed that the breakthrough curve becomes steeper and more sigmoidal with increasing EBCT. They calculated that two columns in series allow a significantly higher specific throughput; 134–175% more than with only one column, depending on the treatment target.

Kunaschk *et al.* (2015) investigated the adsorption behavior of three different GFH adsorbents (tap water (spiked with 50 mg/L phosphate), column with 9 mm inner diameter filled with 6 g GFH, up-flow mode, 1.2 min EBCT). Conventional regeneration with 1 M NaOH reduced the adsorption capacity by up to 85% after four adsorption/desorption cycles. With an energy-dispersive X-ray spectroscopy (EDS), they revealed different calcium-containing compounds which blocked the adsorbent surface. These

deposits interact with the phosphate and disturb the regeneration process. Therefore, they introduced a novel regeneration step using HCl (pH 2.5) prior to alkaline regeneration. With this, they were able to achieve nearly complete recovery of the adsorption capacity. After eight adsorption/desorption cycles, they did not observe any decline in adsorption capacity or changes in the physical properties of two of the adsorbents. One adsorbent was partly dissolved during acidic regeneration.

Kumar *et al.* (2018) used the same acidic-alkaline regeneration approach as Kunaschk *et al.* (2015) in their investigation of two different GFH adsorbents (pH 7.9±0.2 (no buffer, no pH adjustment), 21 °C, WWTP effluent (spiked to 2 mg/L PO_4-P), column with 18 mm inner diameter filled with GFH, up-flow mode, 5 min EBCT, P determination from unfiltered sample). They found that a smaller particle size resulted in up to four times higher adsorption capacities. Although the GFH undergoes no change in specific surface area when grinded, its micropores (< 2 nm) and mesopores (2–50 nm) become more accessible, thus facilitating intraparticle diffusion. In contrast to Kunaschk *et al.* (2015), they observed a change in surface area of the GFH adsorbents after acidic and alkaline regeneration. They assumed that Ca^{II} makes the adsorbent surface more electropositive as it likely first physisorbs before precipitating. The precipitate itself can shift the pH_{PZC} because calcium carbonates often show a $pH_{PZC} > 9$.

Besides physisorption and surface precipitation, ligand exchange is the dominant type of adsorption of phosphate on iron (hydr)oxides (Loganathan *et al.* 2014; Kunaschk *et al.* 2015; Li *et al.* 2016; Kumar *et al.* 2018; Liu *et al.* 2018). During ligand exchange, phosphate adsorbs by forming inner-sphere complexes (Sigg and Stumm 1981; Goldberg and Sposito 1985; Genz *et al.* 2004; Xie *et al.* 2014). Hereby, the formation of various complexes is possible, their structures are shown in Fig. 1.7 (Sigg and Stumm 1981; Goldberg and Sposito 1985; Petrone 2013; Xie *et al.* 2014). Additionally, the formation of ternary complexes is possible in the presence of Ca^{II} (Gao and Mucci 2003; Sperlich 2010). Due to the ligand exchange mechanism, desorption is thus possible by adding NaOH (Sperlich 2010; Kunaschk *et al.* 2015; Kumar *et al.* 2019).

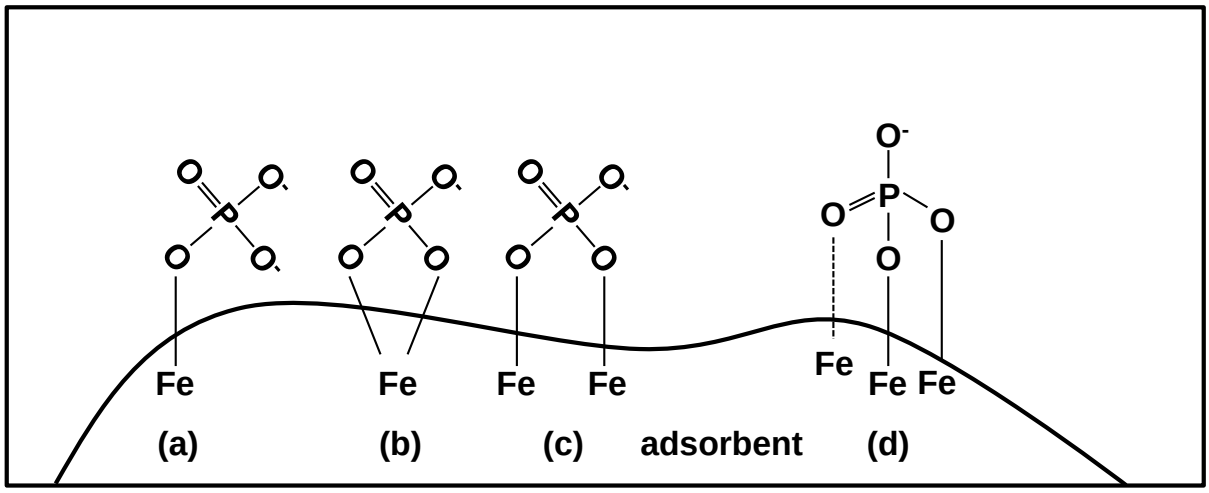

Fig. 1.7: Possible inner-sphere complexes of phosphate on iron (hydr)oxides.(a) monodentate, (b) mononuclear bidentate, (c) binuclear bidentate, (d) tridentate complexes. Modified from Petrone (2013).

1.3.3 Adsorption of Phosphonates on Iron (Hydr)Oxides

Despite the fact that highly water-soluble substances generally do not readily adsorb to sediments and soils, due to their chelating properties phosphonates have a high affinity to adsorb to minerals (Gledhill and Feijtel 1992). Numerous articles show that phosphonates adsorb very well to various adsorbents such as calcite (Xyla *et al.* 1992), cassiterite (Kuys and Roberts 1987), clay (Fischer 1991, 1993; Morillo *et al.* 1997), aluminum oxides (Laiti *et al.* 1995; Gerbino 1996; Laiti and Öhman 1996; Liu *et al.* 2000), iron oxides (Day *et al.* 1997; Barja *et al.* 1999; Nowack and Stone 1999a, 1999b), zinc oxide (Nowack and Stone 1999b), hydroxyapatite (Jung *et al.* 1973; Rawls *et al.* 1982; Amjad 1987; Chirby *et al.* 1988), barite (Black *et al.* 1991), sediments (Fischer 1992, 1993; Dolinger *et al.* 2015; Rott *et al.* 2020b), soils (Steber and Wierich 1986, 1987; Held 1989), sewage sludges (Steber and Wierich 1986, 1987; Fischer 1992, 1993; Nowack 2002a; Dollinger *et al.* 2015), as well as natural adsorbents such as coconut and mussel shells (Kumar *et al.* 2010) and engineered magnetic nanocomposite adsorbents (Rott *et al.* 2018a; Altaf *et al.* 2021a; Altaf *et al.* 2021b; Drenkova-Tuhtan *et al.* 2021; Li *et al.* 2021). Selected studies focusing on the adsorption of phosphonates on various iron (hydr)oxides are described below.

Nowack and Stone (1999a) analyzed the adsorption of eight different phosphonates in ultrapure water on precipitated goethite, an iron oxide-hydroxide. They found that 10 µM NTMP adsorbed almost completely on goethite within a few minutes at pH 7

(buffer: 1 mM 3-(*N*-morpholino)propanesulfonic acid (MOPS), no pH adjustment), 25±0.2 °C, 1 h contact time, 0.42 g/L adsorbent in 30 mL ultrapure water (spiked with 10 µM phosphonate), magnetic stirrer/water bath, 10 mM ionic strength ($NaNO_3$), P determination from membrane-filtered sample (0.2 µm)). When the pH was subsequently raised to 12.2, a slow desorption occurred, which was completely finished after about five hours (desorption at pH 12.2 by adding 1 M NaOH). Even with a contact time of seven days for adsorption, the kinetics of desorption did not change. Thus, it can be assumed that this was pure adsorption on the surface and not the formation of an Fe^{III}-NTMP precipitate. The variation of ionic strength in the range of 1 mM to 1 M $NaNO_3$ showed no effect on adsorption. Furthermore, they investigated the influence of pH on adsorption with the result that an increasing pH led to decreasing adsorption and at pH > 10 the adsorption of many phosphonates became negligible. With 10 µM NTMP, almost complete adsorption occurred at pH values < 7. Experiments with a pH of 7.2 showed that adsorption decreases with increasing number of phosphonate groups: NTMP (three phosphonate groups) > EDTMP (four phosphonate groups) > DTPMP (five phosphonate groups).

In further studies by Nowack and Stone (1999b), they addressed the influence of different metal ions on the adsorption of various phosphonates on goethite (pH 3–12 (no buffer, no pH adjustment), 25±0.2 °C, 1 h contact time, 0.42 g/L adsorbent in 30 mL ultrapure water (spiked with 10 µM phosphonate), magnetic stirrer/water bath, 0.01 M ionic strength ($NaNO_3$), P determination from membrane-filtered sample (0.2 µm)). Again, they found higher phosphonate adsorption with decrasing pH. For five of the six phosphonates investigated, equimolar concentrations of Cu^{II}, Zn^{II}, and Fe^{III} had no discernible effect on adsorption. Only in the case of DTPMP, the adsorption decreased significantly with the addition of Fe^{III}. The addition of Ca^{II} had a very positive effect on the adsorption of the phosphonates. Due to the presence of calcium ions, adsorption still took place at higher pH values. For example, the removal rate of NTMP could be increased from 40% to 100% in the presence of 1 mM Ca^{II} at pH 10 and from 0% to 95% at pH 12. In addition, Ca^{II} also had an effect on the maximum adsorption capacity, which was doubled already at low, equimolar concentrations, compared to a solution without calcium ions. At 1 mM Ca^{II}, this effect increased even more, whereas at 5 mM no further improvement occurred.

The influence of phosphate ions on the adsorption of phosphonates was studied by Nowack and Stone (2006) (pH 7.2 (buffer: 1 mM MOPS, no pH adjustment), 25±2 °C, 24 h contact time, 0.42 g/L adsorbent in 30 mL ultrapure water (spiked with 20–40 µM phosphonate), magnetic stirrer/water bath, 0.01 M ionic strength ($NaNO_3$), P determination from membrane-filtered sample (0.2 µm)). They observed that the presence of phosphate slightly negatively affects the adsorption of phosphonates. The adsorption of phosphate, on the other hand, is significantly disturbed by the presence of phosphonates. Phosphate adsorption was more disturbed with increasing number of phosphonate groups. Phosphate and phosphonates thus compete for the same adsorption sites on goethite.

Boels *et al.* (2010) studied the adsorption of NTMP on iron- and manganese-coated sand, which is a waste product of a large drinking water treatment plant in the Netherlands. The influence of pH, ionic strength, and the presence of competing ions were investigated. They observed that adsorption of NTMP was not suppressed by increasing ionic strength, but even slightly improved (pH 7 (no buffer, no pH adjustment), 25±0.1 °C, 120 h contact time, 0.1 g adsorbent in 75 mL ultrapure water (spiked with 5–300 mg/L NTMP), shaking bath, < 0.01–0.1 M ionic strength (NaCl), P determination from filtered sample). Carbonate (0.61 g/L HCO_3^-) and sulfate (0.288 g/L SO_4^{2-}) were used as competing ions in their experiments. The carbonate and sulfate ions showed only a very slight negative influence on adsorption. This indicates a high selectivity of the coated sand with respect to NTMP. Further experiments showed that the adsorption of NTMP at pH 8 was significantly lower than at pH 7, which was probably due to a lower surface charge of the sand, which had a pH_{PZC} of 8.2. By calculating the free Gibbs energy, they showed that physosorption was presumably the dominating process.

In further studies, Boels *et al.* (2012) showed that NTMP can also adsorb to granular ferric hydroxide (pH 7.85±0.02 (buffer: hydrogen carbonate, pH adjustment), 23.8–24.9 °C, 24 h contact time, 2.6–6.2 g adsorbent in 100 mL synthetic membrane concentrate (10.2–25.4 mg/L NTMP), stirrer/water bath, 0.03 M ionic strength, P determination from membrane-filtered sample (0.45 µm)). The adsorption process was slow, showing the process is controlled by intraparticle diffusion. Again, sulfate ions were found to have no effect on the adsorption of NTMP. Calcium ions, however, have a clearly positive effect on NTMP adsorption on GFH. A Ca^{II}:NTMP molar ratio of 2:1

already doubled the adsorption capacity with respect to NTMP and a Ca^{II}:NTMP molar ratio of 60:1 increased the adsorption capacity even further. This can probably be attributed to the formation of ternary complexes. Desorption experiments in 1 L 0.1 M NaOH followed by washing with 1 L deionized water showed that the GFH is reusable.

Chen *et al.* (2017) performed batch experiments with NTMP-containing sythetic membrane concentrate (pH 8.3 (no buffer, no pH adjustment), 20 °C, 147 h contact time, 10–4,000 mg GFH, synthetic membrane concentrate (2.0–30 mg/L NTMP), orbital shaker, 86.25 mM ionic strength, P determination from membrane-filtered sample (0.45 µm)). Adsorption occurred slowly over a period of 6 days. They showed that NTMP adsorbed strongly on GFH even in the presence of high concentrations of other anions, suggesting inner-sphere complexation. The presence of Ca^{II} increased NTMP adsorption significantly. They found strong phosphonate adsorption even at a relatively high pH of 8.3 and high activation barriers for desorption. Regeneration of GFH by 0.1 M NaOH solution was therefore slow. Around 40–50% of the adsorbed phosphonate was released within 10–24 h, with the remaining percentage being released about an order of magnitude slower. They concluded that conventional regeneration methods are impractical for this application.

In addition to the batch experiments described above, Boels (2012) and Chen *et al.* (2017) also performed fixed-bed column experiments for phosphonate adsorption on GFH. Boels (2012) observed an asymptotic breakthrough curve (BTC), indicating that the adsorption process is controlled by intraparticle diffusion (pH 7.9 (no buffer, no pH adjustment), 294±1 K, synthetic membrane concentrate (10–15 mg/L NTMP), column with 8 mm inner diameter filled with 2.5–4.0 g GFH, up-flow mode, 19–32 s EBCT, 0.03–0.04 M ionic strength, P determination from unfiltered sample). Therefore, breakthrough already occured despite parts of the column not being fully loaded. He found that smaller grain sizes can counteract this and that sulfate, nitrate, magnesium, and potassium ions as well as an increasing ionic strength only have a negligible effect on adsorption. The BTC could be successfully described with a surface diffusion model. For regeneration, 0.1 M NaOH was recirculated for 2.5 h after the 8 h adsorption phase. The regeneration efficiency was significantly dependent on the NaOH volume used. For instance, at 62 BV NaOH about 50% of the NTMP was regenerated, but at 292 BV already about 70%. The BTC of a second cycle after regeneration was similar to that of the first cycle.

Chen *et al.* (2017) also performed column experiments with a synthetic membrane concentrate and GFH and observed slow adsorption kinetics (pH 8.3 (no buffer, no pH adjustment), 20 °C, synthetic membrane concentrate (2.0 mg/L NTMP), column with 0.8 mm inner diameter filled with 2 g GFH, up-flow mode, 2.0 min EBCT, 86.25 mM ionic strength, P determination from unfiltered sample). By varying the NaOH concentration and its flow rate (0.1 and 1.0 M NaOH, 0.05 mL/min and 0.25 mL/min), they found that there was a fast and a slow desorbing NTMP fraction, with the desorption rate of the slow desorbing fraction being limited by equilibrium effects. Thus, the desorption efficiency could be improved by faster flow rate and higher NaOH concentration. However, after a total of almost 12,000 min of regeneration, only 78% of NTMP could be desorbed. Due to incomplete regeneration, 28% less NTMP was adsorbed in the first 6,000 BV of the second cycle compared to the first cycle. Overall, only 2.75 mg P/g was taken up by the GFH compared to 4.38 mg P/g in the first cycle. Experiments with another phosphonate-containing antiscalant (Permatreat 191) over three adsorption/desorption cycles showed similar behavior.

Different phosphonate complexes that can be formed by adsorption on iron (hydr)oxides have been described by Stone *et al.* (2002) and Martínez and Farrell (2017). Stone *et al.* (2002) suggested the formation of monodentate, mononuclear bidentate, mononuclear tridentate, and binuclear bidentate inner-sphere surface complexes. On the one hand, the presence of metal ions can have a negative effect on the adsorption of phosphonates, since the complexation of the metal ions offers phosphonates an alternative reaction to adsorption. On the other hand, at higher pH values ($pH > pH_{PZC}$), metal ions can adsorb to the adsorbent themselves and counteract the repulsion of negatively charged adsorbent surface and negatively charged phosphonate ions due to their positive charge. Multidentate ligands can either form a bridge between metal ions of the adsorbent (e.g. iron in GFH) and dissolved metal ions (e.g. calcium), so-called ligand-like ternary complexes, or the metal ions can form a bridge between surface OH groups and the phosphonate, so-called metal ion-like ternary complexes (Stone *et al.* 2002). These ternary complexes are formed especially in the presence of Ca^{II} (Nowack and Stone 1999b; Boels *et al.* 2012; Chen *et al.* 2017; Martínez and Farrell 2017).

Martínez and Farrell (2017) used a density funtional theory model to calculate possible adsorption mechanisms of NTMP on ferric hydroxide. Besides physisorption, they

found monodentate, mononuclear bidentate, and binuclear bidentate inner-sphere surface complexes. According to their calculations, the formation of monodentate and bidentate complexes of NTMP complexed with Ca^{II} is more energetically favorable than that of uncomplexed NTMP. In addition, their model revealed that complexation with Ca^{II} can also result in a tridentate ternary surface complex in which Ca^{II} bridges between three $\equiv FeO^-$ and three $–P–O^-$ groups. Among all the complexes described, the formation of this ternary complex requires the lowest activation energy.

1.3.4 Influencing Factors on Phosphate and Phosphonate Adsorption on Iron (Hydr)Oxides

Since orthophosphate and phosphonates compete for the same adsorption sites (Nowack and Stone 2006), the following statements apply to both substances. The adsorption capacity increases with increasing temperature (Li *et al.* 2016; Liu *et al.* 2018; Rott *et al.* 2018a; Li *et al.* 2021). The same usually applies to adsorption kinetics, which is particularly relevant for column experiments with short contact times (Kumar *et al.* 2019). The pH value has a strong influence on the adsorption behavior, as it not only determines the surface charge of the adsorbent, but also influences the species distribution of the adsorptive (Li *et al.* 2016). With increasing pH, the adsorption capacity decreases (Nowack and Stone 1999a, 1999b; Boels *et al.* 2010; Li *et al.* 2016; Kumar *et al.* 2019). Increasing ionic strength has either no or a positive influence on adsorption (Nowack and Stone 1999a; Stone *et al.* 2002; Antelo *et al.* 2005; Boels *et al.* 2010; Boels 2012; Wang *et al.* 2015; Cui *et al.* 2016). This indicates the formation of inner-sphere complexes, while a decrease would hint at outer-sphere complexes (Lützenkirchen 1997; Nowack and Stone 1999a; Cui *et al.* 2016).

Municipal wastewater as well as industrial wastewater such as membrane concentrates also contain other ions that can affect adsorption. This influence of other ions on the adsorption of phosphate and phosphonates on iron (hydr)oxides was also studied previously. It is known that multivalent anions adsorb more easily than monovalent anions (Li *et al.* 2016; Liu *et al.* 2018). The monovalent anions choride and nitrate therefore have only a minor impact on the adsorption of phosphate (Gao and Mucci 2003; Chitrakar *et al.* 2006; Li *et al.* 2016; Kumar *et al.* 2019). They adsorb mostly by physisorption (Parfitt 1979; Chitrakar *et al.* 2006), but ligand exchange is also possible

(Parfitt and Russell 1977). Altaf *et al.* (2021a) observed little suppresion of NTMP adsorption in the presence of nitrate. The bivalent anion sulfate can adsorb by physisorption as well as by inner-sphere complexes (Charlet *et al.* 1993; Geelhoed *et al.* 1997; Rietra *et al.* 1999; Wijnja and Schulthess 2000). However, the presence of sulfate usually has no or very little influence on the adsorption of phosphate (Geelhoed *et al.* 1997; Gao and Mucci 2003; Chitrakar *et al.* 2006). The presence of phosphate, on the other hand, suppresses the adsorption of sulfate (Geelhoed *et al.* 1997). Similarly, Boels *et al.* (2010) and Altaf *et al.* (2021a) found only little influence of present sulfate ions on NTMP adsorption. The greatest influence on phosphate adsorption is caused by (hydrogen-)carbonate, which can also adsorb via physisorption and inner-sphere complexes (Su and Suarez 1997; Villalobos and Leckie 2001; Chitrakar *et al.* 2006; Zelmanov and Semiat 2015; Li *et al.* 2016; Mendez and Hiemstra 2019). Chitrakar *et al.* (2006) therefore suggested a selecitivity order of Cl^-, NO_3^-, SO_4^{2-} << CO_3^{2-}, HPO_4^{2-} for adsorption on goethite. Boels *et al.* (2010) found an influence of (hydrogen-)carbonate ions on NTMP adsorption at low phosphonate concentrations. Altaf *et al.* (2021a) found the biggest influence of (hydrogen-)carbonate ions on NTMP adsorption. Natural organic matter (NOM) can also compete for adsorsption sites (Geelhoed *et al.* 1998; Borggaard *et al.* 2005; Antelo *et al.* 2007; Weng *et al.* 2012; Fu *et al.* 2013). Like phosphate and phosphonates, NOM can also be desorbed with NaOH (Genz *et al.* 2008; Schöpke 2013).

Even without directly competing for adsorption sites, ions can influence adsorption. The presence of calcium is thereby of particular interest. Calcium can enhance phosphate adsorption either indirectly, by increasing the electropositivity of the surface, or directly, by forming ternary complexes (Rietra *et al.* 2001; Gao and Mucci 2003; Sperlich 2010; Weng *et al.* 2012; Antelo *et al.* 2015; Talebi Atouei *et al.* 2016; Han *et al.* 2017). Similar but much less pronounced behavior is also known from Magnesium (Trivedi *et al.* 2001). Various studies show the same mechanisms for the adsorption of phosphonates (Nowack and Stone 1999b; Boels *et al.* 2012; Chen *et al.* 2017; Altaf *et al.* 2021a). Which of these mechanisms is actually responsible for the positive influence of calcium ions is, however, controversial.

In addition, the presence of other ions can lead to the formation of precipitates, such as calcium carbonate, calcium phosphates, Ca-HEDP, Ca-NTMP, Ca-DTPMP, Fe^{II}-NTMP, or Fe^{III}-NTMP (Oddo and Tomson 1990; Zholnin *et al.* 1990; Kan *et al.* 1994;

Browning and Fogler 1995, 1996; Pairat *et al.* 1997; Friedfeld *et al.* 1998; Kan *et al.* 2005; Kunaschk *et al.* 2015; Kumar *et al.* 2018). These precipitates can reduce the phosphorus content of the solution either by direct precipitation of phosphorus-containing compounds or by adsorption of phosphorus-containing compounds onto the precipitates (Bartels *et al.* 1979; Chirby *et al.* 1988; Kan *et al.* 2005; Karaca *et al.* 2006; Xu *et al.* 2014).

1.3.5 Research Gaps

Previous studies have shown that granular ferric (hydr)oxide is a promising adsorbent for the adsorption of orthophosphate and phosphonates. While the adsorption of orthophosphate on GFH has been widely studied, there are still gaps regarding the adsorption of various phosphonates. The scientific articles on the adsorption of phosphonates on GFH published so far mostly lack investigations on material stability, regenerability and application to real wastewater in fixed-bed columns. In addition, the studies often investigated relatively high phosphonate concentrations (up to 300 mg/L NTMP), which is significantly higher than the concentrations of real wastewaters such as membrane concentrate.

The ions present in the (waste)water matrix can have a great influence on the adsorption of phosphorus compounds. However, many studies only investigated the influence of individual ions. In real wastewater, though, various ions coexist in parallel and can interact with each other and, therefore, experimental conditions should be representative of realistic solutions. With respect to adsorption of phosphonates, the influence of other single ions was only investigated for the phosphonate NTMP. Also, there are only two publications that have performed fixed-bed column experiments with NTMP and both of them used synthetic wastewater only (Boels 2012; Chen *et al.* 2017). These studies considered a maximum of three adsorption/desorption cycles, so that a prediction on the long-term applicability of GFH is uncertain.

Thus, there are no studies on adsorption of phosphonates other than NTMP (and an unknown mixture of phosphonate compounds) on GFH so far. Furthermore, there are no studies on the adsorption of phosphonates on GFH with real wastewater. Only a few researchers have conducted experiments with real wastewater and phosphonates other than NTMP with other adsorbents (Nowack 2002a; Boels *et al.* 2010; Rott *et al.*

2018a; Drenkova-Tuhtan *et al.* 2021). An intensive literature review has not found any studies on the adsorption of HPAA, not even with other adsorbents.

1.3.6 Previous Experiments

This thesis originated from the research project ‘Investigations on the removal of phosphonates and orthophosphate from wastewater using metal-containing filter materials’ (German title: Untersuchungen zur Elimination von Phosphonaten und ortho-Phosphat aus Abwasser mithilfe metallhaltiger Filtermaterialien), which was kindly funded by Willy-Hager-Stiftung, Stuttgart, Germany (Rott *et al.* 2019).

In this project, further experiments were conducted, which can be seen as the basis of this thesis. For example, 16 different adsorbents were compared (name with source of supply in brackets): FerroSorp Plus and FerroSorp RW (Hego BioTec), K24 Phosphatbinder (Teichpoint), Double P+S (BwF Brauchwasserfilter), Fe-Granulate MP (Metallpulver24), Fe-Granulate Pontax, magnetite, and hematite (Pontax GmbH), Filter sand (Haida), ION Quartz #1, ION Quartz #4, and ION Zeolite (BwF Brauchwasserfilter), IOCS-1 and IOCS-2 (iron coated filter sand), GAC Epibon 8x30 (DonauCarbon), nFe-GAC (GAC impregnated with nano iron particles). nFe-GAC was prepared following Zach-Maor *et al.* (2011b), and IOCS-1 and IOCS-2 were prepared based on Arias *et al.* (2006), Boujelben *et al.* (2008), Jianbo *et al.* (2009), and Dongmei *et al.* (2011). Fig. 1.8 depicts photos of the adsorbents as well as their grain sizes. Since the GFH materials showed the best adsorption capacities in these experiments, the focus of this thesis is on these adsorbents.

Fig. 1.8: Investigated adsorbents and their grain sizes.

Some portions of that project are part of Chapters 2, 3, and 4, complemented by further experiments outside the project. This thesis therefore utilizes results obtained in that project, such as the particle size distribution, bulk density, density, and pH_{PZC} of the adsorbents. In addition, preliminary experiments were carried out in the course of that project, which are not explained in detail in this thesis, such as on material stability, on the influence of the buffers used, on adsorption and desorption kinetics, and on the concentration of NaOH for efficient use as a regeneration solution. Furthermore, experiments were carried out in the project, the results of which are not part of this thesis. For example, experiments were also conducted with other wastewaters, including cooling tower runoff. The phosphonate HPAA is added to this cooling tower runoff as a stabilizer, which is why HPAA was also considered in this thesis.

1.4 Materials and Methods

1.4.1 Experimental Procedure

Despite lab-scale fixed-bed column experiments providing more transferable results regarding the adsorption performance of industrial-scale filter columns (Patel 2019), both batch and fixed-bed column experiments were conducted in this work (Fig. 1.9). In batch experiments, a lower maximum loading is expected than in column experiments, since adsorptive concentration decreases over the duration of the experiment, whereas in column experiments the adsorbent is always exposed to the same influent concentration (Akratanakul *et al.* 1983; Loganathan *et al.* 2014). With GFH, prediction of breakthrough curves from batch experiment results is difficult due to the strong influence of intraparticle diffusion (Sperlich *et al.* 2008). Nevertheless, batch experiments were carried out because they are easy to perform and thus several adsorbents can be compared quickly and influencing parameters as well as adsorption mechanisms can be investigated (Li *et al.* 2016).

Initially, batch experiments with spiked pure water were carried out to compare different GFH adsorbents, for a thermodynamic study, to investigate the influence of pH and phosphonate properties on adsorption of various phosphonates and for first investigations on a possible regeneration of the GFH (Chapter 2). In further batch experiments with spiked pure water, the influence of calcium on the adsorption of various phosphonates as well as the possible precipitation of calcium-phosphonate complexes were investigated. In further batch experiments with membrane concentrate and its synthetic

replicas, the influence of the presence of other ions was examined (Chapter 3). Fixed-bed column experiments were then performed to test the applicability of the GFH over multiple cycles. For this purpose, a spiked pure water solution was first used to evaluate different methods of alkaline regeneration. This was followed by further experiments with real membrane concentrate on the influence of pH, the introduction of a novel acidic regeneration step, and on the effects of replacing the alkaline regeneration solution (Chapter 4).

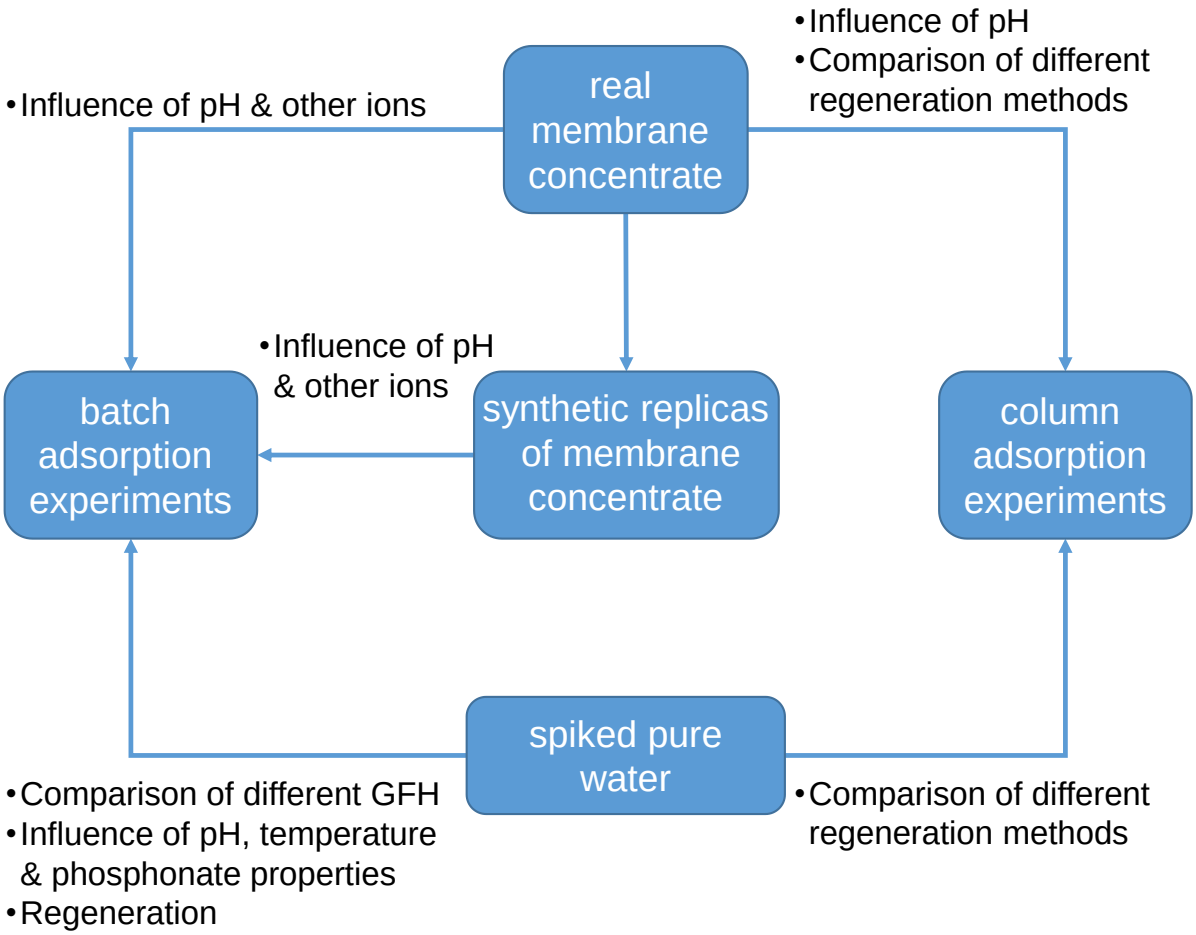

Fig. 1.9: Overview of experimental procedure and used solutions.

The phosphorus-containing solutions were prepared as follows: an appropriate amount of acetic acid (AcOH), 2-(N-morpholino)ethanesulfonic acid (MES), 3-(N-morpholino)propanesulfonic acid (MOPS), 4-(2-hydroxyethyl)-1-piperazinepropanesulfonic acid (EPPS), 3-(cyclohexylamino)-1-propanesulfonic acid (CAPS), 3-(cyclohexylamino)-2-hydroxy-1-propanesulfonic acid (CAPSO), or NaOH were weighed into a volumetric flask and mixed with deionized water to prepare a 0.01 M solution. These buffers were selected for their low ability to complex metal ions. An appropriate amount of

a phosphorus-containing stock solution (with either 1 g/L o-PO_4-P, HPAA-P, PBTC-P, HEDP-P, NTMP-P, EDTMP-P, or DTPMP-P) was then added to achieve the desired initial P concentration. The volumetric flask was then filled up to the ring mark using deionized water, stirred intensively, and the content of the volumetric flask was transferred into a glass bottle. In this bottle, the pH of the solution was now adjusted to 4.0 or 5.0 (for AcOH), 6.0 (for MES), 7.0 (for MOPS), 8.0 (for EPPS), 9.0 (for CAPSO), 10.0 or 12.0 (for CAPS) or 12.0 (for NaOH) by adding HCl or NaOH while stirring. The solutions were stored in the dark at 4 °C for a maximum of two weeks. Before the experiments, the required partial volume from these solutions was brought to room temperature (20 °C).

Prior to the batch experiments, the required amount of adsorbent was first weighed into a 50 mL centrifuge tube (Fig. 1.10). Then, the centrifuge tube was filled up to the 50 mL mark with the desired buffered, phosphorus-containing solution, quickly capped and clamped into the rotator running at 20 rpm (LLG-uniROTATOR 2). From this moment, the contact time began. After the contact time had elapsed, the centrifuge tube was quickly removed from the clamp, the cap was screwed off and a volume of approximately 20 mL of the supernatant was membrane-filtered into an empty glass bottle using a syringe filter (0.45 µm pore size, nylon). From the filtrate, a partial volume of usually 4 mL was transferred using an Eppendorf pipette into a dry 10 mL Duran preparation tube pre-rinsed with HCl and H_2O for P determination. In addition, the pH of each membrane filtrate was determined. Depending on the experimental objective, various parameters such as adsorbent quantity, temperature, pH value, Ca^{II} concentration, or used solutions could be varied.

In an additional batch experiment, the ability of FerroSorp RW to be loaded and unloaded multiple times was investigated. For this purpose, FerroSorp RW was loaded with a solution containing 1 mg/L NTMP-P and then regenerated in a solution of 1 M NaOH. This procedure was repeated five times, and between each repetition it was necessary to perform three rinsing steps with a buffered solution to wash the materials and remove NaOH residues that could unintentionally increase the pH of the solution of the next adsorption step. The material in the centrifuge tubes was weighed before and after the five cycles of adsorption/desorption after drying in order to find out how much material had been lost during the tests. The experiment was performed analogously to the batch adsorption experiments, with contact times of 60, 60, and 15 min

for adsorption, desorption, and rinsing steps, respectively. The turbidity was measured before filtration and the pH after filtration.

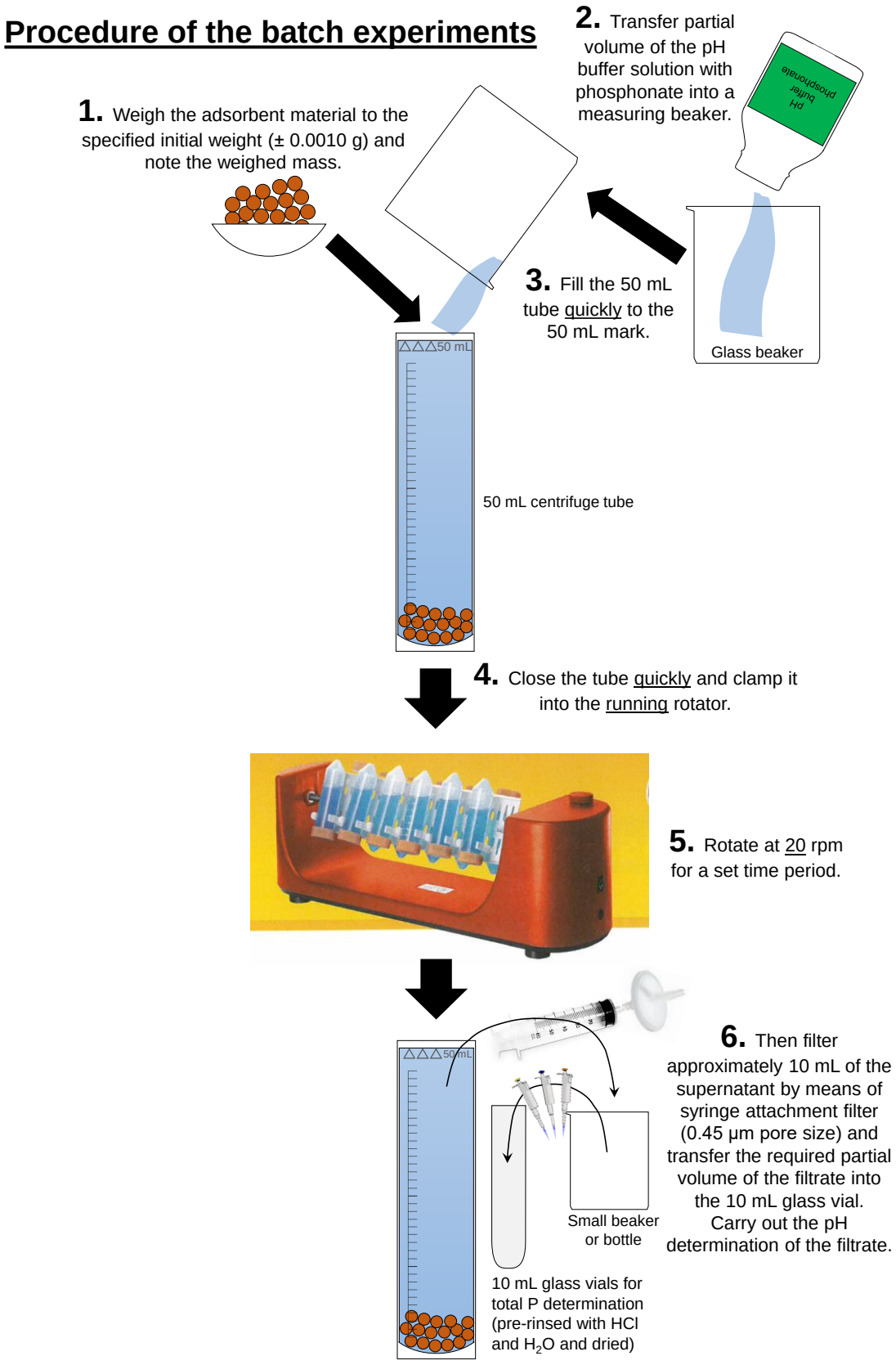

Fig. 1.10: Execution of the batch experiments.

For the experiments with fixed-bed columns, filter columns made of Plexiglas with an inner diameter of 1.6 cm were used. Glass wool and a stainless steel mesh were used both below and above the adsorbent to secure the adsorbent in the column. When the column was fed without adsorbent, but with glass wool and stainless steel mesh, no phosphorus removal could be observed. The design of the columns is shown in Fig. 1.11 and Fig. 1.12 illustrates the setup of an entire column experiment.

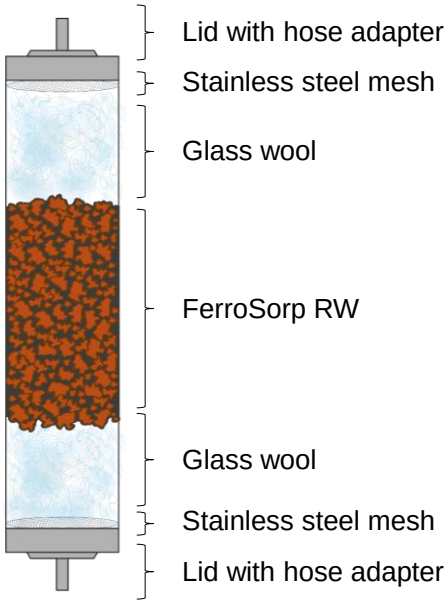

Fig. 1.11: Design of the filter column. Not drawn to scale.

The columns were fed by a peristaltic pump (types used: Ismatec IPC-8 and IPC-12) with the respective phosphonate-containing solution from a 10-liter glass bottle. The columns were operated in an up-flow mode to ensure a uniform flow and avoid channeling (Worch 2012). Regular sampling of the column effluent was carried out.

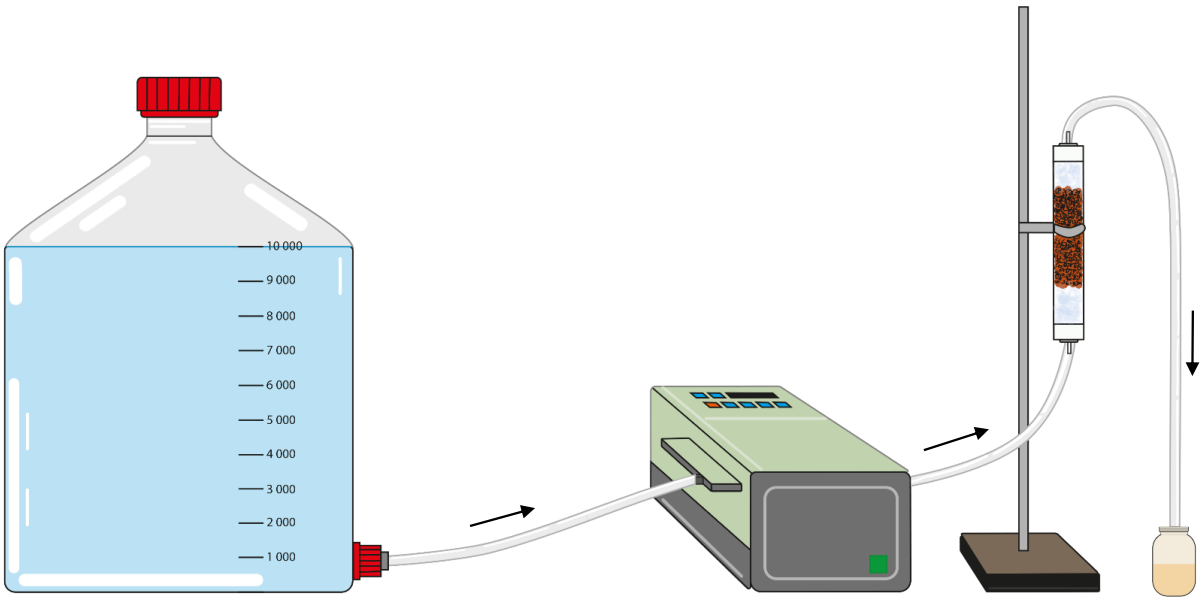

Fig. 1.12: Setup of the fixed-bed column adsorption experiments. Arrows indicate flow direction.

The columns were regenerated acidically (HCl) and alkaline (NaOH). Two different methods were used for both options. In the case of regeneration without recirculation (Fig. 1.13a), the regeneration solution was used once and then collected for analysis. In the case of regeneration with recirculation (Fig. 1.13b), the regeneration solution was fed through the column back into the storage bottle, which was placed on a magnetic stirrer. In the latter method, 10 mL of the NaOH was taken for analysis after each cycle using a volumetric pipette. These 10 mL were then replenished with fresh NaOH. Depending on the experimental objective, parameters such as pH, EBCT, flow rate, regeneration method, number of cycles, or cycle duration could be varied.

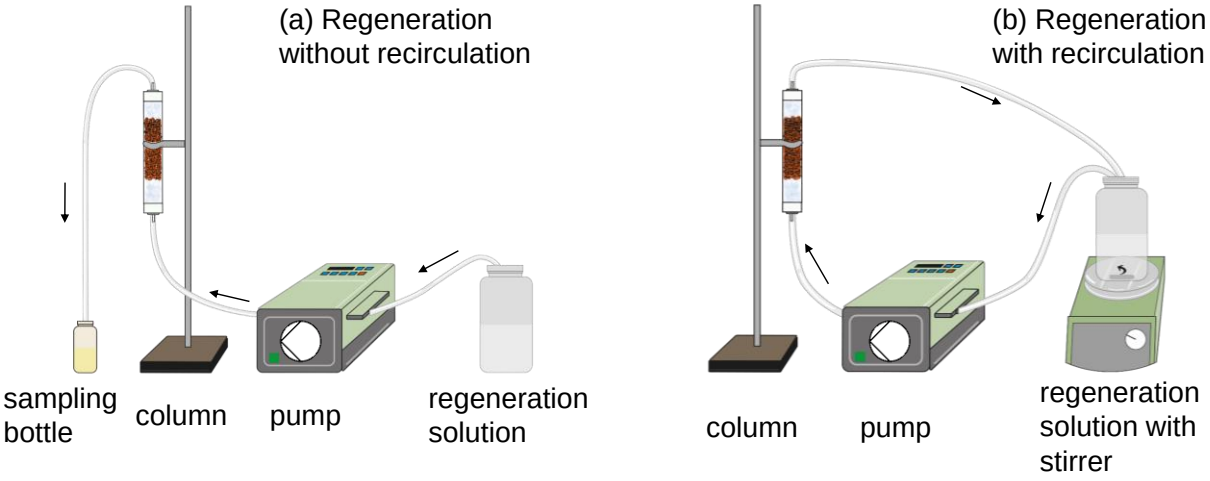

Fig. 1.13: Setup of the fixed-bed column regeneration experiments. Arrows indicate flow direction.

1.4.2 Materials

For a breakdown of reagents, chemicals, adsorbents, and solutions used, please refer to Sections 2.4, 3.4, and 4.4.

The specific surface areas of the adsorbents FerroSorp Plus and FerroSorp RW are manufacturer's specifications. The determination of the specific surface area of all other adsorbents was carried out by Porotec GmbH (Hofheim, Germany) according to DIN 66131. A dynamic measuring method with nitrogen measuring gas at 77 K and a Horiba SA9600 measuring device was used (adsorption up to a relative pressure of $p/p_0 = 0.3$).

The pH drift method was used for the determination of pH_{PZC}. For this, six solutions of each 0.01 M NaCl, 0.01 M KNO_3, and 0.01 M $NaNO_3$ were prepared. The individual solutions were adjusted to pH 2, 4, 6, 8, 10, and 12 using HCl and NaOH. Subsequently, 150 mg of each adsorbent was weighed into 50 mL glass bottles and 50 mL of the respective solutions were added, resulting in a total of 18 samples per adsorbent. Prior to this, the pH of each solution was again checked and notated. At a stirring velocity of approximately 250 rpm, all samples were stirred for 24–65 h on a magnetic stirrer. Thereafter, the samples were membrane-filtered (0.45 µm pore size, nylon filter) and the pH was measured from the filtrate. The delta from pH_{start} and pH_{end} was calculated and plotted versus pH_{start}. The pH at which the delta is close to zero corresponds to the pH_{PZC}.

1.4.3 Phosphorus Analysis

All samples from alkaline regeneration with 1 M NaOH were analyzed for total phosphorus in accordance with ISO 6878. ISO 6878 describes the total P determination by the molybdenum blue method with an acidic peroxydisulfate digestion at > 100 °C for 30 min. However, a longer digestion time is recommended for some phosphonates, so 60 min was used in this thesis based on preliminary experiments. The used procedure is illustrated in Fig. 1.14 and the compositions of the solutions required for phosphorus analysis can be found in Tab. 1.2. More details on the molybdenum blue reaction can be found in the review article by Nagul *et al.* (2015).

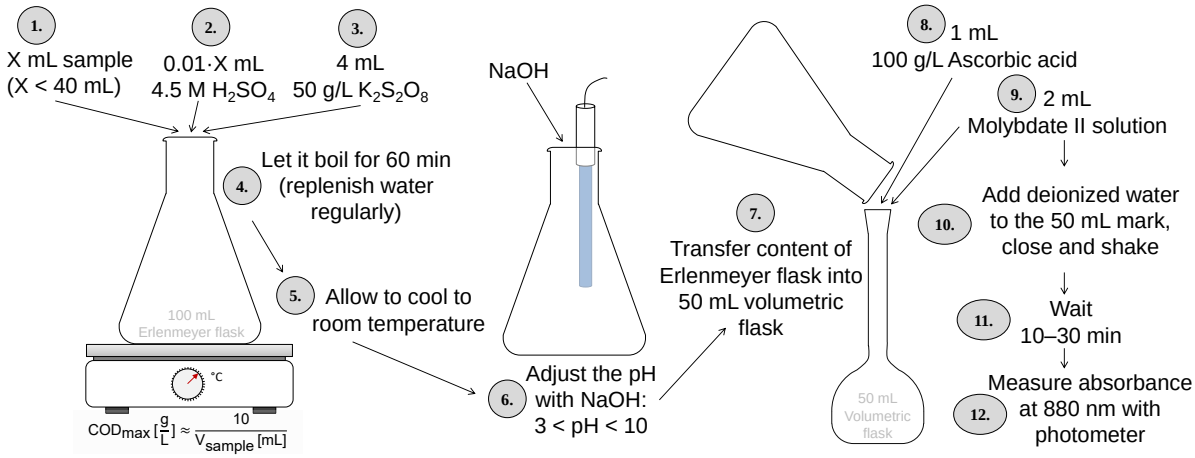

Fig. 1.14: Procedure for the total P determination according to ISO 6878.

Tab. 1.2: Solutions to be used for phosphorus determination according to ISO 6878.

Solution	Chemical formula	Concentration
Potassium peroxydisulfate	$K_2S_2O_8$	50 g/L
L(+)-ascorbic acid	$C_6H_8O_6$	100 g/L
Molybdate I solution:		
Potassium antimony(III) oxide tartrate	$K(SbO)C_4H_4O_6 \cdot ½H_2O$	0,7 g/L
Hexaammonium heptamolybdate	$(NH_4)_6Mo_7O_{24} \cdot 4H_2O$	26 g/L
Sulfuric acid	H_2SO_4	5,40 mol/L
Molybdate II solution:		
Potassium antimony(III) oxide tartrate	$K(SbO)C_4H_4O_6 \cdot ½H_2O$	0,7 g/L
Hexaammonium heptamolybdate	$(NH_4)_6Mo_7O_{24} \cdot 4H_2O$	26 g/L
Sulfuric acid	H_2SO_4	4,14 mol/L
Potassium dihydrogen phosphate standard	KH_2PO_4	1 mg/L P

The total P determination according to ISO 6878 is very time-consuming. To allow the largest possible number of samples to be analyzed in the shortest possible time, Rott *et al.* (2018b) developed a miniaturized form of the total P and o-PO_4 determination based on the ISO method. In that ISO_{mini} method, the total volume of the sample including reagents is 10 mL, whereas this is 50 mL in the ISO method. Accordingly, the amount of solutions to be used in the ISO_{mini} method is reduced to one fifth. In contrast to the ISO method, where the digestion takes place in the Erlenmeyer flask on a hotplate, the digestion in the ISO_{mini} method is conducted in a thermostat. The amount of NaOH to be dosed was determined from several measurements using the ISO method.

Rott *et al.* (2018b) found that at organic buffer concentrations of 0.01 mol/L, the phosphonates were not completely digested. This was due to the $K_2S_2O_8$ concentration according to ISO 6878 being too low. Eq. 1.16 illustrates that a 20-fold excess of the oxidant $K_2S_2O_8$ must be dosed to ensure, for example, total oxidation of the buffer 2-(*N*-morpholino)ethanesulfonic acid (MES).

$$C_6H_{13}NO_4S + 15\ H_2O + 20\ S_2O_8^{2-} \rightarrow 6\ CO_2 + NO_3^- + 41\ SO_4^{2-} + 43\ H^+ \qquad (1.16)$$

According to ISO 6878, however, only an approximately 3.3-fold excess of $K_2S_2O_8$ is dosed (e.g. 0.01 mol/L MES corresponds to 40 µmol MES in 4 mL analyte; in 0.8 mL of the supernatant of a 50 g/L $K_2S_2O_8$ solution, approximately 130 µmol $K_2S_2O_8$ are present). Accordingly, the ISO_{mini} method was modified by a higher $K_2S_2O_8$ dosing amount, depending on the buffer used (4.8 mL of 8.33–66.66 g/L $K_2S_2O_8$ or higher).

Fig. 1.15 summarizes the individual steps of the ISO_{mini} method and the needed $K_2S_2O_8$ dosages depending on different buffers, Fig. 1.16 illustrates the steps for orthophosphate determination with the ISO_{mini} method.

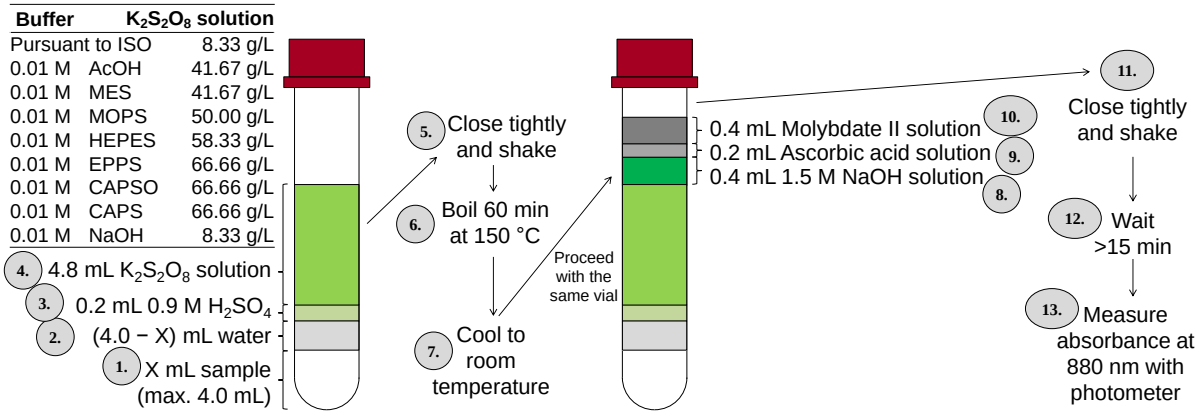

Fig. 1.15: Procedure for total P determination in miniaturized (ISO_{mini}) form based on ISO 6878 (Rott et al. 2018b).

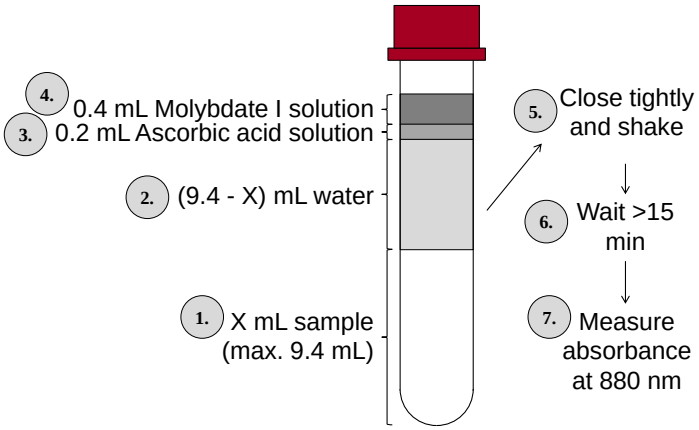

Fig. 1.16: Procedure for orthophosphate determination in miniaturized (ISO_{mini}) form based on ISO 6878.

The applicability of this method was confirmed using various organic buffers at 0.01 M mixed with 1 mg/L NTMP-P and 1 mg/L KH_2PO_4-P standard, at different $K_2S_2O_8$ (oxidizing agent) and NaOH doses and paralleled by P determinations according to ISO 6878 (Rott *et al.* 2018b). Both a blank (deionized water) and a standard (1 mg/L o-PO_4-P) were co-analyzed for internal quality control on each day that phosphorus measurements were made.

1.4.4 Other Analyses

Turbidity (unit: NTU) was measured using the WTW Turb 430 IR turbidimeter (nephelometric, 90 °C scattered light). Chemical oxygen demand (COD) (Hach LCK 1414), Ca^{2+}, Mg^{2+}, chloride (Hach LCK 311), sulfate (Hach LCK 153), and nitrate (Hach LCK 340) were determined using Hach rapid tests (thermostat: HachLange HT200S and Merck Spectroquant TR320, photometer: HachLange DR2800). The alkalinity was determined according to DIN 38409-H7-2 (titration of 100 mL sample with HCl to pH 4.3) (DIN 38409). All other analytical methods used are described in Sections 2.4, 3.4, and 4.4.

2 Batch Studies of Phosphonate Adsorption on Granular Ferric Hydroxides

This Chapter has been published as:

Reinhardt, T., Gómez Elordi, M., Minke, R., Schönberger, H. and Rott, E. 2020. Batch Studies of Phosphonate Adsorption on Granular Ferric Hydroxides. *Water Sci. Technol.*, **81**(1), 10–20. https://doi.org/10.2166/wst.2020.055.

2.1 Research Questions

- Is GFH suitable for adsorption of phosphonates?
- How do the parameters temperature, pH and the phosphonate structure (molecular size and weight, number of phosphonate groups) influence adsorption?
- Is regeneration possible and can GFH be reused in multiple adsorption-desorption cycles?

2.2 Abstract

Phosphonates are widely used in various industries. It is desirable to remove them before discharging phosphonate-containing wastewater. This study describes a large number of batch experiments with adsorbents that are likely suitable for the removal of phosphonates. For this, adsorption isotherms for four different granular ferric hydroxide (GFH) adsorbents were determined at different pH values in order to identify the best performing material. Additionally, the influence of temperature was studied for this GFH. A maximum loading for nitrilotrimethylphosphonic acid (NTMP) was found to be ~12 mg P/g with an initial concentration of 1 mg/L NTMP-P and a contact time of 7 days at room temperature. Then, the adsorption of six different phosphonates was investigated as a function of pH. It was shown that GFH could be used to remove all investigated phosphonates from water and, with an increasing pH, the adsorption capacity decreased for all six phosphonates. Finally, five adsorption-desorption cycles were carried out to check the suitability of the material for multiple reuse. Even after five cycles, the adsorption process still performed well.

2.3 Introduction

The worldwide limits for the discharge of phosphorus into water bodies are becoming increasingly stringent. With regard to phosphorus emission, in addition to orthophosphate, other quantitatively relevant P-containing compounds such as phosphonates should be considered (Fig. 2.1). Phosphonates are complexing agents that are used in domestic detergents, but also in various industries, such as in the textile industry as bleach stabilizers, in drinking water purification as antiscalants, and in industrial detergents (Nowack and Stone 1999a; Boels *et al.* 2012). In only 14 years (1998–2012), the global phosphonate consumption grew by more than 67% from 56,000 t/yr to 94,000 t/yr (Davenport *et al.* 2000; EPA 2013).

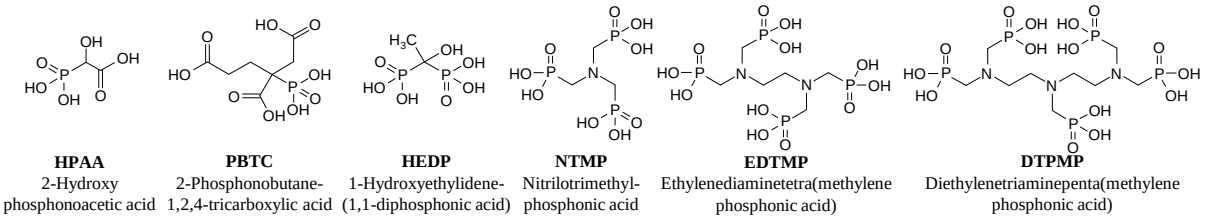

Fig. 2.1: Chemical structures of considered phosphonates.

Phosphonates are suspected of contributing to the eutrophication of water bodies, as UV radiation can promote their degradation to readily available orthophosphate (Matthijs *et al.* 1989; Lesueur *et al.* 2005; Kuhn *et al.* 2018; Rott *et al.* 2018c). Only recent developments in phosphonate analytics have shown that phosphonates accumulate significantly in sediments and suspended solids and, therefore, could lead to long-term environmental impacts (Armbruster *et al.* 2020).

With regard to the removal of phosphonates from wastewater, the use of UV lamps is often limited due to high energy costs and an inability to treat the incoming large volumes of wastewater. During the Fenton and flocculation process, large quantities of sludge are produced, which then must be separated and disposed of expensively. In addition, a very high flocculant concentration is often required to form a sufficient amount of flocs, as phosphonates are very strong complexing agents (Rott *et al.* 2017a; Rott *et al.* 2017b).

A possible alternative for the removal of phosphonates is to use iron-containing filter materials as it utilizes their high adsorption affinity towards metal-containing surfaces. Possible adsorbents range from iron-coated sand (Boels *et al.* 2010) and commercially available granular ferric hydroxides (GFH) (Boels *et al.* 2012; Chen *et al.* 2017) to engineered composite particles (Rott *et al.* 2018a) and minerals such as goethite (Nowack and Stone 1999a). These adsorbents must have both a high adsorption capacity and an effective regenerability for them to be applicable in large-scale wastewater treatment applications.

So far, however, hardly any studies have been published on these properties with regard to iron-containing adsorbents and phosphonates. Furthermore, only one phosphonate is investigated in these studies, although various phosphonates with different properties are used in industrial processes. For instance, an intensive literature re-

search has not revealed any previous investigations on the removal of HPAA. Therefore, in order to close the knowledge gaps mentioned above, this study describes a large number of batch experiments with four different GFH adsorbents likely suitable for the removal of phosphonates.

2.4 Materials and Methods

2.4.1 Reagents and Chemicals

All solutions were prepared with deionized water produced from drinking water using an ion exchanger (Seradest SD 2000) and a filter unit (Seralpur PRO 90 CN). Acetic acid (AcOH) (100%, Ph. Eur.) and hydrochloric acid (32%, AnalaR NORMAPUR) were obtained from VWR Chemicals (Fontenay-sous-Bois, France) and NaOH (≥ 99%, Ph. Eur.) from Merck (Darmstadt, Germany). 2-(*N*-morpholino)ethanesulfonic acid (MES) (≥ 99%), 3-(*N*-morpholino)propanesulfonic acid (MOPS) (≥ 99.5%), 4-(2-hydroxyethyl)-1-piperazinepropanesulfonic acid (EPPS) (≥ 99.5%), 3-(cyclohexylamino)-2-hydroxy-1-propanesulfonic acid (CAPSO) (≥ 99.5%), 3-(cyclohexylamino)-1-propanesulfonic acid (CAPS) (≥ 98%), HEDP·H_2O (≥ 95%), and NTMP (≥ 97%) originated from SigmaAldrich (St. Louis, MO, USA). PBTC, as a technical solution (50%, CUBLEN P 50), as well as EDTMP (5.3% water of crystallization) and DTPMP (16% water of crystallization), both as solids, were obtained from Zschimmer & Schwarz Mohsdorf (Burgstädt, Germany). HPAA, as a technical solution (50%), was purchased from Connect Chemicals (Ratingen, Germany).

2.4.2 Adsorbents

A total of four different GFH adsorbents were investigated, with their properties shown in Tab. 2.1 and macro photographs depicted in Fig. 2.2. Each adsorbent was rinsed once with distilled water over a sieve until the water was clear and then air-dried under a fume hood.

Tab. 2.1: Granular ferric hydroxides investigated in this study.

#	Adsorbent material	Supplier	Grain size after rinsing [mm]	Point of zero charge [pH_{PZC}]	Specific surface [m^2/g]
GFH1	FerroSorp RW	HeGo Biotec	0.5–2.5	8.6	210
GFH2	FerroSorp Plus	HeGo Biotec	0.5–2.5	8.7	230
GFH3	Double P+S	BwF Brauch-wasserfilter	1.25–2.5	8.5	242
GFH4	K24 Phosphat-binder	Teichpoint	2.24–8.0	8.3	279

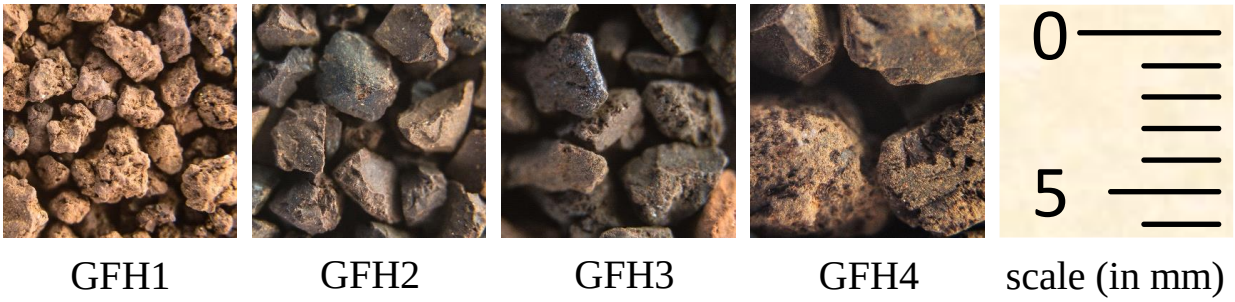

Fig. 2.2: Macro photographs of the different GFH adsorbents.

2.4.3 Experimental Procedure

Buffered solutions containing 1 mg/L P for the six phosphonates in Fig. 2.1 were prepared as follows (pH target value (pH_{start}) with buffer concentration in brackets): pH 4 (0.01 M AcOH), pH 5 (0.01 M AcOH), pH 6 (0.01 M MES), pH 7 (0.01 M MOPS), pH 8 (0.01 M EPPS), pH 9 (0.01 M CAPSO), pH 10 (0.01 M CAPS), and pH 12 (0.01 M CAPS). The pH was set using HCl or NaOH. The required amount of adsorbent was weighed into a 50 mL centrifuge tube, which was then filled with the buffered P-containing solution to the 50 mL mark, immediately closed, and clamped in the overhead rotator running at 20 rpm (LLG-uniROTATOR 2). After the predefined contact time, the centrifuge tube was promptly removed and a volume of approximately 20 mL of the supernatant was filtered into an empty glass bottle using a syringe with an attachable nylon filter (0.45 µm pore width). From the filtrate, total P and the pH (pH_{end}) were determined. The experiments were performed in a single approach, except for Experiment 4 (duplicate approach, i.e. 2 parallel runs), for which the results are presented as mean values with their standard deviations.

In Experiment 1, the NTMP adsorption behavior of four different GFH adsorbents was determined according to the procedure described above for a contact time (t_c) of 1 h and various pH values in order to identify the best performing material (T = 20 °C; pH 4, 6, 8, 10, and 12; t_c = 60 min; initial concentration = 1 mg/L NTMP-P; four different GFH adsorbents). It is noteworthy that this contact time was not sufficient to reach equilibrium. However, since Experiment 1 merely served to compare the adsorption behavior of the four different adsorbents, it was not necessary to reach equilibrium. In Experiment 2, a thermodynamic study on NTMP adsorption on GFH1 was carried out. For this, longer contact times (up to 7 d) were used to allow more time to reach a possible equilibrium. The influence of temperature on NTMP adsorption was investigated in the temperature range of 5–35 °C (T = 5, 20, 35 °C; pH 6; t_c = 60 min – 7 d; initial concentration = 1 mg/L NTMP-P; GFH1). Experiment 2 was carried out in rooms with different temperatures (climatic room 1 with cooling (5° C), laboratory at room temperature (20° C), and climatic room 2 with heating (35° C)) to keep the temperature constant during the experiment. The experiments were not started until the solution had reached the respective room temperature. For Experiments 1 and 2, the initial NTMP concentration remained constant while the GFH dosages varied from 0.74 to 14 g/L in Experiment 1 and from 0.02 to 14 g/L in Experiment 2. In Experiment 3, the adsorption capacity of GFH1 against six phosphonates and the influence of the pH on the adsorption of these compounds were investigated (T = 20 °C; pH 4, 5, 6, 7, 8, 9, 10, and 12; t_c = 60 min; initial concentration = 1 mg/L HPAA-P, PBTC-P, HEDP-P, NTMP-P, EDTMP-P, and DTPMP-P; GFH1). Here, a constant factor of 0.23 g GFH1/µmol of P compound was applied. Experiment 4 investigated the regenerability of GFH1 in 5 cycles (T = 20 °C; pH 6; t_c = 60 min each for adsorption and desorption; t_c = 15 min each for 3 rinsing steps; initial concentration = 1 mg/L NTMP-P; regeneration solution = 1 M NaOH; GFH1). After performing each adsorption step as described above, the supernatant (later to be filtered and analyzed) was decanted. For the desorption steps, the centrifuge tube was then filled with 1 M NaOH solution up to the 50 mL mark, rotated for 60 min, and decanted again (the decanted supernatant was analyzed as well). To remove NaOH residues which could have unintentionally increased the pH of the solution in the next adsorption step, the same procedure was repeated three times in a row with 50 mL of a buffer solution (0.01 M MES; pH 6) before the next cycle began. For both NaOH and buffered solution, fresh solutions

were used in each cycle. The dry weight of GFH1 was determined before and after the five cycles to identify how much material had been lost in the experiment.

2.4.4 Analytical Methods

A modified method based on ISO 6878 (ISO_{mini}, molybdenum blue method), as described by Rott *et al.* (2018b), was used for phosphorus analysis. The applicability of this method was confirmed using various organic buffers at 0.01 M mixed with 1 mg/L NTMP-P and 1 mg/L KH_2PO_4-P standard, at different $K_2S_2O_8$ (oxidizing agent) and NaOH doses and paralleled by P determinations according to ISO 6878 (Rott *et al.* 2018b). All glass materials that came into contact with the sample were thoroughly rinsed with hydrochloric acid (10%) and deionized water prior to the analysis. The digestion was carried out in a HachLange HT200S thermostat. The absorbance was measured with the UV/VIS spectrophotometer Nanocolor UV/VIS II from Macherey-Nagel. For the analysis of the strongly alkaline regeneration solution, the original ISO 6878 method (molybdenum blue method) was used. The pH value was determined with the WTW pH electrode SenTix 81 in combination with the instrument WTW pH91. Scanning electron microscopy was applied using a Zeiss DSM-982 Gemini microscope with a thermal Schottky field emitter. For preparation, individual samples were applied to a sample carrier and fixed with conductive silver. To prevent electrical charging of the granules and gain a clear image, the samples were sputtered with gold using a Leica coater (EM ACE 600). Furthermore, energy-dispersive X-ray spectroscopy (EDS) was performed with an X-ray detector from ThermoScientific (DSM-982 UltraDRY SDD detector).

2.4.5 Model Equations

The Freundlich isotherms were modeled using Eq. 2.1. The parameters K_F and n were determined by non-linear regression using the least-squares method.

$$q = K_F c^{1/n} \tag{2.1}$$

Additionally, the model by Langmuir (Eq. 2.2) was applied to the experimental data. The parameters q_{max} and K_L were determined by non-linear regression using the least-squares method.

$$q = q_{max} \frac{K_L c}{1 + K_L c} \quad (2.2)$$

All model parameters can be found in Tab. S2.1. The Freundlich model led to the best r^2 values, and therefore, only Freundlich isotherms are shown in this study.

For the thermodynamic calculations, Eq. 2.3 and Eq. 2.4 were used. By determining thermodynamic parameters such as the change in enthalpy (ΔH^0), entropy (ΔS^0), and free Gibbs energy (ΔG^0), it was possible to assess whether the sorption process is endothermic or exothermic as well as the strength and spontaneous nature of adsorption (Yan, Liang-guo *et al.* 2015).

$$\Delta G^0 = -RT \ln K_d \quad (2.3)$$

$$\ln K_d = \frac{\Delta S^0}{R} - \frac{\Delta H^0}{RT} \quad (2.4)$$

In Eq. 2.3 and Eq. 2.4, R is the universal gas constant [8.314459 J/(mol K)], T is the temperature [K], and K_d is the dimensionless form of the Freundlich constant. To make the temperature dependent Freundlich constant K_F dimensionless, it was corrected by a factor of 1000 g/L (density of water), according to Milonjic (2007).

The enthalpy and entropy change was determined from the slope and intercept of the plot of ln K_d vs. $1/T$, also known as the Van`t Hoff plot. A positive value of ΔH^0 indicates endothermic adsorption, i.e. the adsorption process consumes energy. An exothermic adsorption is described by a negative value, which means that energy is released. Negative values of ΔG^0 describe an exergonic (spontaneous) adsorption, while positive values of ΔS^0 indicate that the randomness at the solid–solution interface increases during adsorption (Yan *et al.* 2010; Wasielewski *et al.* 2018).

The curves in Fig. 2.6, plotting the adsorption capacity as a function of *pH*, were modeled by the logistic function model (Eq. 2.5). The parameters *a*, *b*, and *d* were determined by non-linear regression using the least-squares method.

$$c_{ads}(pH) = 1 \frac{mg}{L} - \frac{d}{(1+ae^{-b \times pH})} \quad (2.5)$$

The coefficient of determination r^2 was calculated according to Rott *et al.* (2018a). For the species distribution in Fig. 2.6, the pK values from Rott *et al.* (2018a) were used. Additionally, pK values of 1.12, 3.48, 8.00, and 13.48 for HPAA were applied as calculated for 0 M ionic strength, according to ChemAxon Ltd. (2017).

To test the significance of the experimental and modeled data, a Student's t-test was performed. Calculated p-values can be found in Tab. S2.1 and Tab. S2.2.

2.5 Results and Discussion

2.5.1 Experiment 1 – Effect of Adsorbent Nature on NTMP Adsorption

Fig. 2.3 enables a comparison of the adsorption behavior of the four GFH adsorbents examined at a 1 h contact time and different pH values. Since the pH of the solution shifted in the direction of the pH_{PZC} of the GFH during adsorption, the indicated pH ranges describe the ranges between pH_{start} and pH_{end}. All materials generally achieved higher loadings at lower pH values. The adsorbents show a positive net surface charge at pH values below the pH_{PZC}, which increases with increasing deviation to the pH_{PZC}. NTMP is negatively charged over the entire pH range tested so that adsorptive and adsorbent experience a stronger electrostatic attraction at lower pH values (Nowack and Stone 1999a).

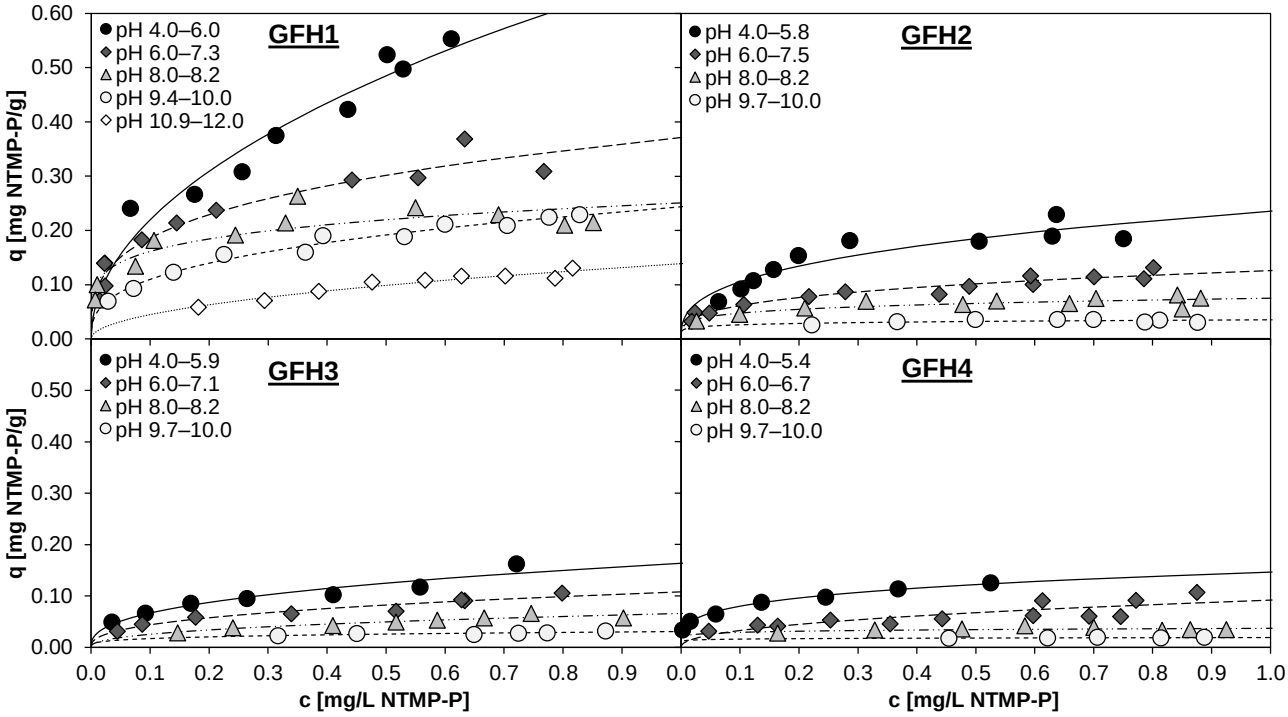

Fig. 2.3: Effect of adsorbent nature on NTMP adsorption with 1 mg/L NTMP-P depending on the pH (buffer: 0.01 M AcOH, 0.01 M MES, 0.01 M EPPS, 0.01 M CAPS) at room temperature (20 °C) (20 rpm, t_c = 1 h). Freundlich models are shown (model constants in Tab. S2.1).

GFH1 was the material with clearly the best performance. For instance, GFH1 achieved a loading of 0.55 mg NTMP-P/g at a pH of 4.0–6.0. In contrast, the second-best GFH (GFH2) had a maximum loading of only 0.23 mg NTMP-P/g. This loading was achieved by GFH1 even at the pH range of 9.4–10.0. Interestingly, GFH4 performed poorly in comparison despite the largest specific surface area (Tab. 2.1). Considering the pH_{PZC} of all investigated adsorbents was in a similar range, the choice of grain size plays a more important role in adsorption.

Two images depicting different sites of GFH1 at 20,000x magnification show that the material has a crystalline structure formed by crystals of different sizes, corroborating a high porosity (Fig. 2.4). The EDS detected mainly Fe, O, and Ca (H is not detected by the EDS technique). The Ca has its origin in the production process in which calcium-containing compounds are used. Ca has been found to have a positive effect on the adsorption of phosphonates (Nowack and Stone 1999b; Boels *et al.* 2012), which could explain why GFH1 had a notably higher loading when compared to the other

GFH adsorbents (≥ 12–19% $CaCO_3$ content in GFH1, for comparison in GFH2 only 5–10%).

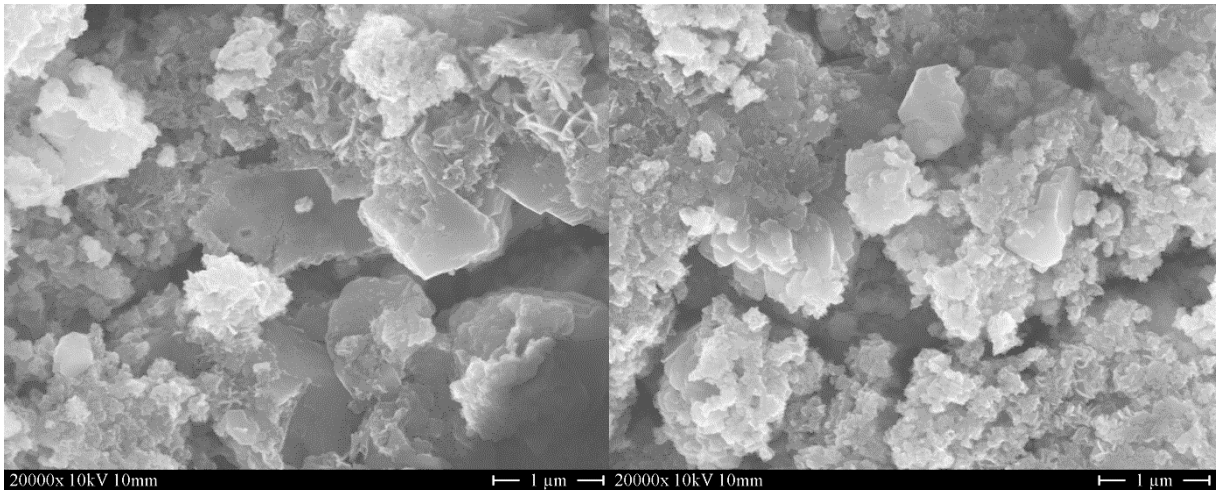

Fig. 2.4: Scanning electron microscope images of GFH1 at a magnification of 20,000x.

Previous experiments (Fig. S2.1) on the stability of the material with respect to the pH had shown that GFH1 was chemically unstable at pH < 6, suggesting poor long-term applicability. Thus, the treatment of phosphonate containing solutions with GFH1 is recommended to be performed at pH values close to 6, despite its remarkably higher short-term efficiency at pH < 6. Since GFH1 proved to be the most efficient of the 4 GFH adsorbents, it alone was tested in the following experiments (2–4).

2.5.2 Experiment 2 – Thermodynamics Study of NTMP Adsorption on GFH1

Additional isotherms with GFH1, the best performing phosphonate in Exp. 1, were prepared at pH 6.0–7.8 and contact times of 1, 3, and 7 d (Fig. 2.5 left). Except for the isotherm after 3 d (r^2 = 0.713), all could be well described with the Freundlich model (r^2 ≥ 0.847; Tab. S2.1).

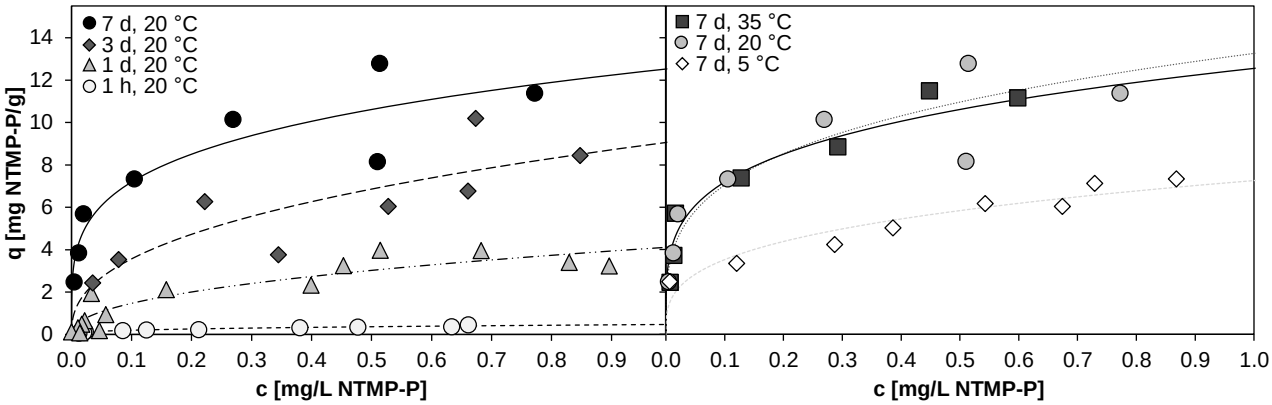

Fig. 2.5: Thermodynamics study of NTMP adsorption on GFH1 with 1 mg/L NTMP-P at an initial pH of 6 (buffer: 0.01 M MES) at different contact times (left) and different temperatures (right) (20 rpm). Freundlich models are shown (model constants in Tab. S2.1).

Since it is known from previous studies that the kinetics increase up to a certain limit with increasing mixing speed, it is likely that a higher agitation would allow faster achievement of equilibrium. Rout *et al.* (2014) showed that the percentage removal of phosphate by adsorption on red soil increased from 88.4% to about 96% when the rotational speed was increased from 100 rpm to 175 rpm. That said, it is not clear whether these experiments at low mixing speed were already in equilibrium after the contact time of 90 minutes. Lin *et al.* (2013) found that although agitation (varying from 0 to 200 rpm) had a considerable influence on the kinetics before equilibrium was reached, it had no noticeable influence on the adsorption of ammonium on zeolite at a 24 hour contact time. However, the influence of mixing speed was not investigated in this study, as the low speed of 20 rpm, chosen in analogy to the experiments of Laiti *et al.* (1995) at 30 rpm, was intended to avoid abrasion of the particles. The adsorbent should be kept as undamaged as possible in order to allow a better comparison with future column experiments, since it is known that the achievable adsorbent load for a given concentration depends on the particle radius of the adsorbent. Thus, isotherms determined with ground material may not accurately reflect the adsorption behavior of the original particles (Worch 2012). Therefore, even after 3 d, equilibrium was not reached. Isotherms not in equilibrium are empirical and any conclusions about a specific adsorption mechanism should be considered with care (Chen *et al.* 2017). However, it can be expected that isotherms gained at 7 d contact time were very close to equilibrium.

At an initial concentration of 1 mg/L NTMP-P, the maximum loading after 7 d was ~12 mg P/g. Experiments with an initial concentration of 5 mg/L NTMP-P and a pH of 6.0–8.0 resulted in a higher maximum loading of about 18 mg P/g (58 mg NTMP/g) due to the stronger gradient between NTMP and GFH1 (Fig. S2.2). In similar investigations, but with a significantly higher initial concentration of 9.3 mg/L NTMP-P and a slightly higher pH of 7.85, Boels *et al.* (2012) found a maximum loading on GFH of ~22 mg NTMP-P/g. On the other hand, at similar conditions (9 mg/L NTMP-P, pH 8.3), Chen *et al.* (2017) found a much lower equilibrium loading of ~9 mg NTMP-P/g after 24 hours (not in equilibrium). Unfortunately, in these studies, the experiments were conducted at pH values at which GFH does not perform optimally, which is why no direct comparison is possible to the results of the current study.

At a temperature of 5 °C, the maximum loading was only ~7 mg P/g (Fig. 2.5 right). Consequently, the adsorption performance was increased when thermal energy was applied. Wang *et al.* (2014) discovered the same behavior for the adsorption of phosphate on iron-coated activated carbon when investigating temperatures of 20, 30, and 40 °C. They explained that as the temperature in the water increases, the surface activity of the adsorbent increases as well. As a result, the interaction forces between adsorbent and adsorptive become stronger (Wang *et al.* 2014). That said, no difference in the maximum loading was found between the temperatures of 20 °C and 35 °C. Therefore, it was concluded that 12 mg P/g (39 mg NTMP/g) is the maximum possible loading of GFH1 at an initial concentration of 1 mg/L NTMP-P and 20 rpm.

The strikingly poorer performance of the adsorbent at low temperatures implies that low wastewater temperatures should be avoided in possible technical implementations for the adsorption of phosphonates on GFH. Therefore, the process is particularly suitable for industries that produce excess waste heat, which can be used to raise the temperature of the wastewater.

Tab. 2.2 shows the results of the thermodynamic calculations. The positive ΔH^0 value indicates an endothermic reaction due to pore size enlargement and/or activation of the adsorbent surface (Yan *et al.* 2010). In addition, the magnitude of ΔH^0 indicates the type of interactions that occur between adsorbent and adsorbate. Values for physisorption are usually below 20 kJ/mol, electrostatic interactions are indicated by a range of 20 to 80 kJ/mol, and chemisorption bond strengths can be from 80 to

450 kJ/mol (Bonilla-Petriciolet *et al.* 2017). Therefore, the adsorption of NTMP on GFH1 may be attributed to physisorption, i.e. the interactions between adsorbent and adsorbate can be dipole-dipole, hydrogen bonds, or van der Waals (Bonilla-Petriciolet *et al.* 2017). This is in line with the findings of Boels *et al.* (2010), who found a value of -10.5 kJ/mol for ΔG^0 and also derived physisorption for the adsorption of NTMP on a GFH. Using their density functional theory model, Martínez and Farrell (2017) found similar results. They concluded that the adsorption of NTMP to GFH is both physisorption, promoted by hydrogen bonding between O atoms in the NTMP and H atoms on the iron hydroxide, and chemisorption. They expect that the initially physically adsorbed NTMP is subsequently converted to chemically bound NTMP in a slower process. The negative values of ΔG^0 describe an exergonic adsorption, i.e. the adsorption occurs spontaneously. The positive value of ΔS^0 indicates that the randomness at the solid–solution interface increased during adsorption. Furthermore, it shows the affinity of NTMP towards GFH1 (Yan *et al.* 2010; Rout *et al.* 2015).

Tab. 2.2: Thermodynamic data of NTMP adsorption on GFH1.

T [K]	ΔG^0 [kJ/mol]	ΔH^0 [kJ/mol]	ΔS^0 [J/K/mol]
278	-20.6	14.5	126.7
293	-23.0		
308	-24.3		

2.5.3 Experiment 3 – Effect of Phosphonates Nature and pH on GFH1 Adsorption Capacity

For all 6 phosphonates, as for NTMP, a decreasing adsorption behavior could be seen with increasing pH (Fig. 2.6). In addition, a reduction of the adsorption affinity was associated with an increasing number of phosphonate groups (PG) and increasing molecular mass. PBTC deviated from this pattern slightly as, at pH < 9, PBTC-P adsorbed in a similar ratio to HEDP-P despite a higher molecular mass than HEDP. For example, at pH 8, for HPAA (1 PG, 156.03 g/mol), PBTC (1 PG, 270.13 g/mol), HEDP (2 PG, 206.03 g/mol), NTMP (3 PG, 299.05 g/mol), EDTMP (4 PG, 436.12 g/mol), and DTPMP (5 PG, 573.20 g/mol), adsorption concentrations of 0.91, 0.84, 0.81, 0.58, 0.41, and 0.36 mg P/L and loadings of 3.92, 3.62, 3.44, 2.50, 1.74, and 1.55 µmol phosphonate/g GFH were found (according to model functions, Tab. S2.2).

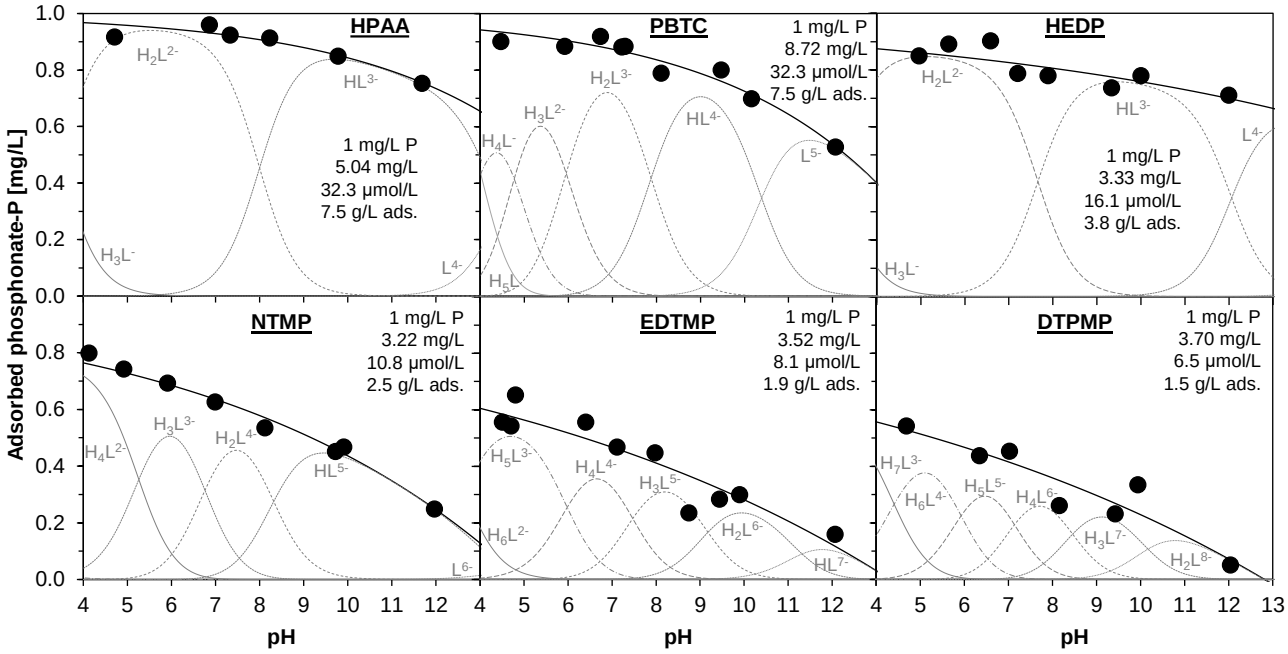

Fig. 2.6: Effect of phosphonates nature and pH on GFH1 adsorption capacity with a dosage of 0.23 g GFH1/µmol phosphonate at room temperature (20 °C) (20 rpm, tc = 1 h). Solutions with 1 mg/L P, buffered at a pH of 4 and 5 (0.01 M AcOH), pH 6 (0.01 M MES), pH 7 (0.01 M MOPS), pH 8 (0.01 M EPPS), pH 9 (0.01 M CAPSO), and pH 10 and 12 (0.01 M CAPS) (model constants in Tab. S2.2).

The three largest molecules investigated all had similar functional groups in varying numbers (NTMP: 1 amino group, 3 methylene phosphonate groups; EDTMP: 2 amino groups, 4 methylene phosphonate groups; DTPMP: 3 amino groups, 5 methylene phosphonate groups), i.e. the molecular size increased in the following order: NTMP < EDTMP < DTPMP. Thus, the observed decrease of phosphonate adsorption with increased molecular size could be expected since larger molecules usually occupy more adsorption sites (Nowack and Stone 1999a). Furthermore, the more phosphonate groups a polyphosphonate has, the higher its negative charge becomes. When these highly negatively charged species adsorb, the adsorption of further phosphonate molecules is disturbed by the transfer of the negative charge to the surface (Nowack and Stone 1999a).

A slight variation in the pattern for PBTC was not extraordinary since this compound contains three carboxyl groups (R-COOH), which are absent in the other phosphonates with the exception of HPAA (one carboxyl group). The deviation from the pattern, however, disappeared as soon as the fully deprotonated PBTC species became dom-

inant at pH > 9. Interestingly, there was still adsorption and no sudden drop of adsorption at pH values higher than the pH_{PZC} for all investigated phosphonates, meaning that adsorption also took place on the adsorbent with a negative net surface charge.

Similar findings regarding the influence of an increasing number of phosphonate groups were reported by Nowack and Stone (1999a, 2006) for phosphonate adsorption on goethite and by Rott *et al.* (2017b) and Klinger *et al.* (1998) for precipitation/flocculation experiments. It is also known that nitrogen-free phosphonates and aminophosphonates show a different behavior during ozonation experiments (Klinger *et al.* 1998; Xu *et al.* 2019). Therefore, if problems arise with the removal of phosphonates from phosphonate containing solutions, it may be sufficient to substitute the corresponding phosphonate in the industrial process with another phosphonate that is easier to remove.

It is important to point out, however, that no final conclusions can be drawn from these experiments on real wastewater, as additional competing ions are present in a wastewater matrix. Phosphonate contaminated industrial wastewaters can be classified into two groups. The first group mostly comprises clear concentrates with low organic loads, high water hardness, and high anion concentrations (e.g. membrane concentrates and cooling wastewater). The second group consists of wastewater with high organic load, such as wastewater from paper and textile industries (Rott *et al.* 2017b). Especially in concentrates, high concentrations of calcium and magnesium can often be found (Sperlich *et al.* 2010; Antony *et al.* 2011; Chen *et al.* 2017). It is known from previous studies that calcium has a positive influence on the adsorption of phosphonates (Nowack and Stone 1999b; Boels *et al.* 2012). Boels *et al.* (2010) showed that anions such as carbonate and sulfate can also influence the adsorption of NTMP. Therefore, further experimentation with real wastewater and on the influence of other ions, which could compete or support phosphonate adsorption, have to be conducted to enable the transferability of the results to future technical realizations for the adsorption of phosphonates on GFH.

2.5.4 Experiment 4 – Regenerability of GFH

Nowack and Stone (1999a) for goethite, as well as Boels *et al.* (2012) and Chen *et al.* (2017) for GFH adsorbents, have already investigated the desorption of NTMP, but only in one, two, and three cycles, respectively. Fig. 2.7 shows that GFH1 could be

loaded and unloaded several times without loss of adsorption capacity. After each adsorption cycle, the total P concentration was ≤ 0.1 mg/L, resulting in a removal efficiency of ≥ 90%.

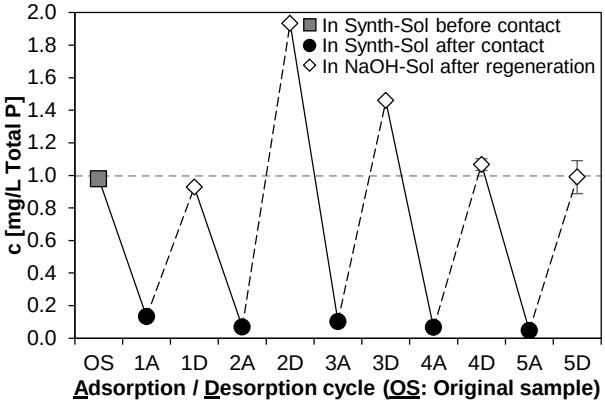

Fig. 2.7: Total P in synthetic solution (Synth-Sol) initially containing 1 mg/L NTMP-P before and after contact with 15 g/L GFH1 initially at pH 6 (0.01 M MES) as well as in 1 M NaOH solution (NaOH-Sol), and after regeneration of GFH1 for five adsorption (A) and desorption (D) cycles (20 °C, 20 rpm, tc = 1 h, 3 rinsing steps for 15 min each with 0.01 M MES solution (pH 6) after each regeneration).

Total P concentrations > 1 mg/L were found in the regeneration solutions, proving that GFH1 already contained phosphorus compounds which were desorbed during the desorption phases with 1 M NaOH solution together with the adsorbed NTMP. Interestingly, these concentrations > 1 mg/L were first found after the second desorption (2D). After this cycle, the P concentration in the regeneration solutions continuously decreased and approached 0.99 mg/L P after 5 cycles. This may be due to a gradual leaching effect of the phosphorus present in the material, as fresh regeneration solution was always used in each desorption step. The fact that after the fifth adsorption step still a very low residual concentration of 0.05 mg/L P was found in the solution (5A) and the total P concentration in the regeneration solution was 0.99 mg/L (5D) indicates that all phosphorus contamination of GFH1 may be washed out, at the latest, by the fifth cycle.

The increase of the pH using a 1 M NaOH solution led to NTMP desorption which can be explained by electrostatic effects (Chen *et al.* 2017). During desorption, hydroxide ions from the NaOH solution interact with the adsorption sites and substitute in place of the adsorbed NTMP, which results in a significantly higher negative net surface charge (Zach-Maor *et al.* 2011a). Additionally, the increase in pH results in an increase

in the negative charge of NTMP ions (Fig. 2.6), leading to electrostatic repulsion. Future experiments should investigate multiple reuse of the regeneration solution.

In addition, by weighing the dry mass of the GFH before and after the experiment, it was determined that 38% of the initial concentration of 15 g/L GFH1 was lost during the five cycles. This was caused by abrasion of GFH1 into finer particles which were then removed partially with the supernatant. Although such a relatively high material loss was recorded, the NTMP removal rates were still high in all cycles, underlining the excellent performance of this material in adsorbing NTMP. Assuming this loss of material occurred linearly, and each desorption step was efficient in desorbing all NTMP, there would still be enough adsorbent (~6 g/L) to remove > 90% P by the time the 9th cycle had been reached (according to the adsorption isotherm in Fig. 2.3). However, such assumptions and calculations are unreliable which is why batch experiments are only indicative experiments. For a higher accuracy, column tests that typically lead to less material loss should be carried out in the future.

2.6 Conclusions

This work showed that GFH could be used to remove all investigated phosphonates from water. For GFH1, the adsorption capacity decreased for all phosphonates with an increasing pH value, and for polyphosphonates, the adsorption capacity decreased with an increasing number of phosphonate groups. To achieve the best performance, the treatment of phosphonate containing solutions should be carried out at pH values close to 6. Additionally, a temperature of 20 °C is adequate for the effective adsorption of NTMP onto GFH1. The treatment of phosphonate containing solutions at low temperatures should be avoided, as the performance of phosphonate adsorption decreases with temperature. It was shown that phosphonates with different properties (molecular size and weight, number of phosphonate groups) behave differently during adsorption. Furthermore, five consecutive adsorption/desorption cycles were carried out showing high adsorption and desorption efficiency, indicating the possible reusability of GFH1 for phosphonate removal. Finally, it needs to be tested with real wastewater to investigate the competing or supporting influence of other ions and in column experiments.

2.7 Acknowledgment

We acknowledge gratefully the Willy-Hager-Stiftung, Stuttgart, for their financial support. We also thank HeGo Biotec GmbH for providing adsorbent samples and Zschimmer & Schwarz Mohsdorf GmbH & Co. KG for the supply of phosphonate samples.

2.8 Supplementary Material

2.8.1 Diagrams

2.8.1.1 Investigations Regarding Material Stability

Buffer solutions with pH values 4, 5, 6, 7, 8, 9, and 10 were prepared containing citric acid monohydrate (99.9%, VWR Chemicals, Fontenay-sous-Bois, France; pH 4 and 5), MOPS (pH 6), HEPES (pH 7 and 8), and disodium tetraborate hexahydrate (≥ 99.5%, p.a., Merck, Darmstadt, Germany; pH 9 and 10) at 0.1 mol/L. The pH was set using HCl or NaOH. The required amount of adsorbent (0.9023 g GFH1, 0.9410 g GFH2, 1.6595 g GFH3, 4.3507 g GFH4) was weighed into a 50 mL centrifuge tube which was then filled with the buffer solution to the 50 mL mark, immediately closed, and clamped in the rotator running at 30 rpm (LLG-uniROTATOR 2). Since the grain sizes of the adsorbents differed considerably from one to another and it was assumed that the outer surface plays the most important role in material stability, the applied masses of the GFH adsorbents were calculated depending on the grain size distribution (the higher the proportion of larger grains, the lower the outer surface, and therefore, the higher the required amount to be tested). After 30 min, the centrifuge tube was promptly removed and the supernatant was transferred into an empty glass bottle. This supernatant was analyzed with regard to turbidity (WTW Turb 430 IR, nephelometric, 90 °C scattered light) and total Fe (Spectroquant Iron Test (0.010–5.00 mg/L Fe) after 1 h digestion with $K_2S_2O_8$ at 120 °C using Spectroquant Crack Set 10).

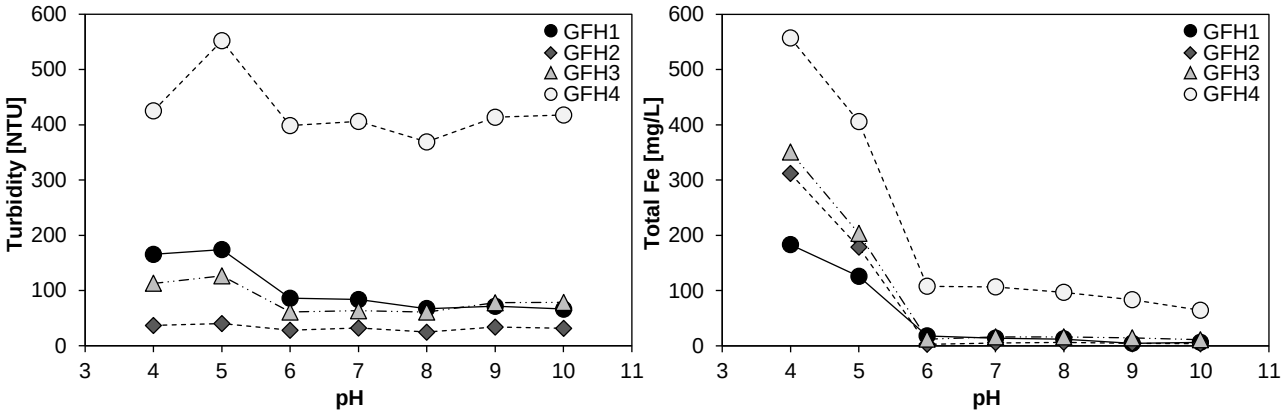

Fig. S2.1: Turbidity formation and iron redissolution in the context of material stability investigations (30 rpm, 30 min, 20 °C) in buffered solutions.

Due to abrasion, turbidity was formed at all pH values (Fig. S2.1 left). The highest turbidity occurred at pH < 6. Whereas the redissolution of Fe was very low for GFH1, GFH2, and GFH3 at pH ≥ 6, significant amounts of Fe were found at pH < 6 in the supernatant (Fig. S2.1 right). Consequently, all GFH adsorbents investigated were mechanically and chemically unstable at pH < 6, which is why they should not be used in this pH range when a long-term stability is required.

2.8.1.2 Adsorption Isotherms at 5 mg/L NTMP-P

Fig. S2.2 depicts the adsorption isotherms gained at different contact times for an initial NTMP-P concentration of 5 mg/L (at a pH of 6.0–7.6 and room temperature).

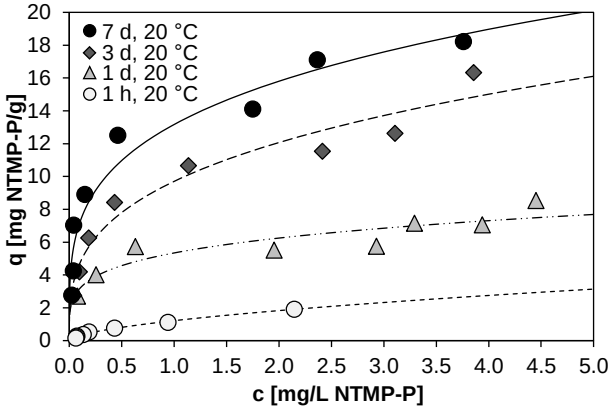

Fig. S2.2: Adsorption isotherms of GFH1 with respect to adsorption of 5 mg/L NTMP-P at an initial pH of 6 (buffer: 0.01 M MES) and different contact times (20 rpm). Freundlich models are shown (model constants in Tab. S2.1).

2.8.2 Constant Values

2.8.2.1 Freundlich Models

Tab. S2.1: Model constants and coefficients of determination for adsorption isotherms.

						Freundlich				Langmuir		
Fig.	Initial NTMP-P	Temp [°C]	Adsorbent	Time	pH	K_F [L/g]	n [-]	r^2 [-]	p [-]	q_{max} [mg/g]	K_L [L/mg]	r^2 [-]
Fig. 2.3	1 mg/L	20	GFH1	1 h	4.0–6.0	0.682	2.032	0.921	0.0002	0.664	4.928	0.824
					6.0–7.3	0.371	3.329	0.934	<0.0001	0.331	19.671	0.910
					8.0–8.2	0.251	5.217	0.797	0.0002	0.227	51.747	0.847
					9.4–10.0	0.244	2.890	0.978	<0.0001	0.250	7.679	0.950
					10.9–12.0	0.139	2.036	0.930	<0.0001	0.156	3.722	0.861
			GFH2	1 h	4.0–5.8	0.236	2.869	0.834	0.0002	0.245	7.010	0.904
					6.0–7.5	0.126	3.225	0.937	<0.0001	0.120	14.166	0.865
					8.0–8.2	0.075	5.076	0.717	0.0009	0.070	22.763	0.760
					9.7–10.0	0.035	7.695	0.302	0.1467	0.040	13.040	0.414
			GFH3	1 h	4.0–5.9	0.164	2.566	0.914	0.0008	0.162	6.975	0.842
					6.0–7.1	0.108	2.554	0.941	0.0001	0.110	6.630	0.870
					8.0–8.2	0.066	2.415	0.897	0.0003	0.079	3.656	0.894
					9.7–10.0	0.031	3.891	0.641	0.0571	0.036	5.764	0.610
			GFH4	1 h	4.0–5.4	0.146	3.815	0.991	<0.0001	0.118	33.491	0.881
					6.0–6.7	0.092	2.237	0.703	0.0012	0.111	3.422	0.682
					8.0–8.2	0.037	9.764	0.268	0.1767	0.039	19.057	0.396
					9.7–10.0	0.019	13.241	0.310	0.3289	0.020	19.236	0.324
Fig. 2.5	1 mg/L	20	GFH1	1 d	6.0–6.3	4.128	2.225	0.852	<0.0001	4.265	6.323	0.885
				3 d	6.0–6.4	9.093	2.458	0.713	0.0092	9.540	5.866	0.689
				7 d	6.0–6.5	12.553	4.133	0.847	0.0011	10.848	46.395	0.851
		5	GFH1	7 d	6.0–6.4	7.257	3.190	0.907	0.0003	8.801	4.192	0.854
		35	GFH1	7 d	6.0–6.6	13.260	3.644	0.941	0.0003	10.672	45.628	0.894
Fig. S2.2	5 mg/L	20	GFH1	1 h	6.0–8.0	1.216	1.698	0.993	<0.0001	2.302	1.351	0.963
				1 d	6.0–7.4	5.342	4.421	0.841	0.0013	7.239	5.609	0.795
				3 d	6.0–7.4	9.701	3.175	0.945	<0.0001	14.474	3.661	0.921
				7 d	6.0–7.5	13.166	3.797	0.936	0.0001	16.963	9.012	0.940

2.8.2.2 Logistic Function Models

Tab. S2.2: Model constants and coefficients of determination for phosphonate adsorption as a function of pH (logistic function model).

	HPAA	PBTC	HEDP	NTMP	EDTMP	DTPMP
a [-]	122384.7	6471.9	3274.0	3199.6	3227.7	2896.8
b [-]	0.264	0.261	0.110	0.146	0.100	0.093
d [mg/L]	1374.50	131.56	264.51	421.55	855.09	885.62
r^2 [-]	0.996	0.947	0.657	0.983	0.858	0.868
p [-]	<0.0001	<0.0001	0.0102	<0.0001	0.0001	0.0022

3 Batch Studies of Phosphonate and Phosphate Adsorption on Granular Ferric Hydroxide (GFH) with Membrane Concentrate and Its Synthetic Replicas

This Chapter has been published as:

Reinhardt, T., Veizaga Campero, A. N., Minke, R., Schönberger, H. and Rott, E. 2020. Batch Studies of Phosphonate and Phosphate Adsorption on Granular Ferric Hydroxide (GFH) with Membrane Concentrate and Its Synthetic Replicas. *Molecules*, **25**(21). https://doi.org/10.3390/molecules25215202.

3.1 Research Questions

- How does the presence of other ions affect adsorption, particularly of calcium?
- Does the Ca^{II} present in GFH also have an effect?
- Do precipitates affect the adsorption/desorption process?

3.2 Abstract

Phosphonates are widely used as antiscalants for softening processes in drinking water treatment. To prevent eutrophication and accumulation in the sediment, it is desirable to remove them from the membrane concentrate before they are discharged into receiving water bodies. This study describes batch experiments with synthetic solutions and real membrane concentrate, both in the presence of and absence of granular ferric hydroxide (GFH), to better understand the influence of ions on phosphonate and phosphate adsorption. To this end, experiments were conducted with six different phosphonates, using different molar Ca:phosphonate ratios. The calcium already contained in the GFH plays an essential role in the removal process, as it can be redissolved, and, therefore, increase the molar Ca:phosphonate ratio. (Hydrogen-)carbonate ions had a competitive effect on the adsorption of phosphonates and phosphate, whereas the influence of sulfate and nitrate ions was negligible. Up to pH 8, the presence of Ca^{II} had a positive effect on adsorption, probably due to the formation of ternary complexes. At pH > 8, increased removal was observed, with either direct precipitation of Ca:phosphonate complexes or the presence of inorganic precipitates of calcium, magnesium, and phosphate serving as adsorbents for the phosphorus compounds. In addition, the presence of (hydrogen-)carbonate ions resulted in precipitation of $CaCO_3$ and/or dolomite, which also acted as adsorbents for the phosphorus compounds.

3.3 Introduction

In recent years, global phosphonate consumption has increased from 56,000 t/yr (1998) to 94,000 t/yr (2012) (Davenport *et al.* 2000; EPA 2013). Phosphonates are complexing agents widely used as antiscalants for softening processes in drinking water treatment (Nowack and Stone 1999a; Boels *et al.* 2012; Armbruster *et al.* 2019). The resulting membrane concentrate is often disposed of into a receiving water body without any further treatment (Squire 2000; Nederlof and Hoogendoorn 2005; Greenlee *et al.* 2009). A recent study shows the effects of wastewater on the occurrence of various phosphonates in rivers (Rott *et al.* 2020b). A significant increase of adsorbed phosphonates in the sediment, which was due to wastewater discharge, was observed. This is of particular interest, since to date, very little is known about the long-term effects of phosphonates in surface waters. Since UV radiation can promote the

degradation of phosphonates to readily available orthophosphate, they can contribute to the eutrophication of water bodies (Lesueur *et al.* 2005; Kuhn *et al.* 2018).

By complexing calcium ions (Nowack 2003) and adsorbing on active growth sites of crystals, phosphonates can inhibit $CaCO_3$ precipitation (Jonasson *et al.* 1996; Yang *et al.* 2001; Tang *et al.* 2008). Due to their threshold effect, they are effective even in substoichiometric concentrations (Kan *et al.* 2005). It is known that phosphonates can adsorb on granular ferric hydroxides (GFH) (Boels *et al.* 2012; Chen *et al.* 2017; Reinhardt *et al.* 2020a) as mono-, bi-, or tridentate complexes (Stone *et al.* 2002; Martínez and Farrell 2017). Calcium ions, whose precipitation is to be prevented by phosphonates, simultaneously have a positive influence on the adsorption of phosphonates on GFH due to the formation of ternary surface complexes (Nowack and Stone 1999b; Martínez and Farrell 2017). The influence of other ions such as magnesium (Chen *et al.* 2017) and sulfate (Boels *et al.* 2012) on the adsorption on GFH has also been investigated in previous studies.

So far, however, hardly any studies have been published on the influence of a mixture of different ions usually present in membrane concentrates on the adsorption of phosphonates on GFH. Although various phosphonates with different properties are used as antiscalants, only one phosphonate, nitrilotrimethylphosphonic acid (NTMP), has been examined in these studies. Furthermore, little attention has been paid thus far to the possible impacts of potential precipitation.

In a previous study, Reinhardt *et al.* (2020a) compared the adsorption of various phosphonates on four different GFH adsorbents. They showed that phosphonates with different properties, such as molecular size and weight, or the number of phosphonate groups, display different behaviors during adsorption. The pH for phosphonate adsorption on GFH should be close to 6. It may be possible to reuse GFH. The authors concluded that further experiments with real wastewater must be conducted in order to investigate the competing or supporting influence of other ions.

With the aim of closing the knowledge gaps mentioned above, this study describes batch experiments with the best-performing GFH used in the previous study. In four experiments, the influence of ions present in membrane concentrate on phosphonate adsorption was investigated (mainly focusing on calcium ions). Additional batches that

did not include GFH were conducted to investigate whether the observed removal could be caused by precipitation. For a better understanding of the process, experiments were first performed with synthetic replicas, before conducting subsequent batches with real membrane concentrate. Fig. 3.1 shows the six investigated phosphonates in this study.

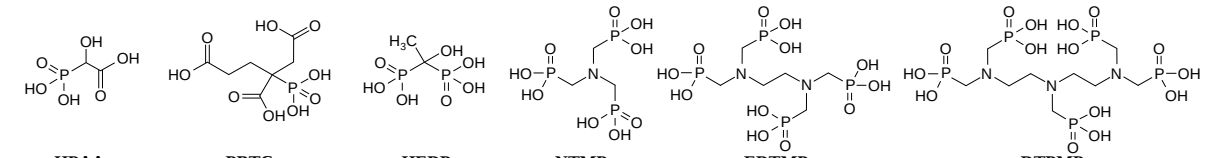

HPAA 2-Hydroxy phosphonoacetic acid | **PBTC** 2-Phosphonobutane-1,2,4-tricarboxylic acid | **HEDP** 1-Hydroxyethylidene-(1,1-diphosphonic acid) | **NTMP** Nitrilotrimethyl-phosphonic acid | **EDTMP** Ethylenediaminetetra(methylene phosphonic acid) | **DTPMP** Diethylenetriaminepenta(methylene phosphonic acid)

Fig. 3.1: Chemical structures of considered phosphonates.

3.4 Materials and Methods

3.4.1 Reagents and Chemicals

All solutions were prepared with deionized water made from drinking water in the laboratory, using an ion exchanger (Seradest SD 2000, ELGA LabWater, Celle, Germany) and a downstream filter unit (Seralpur PRO 90 CN).

Acetic acid (AcOH) (100%, Ph. Eur.) and HCl solution (32%, AnalaR NORMAPUR) were obtained from VWR Chemicals (Fontenay-sous-Bois, France). $NaNO_3$ (> 99%, Ph. Eur.), Na_2SO_4 (≥ 99%, p. a.), $CaCl_2 \cdot 2H_2O$ (≥ 99.5%, p. a.), $MgCl_2 \cdot 6H_2O$ (≥ 99%, Ph. Eur.), KH_2PO_4 (≥ 99.5%, p. a.), and NaOH (≥ 99%, Ph. Eur.) were purchased from Merck (Darmstadt, Germany). $NaHCO_3$ (≥ 99%, Ph. Eur.) was purchased from Carl Roth (Karlsruhe, Germany). Ethylenedinitrilotetraacetic acid disodium salt dihydrate (EDTA-Na_2 dihydrate, Titriplex III, 99–101%, Ph. Eur.) was obtained from Merck (Darmstadt, Germany).

The buffers (2-(*N*-morpholino)ethanesulfonic acid (MES) (≥ 99%), 3-(*N*-morpholino)propanesulfonic acid (MOPS) (≥ 99.5%), 4-(2-hydroxyethyl)-1-piperazinepropanesulfonic acid (EPPS) (≥ 99.5%), 3-(cyclohexylamino)-2-hydroxy-1-propanesulfonic acid (CAPSO) (≥ 99%), and 3-(cyclohexylamino)-1-propanesulfonic acid (CAPS) (≥ 98%) were purchased from Sigma Aldrich (St. Louis, MO, USA).

HPAA was purchased from Connect Chemicals (Ratingen, Germany) as a technical solution (50%). PBTC, as a technical solution (50%, CUBLEN P 50), as well as EDTMP

(5.3% water of crystallization) and DTPMP (16% water of crystallization), both as solids, were supplied by Zschimmer & Schwarz Mohsdorf (Burgstädt, Germany). HEDP·H_2O (≥ 95%) and NTMP (≥ 97%) were purchased from Sigma-Aldrich (St. Louis, MO, USA).

3.4.2 Adsorbent

A previous study comparing the adsorption of phosphonates on different granular ferric hydroxides (GFH) showed that FerroSorp RW had the highest adsorption capacity of the compared adsorbents (Reinhardt *et al.* 2020a). Therefore, FerroSorp RW from HeGo Biotec GmbH was used in this study. Prior to the experiments, the adsorbent was rinsed once over a sieve with distilled water until the water ran clear to remove GFH dust, and then the GFH was air-dried under a fume hood. The screen mesh width was chosen to ensure a maximum separation of 3 Mass-% of the adsorbent as ultrafine particles during the rinsing process. The FerroSorp RW that was used had a grain size of 0.5–2.5 mm after rinsing, a point of zero charge (pH_{PZC}) of 8.6, and a specific surface area of 210 m^2/g. According to the manufacturer, it has a calcium content of ≥ 12–19% (mainly $CaCO_3$).

3.4.3 Membrane Concentrate and Its Synthetic Replicas

The membrane concentrate was taken from a low pressure reverse osmosis (LPRO) plant at a public waterworks. It was a clear (0.11 NTU), colorless solution with a low organic load (16.1 mg/L COD). It was characterized by concentrations of 613 mg/L Ca^{2+} and 75 mg/L Mg^{2+} and the associated exceptionally high level of water hardness, combined with a very high buffer capacity (alkalinity = 26.6 mmol/L). The pH value of the sample was approximately 7.9, the electrical conductivity 3.14 mS/cm, the Cl^- concentration 229 mg/L, the SO_4^{2-} concentration 474 mg/L, and the NO_3^- concentration 67.7 mg/L. The total P of the sample was 1.27 mg/L, and the dissolved P fraction (total P fraction of the membrane-filtered sample) was 1.27 mg/L as well. Thus, the particulate P fraction was negligible. The o-PO_4-P fraction was 0.53 mg/L, and consequently the organic P fraction was 0.74 mg/L P. The antiscalant (DTPMP) was added to the raw water in the waterworks at a dosage of 0.6 mg/L. With an average nanofiltration yield of 80%, the added antiscalant was concentrated by a factor of five. Thus, the membrane concentrate contains approximately 3 mg/L DTPMP, which corresponds to

0.81 mg/L DTPMP-P. Therefore, it is assumed that the organic P fraction consisted almost exclusively of DTPMP. The experiments were started on the day of sampling.

Synthetic replicas of the membrane concentrate were prepared to investigate the influence of different ions. The concentrations of the compounds in the synthetic replicas matched the concentration of the individual compounds in the membrane concentrate. The composition of the synthetic solutions used is shown under the headings A–N in Tab. 3.1, the composition of the membrane concentrate under the heading MC. Preliminary experiments (not described here in detail) showed that the corresponding counterions Na^+ and Cl^- did not have any effect on the adsorption. Since synthetic wastewater lacks the buffering capacity of real wastewater, the addition of an organic buffer (0.01 M) was necessary to keep the pH stable during the adsorption experiments. The influence of the buffers on phosphorus analysis is negligible (Rott *et al.* 2018b).

Tab. 3.1: Composition of the solutions. A–N: synthetic replicas, MC: membrane concentrate.

		Solutions														
Compound	**Unit**	**A**	**B**	**C**	**D**	**E**	**F**	**G**	**H**	**I**	**J**	**K**	**L**	**M**	**N**	**MC**
DTPMP-P	mg/L	0.74	-	0.74	0.74	0.74	0.74	0.74	0.74	0.74	0.74	0.74	0.74	0.74	0.74	0.74
PO_4-P	mg/L	-	0.53	0.53	0.53	0.53	0.53	0.53	0.53	0.53	0.53	0.53	0.53	0.53	0.53	0.53
NO_3^-	mg/L	-	-	-	67.7	-	-	-	67.7	-	-	-	-	-	67.7	67.7
SO_4^{2-}	mg/L	-	-	-	-	474	-	474	474	-	-	-	474	474	474	474
HCO_3^-	mg/L	-	-	-	-	-	1620	1620	1620	-	-	-	-	1620	1620	1620
Ca^{2+}	mg/L	-	-	-	-	-	-	-	-	613	-	613	613	613	613	613
Mg^{2+}	mg/L	-	-	-	-	-	-	-	-	-	75.0	75.0	75.0	75.0	75.0	75.0

3.4.4 Experimental Procedure

Experiments were conducted both with synthetic solutions and with real wastewater. P-containing solutions with different pH values, adjusted with HCl or NaOH, were prepared. For each investigated pH, a buffer was added (target pH value (pH_{target}) with buffer concentration in brackets): pH 5 (0.01 M AcOH), pH 6 (0.01 M MES), pH 7 (0.01 M MOPS), pH 8 (0.01 M EPPS), pH 9 (0.01 M CAPSO), pH 10 (0.01 M CAPS), and pH 12 (0.01 M NaOH).

After the required amount of adsorbent was weighed into a 50 mL centrifuge tube, the tube was filled with the buffered P-containing solution up to the 50 mL mark, immediately capped, and then clamped in the overhead rotator (LLG-uniROTATOR 2) running at 20 rpm. The centrifuge tube was removed after a contact time of seven days, and approximately 20 mL of the supernatant was filtered into an empty glass bottle using a two-part disposable syringe (Norm-Ject, 20 mL, Henke Sass Wolf, Tuttlingen, Germany) with an attachable 0.45 µm nylon filter (Sartorius Stedim Biotech GmbH, Göttingen, Germany). A previous study showed that the relatively long contact time of seven days was necessary to achieve equilibrium (Reinhardt *et al.* 2020a). This contact time could have been reduced by grinding the adsorbent or by a higher rotation speed, which would have led to more abrasion of the adsorbent. Since it is known that the particle radius of the adsorbent has an influence on the adsorption behavior (Worch 2012), the adsorbent should be left as undamaged as possible to allow a better comparison with future column experiments. In a possible future engineering application with filter columns, however, significantly shorter contact times can be achieved, since no equilibrium is necessary in this case. Total P (dissolved), orthophosphate-P, and pH (pH_{end}) were determined from the filtrate. As it is possible for pH_{end} to deviate from pH_{target}, the figures show pH_{end}, which is considered to be more relevant.

Dissolved phosphonates are part of the dissolved unreactive phosphorus (DUP) fraction in wastewater, which corresponds to the difference between dissolved P (total P of membrane-filtered sample) and orthophosphate-P (Rott *et al.* 2020a). Therefore, organic P concentrations in mg/L were calculated in accordance with Eq. 3.1.

$$c(DUP) = c(\text{dissolved P}) - c(\text{o-}PO_4\text{-P}) \quad (3.1)$$

Experiment 1 served to investigate the influence of Ca^{II} on the adsorption of different phosphonates on GFH. Two different molar ratios of Ca:phosphonate, 0:1 and 2:1, at different pH values were considered. Tab. 3.2 shows the phosphonate concentrations used in Experiment 1, which was conducted with and without adsorbent to investigate the relevance of precipitation (T = 20 °C; pH 5, 6, 7, 8, 9, 10, and 12; t_c = 7 d; initial concentration = 16.1 mg/L HPAA, PBTC, HEDP, NTMP, EDTMP, or DTPMP; Ca:phosphonate 0:1 and 2:1; 0.2 g GFH/L and without GFH).

Tab. 3.2: Different concentrations of phosphonates used in Experiment 1.

	Phosphonate		Phosphonate-P
	mg/L	**µmol/L**	**mg/L**
HPAA	16.1	103	3.19
PBTC	16.1	59.6	1.85
HEDP	16.1	78.1	4.84
NTMP	16.1	53.8	5.00
EDTMP	16.1	36.9	4.57
DTPMP	16.1	28.1	4.35

The objective of Experiment 2 was to examine the influence of Ca^{II} on the adsorption of NTMP and DTPMP at higher Ca^{II} concentrations than in Experiment 1. These two phosphonates were selected as salient representatives of organophosphonates, as they are widely used in industrial applications, and the membrane concentrate investigated in this study contained DTPMP. The experiment was performed at seven different pH values and seven different molar ratios of Ca:phosphonate. These were: 0:1, 1:1, 2:1, 3.67:1, 5:1, 7.33:1, and 18.33:1. The adsorption process was investigated both with FerroSorp RW and without adsorbent to investigate the relevance of precipitation (T = 20 °C; pH 5, 6, 7, 8, 9, 10, and 12; t_c = 7 d; initial concentration = 16.1 mg/L NTMP or DTPMP; Ca:phosphonate 0:1–18.33:1; 0.2 g GFH/L and without GFH).

The aim of Experiment 3 was to investigate at which phosphonate and Ca^{II} concentrations and molar Ca:phosphonate ratios phosphonates can be removed without the dosing of GFH, and which factors are decisive in this process. At pH 8 and 9, the NTMP and DTPMP concentrations 3.22 mg/L, 16.1 mg/L, 32.2 mg/L, and 80.5 mg/L (Tab. 3.3) with the molar Ca:phosphonate ratios 0:1, 1:1, 2:1, 5:1, 10:1, 25:1, and 60:1 were examined (T = 20 °C; pH 8 and 9; t_c = 7 d; initial concentration = 3.22–80.5 mg/L NTMP or DTPMP; Ca:phosphonate 0:1–60:1; without GFH). Additionally, the five highest calcium concentrations were investigated using the same procedure, but in the absence of NTMP and DTPMP, to test possible precipitation of $CaCO_3$ and $Ca(OH)_2$. Ca^{2+} concentrations before (Ca_{start}) and after (Ca_{end}) the contact time were determined from the filtrate. This experiment was carried out using a duplicate approach.

Tab. 3.3: Different concentrations of phosphonates used in Experiment 3.

	Phosphonate		Phosphonate-P
	mg/L	**µmol/L**	**mg/L**
NTMP	3.22	10.8	1.0
	16.1	53.8	5.0
	32.2	108	10
	80.5	269	25
DTPMP	3.22	5.61	0.9
	16.1	28.1	4.4
	32.2	56.1	8.7
	80.5	140	22

Experiment 4 focused on the membrane concentrate from a drinking water treatment plant, and on its synthetic replicas. The membrane concentrate was reproduced synthetically step by step to investigate the influence of different ions (T = 20 °C; pH 5, 6, 7, 8, 9, 10, and 12; t_c = 7 d; for the initial concentration see Section 3.4.3; 0.1 g GFH/L and without GFH).

PHREEQC Interactive 3 with the Minteq.v4 database was used to predict possible precipitates.

3.4.5 Analytical Methods

For phosphorus analysis, a modification of the ISO 6878 (ISO 6878) method was used (ISO_{mini}). The ISO_{mini} molybdenum blue method has been described in detail by Rott et al. (Rott *et al.* 2018b). Prior to analysis, all glass materials that came into contact with the sample were thoroughly rinsed with 10% hydrochloric acid and deionized water. Digestion was performed in a HachLange HT200S thermostat. Absorbance measurements were carried out with a Nanocolor UV/VIS II spectrophotometer from Macherey-Nagel. A WTW SenTix 81 pH electrode in combination with the WTW pH91 instrument was used to determine the pH. In order to determine Ca^{2+}, DIN 38406-3 was used (DIN 38406-3). A total sample volume of 50 mL of the solution to be analyzed was transferred into an Erlenmeyer flask with a volumetric pipette. A total of 2 mL of 2 M sodium hydroxide solution and a spatula tip of indicator were added to the flask.

The solution was titrated with 0.01 M ethylenediaminetetraacetic acid (EDTA) solution while stirring, until the color changed completely.

3.5 Results and Discussion

3.5.1 Experiment 1 – Adsorption Behavior of Six Phosphonates in the Presence of and Absence of Ca^{II}

Fig. 3.2 enables a comparison of the adsorption behavior of six different phosphonates at molar Ca:phosphonate ratios of 0:1 and 2:1, with a contact time of seven days and different pH values. Additionally, the removal rates in the absence of GFH are shown, in order to determine the relevance of precipitation. The phosphonates in Fig. 3.2 were sorted in the order of the increasing number of phosphonate groups (PG): HPAA (1 PG), PBTC (1 PG), HEDP (2 PG), NTMP (3 PG), EDTMP (4 PG), DTPMP (5 PG).

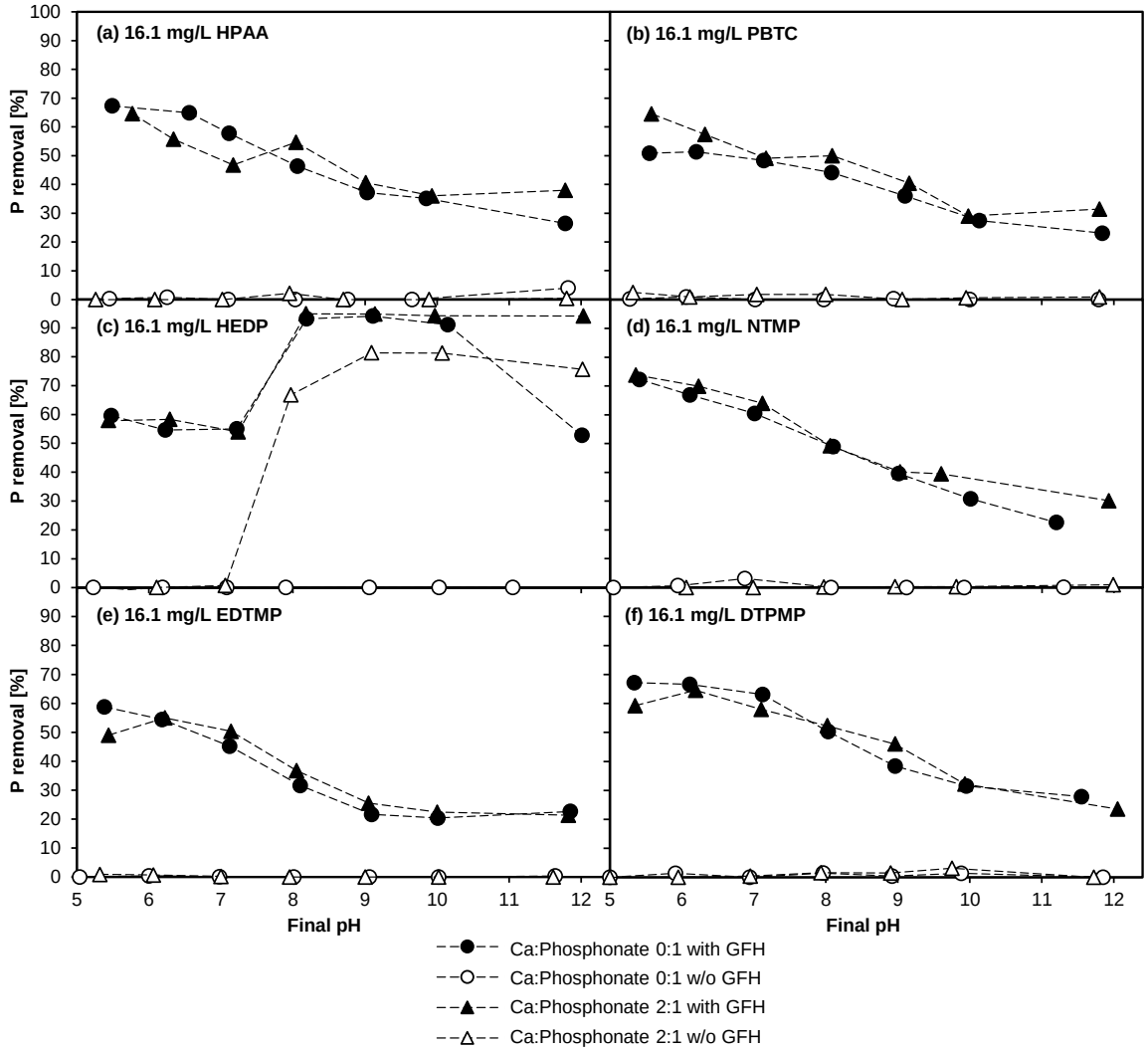

*Fig. 3.2: Influence of Ca^{II} presence on phosphonate adsorption (T = 20 °C; t_c = 7 d; initial phosphonate concentration = 16.1 mg/L; 0.2 g GFH/L and without GFH). (**a**): 16.1 mg/L HPAA, (**b**): 16.1 mg/L PBTC, (**c**): 16.1 mg/L HEDP, (**d**): 16.1 mg/L NTMP, (**e**): 16.1 mg/L EDTMP, (**f**): 16.1 mg/L DTPMP.*

For all phosphonates, except HEDP, the removal rates decreased with increasing pH to a similar extent (removal rates at pH_{target} 5 and 12): HPAA from 67% to 27%, PBTC 65% to 23%, NTMP 74% to 23%, EDTMP 59% to 24%, DTPMP 66% to 24%. The difference in the removal rate between the solutions in the presence of and absence of Ca^{II} was always less than 13%. Therefore, no major influence of Ca^{II} on phosphonate removal was observed. This stands in contradiction to several previous studies. Nowack and Stone (1999b) investigated the adsorption of HEDP, NTMP, EDTMP, and DTPMP on goethite and found that excess Ca^{II} concentrations significantly increased the maximum loading. Even at an equimolar Ca:NTMP ratio, the maximum loading for NTMP almost doubled. Similarly, Boels *et al.* (2012) observed a near doubling of the maximum loading of GFH at a molar Ca:NTMP ratio of 2:1. At a molar ratio of 60:1, it

was possible to increase the loading even further. Rott *et al.* (2018a) also found a positive influence of Ca^{II} on the adsorption of NTMP and DTPMP on magnetic adsorbent particles (ZnFeZr-oxyhydroxide). In addition, Chen *et al.* (2017) found a positive influence of the hardness ions calcium and magnesium on NTMP adsorption on GFH. The aforementioned studies attribute this behavior mainly to the potential formation of ternary complexes. Ternary complexes can build a bridge between the GFH surface and phosphonates, leading to an increased adsorption (Stone *et al.* 2002; Boels *et al.* 2012; Martínez and Farrell 2017).

In the batches without GFH, no removal could be detected. Thus, for this experiment, precipitation can be excluded as the cause of phosphorus removal. HEDP, however, deviated clearly from the behavior of the other phosphonates. In the presence of GFH, it showed a removal of 60% (pH_{target} 5) to 53% (pH_{target} 12), whereas the removal at pH_{target} 8 to 10 was > 90%.

A closer look at the behavior of HEDP reveals two particularly noteworthy aspects. First, with a molar Ca:phosphonate ratio of 2:1, phosphorus was removed even in the absence of GFH, and second, in the presence of GFH, phosphorus was removed without the addition of Ca^{II}. In the latter case, about 67% of the phosphorus was removed at pH 8.0, about 81% at pH 9.1 and 10.1, and about 76% at pH 12.0. The removal of phosphorus even without the dosing of GFH suggests precipitation of $CaCO_3$ or Ca-HEDP complexes. According to calculations performed with PHREEQC, at a calcium concentration of 156.2 µmol/L, more than 7.2 mmol/L of (hydrogen-)carbonate would be necessary to precipitate $CaCO_3$ at pH 8.0. These calculations do not consider HEDP, which complexes at least parts of the Ca^{II} and additionally inhibits precipitation of $CaCO_3$ (Garcia *et al.* 2001; Nowack 2003). Since deionized water was used in the experiments, and the samples were rotated in closed centrifuge tubes (closed system), the (hydrogen-)carbonate content (from airborne CO_2) of the solutions is expected to be low. Therefore, the formation of $CaCO_3$ is unlikely.

Another explanation for the observed HEDP removal in the absence of GFH could be the precipitation of Ca-HEDP complexes. Several researchers have investigated various different calcium-phosphonate precipitates, such as Ca-HEDP (Browning and Fogler 1996), Ca-NTMP (Pairat *et al.* 1997; Kan *et al.* 2005), and Ca-DTPMP (Kan *et al.* 1994). However, these studies were conducted using relatively high phosphonate

concentrations. In another study, Zhang *et al.* (2010) found more Ca-phosphonate precipitation for HEDP as compared with other phosphonates. The authors concluded that the order of solubility of the Ca-phosphonate complexes was as follows: PBTC > DTPMP > EDTMP > NTMP > HEDP. This corresponds with the results of the current study and the findings of Amjad *et al.* (2003), who found a calcium ion tolerance of PBTC >> HEDP.

Interestingly, between pH 8 and 10, a peak in phosphorus removal was observed without the addition of Ca^{II}. The reason for this could be the dissolution of calcium from the GFH. The redissolved Ca^{II} could then lead to precipitation. To investigate this in more detail, a 0.01 M CAPSO solution at pH 9 with 0.2 g/L GFH was rotated with a contact time of seven days (without a phosphonate). A Ca^{2+} concentration of 11.0 ± 1.1 mg/L could then be observed in the membrane-filtered supernatant. According to the manufacturer's statement specifying ≥ 12–19% calcium content in the GFH, a dosage of 0.2 g/L GFH would result in a maximum calcium concentration in the solution of 24 to 38 mg/L, if completely redissolved. Therefore, it can be assumed that approximately 29% to 46% of the Ca^{II} was redissolved.

Those measurements may explain why no positive effect of Ca^{II} on the removal of phosphorus was observed with the other five phosphonates. A calcium concentration of 11.0 mg/L (as redissolved from the GFH) already corresponds to the following molar Ca:phosphonate ratios: Ca:HPAA 2.7:1, Ca:PBTC 4.6:1, Ca:HEDP 3.5:1, Ca:NTMP 5.1:1, Ca:EDTMP 7.5:1, and Ca:DTPMP 9.9:1. Therefore, although no Ca^{II} was added, the positive effect of Ca^{II} had probably already been achieved by redissolution from the GFH. This shows the important role of the $CaCO_3$ content of the GFH and also explains the deviation between these results and those found in previous publications.

In conclusion, Experiment 1 yielded two findings: First, the redissolved calcium from the GFH had a positive effect on phosphonate adsorption, possibly attributable to the formation of ternary complexes. Second, at the given conditions, HEDP was found to precipitate presumably as Ca-phosphonate complexes, which also increases its removal rate.

3.5.2 Experiment 2 – Adsorption Behavior of NTMP and DTPMP in the Presence of Ca^{II} in Higher Concentrations

The aim of Experiment 2 was to investigate the influence of Ca^{II} in higher concentrations than those in Experiment 1 on the adsorption of NTMP and DTPMP on GFH. Fig. 3.3 shows the results of batches with NTMP and DTPMP in the presence of and absence of GFH over different pH values from 5 to 12.

According to Fig. 3.3b, in the batches without adsorbent, no removal of NTMP took place up to a molar Ca:NTMP ratio of 7.33:1. A different behavior was observed when Ca^{II} was added in a molar Ca:NTMP ratio of 18.33:1. NTMP was removed at particular pH values: ~89% at pH 8.1, ~93% at pH 9.0, ~98% at pH 9.8, and ~28% at pH 12.0. A possible explanation for this behavior could be $CaCO_3$ or Ca-NTMP precipitation. According to calculations performed with PHREEQC, more than 0.8 mmol/L of (hydrogen-)carbonate would be necessary at a calcium concentration of 986.3 µmol/L to precipitate $CaCO_3$ at pH 8.1. These calculations do not consider NTMP, which complexes at least parts of the Ca^{II} and inhibits precipitation of $CaCO_3$ (Nowack 2003; Tang *et al.* 2008). The (hydrogen-)carbonate content of the solutions should be low due to the use of deionized water in the experiments, and due to the rotation of the samples in closed centrifuge tubes (closed system). Thus, the formation of $CaCO_3$ is unlikely.

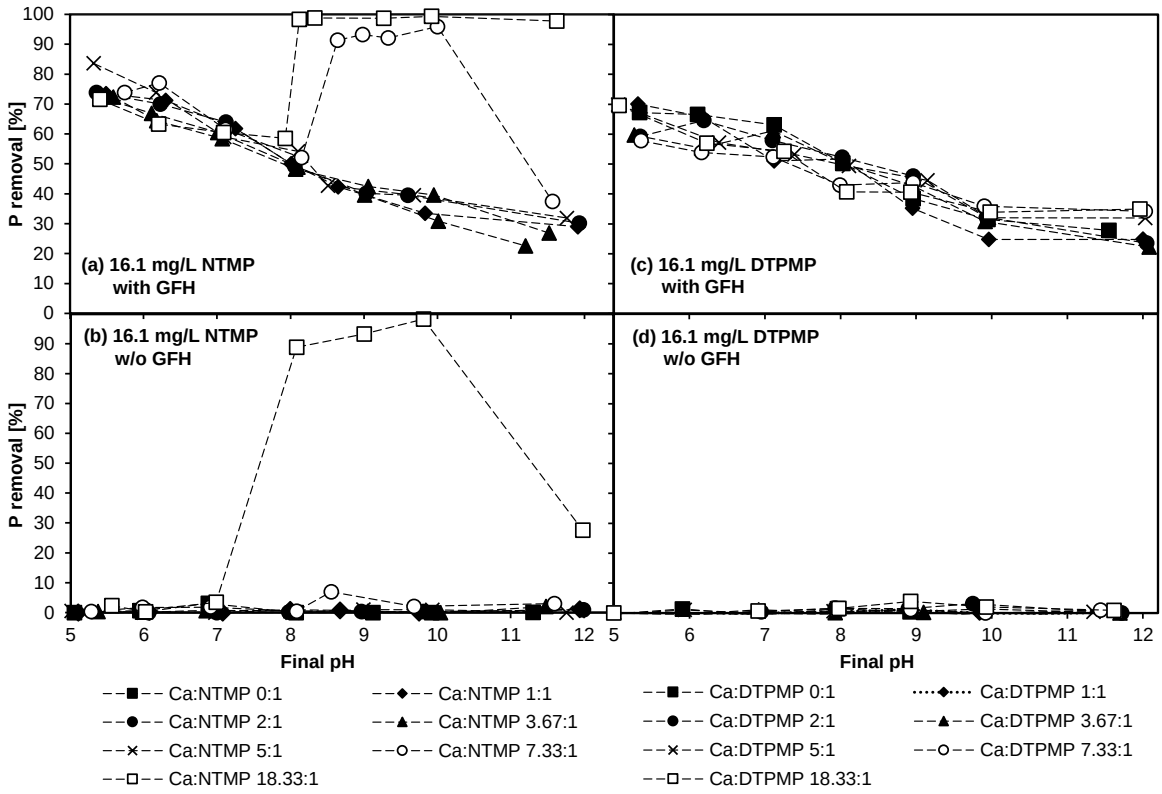

*Fig. 3.3: Influence of various molar Ca:phosphonate ratios on phosphonate adsorption (T = 20 °C; t_c = 7 d; initial concentration = 16.1 mg/L phosphonate; 0.2 g GFH/L and without GFH). (**a**): 16.1 mg/L NTMP with GFH, (**b**): 16.1 mg/L NTMP without GFH, (**c**): 16.1 mg/L DTPMP with GFH, (**d**): 16.1 mg/L DTPMP without GFH.*

In the case of added GFH adsorbent (Fig. 3.3a), the adsorption of NTMP was nearly identical at molar Ca:NTMP ratios of up to 5:1. At a molar ratio of 7.33:1, between pH 8.5 and 10.0, and at 18.33:1, between pH 8.1 and 11.6, increased removal occurred. Interestingly, when comparing the batches with (Fig. 3.3a) and without (Fig. 3.3b) GFH, a discrepancy can be observed. If precipitates were the reason for an increased removal, a removal of phosphorus should have also been seen at a molar Ca:NTMP ratio of 7.33:1 from pH 8.5 to 10.0 and at a molar ratio of 18.33:1 at pH 12, as observed in the batches without GFH. However, this can be explained again by the redissolution of calcium from the GFH, which may have led to a higher availability of Ca^{II} in the batches with GFH than indicated by the molar ratios in Fig. 3.3.

In Fig. 3.3c,d the behavior of DTPMP is shown. In the batches without GFH (Fig. 3.3d), no removal of DTPMP took place throughout all pH values and all molar Ca:DTPMP ratios tested. Therefore, a precipitation of $CaCO_3$ or Ca-DTPMP can be excluded. It is known that DTPMP, unlike other organophosphonates such as HEDP, NTMP, and EDTMP, does not precipitate as 1:1 complexes (Popov *et al.* 2002). The batches with

DTPMP and GFH (Fig. 3.3c) show the typical behavior of phosphonates on iron-containing surfaces, namely a decreasing adsorption capacity with increasing pH (Nowack and Stone 1999a, 1999b, 2006; Reinhardt *et al.* 2020a). The differences in phosphorus removal among the different molar Ca:DTPMP ratios do not show any pattern; therefore, they must have been due to inaccuracies that commonly arise when conducting experiments. Certain deviations in the results of these experiments are to be expected, since some of the input variables may already differ slightly, such as the weighed adsorbent mass, homogeneity of the GFH, pH_{end} value, and so on. Repetitions of selected batches produced similar results (not shown in the figures for better readability). However, despite these deviations, tendencies can still be clearly identified.

In conclusion, the batches with NTMP showed precipitation, which presumably consisted of Ca-NTMP complexes, whereas the batches with DTPMP did not show any precipitation. This corresponds with data found in the literature: Zhang *et al.* (2010) observed that Ca-NTMP complexes have a lower solubility than Ca-DTPMP complexes. Furthermore, Gledhill and Feijtel (1992) stated that Ca-NTMP complexes have higher stability constants than Ca-DTPMP complexes at any given pH. Taken together, these conclusions indicate that there are more Ca-NTMP than Ca-DTPMP complexes at any given pH, but the solubility of the Ca-NTMP complexes is lower.

3.5.3 Experiment 3 – Investigations on NTMP and DTPMP Precipitation

Since the previous experiments had shown that precipitation is responsible for increased removal, the aim of Experiment 3 was to investigate this phenomena in more detail. The experiment was necessary because it does not seem to be possible to predict the precipitation of Ca-phosphonate complexes on the basis of the existing data. Depending on the experimental conditions (molar Ca:phosphonate ratio, pH, ionic strength, temperature) different complexes can precipitate (Kan *et al.* 1994; Pairat *et al.* 1997), but reliable solubility products have been published only for some of them. In addition, the presence of calcium can have an effect on the pK_a values of the phosphonates (Browning and Fogler 1996). Additionally, a critical evaluation showed that the stability constants of DTPMP are not reliable, due to difficulties in synthesis and purification (Popov *et al.* 2002).

Different phosphonate concentrations and molar Ca:phosphonate ratios were applied (Tab. 3.4 and 3.5). The pH values 8 and 9 were examined, as the previously described increased removal of phosphonates started in this pH range. Higher pH values were not investigated, because lower pH values are recommended for the adsorption of phosphonates on GFH (Reinhardt *et al.* 2020a). In Tab. 3.4 and 3.5, removal rates higher than 90% are highlighted in dark gray, and removal rates ≥ 5% and ≤ 90% are highlighted in light gray. Removal rates of less than 5% were considered to be measurement inaccuracies, as were negative values (which were within the 5% inaccuracy range). Standard deviations are shown in Tab. S3.1 and S3.2. Calcium concentrations that are discussed separately are highlighted in bold type.

Tab. 3.4: Removal of NTMP by precipitation at different calcium concentrations and pH values (T = 20 °C; t_c = 7 d; no GFH added). Standard deviations are shown in Tab. S3.1.

	NTMP [mg/L]											
	3.22	**16.1**	**32.2**	**80.5**	**3.22**	**16.1**	**32.2**	**80.5**	**3.22**	**16.1**	**32.2**	**80.5**
	Calcium [mmol/L]				**Removal at pH 8 [%]**				**Removal at pH 9 [%]**			
Ca:NTMP 0:1	0.00	0.00	0.00	0.00	1	0	1	0	3	0	1	2
Ca:NTMP 1:1	0.01	0.05	0.11	0.27	3	0	2	1	−1	0	1	2
Ca:NTMP 2:1	0.02	0.11	0.22	**0.54**	1	0	1	1	0	1	2	**91**
Ca:NTMP 5:1	0.05	0.27	**0.54**	1.35	2	1	2	99	4	2	**78**	99
Ca:NTMP 10:1	0.11	**0.54**	1.08	2.69	1	3	95	99	4	**64**	100	100
Ca:NTMP 25:1	0.27	1.35	2.69	6.73	1	94	99	100	3	97	100	100
Ca:NTMP 60:1	0.65	3.23	6.46	16.1	0	97	99	100	2	99	100	100

Tab. 3.4 shows the results of the batches with NTMP at different calcium concentrations. In the batches without Ca^{II} and with a molar Ca:NTMP ratio of 1:1, no removal of phosphorus was observed. The same applies to the batches with 3.22 mg/L NTMP at all molar Ca:NTMP ratios. At higher NTMP concentrations, phosphorus was removed almost completely above particular calcium concentrations. At pH 9, the removal started at lower molar Ca:NTMP ratios than at pH 8 (e.g., with 80.5 mg/L NTMP at pH 9, a molar Ca:NTMP ratio of 2:1 was sufficient for a removal of 91%, whereas at pH 8 no removal occurred).

The three batches with the same Ca^{II} concentration of 0.54 mmol/L highlight an interesting aspect (highlighted in bold type). The NTMP removal at pH 9 increased with

increasing NTMP concentration from 64 ± 0.4% at 16.1 mg/L, and 78 ± 1.9% at 32.2 mg/L, up to 91 ± 0.2% at 80.5 mg/L. This indicates a precipitation of Ca-NTMP complexes, since a possible precipitation of $CaCO_3$ would have been inhibited by increasing concentrations of NTMP, due to its scale inhibition effect (Tang *et al.* 2008).

In Tab. 3.5 the results of the DTPMP batches at different calcium concentrations are shown. At molar Ca:DTPMP ratios of up to 2:1 and at 3.22 mg/L DTPMP, no removal of phosphorus was observed. At higher DTPMP concentrations, however, phosphorus was at least partially removed at particular Ca^{II} concentrations. Similar to NTMP, at pH 9, DTPMP was removed at lower molar Ca:DTPMP ratios than at pH 8.

Tab. 3.5: Removal of DTPMP by precipitation at different calcium concentrations and pH values (T = 20 °C; t_c = 7 d; no GFH added). Standard deviations are shown in Tab. S3.2.

	DTPMP [mg/L]											
	3.22	**16.1**	**32.2**	**80.5**	**3.22**	**16.1**	**32.2**	**80.5**	**3.22**	**16.1**	**32.2**	**80.5**
	Calcium [mmol/L]				**Removal at pH 8 [%]**				**Removal at pH 9 [%]**			
Ca:DTPMP 0:1	0.00	0.00	0.00	0.00	−2	−1	−1	−1	−2	0	2	−1
Ca:DTPMP 1:1	0.01	0.03	0.06	0.14	−1	1	−4	−1	2	0	4	0
Ca:DTPMP 2:1	0.01	0.06	0.11	0.28	0	−1	−4	−1	−1	0	−2	0
Ca:DTPMP 5:1	0.03	0.14	0.28	**0.70**	0	1	0	0	−1	0	−1	**62**
Ca:DTPMP 10:1	0.06	0.28	0.56	**1.40**	0	0	0	**74**	−4	0	47	91
Ca:DTPMP 25:1	0.14	**0.70**	**1.40**	3.51	−1	−1	**56**	90	−1	**0**	88	94
Ca:DTPMP 60:1	0.34	1.68	3.37	8.42	0	54	84	93	−6	85	92	96

At pH 8 and 16.1 mg/L DTPMP, a removal of 54% was observed at a molar Ca:DTPMP ratio of 60:1. At a concentration of 12 mM Ca and 0.73 µM DTPMP (0.42 mg/L) at 70 °C, Kan *et al.* (1994) found a crystalline Ca-DTPMP precipitate. Yan, Fei *et al.* (2015) also assumed precipitation of a Ca-DTPMP complex in their experiments with residual concentrations of 0.06 mM DTPMP and approximately 0.8 mM calcium.

An increased removal rate of DTPMP was observed at a constant Ca^{II} concentration of 0.70 mmol/L, paralleled by increasing DTPMP concentrations (Tab. 3.5) (i.e., at pH 9; no removal was found at 16.1 mg/L DTPMP, but at 80.5 mg/L DTPMP, 62 ± 1.9% was removed). Moreover, at pH 8, at a Ca^{II} concentration of 1.40 mmol/L and 32.2 mg/L DTPMP, 56 ± 1.4% was removed, whereas at 80.5 mg/L DTPMP, a higher

removal rate of 74 ± 0.3% was observed. This indicates that precipitation of Ca-DTPMP complexes occurred, as it was observed for NTMP (Tab. 3.4).

The results of Experiment 3 match the results from Experiment 2, in which the same concentration of 16.1 mg/L NTMP and DTPMP was used. In conclusion, NTMP and DTPMP demonstrated similar behavior. However, at comparable molar Ca:phosphonate ratios, NTMP showed a higher removal than DTPMP. This corresponds with the findings of Zhang *et al.* (2010), who found the solubility of Ca-DTPMP complexes to be higher than that of Ca-NTMP complexes.

To gain more knowledge as to which substances are precipitated, further batches were investigated with the five highest Ca^{II} concentrations used in Experiment 3 in the absence of phosphonate. In this case, the calcium concentration was measured in the membrane filtrate after seven days of rotation (Tab. 3.6). Ca_{start} deviated only ±3.4% from the target calcium concentration (Ca_{target}). Therefore, this deviation is assumed to represent the degree of measurement inaccuracy inherent in this calcium determination method.

Tab. 3.6: Change in calcium concentration in the absence of phosphonates (T = 20 °C; pH = 8 and 9; t_c = 7 d; no GFH added). Ca_{target}: target starting concentration, Ca_{start}: actual starting concentration, Ca_{end}: final concentration, Deviation: Ca_{start}/Ca_{end}.

pH_{start}	pH_{end}	Ca_{target} [mmol/L]	Ca_{start} [mmol/L]	Ca_{end} [mmol/L]	Deviation [%]
8.01	8.04	3.51	3.44	3.42	0.6
7.99	8.00	6.46	6.35	6.40	−0.8
8.01	8.04	6.73	6.80	7.00	−2.9
8.00	8.03	8.42	8.40	8.20	2.4
8.00	8.03	16.10	15.90	16.00	−0.6
9.01	9.01	3.51	3.60	3.64	−1.0
8.98	8.99	6.46	6.30	6.10	3.2
9.01	9.02	6.73	6.50	6.40	1.5
8.97	8.96	8.42	8.45	8.50	−0.6
8.99	8.97	16.10	15.60	15.35	1.6

The initial and final pH values are nearly identical. A precipitation of $CaCO_3$, however, would have resulted in a pH decrease (calculations performed with PHREEQC) that should have been noticeable, even though a buffer was used. The deviation between the initial and final concentration of Ca^{2+} varied between −3% and +3%. The negative

deviations are attributable to batches in which the measured final concentration was above the measured initial concentration. As this is not possible, the negative values indicate the measurement error of the analysis method. As the positive deviations are of the same order of magnitude, it is assumed that the deviations within this range are due to measurement inaccuracies, which is also in line with the deviations between Ca_{start} and Ca_{target} as mentioned above. It can be concluded that neither $CaCO_3$ nor $Ca(OH)_2$ precipitated. Since precipitation only occurred in the presence of the phosphonates, this is another indication that the precipitates were Ca-phosphonate complexes.

3.5.4 Experiment 4 – Adsorption Behavior of Membrane Concentrate and Its Synthetic Replicas

3.5.4.1 Adsorption of DTPMP and Orthophosphate

The aim of Experiment 4 was to analyze the respective competitive or synergistic effects of ions on phosphorus removal. To this end, batch adsorption experiments with the real membrane concentrate and its synthetic replicas were conducted. For a better understanding of the results, they have been broken down as follows: Fig. 3.4a,b show the influence of anions in the presence of and absence of GFH, and Fig. 3.4c,d show the influence of cations with and without GFH present. Fig. 3.5 shows the results for orthophosphate with the same layout.

The adsorption of DTPMP on GFH in the presence of negatively charged compounds is depicted in Fig. 3.4a. As observed in previous studies (Nowack and Stone 1999a, 1999b, 2006; Reinhardt *et al.* 2020a), the adsorption capacity decreased with increasing pH. Furthermore, in the mere presence of DTPMP (solution A), the removal was higher than in all other combinations with anions. By comparing solution A (only DTPMP in the solution) with solution B (only orthophosphate in the solution, Fig. 3.5a), a slightly higher adsorption of orthophosphate becomes apparent. This could be attributed to the large difference in molecular size.

In the presence of DTPMP and orthophosphate (solution C), the removal of DTPMP was slightly suppressed. This is in line with the findings of Nowack and Stone (2006), who observed the suppression of phosphate adsorption in the presence of phosphonates, and the lowering of phosphonate adsorption in the presence of phosphate.

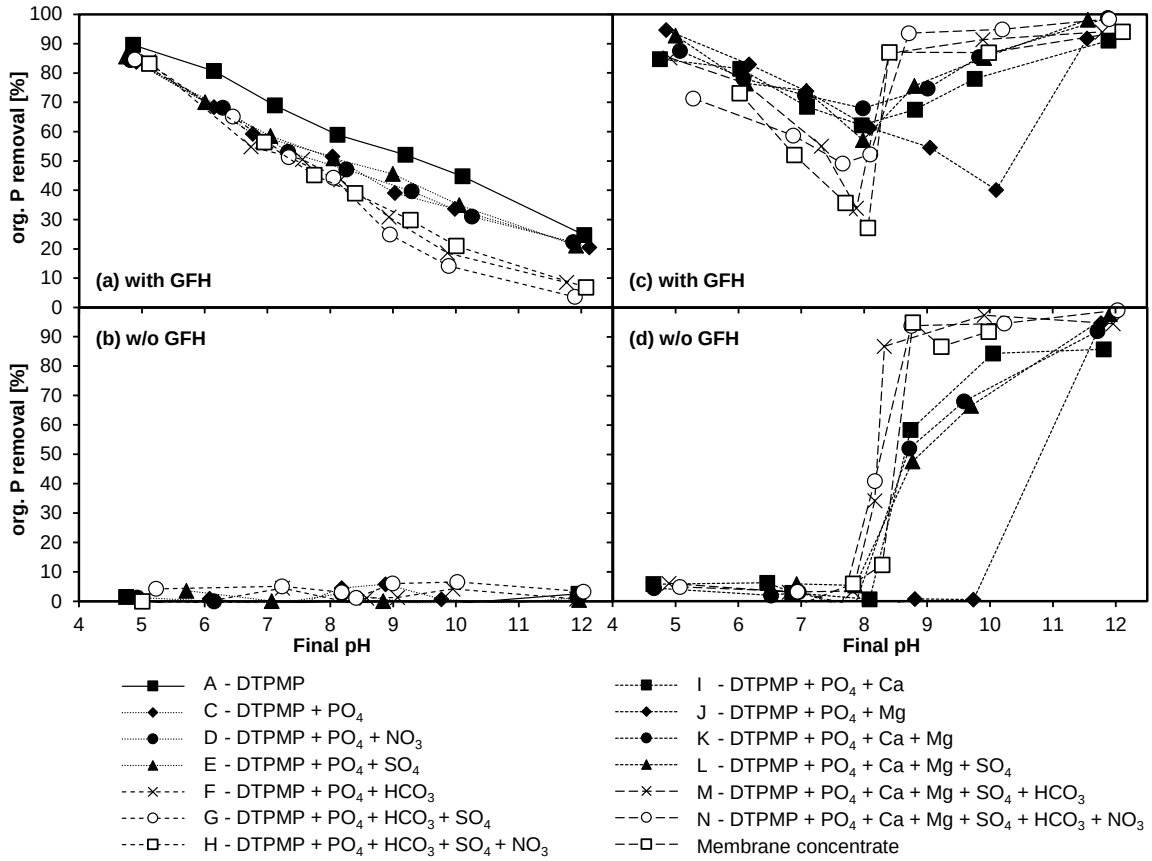

*Fig. 3.4: Organic P removal from synthetic replicas and real membrane concentrate (T = 20 °C; t_c = 7 d; initial concentrations: see Section 3.4.3; 0.1 g GFH/L and without GFH). (**a**): solutions A, C-H with GFH, (**b**): solutions A, C-H without GFH, (**c**): solutions I-N and membrane concentrate with GFH, (**d**): solutions I-N and membrane concentrate without GFH.*

3.5.4.2 Influence of Anions

When nitrate was added (solution D), no influence was observed. Although nitrate can adsorb on GFH (Rahimi *et al.* 2016), there seems to be no competition for the same adsorption sites. Similarly, Zelmanov and Semiat (2015) could not detect any influence of nitrate on the adsorption of orthophosphate on iron oxide/hydroxide nanoparticle-based agglomerates.

The presence of sulfate (solution E, Fig. 3.4a and 3.5a) also had no observable effect on the adsorption of phosphorus compounds. This is consistent with the results of Boels *et al.* (2010), who found only a minor influence of sulfate on the adsorption of NTMP on waste filtration sand, and with Boels *et al.* (2012), who observed no influence of sulfate ions on NTMP adsorption on GFH. Although only very few investigations

have been published on the effect of sulfate on phosphonate adsorption, several studies have investigated the possible competitive adsorption of sulfate and orthophosphate. According to a study by Geelhoed *et al.* (1997), in which the competitive adsorption of sulfate and orthophosphate on goethite was analyzed, phosphate proved to be much more competitive than sulfate, despite the ability of sulfate to form inner-sphere complexes. The presence of sulfate resulted only in a small decrease in phosphorus adsorption at pH < 4. Moreover, Violante *et al.* (2002) also found that sulfate competed only poorly with orthophosphate for adsorption sites of minerals and soils at pH values above 5. Genz *et al.* (2004) could not detect any influence of sulfate ions when a membrane bioreactor filtrate was spiked with sulfate prior to phosphorus removal with GFH. Thus, the results of the current study regarding the influence of nitrate und sulfate ions are in line with those found in the literature.

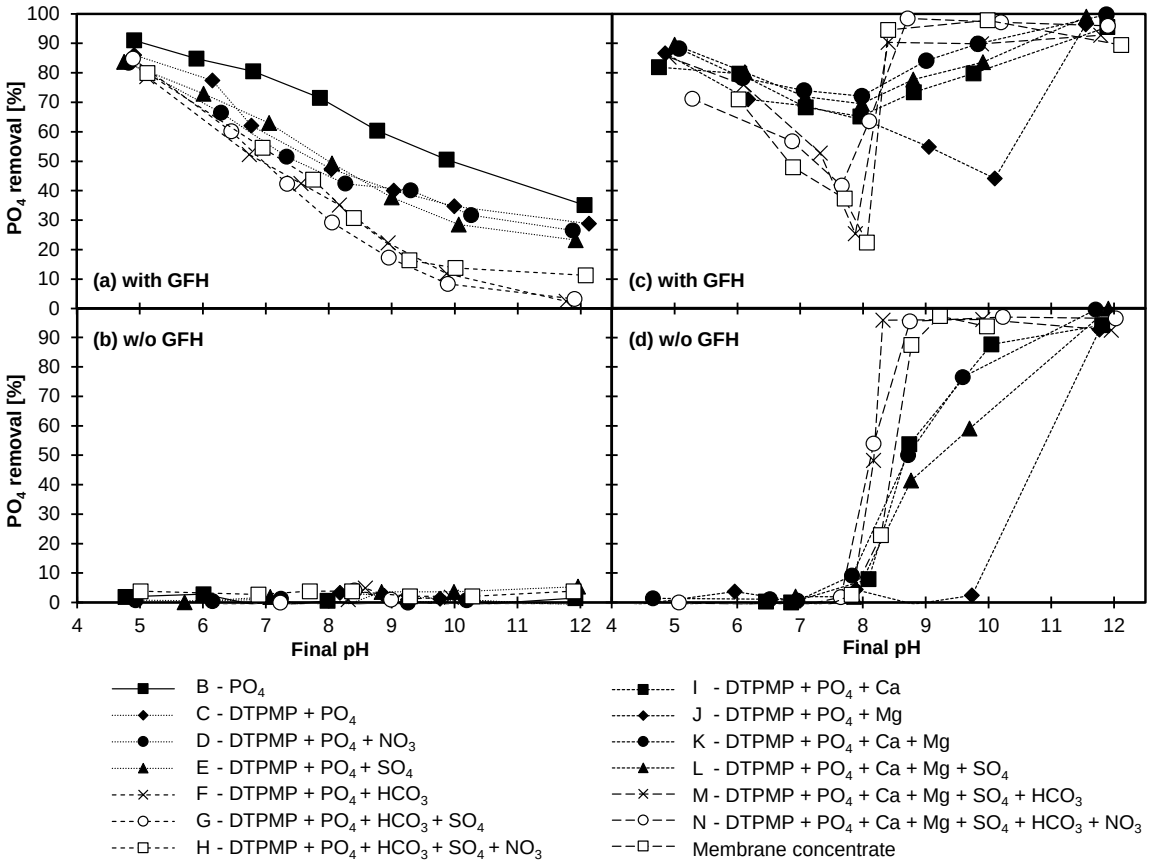

*Fig. 3.5: Phosphate removal from synthetic replicas and real membrane concentrate (T = 20 °C; t_c = 7 d; initial concentration see Section 3.4.3; 0.1 g GFH/L and without GFH). (**a**): solutions B-H with GFH, (**b**): solutions B-H without GFH, (**c**): solutions I-N and membrane concentrate with GFH, (**d**): solutions I-N and membrane concentrate without GFH.*

With the addition of (hydrogen-)carbonate (solution F, Fig. 3.4a and 3.5a), the adsorption of organic phosphorus decreased slightly at pH 5 to 7, and distinctly from pH 8 to 12. Boels *et al.* (2010) found that (hydrogen-)carbonate ions interfered with the adsorption of NTMP at low concentrations. Another study conducted by Su and Suarez (1997) found that (hydrogen-)carbonate lowered the electrophoretic mobility and reduced the pH_{PZC} of iron oxide adsorbents, suggesting inner-sphere carbonate adsorption. Lowering the pH_{PZC} would lead to greater electrostatic repulsion between DTPMP, which is highly negatively charged at high pH values, and GFH. A study investigating the adsorption of orthophosphate on iron oxide/hydroxide nanoparticle-based agglomerates showed a significant impact of (hydrogen-)carbonate concentration. Experiments with an initial P concentration of 10 ppm resulted in a residual P concentration of < 0.05 ppm with no (hydrogen-)carbonate ions, and of 0.55 ppm in the presence of 1250 ppm (hydrogen-)carbonate ions (pH 7.5) (Zelmanov and Semiat 2015). This is also in line with the findings of Chitrakar *et al.* (2006), who stated the order of selectivity for phosphate adsorption on goethite at pH 8 as Cl^-, NO_3^-, SO_4^{2-} << CO_3^{2-}, HPO_4^{2-}. A study investigating the adsorption of carbonate found that phosphate has a higher affinity towards ferrihydrite than carbonate. A high concentration of carbonate ions was needed before a significant suppression of phosphate adsorption was observable, which increased with increasing pH (Mendez and Hiemstra 2019). In the current study, such a high concentration of (hydrogen-)carbonate ions was present. The increased competition for adsorption sites at pH > 8 could be attributed to the presence of bivalent CO_3^{2-} ions and the resulting greater electrostatic attraction. The additional presence of sulfate (solution G) or sulfate and nitrate (solution H) resulted in no further reduction of adsorption. Fig. 3.4b and 3.5b show that, without GFH, there was no noteworthy removal of organic phosphorus and phosphate. Thus, precipitation can be excluded.

3.5.4.3 Influence of Cations

Fig. 3.4c,d and 3.5c,d show the effect of the two hardness ions calcium and magnesium on the removal of DTPMP and phosphate in the presence of and absence of GFH. The figures also illustrate the effect of the two cations in combination with the previously investigated anions up to a near-complete synthetic replication of the membrane concentrate, as well as with the original membrane concentrate.

As shown in Fig. 3.4c and 3.5c, a noticeable change was observed with the addition of cations, indicating a possible synergistic interaction. The distinct tendency towards a drastically enhanced adsorption at pH values > 8 even resulted in a removal increase of up to > 60 percentage points (e.g., at pH 12, from ~30% (solution C) to > 90% in the presence of Ca^{II} (solutions I to N)). However, at pH values > 8, a removal was also observable without GFH (Fig. 3.4d and 3.5d). Thus, precipitation must have occurred in some form at pH > 8.

Interestingly, up to pH 8, the combination of DTPMP, PO_4-P, and Ca^{II} (solution I) resulted in a higher removal of organic phosphorus than the combination of only DTPMP and PO_4-P (solution C). The higher removal was comparable to the removal achieved for solution A (mere presence of DTPMP). The same kind of effect was observed with the solution with additional Mg^{II} (solution J, up to pH 10) and the solution with additional Ca^{II} and Mg^{II} combined (solution K). Up to pH 8, however, no removal by precipitation was observed in the absence of GFH (Fig. 3.4d and 3.5d). Thus, at pH < 8, the enhanced removal by Ca^{II} and Mg^{II} ions must have been due mainly to the formation of ternary complexes (Martínez and Farrell 2017). These results stand in agreement with those of previous studies that have shown that excess Ca^{II} concentrations can substantially increase the maximum surface coverage of phosphonates (Nowack and Stone 1999b; Boels *et al.* 2010; Chen *et al.* 2017; Rott *et al.* 2018a). Various studies have attributed this behavior to the formation of ternary complexes. Excess magnesium is known to have similar effects (Lin *et al.* 2020).

3.5.4.4 Combined Influence of Anions and Cations

The additional presence of sulfate ions (solution L) did not lead to altered behavior. When (hydrogen-)carbonate was added to solutions with Ca^{II} and Mg^{II} (solutions M and N), up to pH 8, a lower removal of organic phosphorus and PO_4-P was observed as compared with other solutions containing cations (solutions I to L). This supports the already noted assumption that (hydrogen-)carbonate is a competing ion for phosphonates.

Above pH 8, on the other hand, even in the absence of GFH, organic phosphorus and PO_4-P was removed (Fig. 3.4d and 3.5d). This proves that the removal observed in this pH range in the presence of GFH must have at least in part been attributable to

precipitation. A calcium concentration of 15.3 mmol/L in solutions I to N resulted in a molar Ca:DTPMP ratio of about 3200:1. This very high ratio was not investigated in Experiment 3, but given the tendency of the results in Tab. 3.5, it seems possible that above a certain molar Ca:DTPMP ratio, precipitation will occur even at low DTPMP concentrations. Furthermore, since orthophosphate was present in all solutions, the precipitation of hydroxyapatite ($Ca_5(PO_4)_3OH$) was likely at pH > 8 (calculations performed in PHREEQC). Therefore, the enhanced removal for the solutions I, K, and L at pH > 8 can be ascribed to the precipitation of hydroxyapatite and/or Ca-DTPMP complexes. Both of these precipitates would lead to a removal of organic phosphorus, either by direct precipitation (Ca-DTPMP complexes) or adsorption on the precipitate (hydroxyapatite) (Bartels *et al.* 1979). In the absence of calcium but with magnesium present (solution J), the observed precipitation was shifted towards the more alkaline pH range (pH > 10), which is consistent with the observation that in the presence of GFH at pH > 10 an increased removal occurred. Calculations performed with PHREEQC predict precipitation of $Mg(OH)_2$, which is a known adsorbent for phosphorus compounds (Lin *et al.* 2019), from pH 10 onwards.

With additional (hydrogen-)carbonate ions (solutions M and N), a stronger removal and, thus, a stronger precipitation occurred, compared with the previously discussed solutions (without GFH, Fig. 3.4d and 3.5d). Calculations performed with PHREEQC, without taking DTPMP into account, showed that the solubility limit of $CaCO_3$, dolomite ($CaMg(CO_3)_2$), and hydroxyapatite was exceeded in solutions M and N from pH 7 onwards. Since no precipitation occurred at pH 7, this precipitation must have been impeded by the phosphonate. Above pH 8, however, these three compounds could be precipitated and all of them, as possible adsorbents, could have led to the removal of phosphorus (Bartels *et al.* 1979; Chirby *et al.* 1988; Kan *et al.* 2005; Karaca *et al.* 2006; Xu *et al.* 2014). In keeping with the enhanced precipitation observed at pH > 8, removal also increased in the batches with GFH at higher pH values (Fig. 3.4c and 3.5c).

The behavior of solution N, the near-complete synthetic replica of the membrane concentrate, and the real membrane concentrate were very similar. Therefore, it can be concluded that all ions that strongly influence phosphonate adsorption were considered in the replica. In conclusion, the competing effect of anions present in the membrane concentrate on phosphonate adsorption can be ranked as follows: HCO_3^- >> SO_4^{2-}, NO_3^-. Particularly at pH values > 8, Ca^{II} has a positive effect on phosphorus

removal, mainly due to precipitation. The same applies to Mg^{II} at pH values > 10. The influence of the investigated ions on adsorption of DTPMP and PO_4-P is nearly identical.

3.6 Conclusions

The influence of different compounds in membrane concentrate on the adsorption of phosphonates and phosphate on GFH was investigated. Of all phosphonates tested, HEDP was the phosphonate with the lowest calcium tolerance (precipitation already at a molar Ca:HEDP ratio of 2:1 after seven days contact time). The calcium already contained in the GFH plays an essential role in the removal process, as it can be redissolved, causing a positive effect on the removal of phosphonates. A further increase in Ca^{II} concentration also caused precipitation of the phosphonates NTMP and DTPMP at pH values > 8, likely as Ca-phosphonate complexes. NTMP and DTPMP showed a similar adsorption behavior, but the solubility of Ca-NTMP complexes was lower than that of Ca-DTPMP complexes. Experiments with membrane concentrate and its synthetic replicas showed that HCO_3^- has a competing effect on phosphorus adsorption, whereas the influence of SO_4^{2-} and NO_3^- is negligible. Up to pH 8, the presence of Ca^{II} has a positive effect on adsorption, probably due to the formation of ternary complexes. The presence of Ca^{II} (at pH > 8) and Mg^{II} (at pH > 10) led to the formation of precipitates that served as adsorbents for phosphorus compounds, either through direct precipitation of Ca-phosphonate complexes, or through the formation of inorganic precipitates of calcium, magnesium, and phosphate. An additional presence of (hydrogen-)carbonate ions resulted in precipitation of $CaCO_3$ and/or dolomite, which also acted as adsorbents for phosphorus compounds. The influence of the investigated ions on the adsorption of DTPMP and PO_4-P is nearly identical. It can be assumed that membrane concentrate with its high content of Ca^{2+} and Mg^{2+} is well suited for treatment with GFH. Since Ca^{II} is redissolved from GFH, future experiments should examine whether sufficient phosphonate is still removed after multiple use. In addition, it is important to investigate whether the precipitates interfere with the adsorption or regeneration process.

3.7 Funding and Acknowledgment

We would like to acknowledge our gratitude to the Willy-Hager-Stiftung, Stuttgart, for their financial support. We would like to thank HeGo Biotec GmbH for providing adsorbent samples, and Zschimmer & Schwarz Mohsdorf GmbH & Co. KG for supplying us with phosphonate samples.

3.8 Supplementary Material

3.8.1 Standard Deviations

Experiment 3 was carried out in a duplicate approach. Tab. S3.1 and S3.2 show the sample standard deviations of the results. The sample standard deviation was calculated according to Eq. S3.1, where N is the number of observations on the sample, x_i the observed sample value, and $\bar{x}$ the mean value of these observations.

$$s = \sqrt{\frac{1}{N-1}\sum_{i=1}^{N}(x_i - \bar{x})^2}, \quad \text{(S3.1)}$$

Tab. S3.1: Removal of NTMP by precipitation at different calcium concentrations and pH values with standard deviations (T = 20 °C; t_c = 7 d; no GFH added).

	NTMP [mg/L]							
	3.22	**16.1**	**32.2**	**80.5**	**3.22**	**16.1**	**32.2**	**80.5**
	Removal at pH 8 [%]				**Removal at pH 9 [%]**			
Ca:NTMP 0:1	0.6±1.1	-0.1±0.5	1.1±0.0	0.0±0.4	2.6±0.3	0.2±0.2	0.7±0.7	2.4±1.0
Ca:NTMP 1:1	2.6±1.8	0.3±0.1	1.5±0.1	1.1±0.2	-1.2±0.1	0.2±0.3	0.8±0.2	2.2±0.3
Ca:NTMP 2:1	0.9±0.5	0.2±0.5	1.4±0.1	0.8±0.2	-0.3±0.4	1.4±0.6	1.9±0.2	91.3±0.2
Ca:NTMP 5:1	1.5±0.2	1.2±0.2	1.7±0.1	98.7±0.6	4.3±0.8	1.6±1.3	78.2±1.9	99.4±0.3
Ca:NTMP 10:1	0.7±0.2	2.6±2.2	95.4±2.1	99.5±0.5	3.6±1.1	63.7±0.4	99.6±0.2	99.5±0.1
Ca:NTMP 25:1	1.1±2.4	94.0±0.2	99.0±0.0	99.7±0.1	2.7±0.6	97.0±1.9	100.1±0.2	100.1±0.3
Ca:NTMP 60:1	0.3±0.4	96.6±2.2	99.4±0.0	99.6±0.0	2.0±0.4	98.6±0.7	100.4±0.0	100.1±0.0

Tab. S3.2: Removal of DTPMP by precipitation at different calcium concentrations and pH values with standard deviations (T = 20 °C; t_c = 7 d; no GFH added).

	DTPMP [mg/L]							
	3.22	**16.1**	**32.2**	**80.5**	**3.22**	**16.1**	**32.2**	**80.5**
	Removal at pH 8 [%]				**Removal at pH 9 [%]**			
Ca:DTPMP 0:1	-1.5±0.6	-1.1±1.3	-1.2±1.0	-0.6±0.4	-1.6±0.1	0.1±0.1	1.8±2.3	-0.6±0.2
Ca:DTPMP 1:1	-1.4±0.4	1.4±1.5	-4.0±1.1	-1.3±0.7	1.7±4.8	-0.3±0.3	3.7±3.3	-.03±0.1
Ca:DTPMP 2:1	-0.1±0.6	-0.8±1.5	-3.9±0.3	-0.8±0.4	-1.5±0.0	0.2±0.3	-1.5±0.0	-0.3±0.5
Ca:DTPMP 5:1	0.0±1.2	1.0±1.4	0.5±1.5	0.0±0.3	-1.4±0.1	-0.3±0.5	-1.5±1.3	61.9±1.9
Ca:DTPMP 10:1	0.3±0.4	0.0±0.7	-0.1±0.0	73.8±0.3	-4.5±3.0	0.3±0.3	47.0±0.3	91.2±0.3
Ca:DTPMP 25:1	-1.2±0.7	-0.6±3.6	55.6±1.4	90.3±0.1	-1.2±1.6	0.3±0.3	87.7±0.6	94.3±0.1
Ca:DTPMP 60:1	0.0±0.4	54.2±0.2	83.7±0.3	93.3±0.6	-6.2±2.4	84.7±0.2	92.2±0.1	95.6±0.1

4 Fixed-Bed Column Studies of Phosphonate and Phosphate Adsorption on Granular Ferric Hydroxide (GFH)

This Chapter has been published as:

Reinhardt, T., Rott, E., Schneider, P. A., Minke, R. and Schönberger, H. 2021 Fixed-Bed Column Studies of Phosphonate and Phosphate Adsorption on Granular Ferric Hydroxide (GFH). *Process Safety and Environmental Protection*, **153**, 301–310. https://doi.org/10.1016/j.psep.2021.07.027.

4.1 Research Questions

- Is NaOH as regeneration solution reusable over many cycles?
- Can precipitation be prevented by lowering the pH of the membrane concentrate?
- Can the precipitates be removed subsequently with a novel regeneration method using HCl?

4.2 Abstract

The use of phosphonates as antiscalants in membrane processes is common. Before they are discharged into the receiving water, they should be removed from the membrane concentrate to protect the aquatic environment. This study conducted fixed-bed column experiments on the adsorption of diethylenetriaminepenta(methylene phosphonic acid) (DTPMP) and orthophosphate on granular ferric hydroxide (GFH). The objective was to investigate the adsorption and desorption performance using real membrane concentrate, while testing both the usability of the GFH and that of the regeneration solutions over multiple cycles. Whereas a synthetic solution with DTPMP allowed almost complete regeneration, the adsorption performance with real membrane concentrate at the original pH ≅ 8 decreased significantly. This could be attributed to the precipitation of calcium compounds which disturbed the adsorption/desorption process. With the introduction of a novel acidic regeneration step to remove the precipitates, an adsorption performance of 95% over 20 cycles was achieved. The hydrochloric acid (HCl) can be reused when its pH is kept constant by a pH control. The sodium hydroxide solution (NaOH) for alkaline regeneration can be reused several times. However, the desorption performance decreased significantly when its electrical conductivity dropped below 90 mS/cm. Replacing the NaOH regularly can significantly improve the desorption performance.

4.3 Introduction

The global consumption of phosphonates increased by almost 70% from 1998 (56,000 t/yr) to 2012 (94,000 t/yr) (Davenport *et al.* 2000; Nowack 2003; EPA 2013). Since 2017, EU Regulation No 648/2004 has limited the use of phosphorus to a maximum of 0.3 g per standard dose in consumer automatic washing detergents (EU 2004). In Germany alone, this has led to an increase in the use of phosphonates in detergents, cleaning and maintenance products by over 60% from 4,673 tons in 2015 to 7,613 tons in 2019 (IKW 2021). It can therefore be assumed that phosphonate consumption has increased significantly across Europe since the estimate by EPA (2013). This increase puts phosphonates under increased scientific and regulatory attention (Rott *et al.* 2018c). In addition to their consumption in many industrial processes, phosphonates are frequently used in drinking water treatment as complexing agents for softening processes (Nowack and Stone 1999a; Boels 2012; Armbruster *et al.* 2019).

The resulting concentrates are often discharged into receiving waters without treatment (Squire 2000; Nederlof and Hoogendoorn 2005; Greenlee *et al.* 2009). Phosphonates, however, are known to adsorb and accumulate on sediment in rivers (Rott *et al.* 2020b). While phosphonates are often poorly biodegradable, they would likely contribute to the eutrophication of water bodies due to degradation by UV radiation (Lesueur *et al.* 2005; Kuhn *et al.* 2018; Rott *et al.* 2018c).

Phosphonates are known to adsorb well on mineral surfaces such as iron (hydr)oxides (Fischer 1991; Nowack and Stone 1999a). Several studies have been conducted on the adsorption of phosphonates and phosphate on granular ferric (hydr)oxide (GFH) in batch experiments (Genz *et al.* 2004; Sperlich 2010; Boels 2012; Chen *et al.* 2017; Reinhardt *et al.* 2020b). Adsorption capacities from these batch experiments are usually estimated under equilibrium conditions, which could take from several minutes up to many days to achieve (Nowack and Stone 1999a; Boels 2012; Chen *et al.* 2017). Additionally, since the experiments are often performed under different conditions, it is difficult to compare the adsorption capacities (Kumar *et al.* 2019). So far, there have been few studies on the adsorption/desorption behavior of phosphonates on GFH in fixed-bed columns over several cycles (Boels 2012; Chen *et al.* 2017; Reinhardt *et al.* 2020a). Reusability of adsorbents, however, is important for economic and environmental reasons (Kumar *et al.* 2018). To investigate the reusability, experiments with multiple adsorption/desorption cycles using an appropriate regeneration mode are a suitable approach. Batch experiments have shown that phosphonates and orthophosphate could be desorbed from GFH with sodium hydroxide solution (NaOH) (Boels 2012; Chen *et al.* 2017; Reinhardt *et al.* 2020a).

In a previous study, Reinhardt *et al.* (2020b) showed that, in addition to adsorption of phosphonates and orthophosphate from the membrane concentrate on GFH, calcium-containing precipitates can form and calcium can redissolve from the GFH. It is unclear whether these precipitates interfere with adsorption and whether the GFH can be used repeatedly despite this calcium redissolution.

Therefore, this study focuses on column experiments for the adsorption of phosphorus as both phosphonate and orthophosphate from a synthetic solution and real membrane concentrate onto GFH. The membrane concentrate used in this study contains the phosphonate diethylenetriaminepenta(methylene phosphonic acid) (DTPMP) as well

as orthophosphate and has a high water hardness. The chemical structure of DTPMP is shown in Fig. 4.1. The objective of the study was to investigate the adsorption and desorption performance of fixed-bed GFH columns fed with real membrane concentrate. For this purpose, different types of alkaline regeneration with sodium hydroxide solution were first examined. Due to the high water hardness of the membrane concentrate, calcium-containing precipitates may occur. Therefore, two different approaches were considered to prevent or redissolve these precipitates. To prevent precipitation, the pH of the membrane concentrate was lowered to 6, and in addition to the common alkaline regeneration, a novel approach for phosphonate loaded GFH with an additional acidic regeneration step was investigated to redissolve possible precipitates. This approach was previously suggested for the desorption of orthophosphate from GFH in experiments with calcium precipitates (Kunaschk *et al.* 2015; Kumar *et al.* 2018). Lastly, an attempt was made to optimize the desorption performance by replacing the sodium hydroxide solution. The columns were operated for up to 24 cycles.

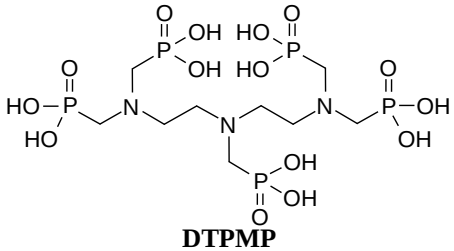

DTPMP
Diethylenetriaminepenta(methylene phosphonic acid)

Fig. 4.1: Chemical structure of DTPMP.

4.4 Materials and Methods

4.4.1 Reagents and Chemicals

HCl (32%, AnalaR NORMAPUR) was purchased from VWR Chemicals (Fontenay-sous-Bois, France). Sulfuric acid (95–97%, EMSURE, Ph. Eur.), NaOH (≥ 99%, Ph. Eur.), and ethylenedinitrilotetraacetic acid disodium salt dihydrate (EDTA-Na_2 dihydrate, Titriplex III, 99–101%, Ph. Eur.) were obtained from Merck (Darmstadt, Germany). The buffer 4-(2-hydroxyethyl)-1-piperazinepropanesulfonic acid (EPPS) (≥ 99.5%) was purchased from SigmaAldrich (St. Louis, MO, USA) and DTPMP (16%

water of crystallization) was supplied by Zschimmer & Schwarz Mohsdorf (Burgstädt, Germany).

All solutions were prepared with deionized water, which was prepared from drinking water using ion exchange (Seradest SD 2000) and filtration (Seralpur PRO 90 CN).

4.4.2 Adsorbent

FerroSorp RW from HeGo Biotec GmbH (Berlin, Germany) was used in all experiments, owing to its high phosphonate adsorption capacity (Reinhardt *et al.* 2020a). To remove GFH dust, the adsorbent was washed with deionized water over a sieve prior to use until the water became clear, then air-dried. A maximum permitted loss of 3 mass-% of the adsorbent as ultra-fine particles during rinsing was ensured by selecting a suitable screen mesh size. The FerroSorp RW had a final grain size of 0.5–2.5 mm, a specific surface area of 210 m²/g, and a point of zero charge (pH_{PZC}) of 8.6. The calcium content was 12–19% (mainly as $CaCO_3$), according to the manufacturer.

4.4.3 Membrane Concentrate

The membrane concentrate was taken from a public waterworks that operates a low-pressure reverse osmosis (LPRO) plant to reduce water hardness. The membrane concentrate was a clear (0.28±0.23 NTU) and colorless solution that showed a low organic load with a COD of 16.0±0.2 mg/L. It had an exceptionally high water hardness, due to very high concentrations of 594±42 mg/L Ca^{2+} and 86.9±10.5 mg/L Mg^{2+}, and a high buffer capacity (alkalinity: 25.3±1.7 mmol/L). The electrical conductivity of the sample was 3.18±0.15 mS/cm, the pH was approximately 7.9, the SO_4^{2-} concentration 463±120 mg/L, the NO_3^- concentration 67.7 mg/L, and the Cl^- concentration 231±33 mg/L. Since the total P of both the filtered and raw sample were the same (1.32±0.06 mg/L), the incoming particulate P fraction was negligible. The o-PO_4-P fraction was 0.55±0.02 mg/L and, by difference, the organic P fraction amounted to 0.77±0.05 mg/L P. The analytical values given are from analyses of the membrane concentrate on four different sampling days. Since the antiscalant (DTPMP) is added to the raw water in the waterworks at a dosage of 0.6 mg/L and the average yield of the LRPO is ~80%, the added antiscalant is concentrated by a factor of five and the

membrane concentrate thus contains approximately 3 mg/L DTPMP. As this corresponds to 0.81 mg/L DTPMP-P, it is assumed that almost the entire organic P fraction consisted of DTPMP. Weekly samples were taken and stored in sealed 5-L HDPE canisters. They were filled to the maximum, minimizing the headspace, so that to minimize interaction with gas phase CO_2.

In addition, a synthetic solution containing 0.77 mg/L DTPMP-P was used as it is present in the real membrane concentrate. Since synthetic wastewater does not have the buffering capacity of real wastewater, an organic buffer (0.01 M EPPS) was added to maintain pH during the adsorption experiments. The influence of EPPS on the adsorption of DTPMP on GFH, as well as on phosphorus analysis, was found to be negligible in previous batch experiments (Rott *et al.* 2018b). The pH was adjusted with NaOH.

4.4.4 Experimental Procedure

Column experiments were performed with both a synthetic solution and real membrane concentrate. A process schematic of the experimental setup can be seen in Fig. 4.2, showing the adsorption process on the left and the various regeneration options on the right. The Plexiglas columns, with an inner diameter of 1.6 cm, were filled with 5.3 g FerroSorp RW resulting in 10 mL of bed volume (BV) and a bed height of 5 cm. Glass wool and a stainless steel mesh were installed below and above the adsorbent to secure it in the column. The columns, operated in an up-flow mode, were fed with the phosphonate-bearing solution from a 10-liter glass bottle by a peristaltic pump with a flow rate range of 0.21–21 mL/min (Ismatec IPC, Wertheim, Germany). The empty bed contact times (EBCTs) and hence the flow rates were chosen to result in a cycle duration of 24 h and with the aim of maintaining the effluent concentration at $c/c_0 < 0.2$ over multiple cycles. Total P, orthophosphate-P, and pH were analyzed in regularly sampled effluent flow. Each sample consisted of 10 min of accumulated outflow from the column.

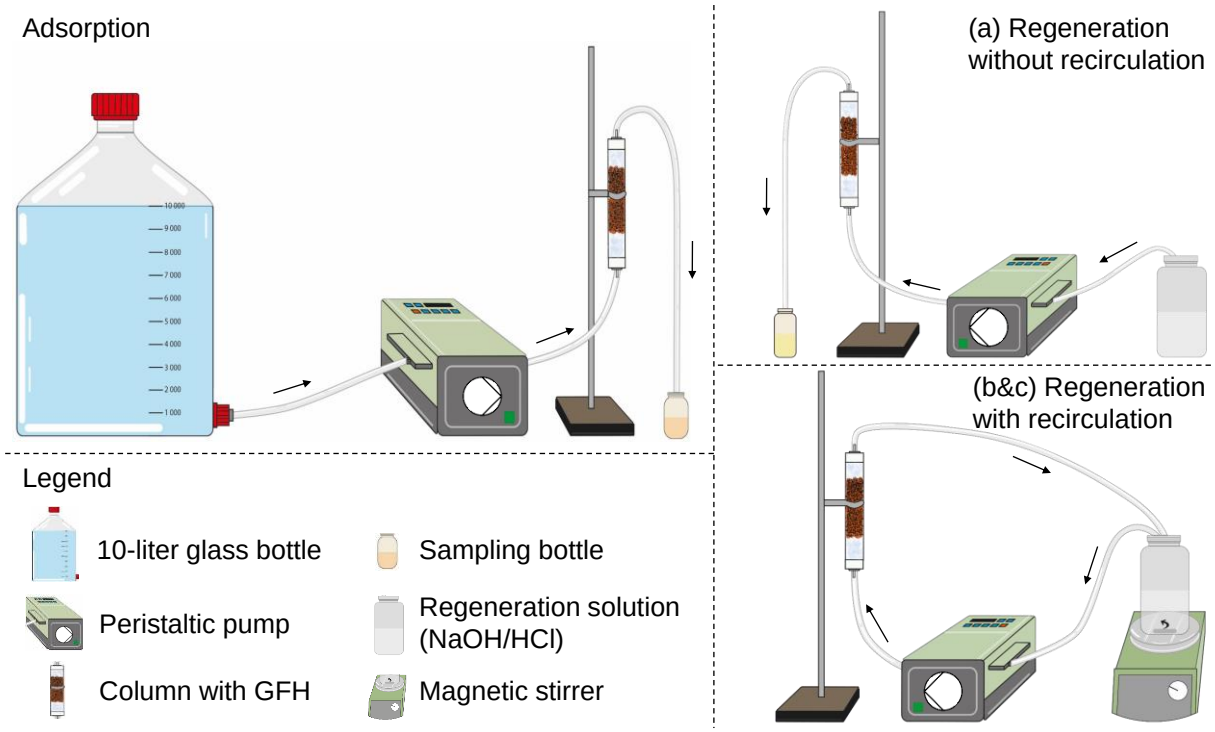

Fig. 4.2: Schematic diagram of experimental setup.

In this study, alkaline regeneration was used to desorb phosphonate and orthophosphate ions and acidic regeneration was applied to remove calcium-containing precipitates. The alkaline regeneration was performed with 1 M NaOH at an upward feed flow rate of 21 mL/min. Three different types of alkaline regeneration were investigated. In regeneration method (a), fresh 1 M NaOH was used for regeneration in each cycle (Fig. 4.2 (a)). In method (b), fresh 1 M NaOH was used for each cycle, but the NaOH was recirculated during the regeneration step. Finally, in method (c), the same NaOH was recirculated for all cycles without replacing it (Fig. 4.2 (b&c)). In all experiments, 200 mL of NaOH was used and in regeneration methods (b) and (c), this was stirred during the regeneration step. Before and after the alkaline regeneration, the columns were rinsed with 20 BV of tap water to avoid precipitation resulting from direct contact between the membrane concentrate and NaOH. The columns were stored in tap water over the weekends.

The acidic regeneration step was conducted with hydrochloric acid (HCl) at pH 2.5 (3.16 mM HCl) at feed flow rate of 21 mL/min (Fig. 4.2 (b&c)). In the experiments where the pH of the HCl was controlled, a 1 M HCl refresh solution was added using a Dosimat (Metrohm, Herisau, Switzerland) dosing pump. Specialized software, a

Greisinger GMH 3530 pH meter and a GE probe with integrated temperature compensation (GHM Messtechnik GmbH, Regenstauf, Germany) were employed in the pH feedback controller.

Experiment 1 (columns A–C) served to investigate the influence of the three different alkaline regeneration methods described above using a synthetic DTPMP solution. In Experiment 2 (columns D&E), column experiments were performed with membrane concentrate at initial pH ≅ 8, and adjusted to pH 6 with HCl to investigate the effect of pH on the extent of precipitation. In Experiment 3 (columns F1–G2), an acidic regeneration step was introduced to evaluate the removal of surface precipitates. This involved two approaches: the use of fresh HCl in each cycle vs. reuse of HCl over all cycles with pH control (addition of 1 M HCl) to stabilize the solution to pH ≅ 2.5. Thus, a possible reduction of HCl consumption was investigated. This experiment was carried out in duplicate. The objective of Experiment 4 (column H) was to investigate whether the efficiency of regeneration could be improved by replacing the NaOH when its electrical conductivity dropped below 90 mS/cm. A detailed overview of the operational parameters of the different columns in Experiments 1–4 can be found in Tab. 4.1, the feed flow rates as well as the concentrations of NaOH and HCl were selected by preliminary experiments.

Organic P concentrations in mg/L were calculated according to Eq. 4.1:

$$c(\text{organic P}) = c(\text{dissolved P}) - c(\text{o-PO}_4\text{-P}) \quad (4.1)$$

The cumulative adsorption efficiency (in %) was calculated according to Eq. 4.2:

$$\text{Eff}_{\text{ads}} = \frac{\sum_{i=1}^{n} m_{\text{P,ads,i}}}{\sum_{i=1}^{n} m_{\text{P,in,i}}} 100\% \quad (4.2)$$

where $m_{P,ads,i}$ and $m_{P,in,i}$ are the total P loads (in mg) adsorbed in cycle *i* and fed into the column with the influent, respectively, and *n* the number of cycles. The adsorbed total P load $m_{P,ads,i}$ in each cycle was calculated by plotting the column effluent concentration versus bed volumes. The area under the curve was determined and then subtracted from the load that had entered the column, which gives the amount adsorbed.

The cumulative desorption efficiency (in %) was calculated following Eq. 4.3:

$$Eff_{des} = \frac{\sum_{i=1}^{n} m_{P,des,i}}{\sum_{i=1}^{n} m_{P,ads,i}} 100\% \quad (4.3)$$

where $m_{P,des,i}$ and $m_{P,ads,i}$ are the total P loads (in mg) desorbed and adsorbed in cycle *i*, respectively, and *n* the number of cycles. The desorbed total P load $m_{P,des,i}$ in each cycle was calculated by multiplying the NaOH volume with the total P concentration in the regeneration solution. The desorbed loads from previous cycles were subtracted from this.

Tab. 4.1: Operational parameters of columns in Experiments 1–4.

	Experiment							
	1			2		3		4
	Column							
	A	B	C	D	E	F1&2	G1&2	H
Adsorption								
Inflow DTPMP-P [mg/L]	0.77	0.77	0.77	0.77 ±0.05	0.77 ±0.05	0.77 ±0.05	0.77 ±0.05	0.77 ±0.05
Inflow PO_4-P [mg/L]	-	-	-	0.55 ±0.02	0.55 ±0.02	0.55 ±0.02	0.55 ±0.02	0.55 ±0.02
Inflow total P [mg/L]	0.77	0.77	0.77	1.32 ±0.06	1.32 ±0.06	1.32 ±0.06	1.32 ±0.06	1.32 ±0.06
pH	8	8	8	8	6	8	8	8
Flow rate [mL/min]	3.33	3.33	3.33	3.33	3.33	2.5	2.5	2.5
BV [mL]	10	10	10	10	10	10	10	10
BV/h	20	20	20	20	20	15	15	15
EBCT [min]	3	3	3	3	3	4	4	4
Duration [h]	21.5	21.5	21.5	23	23	20	20	20
Alkaline regeneration (1 M NaOH)								
Flow rate [mL/min]	21	21	21	21	21	21	21	21
Duration [min]	120	120	120	15	15	15	15	15
Regeneration method	(a)	(b)	(c)	(c)	(c)	(c)	(c)	(c)
Acidic regeneration (HCl pH 2.5)								
Flow rate [mL/min]	-	-	-	-	-	21	21	21
Duration [h]	-	-	-	-	-	3	3	3
Recirculation with pH control	-	-	-	-	-	no	yes	no
Total adsorption/desorption cycle								
Cycle duration [h]	24	24	24	24	24	24	24	24
Number of cycles	17	17	17	8	20	20	20	24
Number of weeks	5	5	5	2	5	5	5	6

4.4.5 Analytical Methods

A modification of the molybdenum blue method (ISO 6878) was used for phosphorus analysis (ISO_{mini}), which was thoroughly described by Rott *et al.* (2018b). Before the analysis, any glassware that came in contact with the sample was carefully rinsed with 10% HCl and deionized water. The samples analyzed for total P were digested in a HachLange HT200S thermostat. Absorbance measurements were performed using a Macherey-Nagel Nanocolor UV/VIS II spectrophotometer. The strongly alkaline regeneration solution was analyzed by the original ISO 6878 method. For pH determination, a WTW SenTix 81 pH electrode was used in combination with the WTW pH91 instrument. Electrical conductivity was measured using the WTW TetraCon 925 conductivity electrode in combination with the WTW Multi 3430 meter. For Ca^{2+} determination, a sample volume of 50 mL of the solution to be analyzed was pipetted into an Erlenmeyer flask (DIN 38406-3). Then, 2 mL of a 2 M NaOH and a spatula tip of indicator were added to the flask. This solution was titrated with 0.01 M EDTA solution under stirring until a complete color change was observed. Iron analysis was performed with a Spectroquant Iron Test, the sample was pre-treated with a Spectroquant Crack Set 10 (Merck, Darmstadt, Germany).

4.5 Results and Discussion

4.5.1 Experiment 1 – Influence of Different Alkaline Regeneration Methods

Fig. 4.3 shows the performance of the 17 adsorption/desorption cycles with the synthetic solution, using three different regeneration methods. Over the 17 adsorption cycles, a total of 54.1 mg P entered each column. The cumulative adsorption performance over all cycles was 92, 91, and 90% for regeneration methods (a), (b), and (c), respectively. Therefore, all three columns demonstrated effective and comparable adsorption performance. The adsorption performance decreased linearly over the 17 cycles. In column C, for example, adsorption efficiency was only 83% in the 17^{th} cycle. This could be attributed to the linearly increasing residual load on the GFH due to the incomplete regeneration, which already occupies adsorption sites. This may also indicate that the EBCT of 3 min for experiments at pH 8 is too short to achieve satisfying effluent values.

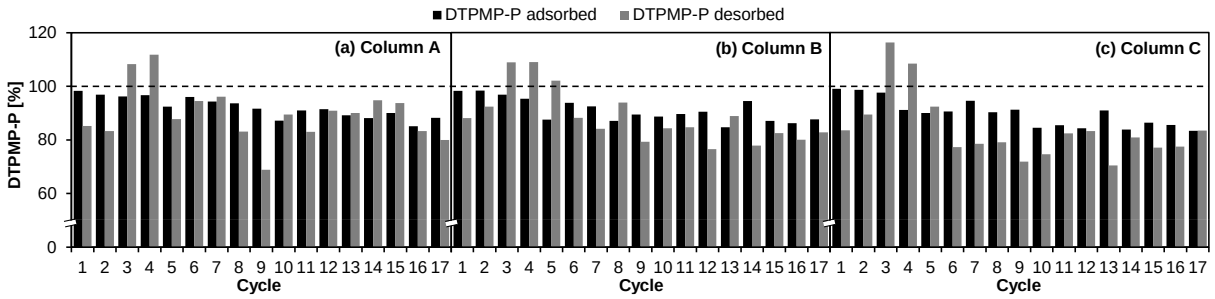

Fig. 4.3: Performance of 17 adsorption/desorption cycles with synthetic solution (adsorption: synthetic solution with 0.77 mg/L DTPMP-P, pH 8, 3 min EBCT; alkaline regeneration: 1 M NaOH, 120 min). (a) Regeneration with fresh NaOH in each cycle, no recirculation of NaOH; (b) regeneration with fresh NaOH in each cycle, recirculation of NaOH; (c) no replacement of NaOH, recirculation of NaOH. Dashed line shows inflow (100%).

GFH belongs to the group of oxidic adsorbents, consisting of crystalline structures. In these adsorbents, negatively charged oxygen or hydroxide ions and positively charged metal ions are ordered in such a way that their positive and negative charges compensate each other. However, this regular structure is disturbed at the surface and the charges have to be neutralized by protons and hydroxide ions in aqueous solutions. Thus, the surface of oxidic adsorbents such as GFH is covered with surface OH groups. Subject to the pH of the solution, these surface OH groups undergo protonation or deprotonation. At pH_{PZC}, which is 8.6 for the GFH used in this study, the total net surface charge equals zero (Worch 2012). Adsorption of phosphonates on GFH can be both physical, i.e., by electrostatic attraction and hydrogen bonding with the surface OH groups, and chemical, i.e., by ligand exchange with the surface OH groups and covalent bonds with metallic cations (Chen *et al.* 2017; Martínez and Farrell 2017). The same applies to the adsorption of phosphate (Kumar *et al.* 2019). At the pH values investigated in this study ranging from 6 to 8, phosphonates and phosphate are present as negatively charged anions. Therefore, their adsorption is favored at pH values below pH_{PZC}, since the surface of the GFH is then positively charged and electrostatic attraction occurs. To reverse the adsorption process, 1 M NaOH was used, as this is considered as common practice for the regeneration of GFH materials and was confirmed by preliminary experiments (Kartashevsky *et al.* 2015; Kunaschk *et al.* 2015; Kalaitzidou *et al.* 2016; Chen *et al.* 2017). The increase in pH by the 1 M NaOH leads to an increase in the negative charge of the phosphonate and phosphate ions and to

a negative net surface charge of the GFH, resulting in electrostatic repulsion (Chen *et al.* 2017).

The cumulative desorption performance over the 17 cycles was 90, 89, and 84% for columns A, B, and C, respectively. This shows near-complete regeneration of the columns with regeneration methods (a) and (b), while the recirculation of NaOH (method (c)) resulted in a slightly poorer desorption performance, due to the ongoing exhaustion of the NaOH. With regeneration method (c), the electrical conductivity of the regeneration solution decreased from 178 mS/cm in the virgin 1 M NaOH to 90 mS/cm in the NaOH after 17 cycles. The regeneration mechanism involves ligand exchange of phosphate and DTPMP for OH^- ions (Drenkova-Tuhtan *et al.* 2017; Rott *et al.* 2018a). Furthermore, it is known that the contribution of OH^- ions to electrical conductivity is much higher than that of phosphate ions (Levlin 2010). Thus, the decrease in electrical conductivity is a good indicator for the exhaustion of the regeneration capacity. The values of desorption efficiency above 100% in Fig. 4.3 can be explained by the desorption of DTPMP and orthophosphate, which had not been removed in the previous cycles. In addition, the GFH used also contains phosphorus itself, which can desorb by contact with NaOH (Reinhardt *et al.* 2020a).

After the 17 cycles, the loading was 0.97, 1.06, and 1.46 mg P/g GFH for columns A, B, and C, respectively. In a batch experiment with an initial concentration of 1 mg/L DTPMP-P at pH 8, a maximum loading of 10.2 mg P/g GFH was determined (Fig. S4.1). This value cannot be compared directly due to different boundary conditions (batch vs. column, different initial concentrations, different contact times, etc.). Nonetheless, if the comparison is made, this would imply that the column with the highest loading was only 14.3% loaded after the 17 cycles. Assuming a further linear increase in the residual loading, the column would be completely loaded after 90 cycles. However, since the adsorption performance decreases with increasing residual loading, the effluent quality would be expected to decrease in the subsequent cycles. After 17 cycles, the total P concentration in the regenerate of Column C was 102 mg/L, which, compared to the concentration of the synthetic solution, is a 137-fold P enrichment.

In conclusion, Experiment 1 shows that the GFH can be reused over multiple cycles. However, in Experiment 1, a synthetic solution was used without competing ions, such as those present in the membrane concentrate. Although the desorption performance

was slightly lower when the NaOH was reused in column C, this regeneration method was used in the following experiments because it has vast economic and environmental advantages due to less consumption of NaOH.

4.5.2 Experiment 2 – Influence of pH of the Membrane Concentrate

Experiment 2 was carried out with the raw membrane concentrate at pH ≅ 8 (Fig. 4.4 (a), column D) and the membrane concentrate adjusted to pH 6 with HCl (Fig. 4.4 (b), column E). The duration of alkaline regeneration was reduced to 15 min as part of further optimization. For comparison, breakthrough curves without the regeneration step are shown in Fig. S4.2. GFH adsorbents are porous media whose surface area consists largely of micropores with a pore size < 2 nm (Kumar *et al.* 2019). This has the advantage of providing a high specific surface area, even in granular form. However, adsorption on such adsorbents is often limited by intraparticle diffusion (Kumar *et al.* 2018). Fig. S4.2 shows an asymptotic breakthrough curve at both pH values. This suggests that the intraparticle diffusion processes are slow and breakthrough already occurs even though there is still considerable free adsorption capacity on the adsorbent.

At pH ≅ 8, the desorption performance decreased sharply over the eight cycles and the adsorption performance was also unsatisfactory (Fig. 4.4 (a)). The adsorption performance dropped from over 90% in the first two cycles to 29% in the 8th cycle. During the same period, the desorption performance dropped from 50% to 2%. The loading of the GFH was 4.24 mg P/g GFH after the 8th cycle. Thus, compared to the maximum loading from a batch experiment with 1 mg/L DTPMP-P (Fig. S4.1), there should still be sufficient free capacity for further cycles. Nevertheless, the adsorption performance decreased strongly and the effluent concentration of the column reached values of $c/c_0 > 0.8$ already in the 3rd cycle (Fig. S4.3).

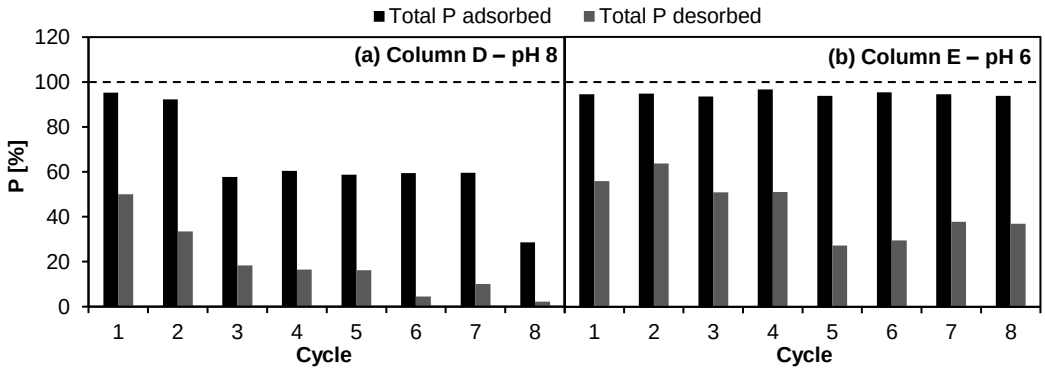

Fig. 4.4: Performance of 8 adsorption/desorption cycles with membrane concentrate (adsorption: 3 min EBCT; alkaline regeneration according to method (c): 1 M NaOH, 15 min). (a) Membrane concentrate, pH ≅ 8, (b) membrane concentrate, pH set to 6 with HCl. Dashed line shows inflow (100%).

The performance of an adsorbent may decrease during use for a number of reasons: Incomplete desorption of the adsorbate, loss of active sites caused by wear of the adsorbent, and structural changes such as surface area, porosity, type of iron (hydr)oxide, or crystallinity during adsorption and regeneration, but also surface precipitation (Cabrera *et al.* 1981; Chitrakar *et al.* 2006; Kunaschk *et al.* 2015; Kumar *et al.* 2018). Besides its purpose of desorbing adsorbed phosphonate and orthophosphate from the surface, NaOH can also lead to such surface precipitation of various compounds. Possible precipitates include hydroxyapatite, dolomite, $CaCO_3$ and/or Ca-DTPMP complexes (Reinhardt *et al.* 2020b). In a study on the adsorption of phosphate on akagaenite, it was observed that complete regeneration was possible with an alkaline solution (Deliyanni *et al.* 2007). Another study with a GFH rich in akagaenite showed a desorption performance of over 80% in the first cycle, but in further adsorption/desorption cycles the regeneration efficiency decreased further (Sperlich 2010). Similar results were also reported in experiments on adsorption of the phosphonate NTMP on GFH (Chen *et al.* 2017). Similar to the results in the present study, in the experiments with phosphate-spiked drinking water from Kunaschk *et al.* (2015), after the first regeneration cycle, the used GFH showed a performance comparable to the initial loading. After the third cycle, however, the volume of solution that could be treated with the adsorbent decreased significantly to below 40% of the initial amount. In addition to the different adsorbents used, the main difference in the aforementioned studies are the water matrices. Similar to Experiment 1 in this study, complete regeneration was possible in the experiment from Deliyanni *et al.* (2007) using phosphate-spiked deionized

water. This suggests that in the experiments conducted by Sperlich (2010), Chen *et al.* (2017), and Kunaschk *et al.* (2015), regeneration performance was affected by other ions. Kunaschk *et al.* (2015) revealed with EDS analyses that calcium-containing precipitates likely formed on the surface of the GFH. These precipitates can cover the pores of the GFH, making adsorption sites inaccessible, and bury adsorbed phosphorus compounds (Li and Stanforth 2000; Kunaschk *et al.* 2015). This may also be the reason for the rapid increase in effluent concentration to $c/c_0 > 0.8$ in the 3rd cycle in column D, as a clearly visible white precipitate formed in the column. When HCl was added to this precipitate, strong CO_2 gas formation occurred, which indicates that carbonate was a major component of the precipitate.

Fig. 4.4 (b) shows the first eight cycles of column E with the membrane concentrate set to pH 6. In comparison with column D (Fig. 4.4 (a)), it is clearly seen that the adsorption performance was significantly better, consistently above 93%. Previous studies have already shown that GFH has higher adsorption capacities at lower pH for phosphate and phosphonates, due to the more positively charged surface (Nowack and Stone 1999a; Genz *et al.* 2004; Reinhardt *et al.* 2020a).

The desorption performance decreased from 56% in the first cycle to 37% in the eighth cycle. Previous studies have already established a correlation between decreasing desorption capacity and declining electrical conductivity (Drenkova-Tuhtan *et al.* 2017; Rott *et al.* 2018a), as well as increasing P concentration in the regeneration solution (Kumar 2018). Furthermore, DTPMP and orthophosphate can be transported further into the pores by intraparticle diffusion, and phosphorus in micropores can impede desorption (Cabrera *et al.* 1981). Thus, parts of the phosphorus compounds cannot be desorbed due to the strong binding on the GFH, resulting in less free adsorption capacity in the following cycles (Genz *et al.* 2004; Kalaitzidou *et al.* 2016). Additionally, adsorption sites can be destroyed by the regeneration process (Kalaitzidou *et al.* 2016; Kumar *et al.* 2018). Interestingly, the desorption performance varied strongly between the first four cycles and between cycles 5 to 8. While the cumulative desorption performance was 55% in the first four cycles, it was only 33% in the following four cycles. As it happened, cycles four and five were separated by the weekend, during which the experiment was stopped.

Column E was run for a total of 20 cycles and the effluent concentration remained below c/c_0 = 0.2 during the entire experiment, except for single measurements that exceeded this value (Fig. S4.3). However, these measurements occurred only for samples taken in the first 45 min of a cycle. This indicates that although the columns were rinsed with tap water after alkaline regeneration, parts of the regenerate likely remained inside the column. Therefore, it is possible that a high pH was still present in the pores of the GFH. If the pH in the pores is > pH_{PZC}, this results in increased adsorption of calcium. Calcium is likely to first accumulate on the surface of the adsorbent before forming calcium carbonate precipitates (Kumar *et al.* 2018). In addition, the calcium concentration close to the adsorbent surface is expected to be higher than in bulk solution (Antelo *et al.* 2015). Therefore, it is possible that surface precipitation occurred in the pores of the GFH over the weekend, which in turn may have led to the deteriorated desorption performance. In further studies, the GFH should therefore be completely neutralized before the next cycle, if necessary with an acidic solution to accelerate the process. However, despite the good adsorption performance of ≥ 90% over all 20 cycles, setting the pH to 6 in the membrane concentrate is not recommended due to its strong alkalinity. Moreover, stoichiometrically, the same amount of acid would presumably be required to adjust the pH value to 6 ahead of the reverse osmosis. Consequently, the antiscalant DTPMP could be omitted, since in this pH range the precipitation of $CaCO_3$, the avoidance of which is the goal of the use of DTPMP in the membrane concentrate used in this study, would no longer occur. However, this experiment showed that GFH can be used to remove phosphonate and orthophosphate from membrane concentrate if precipitation can be prevented or minimized, as done in this experiment by lowering the pH of the membrane concentrate to pH 6.

In conclusion, complete regeneration with 1 M NaOH was not possible at either pH 6 or initial pH ≅ 8. Nevertheless, regeneration resulted in additional adsorption capacity, allowing column E to operate for 20 cycles with low effluent values. Since precipitation of calcium compounds strongly affects the adsorption/desorption cycles, these precipitates should either be avoided or chemically removed. Therefore, in the following experiments, an additional step with an acidic regeneration was introduced.

4.5.3 Experiment 3 – Influence of a Novel Acidic Regeneration Step

In Fig. 4.5 the effluent concentration, the electrical conductivity, and the P concentration of the regenerate are plotted over the bed volumes, for columns F1&F2 and G1&G2 operated in two parallel runs over a total of 20 adsorption/desorption cycles. While in columns F1&F2 in each cycle fresh HCl was used for acidic regeneration, in columns G1&G2 the same HCl was used over all cycles and the pH was controlled to a setpoint of 2.5. The EBCT was increased to 4 min to counteract the poorer adsorption performance at pH 8, compared to Experiment 2 at pH 6.

Compared to the results at pH ≅ 8 from Experiment 2, a significant improvement in adsorption performance can be seen, which can be attributed to the acidic regeneration step. Previous studies on the adsorption of phosphate on GFH showed that the calcium-containing precipitates can interact with the adsorbed phosphate and interfere with alkaline desorption (Kunaschk *et al.* 2015; Kumar *et al.* 2018). According to Kunaschk *et al.* (2015), these precipitates can bury the phosphorus underneath. As the above-mentioned precipitates redissolve in an acidic pH range, Kunaschk *et al.* (2015) recommended an acidic regeneration before the alkaline regeneration to remove the precipitates first before desorbing the phosphate. To find a suitable pH value, they performed calculations in PHREEQC, according to which a pH of 2.5 is necessary for rapid redissolution of those calcium compounds. Despite the low stability of GFH adsorbents in acidic environments, only very small portions of different GFH adsorbents dissolved during acidic regeneration at pH 2.5 in the experiments of Kunaschk *et al.* (2015) and Kumar *et al.* (2018).

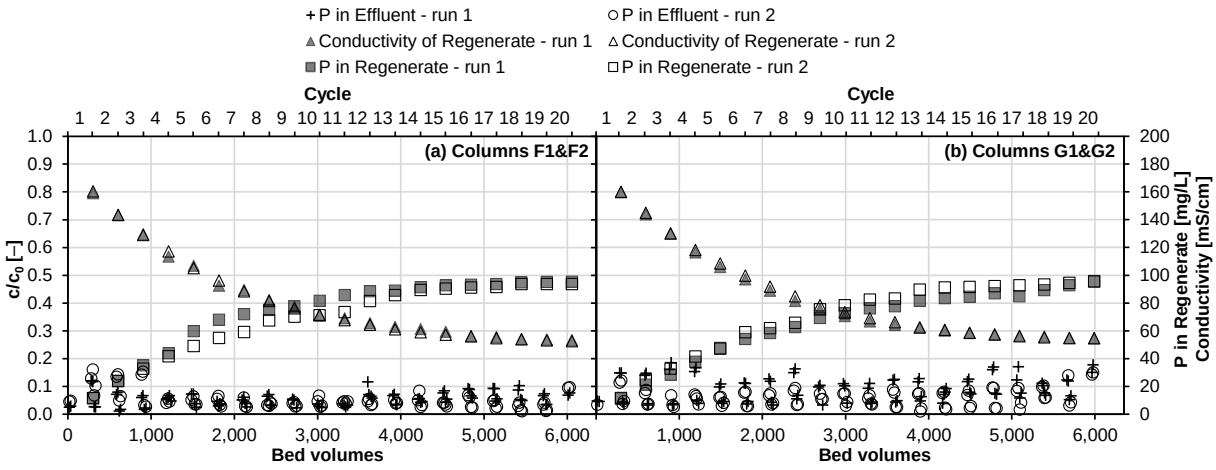

Fig. 4.5: c/c_0 vs. bed volumes for 20 adsorption/desorption cycles with membrane concentrate (adsorption: pH ≅ 8, 4 min EBCT; acidic regeneration: HCl (pH 2.5), 3 h; alkaline regeneration according to method (c): 1 M NaOH, 15 min). (a) Regeneration with fresh HCl in each cycle, no recirculation of HCl, (b) recirculation of HCl with pH control.

Fig. 4.5 (a) shows that the effluent concentration of the columns F1&F2 was always $c/c_0 \leq 0.12$ after the third cycle. The higher effluent concentrations in the first cycles can probably be ascribed to the pre-existing phosphorus loading on the GFH, as shown in a previous study (Reinhardt *et al.* 2020a). Over all 20 cycles, the cumulative adsorption performance was 95%. The cumulative desorption performance, on the other hand, was only 25%. Interestingly, in the first seven cycles, the cumulative desorption performance was still 50%. A similar behavior can also be seen with columns G1&G2 in Fig. 4.5 (b). The effluent concentrations were slightly higher than in columns F1&F2 with $c/c_0 \leq 0.18$, which is also reflected in a slightly lower cumulative adsorption efficiency of 93%. The cumulative desorption efficiency was 26%. Again, the desorption efficiency in the first seven cycles was significantly higher (47%) than over the complete series of cycles. At this point, Fig. 4.5 (a) & (b) show a flattening of the P concentration curve for the regenerate. This occurred as soon as the electrical conductivity of the regenerate dropped below 90 mS/cm. After this point, the desorption efficiency was only ≤ 20% in most cycles. This indicates that the capacity of the regeneration solution decreased at this conductivity level. The average loading after 20 cycles was 10.7 mg P/g GFH for columns F1&F2 and 10.2 mg P/g GFH for columns G1&G2. Thus, compared to the maximum loading from a batch experiment with 1 mg/L DTPMP-P and 1 mg/L PO_4-P (Fig. S4.1), where the measured maximum loadings were 10.2 and

11.5 mg P/g GFH, respectively, the loadings from the columns were near maximum. However, column experiments can be expected to use the adsorption capacity more efficiently, since the adsorbent is continually exposed to the same influent concentration, compared to the decreasing concentration in batch experiments, and therefore, higher maximum loadings are expected in column experiments (Akratanakul *et al.* 1983; Loganathan *et al.* 2014).

The difference between columns F1&F2 and G1&G2 was in the HCl used. In a practical implementation, the regeneration solutions should be used several times to reduce costs and waste streams to be treated. More than 370 BV of HCl was used for acidic regeneration in these experiments. To reduce the amount, the same HCl was used in columns G1&G2 in each cycle. However, to maintain its regeneration capacity, fresh 1 M HCl was added continuously as part of a pH control. In columns F1&F2, almost 3.8 L of HCl with pH 2.5 was consumed per cycle for acidic regeneration, corresponding to a consumption of 12.0 mmol HCl per cycle. In columns G1&G2, on the other hand, 1 L of HCl with a pH of 2.5 was always reused. For pH regulation, an average of 14.7 mmol HCl per cycle was added, which corresponds to a total of less than 300 mL 1 M HCl over all cycles. Thus, although the amount of H^+ consumed increased when HCl was reused, after 20 cycles in this laboratory experiment, only about 1.3 L (130 BV) of waste stream was produced, compared to over 75 L (750 BV) without reuse.

The increase in H^+ consumption can be explained by the buffering effect associated with the redissolution of calcium precipitates. For comparison, the acid consumption in Experiment 2, used to adjust the membrane concentrate to pH 6, was 18.2±2.4 mmol HCl per liter of membrane concentrate. This corresponds to an H^+ consumption of 82.1 mmol per cycle, reflecting the strong buffering capacity of the membrane concentrate and clearly demonstrating that acidic regeneration is more efficient.

In an additional experiment with recirculation of HCl, but without pH regulation, a change in pH value over the regeneration time was observed. Tab. 4.2 clearly shows that the pH increased significantly towards the neutral pH range over the 180 min of acidic regeneration. This was due to the buffering effect of the (hydr)oxide surface. This increase in pH can also indicate that possibly only the lower part of the column is

regenerated, since the pH in the upper part of the column may already be too high for redissolution of the calcium precipitates.

Tab. 4.2: Progression of the pH in HCl over the regeneration period during one cycle without pH control.

Contact time [min]	pH
0	2.5
15	2.7
30	3.1
45	3.9
60	5.2
90	6.3
120	6.7
180	7.1

Acidic and alkaline regeneration can also lead to recrystallization of the GFH, i.e. change of its physical and chemical properties, such as surface area, porosity, or loss of active sites. This change in adsorbent can result in different types and amounts of surface hydroxyl groups, which can, in turn, affect phosphate adsorption. Kumar *et al.* (2018) found that for FerroSorp Plus, a GFH from the manufacturer of the GFH used in this study, no change in the type of iron hydroxide was detectable. Nevertheless, there were differences in the hyperfine field, suggesting that the ferrihydrite was present in a more ordered species after regeneration. The specific surface area of the GFH increased by up to 56%, but this was probably due to the removal of surface precipitates. In another study by Chitrakar *et al.* (2006), for example, it was found that the crystallinity of goethite increased by regeneration with NaOH, accompanied by a decrease in adsorption capacity. In contrast, regeneration of akagaenite showed no effect on crystallinity even after ten cycles (Chitrakar *et al.* 2006).

After 20 cycles, the acidic and alkaline regeneration solutions were analyzed for phosphorus, calcium, and iron. Whereas there was an average of only 0.3 mg/L Fe in the NaOH of the columns F1&F2 and G1&G2, no iron was detected in the HCl. The solubility of iron hydroxide increases significantly in the acidic and alkaline range compared to the neutral pH range (Liu and Millero 1999). The fact that no iron was found in the HCl could indicate that initially dissolved iron precipitated again in the upper part of the column due to the increase of the pH (Tab. 4.2), as already observed by Kunaschk *et*

al. (2015). As expected, no calcium could be detected in the NaOH, but an average concentration of 3.7 g/L was detected in the HCl after the 20 cycles of columns G1&G2. This clearly shows that acidic regeneration removes large amounts of calcium from the adsorbent, namely calcium-containing precipitates, adsorbed calcium ions, or calcium embedded in the GFH itself. While calcium carbonate or different calcium phosphates can redissolve due to their increasing solubility at low pH, adsorbed calcium can desorb due to electrostatic interactions caused by the more positively charged GFH surface at low pH. The alkaline regeneration solutions of columns F1&F2 and G1&G2 had a P concentration of 96 mg/L, resulting in a nearly 73-fold enrichment compared to the initial P concentration in the membrane concentrate. In the HCl, however, only 0.08 mg/L P was found after 20 cycles in columns G1&G2. Accordingly, the redissolved calcium compounds do not appear to be phosphate-containing species, but likely calcium carbonate.

In conclusion, the addition of an acidic regeneration step to the process significantly increased the adsorption performance at pH 8. Reuse of the acid is possible with pH control. Calcium is found solely in the HCl, while phosphorus is removed almost exclusively during alkaline regeneration. Since the adsorption performance decreased significantly after the electrical conductivity of the NaOH fell below 90 mS/cm, the alkaline regeneration solution was replaced at this point in Experiment 4.

4.5.4 Experiment 4 – Influence of Replacing the Alkaline Regeneration Solution

Fig. 4.6 shows the adsorption and desorption performance from an acidic and alkaline regeneration experiment with 24 cycles, where the NaOH was replaced when its electrical conductivity dropped below 90 mS/cm. The cumulative adsorption efficiency of column H was 95%. The average P concentration in the three final alkaline regeneration solutions was 69 mg/L, corresponding to an approximately 52-fold increase in concentration compared to the initial P concentration in the membrane concentrate. Compared to the 73-fold increase in Experiment 3, this seems to be a poorer performance, but this is due to the fact that replacing the NaOH stops the accumulation of P in the regenerate. The cumulative desorption efficiency, on the other hand, reached 46%. Thus, the replacement of NaOH almost doubled the cumulative desorption performance from 25% to 46%.

A mass balance per g GFH in the column over all 24 cycles gives a total P load in the column feed of 17.9 mg P, of which 17.1 mg P could be adsorbed and 0.8 mg P left the column along with the effluent. Of the 17.1 mg P adsorbed, 0.1 mg P was found in the HCl for acidic regeneration and 7.8 mg P in the NaOH for alkaline regeneration. This could also include P from the raw GFH, which already contains 0.5 to 0.7 mg P/g GFH according to the manufacturer. Accordingly, after 24 cycles, the loading was 9.3 mg P/g GFH and, consequently, despite four additional cycles, the loading was lower compared to the columns in Experiment 3.

Overall, the adsorption performance was high, with column effluent values c/c_0 consistently lower than 0.14, with a total of about 7,200 BV treated. This was despite the fact that the EBCT was relatively short with 4 min in this study; in practical treatment systems, EBCTs of up to 30 min are common (Worch 2012). Increasing the EBCT could further improve the adsorption performance. In addition, a series of columns is possible if a higher GFH efficiency is desired (Sperlich 2010).

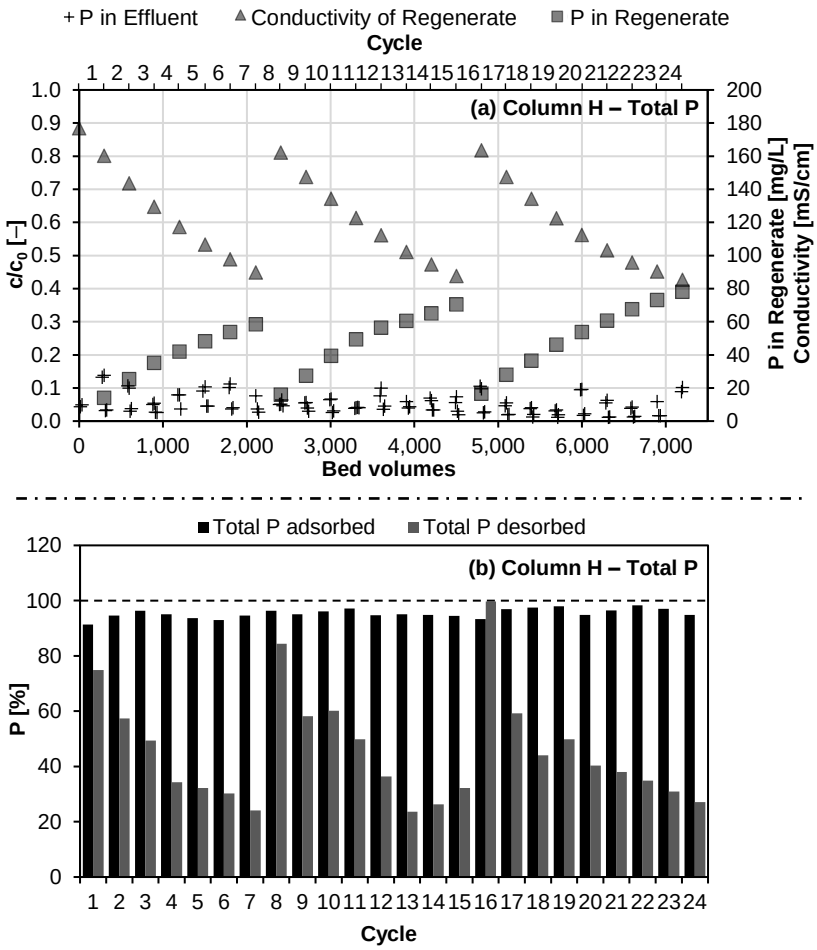

Fig. 4.6: 24 adsorption/desorption cycles with membrane concentrate (adsorption: pH ≅ 8, 4 min EBCT; acidic regeneration: HCl (pH 2.5), 3 h; alkaline regeneration according to method (c): 1 M NaOH, 15 min, replacement if conductivity < 90 mS/cm). (a) c/c_0 vs. bed volumes, (b) adsorption/desorption performance. Dashed line shows inflow (100%).

Looking at the distribution of adsorption and desorption performance in more detail, it can be seen that the orthophosphate and organic phosphorus fractions behave similarly. While the cumulative adsorption performance with respect to orthophosphate is 98% and the cumulative desorption performance is 47%, slightly poorer values of 94% and 45%, respectively, are shown for organic phosphorus (Fig. S4.4). However, this deviation could also be due to experimental scatter without statistical significance.

After these laboratory experiments, an accurate estimate of the operating costs is not yet possible. However, this experiment shows that replacing the NaOH when its electrical conductivity drops below a certain value can enhance desorption performance. Further studies could optimize this. A good compromise should be found between the

desorption performance as well as the use of resources and the waste streams to be discarded. Besides replacing the NaOH, refreshing the NaOH could also be an option. Similar to the pH control of the HCl in Experiment 3, an addition of fresh NaOH depending on the measured electrical conductivity could also be promising. A similar approach has already been successfully demonstrated in a study by Kuzawa *et al.* (2006).

4.6 Conclusions

The novelty of this work involves the first study of adsorption behavior of phosphonates and orthophosphate with real membrane concentrate in a fixed-bed column. Previous studies investigated synthetic wastewater in a maximum of three adsorption/desorption cycles, while this study considered up to 24 cycles run over a 6-week period. Additionally, the acidic regeneration step was firstly applied to phosphonate containing wastewater.

This study shows that GFH can be used over multiple cycles. While a synthetic solution with DTPMP, without other competing ions or synergistic effects, allowed almost complete regeneration of GFH with 1 M NaOH, the regeneration performance with real membrane concentrate decreased significantly, likely due to the formation of surface precipitates. In experiments with membrane concentrate at the initial pH of ≅ 8, the adsorption performance decreased rapidly in 8 cycles, with only 29% in the 8^{th} cycle. This can be attributed to the precipitation of calcium compounds.

When the pH was lowered to 6, a column could be run for 20 cycles with consistently low P effluent concentrations and an adsorption efficiency of > 93%. However, due to the strong buffering capacity of the membrane concentrate, the acid consumption is very high and the acidification of membrane concentrate is not recommended. The NaOH for alkaline regeneration can be reused several times, which helps to save resources and minimizes waste.

In further experiments, an acidic regeneration step was added to the process to remove Ca-containing precipitates accumulating over time in the column. With this, even an adsorption performance of 95% over 20 cycles was achieved. Reuse of the HCl is possible if the pH is kept constant at 2.5 by a pH control.

Calcium was removed only during acidic regeneration, while DTPMP and orthophosphate were removed almost exclusively by alkaline regeneration. The dissolution of iron from the GFH was negligible. Since the desorption capacity decreased significantly when the electrical conductivity of the NaOH sank below 90 mS/cm, this can serve as an indicator for a deterioration in the regeneration capacity. Regular replacement of the NaOH can significantly improve the desorption performance.

4.7 Acknowledgments

We would like to acknowledge our gratitude to the Willy-Hager-Stiftung, Stuttgart, Germany for their financial support. We would also like to thank HeGo Biotec GmbH for providing FerroSorp RW samples and Zschimmer & Schwarz Mohsdorf GmbH & Co. KG for supplying us with a DTPMP sample. Special thanks to Adriana Noelia Veizaga Campero, who provided the schematic diagrams in Fig. 4.2.

4.8 Supplementary Material

4.8.1 Figures S1–S4

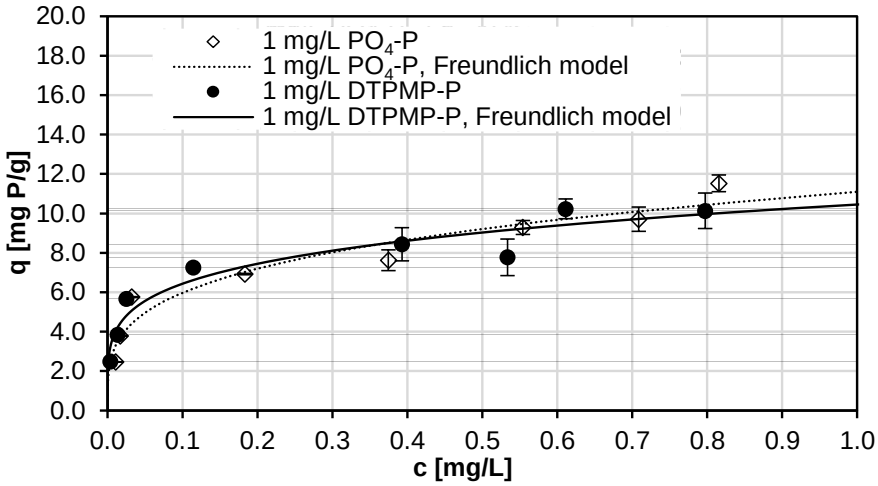

Fig. S4.1: Adsorption of orthophosphate and DTPMP with an initial concentration of 1 mg/L P on GFH at pH 8 (buffer: 0.01 M EPPS) at room temperature (20 °C) (20 rpm, 7 d contact time). Freundlich models are shown (PO_4-P: K_F = 11.093, n = 3.723; DTPMP-P: K_F = 10.451, n = 4.745).

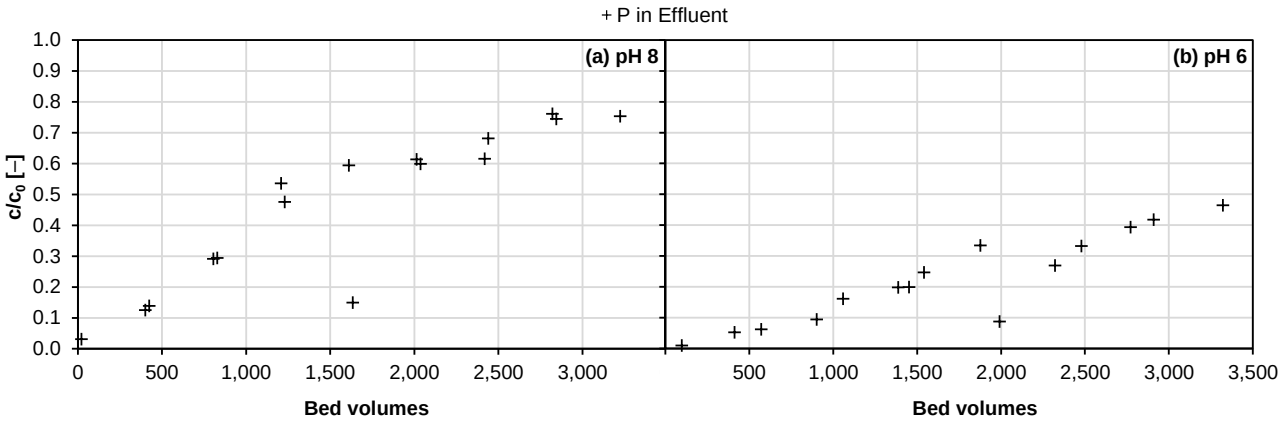

Fig. S4.2: Column breakthrough profiles with membrane concentrate without regeneration (3 min EBCT). (a) pH ≅ 8, (b) pH 6.

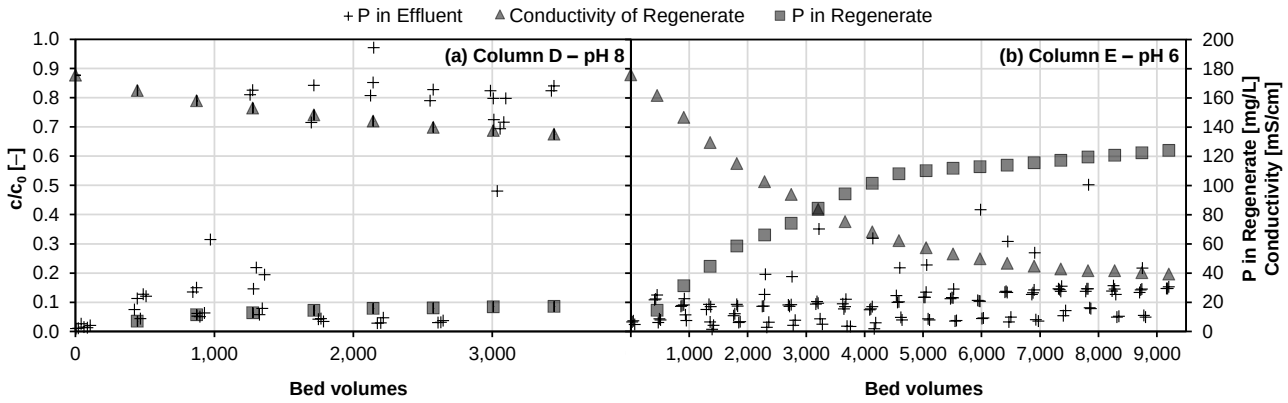

Fig. S4.3: c/c_0 vs. bed volumes for adsorption and desorption cycles with membrane concentrate (adsorption: 3 min EBCT; alkaline regeneration: 1 M NaOH, 15 min). (a) 8 cycles at pH ≅ 8, (b) 20 cycles at pH 6.

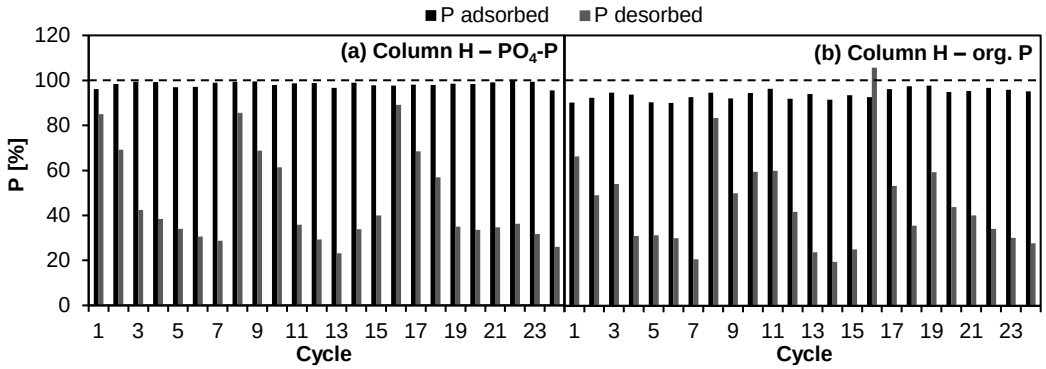

Fig. S4.4: Performance of 24 adsorption/desorption cycles with membrane concentrate (adsorption: pH ≅ 8, 4 min EBCT; acidic regeneration: HCl (pH 2.5), 3 h; alkaline regeneration according to method (c): 1 M NaOH, 15 min, replacement if conductivity < 90 mS/cm). (a) Orthophosphate, (b) organic phosphorus. Dashed line shows inflow (100%).

5 General Discussion

5.1 Summary of Main Findings and Conclusions

In this work, the adsorption of phosphonates other than NTMP on GFH was studied for the first time. In addition, real wastewater was used for these investigations for the first time and the influence of various ions, either positive or negative, on adsorption was examined in detail. The operation of filter columns on a laboratory scale over a period of up to six weeks allowed to draw conclusions about a potential long-term use of the adsorbent. This helped to close the research gaps described in Section 1.3.5. The key finding of this work was that the removal of phosphonates and orthophosphate from real membrane concentrate is possible by adsorption on GFH in fixed-bed columns with a possible reuse of the adsorbent for more than 20 adsorption/desorption cycles.

The results presented in Chapter 2 showed, that among the four GFH adsorbents investigated, FerroSorp RW proved to be the most suitable in batch experiments. Adsorption capacity for all investigated phosphonates decreased with increasing pH. The treatment of phosphonate-containing solutions should be carried out at pH values close to 6 to ensure a high adsorption capacity while maintaining material stability. The maximum loading of GFH was ~12 mg NTMP-P per g GFH in batch experiments with an initial concentration of 1 mg/L NTMP-P and a contact time of 7 days at room temperature. However, the maximum loading of the GFH dropped significantly by > 40% at low wastewater temperatures (5 °C). Low temperatures should therefore be avoided if possible in a potential technical implementation. For the investigated polyphosphonates HEDP, NTMP, EDTMP, and DTPMP, the adsorption capacity decreased with increasing number of phosphonate groups and molecular size and weight. Batch regeneration experiments showed that the phosphorus-containing compounds could be successfully desorbed from GFH with 1 M NaOH and that the GFH could subsequently be reused in five adsorption/desorption cycles.

Further batch experiments described in Chapter 3 investigated the influence of calcium on the adsorption of phosphonates on GFH. It was found that calcium redissolved from the GFH itself, which had a positive influence on phosphonate adsorption, possibly

due to the formation of ternary complexes. Batch experiments with six different phosphonates and various molar Ca:phosphonate ratios in the presence of and absence of GFH revealed that at pH > 8 precipitation can occur after a contact time of seven days. The precipitates are likely Ca-phosphonate complexes. HEDP showed the lowest calcium tolerance with precipitation already at a molar Ca:HEDP ratio of 2:1. After a further increase in the calcium and phosphonate concentrations, precipitation was also observed for NTMP and DTPMP, with the solubility of the Ca:NTMP complexes being lower than that of Ca:DTPMP complexes. In further batch experiments with membrane concentrate and its synthetic replicas, the influence of the ions present in membrane concentrate on DTPMP and orthophosphate adsorption was investigated. The influence of the investigated ions on the adsorption of DTPMP and orthophosphate was nearly identical. The results showed that HCO_3^- had a competitive effect on adsorption, while the influence of SO_4^{2-} and NO_3^- was negligible. The presence of Ca^{II} had a positive effect on the adsorption of DTPMP and orthophosphate up to a pH of 8, presumably due to the formation of ternary complexes. At pH > 8, the presence of Ca^{II} and at pH > 10, the presence of Mg^{II} resulted in precipitation. These precipitates resulted in removal of DTPMP and orthophosphate, either by direct precipitation of the phosphorus-containing compounds, or by their adsorption onto the precipitates. The precipitates could be inorganic precipitates of calcium, magnesium, and phosphate or Ca:DTPMP complexes. The presence of (hydrogen-)carbonate leads to the precipitation of $CaCO_3$ and/or dolomite, both of which can also act as adsorbents for DTPMP and orthophosphate. Due to its high content of Ca and Mg, which can have a positive effect on the adsorption of DTPMP and orthophosphate on GFH, it can be assumed that the studied membrane concentrate is well suited for treatment with GFH.

Lastly, fixed-bed column experiments with a synthetic solution containing DTPMP and real membrane concentrate containing DTPMP and orthophosphate were performed at laboratory scale to test the applicability of the GFH over multiple cycles. Experiments with the synthetic solution showed that the GFH can be successfully used over multiple cycles and the NaOH for regeneration can be reused. Despite that the desorption performance with reuse of the NaOH was slightly lower than with use of fresh NaOH in each cycle, the reuse is recommended due to its vast economic and environmental advantages due to less consumption of NaOH. While experiments with a synthetic

solution containing DTPMP showed almost complete regeneration, the adsorption performance with real membrane concentrate decreased significantly from over 90% in the first two adsorption/desorption cycles to 29% in the 8th cycle at pH ≅ 8. As the main difference between these experiments was the absence of other ions with competitive or synergistic effects in the synthetic solution, this could be attributed to the precipitation of calcium compounds which disturbed the adsorption/desorption process. Therefore, to maintain good adsorption performance over multiple cycles, these precipitates should be either prevented or removed. In experiments to prevent precipitation, the pH of the membrane concentrate was reduced from original pH ≅ 8 to pH 6 by adding HCl. Although this also did not allow complete regeneration, the regeneration resulted in additional adsorption capacity, and therefore, a column could be operated for 20 adsorption/desorption cycles with consistently low P effluent concentrations and with an adsorption efficiency of > 93%. However, the strong buffering capacity of the membrane concentrate results in very high acid consumption and acidification of the membrane concentrate is therefore not recommended. In experiments for the subsequent removal of precipitates, a novel acidic regeneration step using HCl to remove Ca-containing precipitates accumulating in the column over time was introduced. This allowed an adsorption performance of 95% over 20 adsorption/desorption cycles at the original pH 8 of the membrane concentrate, i.e. without prior reduction of the pH value. Reuse of the HCl for the acidic regeneration step was possible if the pH was kept constant by a pH control and the dissolution of iron from the GFH was negligible during acidic regeneration. Calcium was removed only during acidic regeneration, while DTPMP and orthophosphate were removed almost exclusively by alkaline regeneration. Thus, the redissolved calcium-containing precipitates did not appear to be phosphate-containing species, but likely calcium carbonate. The reusability of NaOH was also confirmed in the experiments with real membrane concentrate and the electrical conductivity of NaOH can serve as an indicator for the deterioration of the regeneration capacity. Regular replacement of the NaOH can significantly improve the desorption performance.

The results of this thesis show that granular ferric hydroxide is basically a suitable adsorbent for the removal of phosphonates and orthophosphate from membrane concentrate. However, prior to a possible technical implementation, the process should be further optimized. Possible optimizations are mentioned in the outlook (Section 5.2). It

must also be considered that this procedure would mean a significant additional workload for the operating staff in waterworks and that the process generates new streams that have to be treated as well. However, the generated phosphorus-containing aqueous stream has a much smaller volume and higher concentration.

5.2 Outlook

Replacement of Antiscalant

From an environmental perspective, replacement of the phosphonate-containing antiscalant should be prioritized over treatment of the phosphonate-containing membrane concentrate. In addition to phosphorus-containing antiscalants, which include condensed polyphosphates and phosphonates, there is also a group of phosphorus-free antiscalants (Ketrane *et al.* 2009; Hasson *et al.* 2011; Yu *et al.* 2020). More stringent requirements and increasing environmental concerns have led to increased scientific interest in so-called green antiscalants in recent years (Akın *et al.* 2008; Ketsetzi *et al.* 2008; Martinod *et al.* 2008; Hasson *et al.* 2011; Chaussemier *et al.* 2015; Chen *et al.* 2015; Zhang *et al.* 2016). These are characterized by ready biodegradability and low mobility to minimize environmental impact (Hasson *et al.* 2011). Possible green alternatives include the polymers poly(aspartic acid) (PASP), polyepoxysuccinic acid (PESA), carboxymethyl inulin (CMI), and their derivatives (Hasson *et al.* 2011; Chaussemier *et al.* 2015; Yu *et al.* 2020). All of them have good chelating properties and dispersibility, and their applicability has already been proven in several studies, some of them under real field conditions (Baraka-Lokmane *et al.* 2009; Boels and Witkamp 2011; Hasson *et al.* 2011; Kırboga and Oner 2012; Chaussemier *et al.* 2015; Chen *et al.* 2015; Zhang *et al.* 2016; Yu *et al.* 2020). The inhibition mechanisms involve complexation of calcium ions, adsorption of the antiscalant on the crystal surface and/or delaying nucleation (Boels and Witkamp 2011; Hasson *et al.* 2011; Chhim *et al.* 2020). Mixing two antiscalants with different inhibition mechanisms can result in improved efficacy (Chhim *et al.* 2020). Experiments to substitute the phosphonates NTMP and HEDP (Boels and Witkamp 2011) as well as DTPMP (Baraka-Lokmane *et al.* 2009) with green antiscalants showed promising results. For instance, Boels and Witkamp (2011) found a mitigation of spontaneous precipitation and a reduction of the calcite growth rate in the order of CMI > NTMP > HEDP. An approximately 2.7-fold higher molar concentration of NTMP was required to ensure comparable inhibition of

calcite precipitation as with CMI. Whether these alternative antiscalants can efficiently prevent membrane fouling should be further investigated. The polymer chains of the aforementioned substances can be broken down by non-enzymatic degradation pathways such as chemical hydrolysis, but can also be biodegraded enzymatically by bacteria, fungi and algae. Besides water, biomass, CO_2, and CH_4, other natural substances such as humic matter are produced as degradation products (Gross and Kalra 2002; Hasson *et al.* 2011).

Possible Improvement of Adsorption/Desorption Process

Although this work demonstrated the applicability of GFH for the treatment of membrane concentrate, the process should be further optimized. Several ideas for this are briefly addressed below.

The EBCT of 3 or 4 minutes chosen in the experiments was comparatively short; in practice, EBCTs of up to 30 minutes are common (Worch 2012). The chosen EBCTs were selected to achieve an adsorption/desorption cycle duration of 24 hours. As the experiments were performed without automation, this allowed the samples to be taken and the regeneration cycles to be carried out manually during daytime. Furthermore, a large number of adsorption/desorption cycles could be carried out within a reasonable time frame. As described in Chapter 4 in this thesis, as well as by Boels (2012) for NTMP adsorption and by Sperlich (2010) for orthophosphate adsorption on GFH, the asymptotic shape of the breakthrough curve indicates slow intraparticle diffusion. Thus, breakthrough already occurs although parts of the bed are still far from their maximum loading at equilibrium condition. Smaller particle sizes can significantly reduce the influence of intraparticle diffusion (Sperlich 2010; Boels and Witkamp 2011; Kumar *et al.* 2018). Although specific surface area often remains similar when grinding porous adsorbents such as GFH, the pores become more accessible (Kumar *et al.* 2018). For instance, Kumar *et al.* (2018) found that despite having similar surface area, GFH with a grain size of 0.25–0.325 mm showed a more than 4-fold higher adsorption capacity than GFH with a grain size of 1–1.25 mm. A higher EBCT leads to a steeper and more sigmoidal breakthrough curve as well (Sperlich 2010). Therefore, further research should be carried out to investigate the possible increase in adsorption performance of the columns by using GFH with smaller particle sizes and longer contact times. The operation of several columns in series can also lead to an increase in the performance

of the columns. For instance, Sperlich (2010) was able to show by analyzing breakthrough data that two columns filled with GFH for phosphate adsorption operated in series use the adsorbent 134–175% more efficiently compared to a single column. Multiple adsorber systems with series connection, where one of the adsorbers is out of operation for its regeneration while the others are running, are common practice (Worch 2012).

Further research should also look at optimizing the acidic regeneration. As described in Chapter 4, the pH of the HCl increased significantly during acidic regeneration due to the buffering capacity of the GFH surface. Therefore, the pH may only be sufficiently low to redissolve the calcium-containing precipitates in the lower part of the column. Kunaschk *et al.* (2015) simulated the dissolution of various calcium compounds with the result that dissolution caused the pH to increase. They therefore suggested the pH value in the column effluent as a possible indicator, since it can only reach the input value when all calcium compounds are redissolved. Future research should therefore choose a longer HCl contact time during acidic regeneration until the pH in the effluent is equal to that in the influent of the column. However, special attention should be paid to possible redissolution of iron from the GFH. Although no redissolution of iron was observed in this thesis, this could change at lower pH values in the effluent of the column. The studies of Kunaschk *et al.* (2015) and Kumar *et al.* (2018) showed varying amounts of redissolved iron from different GFH adsorbents, but often the iron redissolution was in the range of only 0.001% to < 0.03% of the GFH mass in the column per cycle.

A greater focus on the alkaline regeneration solution could lead to a more efficient process. As described in Chapter 4, the desorption performance decreased significantly as soon as the electrical conductivity of the regeneration solution fell below 90 mS/cm. The decrease in electrical conductivity indicates a decrease in OH^- ion concentration. Therefore, it should be investigated whether it is possible to replenish the regeneration solution with fresh NaOH as previously shown by Kuzawa *et al.* (2006) and Kartashevsky *et al.* (2015). However, it is also possible that the desorption performance decreases with increasing phosphorus concentration in the regeneration solution. To counteract this, precipitation of the phosphorus-containing compounds with calcium is conceivable. This has already been investigated for both phosphate-

and phosphonate-containing sodium hydroxide solution with $CaCl_2$ and $Ca(OH)_2$ (Kuzawa *et al.* 2006; Boels 2012; Kartashevsky *et al.* 2015). For instance, Boels (2012) found an NTMP removal from the regeneration solution between 91% and 97% depending on the used molar Ca:NTMP ratio (7:1 to 13:1) using $CaCl_2$. Precipitation with iron and aluminum salts is also possible (Yeoman *et al.* 1988; Rott *et al.* 2017b). Another possible alternative is the separation of phosphorus-containing compounds by nanofiltration. Boels (2012) was able to run a nanofiltration with a retention of 99.4% NTMP and an NaOH recovery of 91%. Future research should investigate whether phosphonates recovered in this way can subsequently be reused or if they are still present in a complexed form.

Further insights could also be gained from analyses of the adsorbent itself. For instance, it should be investigated whether the GFH is structurally altered by acidic and alkaline regeneration and whether this has an effect on its performance. Additional EDS analyses could provide insight into whether calcium-containing compounds are still present in the column, especially in the upper part.

Treatment of Waste Streams

The proposed process produces wastewater streams that require further treatment, both the alkaline and acidic regeneration solutions. After 20 adsorption/desorption cycles, no calcium, 0.3 mg/L iron, and 96 mg/L P were found in the sodium hydroxide solution. In contrast, no iron, 3.7 g/L calcium, and only 0.08 mg/L P were found in the hydrochloric acid. However, as the initially dissolved iron may have precipitated again in the upper part of the column due to the increase of the pH, the longer HCl contact time already proposed could lead to iron being found in the hydrochloric acid. Further research should also investigate whether other substances are present in the two wastewater streams that require treatment.

The concentrated phosphorus in the alkaline regeneration solution should be removed before discharging it into water bodies after neutralization. The multiple reuse of the alkaline regeneration solution leads to a concentration of the phosphorus therein. The experiment described in section 4.5.3 led to a nearly 73-fold enrichment. The concentration as well as the volume of the different streams are visualized in Fig. 5.1. As discussed above, the phosphorus-containing compounds could either be precipitated

(Kuzawa *et al.* 2006; Boels 2012; Kartashevsky *et al.* 2015; Rott *et al.* 2017b) or separated by nanofiltration (Boels 2012). A disadvantage of precipitation is the resulting sludge, which must be separated and further processed. Additionally, a part of the added Ca^{II} remains in the regeneration solution (Boels 2012). Future research should also investigate if this Ca^{II} would lead to precipitation in the columns during regeneration.

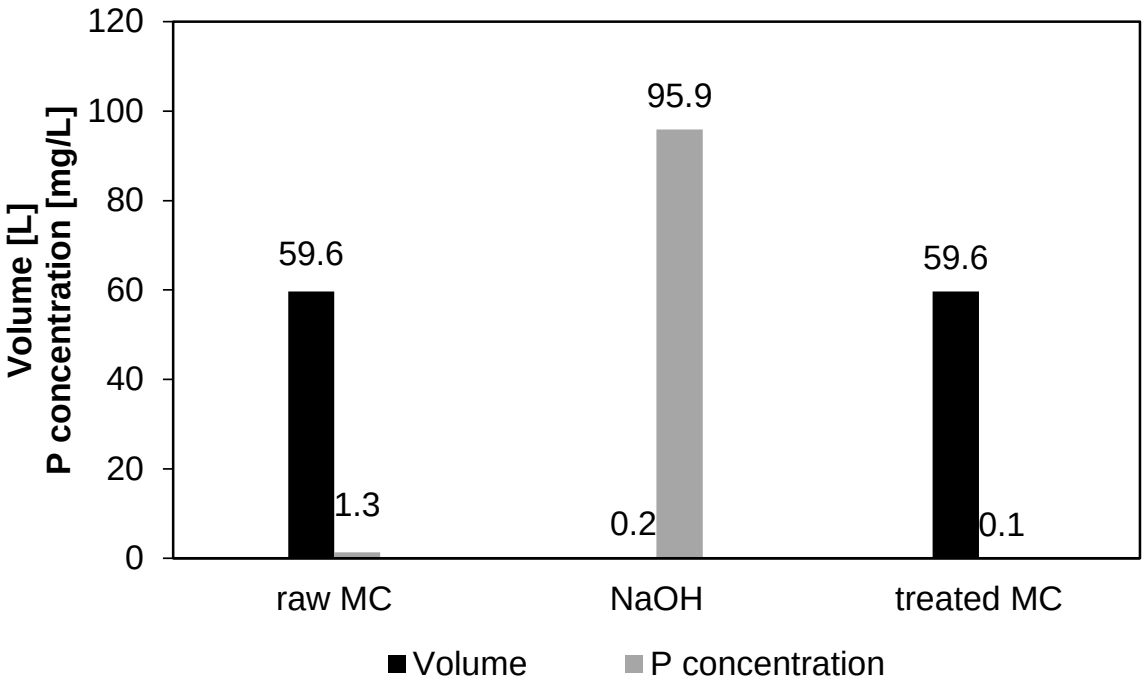

Fig. 5.1: Volume of membrane concentrate (MC) and alkaline regeneration solution (NaOH) that has passed through the column in 20 adsorption/desorption cycles and the corresponding phosphorus concentrations.

The acidic regeneration solution must also be discarded. Future research should investigate whether the calcium present in it can be used to precipitate the phosphorus in the alkaline regeneration solution by mixing the two streams. Calcium is present in excess, as the NaOH contained approximately 0.62 mM DTPMP and the HCl contained approximately 92 mM calcium after 20 adsorption/desorption cycles.

Alternative Treatment Methods For Membrane Concentrate

For the removal of phosphonates from membrane concentrate, other methods than adsorption on GFH are also possible. These include various advanced oxidation processes such as ozone treatment (Klinger *et al.* 1998; Greenlee *et al.* 2014; Xu *et al.*

2019), Fenton process (Rott *et al.* 2017a), and numerous combinations of UV treatment with other chemicals such as UV/Fe^{II} (Lesueur *et al.* 2005; Rott *et al.* 2017a), UV/Fe^{III} (Sun *et al.* 2019), UV/chlorine (Huang *et al.* 2019), UV/persulfate (Wang, Zhi *et al.* 2019), UV/H_2O_2 (Xu *et al.* 2019), and photo-Fenton (Rott *et al.* 2017a). Oxidative degradation yields orthophosphate, which can subsequently be precipitated. Furthermore, precipitation/flocculation processes with the application of iron, aluminum, or calcium salts are possible (Klinger *et al.* 1998; Fettig *et al.* 2000; Rott *et al.* 2017b).

The same membrane concentrate used in this thesis has also been used in previous studies regarding the applicability of the most promising methods of the above, namely precipitation/flocculation with Fe^{III}, Al^{III}, and $Ca(OH)_2$, as well as UV/Fenton and UV/Fe^{II} processes (Rott *et al.* 2017a; Rott *et al.* 2017b). It was found that the precipitation/flocculation process has economic advantages over the oxidative UV/Fenton and UV/Fe^{II} processes.

Contribution to Reducing the Discharged Phosphonate Load Into Water Bodies

According to the load balance by Rott (2016), there were about 4,200–5,200 t of phosphonates in raw wastewater from direct dischargers in Germany in 2012. Considering the six phosphonates investigated in this thesis, this would amount to approximately 480–1,620 t of phosphonate-P. Cooling waters and membrane concentrates accounted for 65–90% of this, i.e. 2,730–4,680 t of phosphonates. According to Gartiser and Ulrich (2002), about 1,500–2,200 t of phosphonates were used in cooling water conditioning in 2001. This would yield an annual load of 530–3,180 t of phosphonates in membrane concentrates, which are often discharged into water bodies without further treatment. If a nationwide technical implementation of the adsorption process on GEH resulted in an elimination efficiency of 90% of the phosphonate load, the phosphonate discharge into water bodies could be reduced by about 480–2,860 t per year. It should be noted that the figures used have a different temporal origin and are therefore not directly comparable with each other. It is nevertheless assumed that the extrapolation gives a sufficiently accurate order of magnitude. It should also be taken into account that phosphonate consumption has been increasing in recent years, which would result in higher values at present.

For comparison, the total phosphorus discharge from point sources, i.e., municipal wastewater treatment plants and industrial direct dischargers, to water bodies in Germany was approximately 7,820 t P in 2012-2014 (UBA 2017). The phosphonate load in raw wastewater from direct dischargers in Germany thus corresponds to about 6–21% of the phosphorus load entering German waters from point sources. Orthophosphate-P accounts for approximately 61% of the total phosphorus load (LUBW 2015). While phosphonate concentrations in water bodies are mostly in the single-digit µg/L range (see section 1.2.4.3), the total phosphorus concentration in the Rhine river in 2019, for example, was 64 µg P/L as an annual mean (BfG 2021b). More rarely phosphonate concentrations in the double-digit µg/L range can be found, but these usually occur in samples taken near discharge of phosphonate-containing wastewater (see section 1.2.4.3). The annual mean orthophosphate concentration in the Rhine river in 2019 was 23 µg P/L (BfG 2021b). Accordingly, the phosphonate-P concentration is approximately a factor of 10 to 30 below the orthophosphate concentration in the Rhine river, but is still not negligible. Especially since the phosphonates accumulate strongly in the sediment due to their high adsorption affinity.

Cost Assessment

In the research project described in Section 1.3.6, from which this thesis originated, a rough cost comparison between the precipitation/flocculation processes and adsorption on GFH was carried out (Rott *et al.* 2019). For the cost comparison, the investment costs (tanks/filter columns, dosing stations, PLC control, sludge treatment equipment) and operating costs were considered. The latter are mainly composed of personnel costs, disposal costs, electricity costs, maintenance costs and costs of the dosed chemicals. The cost calculation was kept simple and did not take into account the development of interest rates and depreciation periods. Tab. 5.1 summarizes the specific investment costs and operating costs for a treatment plant for P removal from membrane concentrate. Costs for pumps and piping were generously included in the tank costs in Tab. 5.1. A detailed description of the composition of the costs can be found in Rott *et al.* (2019).

Tab. 5.1: Specific investment costs and operating costs, pc.: piece.

Investment costs		**Operating costs**	
Component	**Price**	**Item**	**Price**
Reservoir	1,000 €/m³	FerroSorp RW	1.75 €/kg
Dosing station	5,000/pc.	NaOH	0.028 €/mol
Stirring tank	1,000 €/m³	H_2SO_4	0.020 €/mol
Filter column	1,000 €/m³	HCl	0.010 €/mol
PLC (control)	10,000 €/pc.	Fe^{III}	1.56 €/kg
Sedimentation tank	1,000 €/m³	Al^{III}	6.50 €/kg
Chamber filter press	16,000 €/pc.	$Ca(OH)_2$	0.10 €/kg
Filter cake tank	1,000 €/m³	Electricity	0.05 €/kWh
Acid/base reservoir	1,000 €/m³	Personnel	40 €/h
		Sludge disposal	50 €/t
		Acid/base disposal	50 €/m³

The costs of the precipitation/flocculation method depend strongly on the treatment target. For example, in the laboratory experiments by Rott *et al.* (2017b), both using Fe^{III} and using Al^{III}, a β-value of 6 (14 mg/L Fe^{III}, 7 mg/L Al^{III}) was required to remove 85% total P and a β-value of 25 (59 mg/L Fe^{III}, 28 mg/L Al^{III}) was required to remove 90%. The situation was similar for $Ca(OH)_2$. As such, for 85% removal, 400 mg/L $Ca(OH)_2$ was required and for 90% removal, 1,000 mg/L $Ca(OH)_2$ was required. Treatment of the total wastewater volume of 1,000 m³/d with a P removal target of 85% results in investment costs of about 174,000 € for precipitation/flocculation with Fe^{III} or Al^{III}, or 181,000 € for the use of $Ca(OH)_2$. The operating costs sum up to 0.13 €/m³, 0.15 €/m³, and 0.23 €/m³ for precipitation/flocculation with Fe^{III}, Al^{III}, and $Ca(OH)_2$, respectively. Over a ten-year period, therefore, total costs (investment and operating costs) of 660,000 €, 736,000 €, and 1,024,000 €, respectively, are incurred for the use of Fe^{III}, Al^{III}, and $Ca(OH)_2$. With a P removal target of 90%, these costs increase to 967,000 €, 1,286,000 €, or 1,559,000 €. When $Ca(OH)_2$ is used, 20–25 times more sludge is produced than when Fe^{III} and Al^{III} are used, which is noticeable in the sludge disposal costs. Thus, the amount of the operating cost is: $Fe^{III} < Al^{III} < Ca(OH)_2$. However, precipitation by means of $Ca(OH)_2$ turned out to be an effective method for total P removal and simultaneous water softening for membrane concentrates with a high Ca^{2+} and HCO_3^- content, since $CaCO_3$ and $Ca(OH)_2$ precipitated already at pH values slightly above 8 (Rott *et al.* 2017b). Fig. 5.2 gives an overview of the investment and operating costs for the precipitation/flocculation methods.

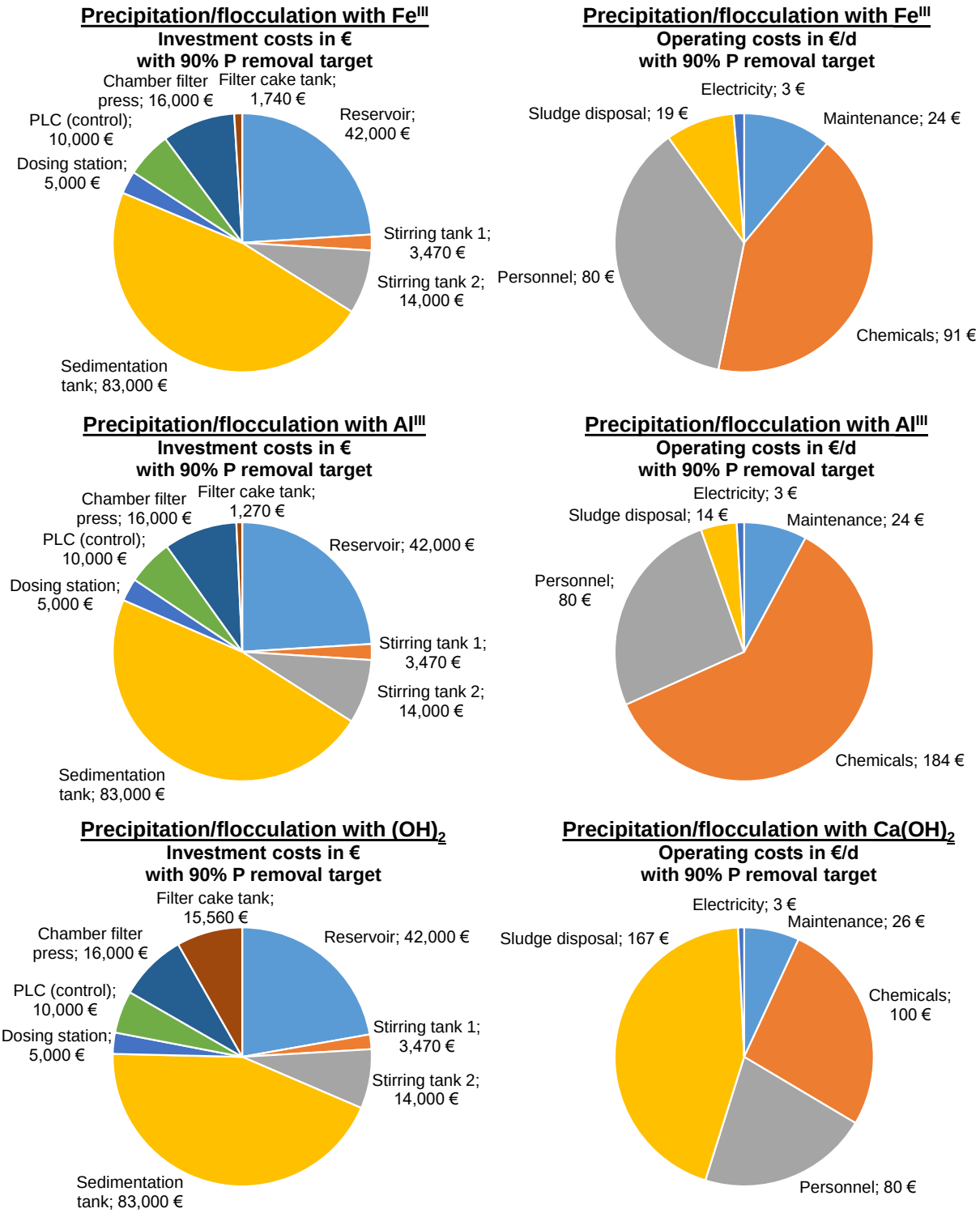

Fig. 5.2: Distribution of investment and operating costs for precipitation/flocculation with Fe^{III}, Al^{III}, and $Ca(OH)_2$ for the treatment of 1,000 m³/d (Rott et al. 2019).

The cost assessment for the GFH adsorption process by Rott *et al.* (2019) was carried out based on the adjustment of the pH value of the membrane concentrate by H_2SO_4 to pH 6 and with an EBCT of 3 minutes. The novel regeneration with HCl had not yet

been investigated at the time of the report. Usually, several columns are connected in parallel or in series so that during a regeneration process one column can be regenerated while the remaining columns can be continuously used for adsorption. In accordance with the experience gained from the laboratory experiments, the possibility of reusing the GFH 24 times was considered for the cost assessment, although likely even more cycles are possible. The NaOH solution for regeneration is also used over 24 cycles, before being replaced with fresh NaOH. The treatment of the alkaline regeneration solution, which accumulates phosphorus during the operation of the filter columns, was considered in the calculations with disposal costs of 50 €/m³. For treatment of the total wastewater volume, Rott *et al.* (2019) estimated investment costs of 70,500 € and operating costs of 0.41 €/m³. The largest cost factor here is the sulfuric acid used to adjust the pH. For a period of ten years the total costs sum up to 1,571,000 €.

For the novel acidic regeneration presented in Chapter 4, a rough cost assessment was performed with the same calculation methods as by Rott *et al.* (2019), likewise for 24 possible cycles until the NaOH and GFH are replaced, but with an EBCT of 4 minutes. Analogous to the disposal costs of the NaOH, 50 €/m³ were also assumed for the disposal of the acidic regeneration solution HCl. This resulted in investment costs of 90,500 € and operating costs of 0.32 €/m³. Accordingly, operating costs were reduced by about 22%, despite the higher EBCT, which results in additional demand for GFH and NaOH. The total cost for ten years in this case is 1,249,000 €. Tab. 5.2 shows the costs for a ten-year period for the different methods described.

Tab. 5.2: Cumulative investment and operating costs for a period of ten years for the treatment of 1,000 m³/d.

Treatment method	P removal	Costs for a ten-year period
Precipitation/flocculation with Fe^{III}	85%	660,000 €
	90%	967,000 €
Precipitation/flocculation with Al^{III}	85%	736,000 €
	90%	1,286,000 €
Precipitation/flocculation with $Ca(OH)_2$	85%	1,024,000 €
	90%	1,559,000 €
Adsorption on GFH with pH adjustment	93%	1,571,000 €
Adsorption on GFH with acidic regeneration	95%	1,249,000 €

Thus, the costs of the GFH adsorption process are already in a comparable range to precipitation/flocculation, despite its better P removal efficiency of 95%. The slightly higher costs of the filtration process compared to the precipitation/flocculation process can be compensated by the much smaller construction volume. Additionally, as described above, there is still great potential for optimization, so that further cost reductions are likely possible and the GFH adsorption process could become more cost-efficient as the precipitation/flocculation process. Fig. 5.3 shows the investment and operating costs for adsorption on GFH with pH adjustment and acidic regeneration.

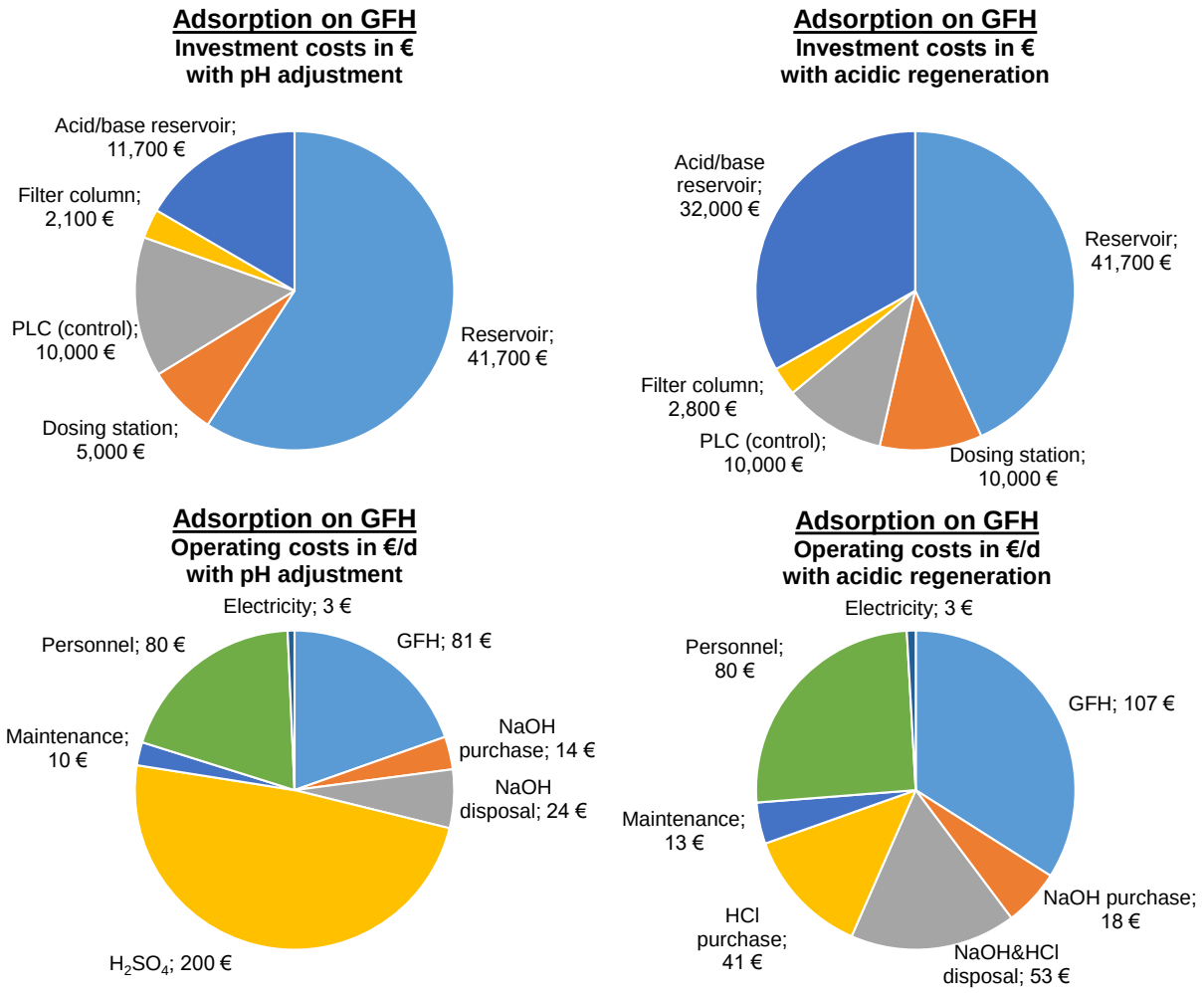

Fig. 5.3: Distribution of investment and operating costs for adsorption on GFH with pH adjustment and acidic regeneration for the treatment of 1,000 m³/d (Rott et al. 2019).

Conclusion

In conclusion, more research is recommended before starting technical implementation of membrane concentrate treatment with GFH. However, the results of this thesis prove that adsorption on GFH is a potential treatment method for membrane concentrate and a rough cost estimation shows that it can compete with precipitation/flocculation processes. Treatment of membrane concentrate with GFH could therefore be a way to reduce the discharge of phosphonates to water bodies and thus reduce potential environmental impacts such as their adsorption to sediments, the long-term effects of which are not yet known.

References

AAW 1984 *Internal Report 452/84806,* Albright and Wilson Ltd. Cited by OECD SIDS 1996.

AbwV 2004 *Ordinance on Requirements for the Discharge of Waste Water into Waters*: *AbwV*.

Akın, B., Öner, M., Bayram, Y. and Demadis, K. D. 2008 Effects of Carboxylate-Modified, “Green” Inulin Biopolymers on the Crystal Growth of Calcium Oxalate. *Crystal Growth and Design*, **8**(6), 1997–2005.

Akratanakul, S., Boersma, L. and Klock, G. O. 1983 Sorption processes in soils as influenced by pore water velocity: 2. Experimental Results. *Soil Science*, **135**(6), 331–341.

Altaf, R., Lin, X., Tadda, M. A., Zhu, S. and Liu, D. 2021a Modified magnetite adsorbent (Zr–La@Fe_3O_4) for nitrilotrismethylenephosphonate (NTMP) removal and recovery from wastewater. *Journal of Cleaner Production*, **278**, 123960.

Altaf, R., Lin, X., Zhuang, W., Lu, H., Rout, P. R. and Liu, D. 2021b Nitrilotrismethylenephosphonate sorption from wastewater on zirconium-lanthanum modified magnetite: Reusability and mechanism study. *Journal of Cleaner Production*, **314**, 128045.

Amjad, Z. 1987 The influence of polyphosphates, phosphonates, and poly(carboxylic acids) on the crystal growth of hydroxyapatite. *Langmuir*, **3**(6), 1063–1069.

Amjad, Z., Zuhl, R. W. and Zibrida, J. F. 2003 *Factors Influencing the Precipitation of Calcium-Inhibitor Salts in Industrial Water Systems,* Association of Water Technologies, Inc., 2003 Annual Convention, Phoenix, AZ.

Antelo, J., Arce, F., Avena, M., Fiol, S., López, R. and Macías, F. 2007 Adsorption of a soil humic acid at the surface of goethite and its competitive interaction with phosphate. *Geoderma*, **138**(1-2), 12–19.

Antelo, J., Arce, F. and Fiol, S. 2015 Arsenate and phosphate adsorption on ferrihydrite nanoparticles. Synergetic interaction with calcium ions. *Chemical Geology*, **410**, 53–62.

Antelo, J., Avena, M., Fiol, S., Lopez, R. and Arce, F. 2005 Effects of pH and ionic strength on the adsorption of phosphate and arsenate at the goethite-water interface. *Journal of Colloid and Interface Science*, **285**(2), 476–486.

Antony, A., Low, J. H., Gray, S., Childress, A. E., Le-Clech, P. and Leslie, G. 2011 Scale formation and control in high pressure membrane water treatment systems: A review. *Journal of Membrane Science*, **383**(1–2), 1–16.

Arias, M., Da Silva-Carballal, J., Garcia-Rio, L., Mejuto, J. and Nunez, A. 2006 Retention of phosphorus by iron and aluminum-oxides-coated quartz particles. *Journal of Colloid and Interface Science*, **295**(1), 65–70.

Armbruster, D., Müller, U. and Happel, O. 2019 Characterization of phosphonate-based antiscalants used in drinking water treatment plants by anion-exchange chromatography coupled to electrospray ionization time-of-flight mass spectrometry and inductively coupled plasma mass spectrometry. *Journal of Chromatography A*, **1601**, 189–204.

Armbruster, D., Rott, E., Minke, R. and Happel, O. 2020 Trace-level determination of phosphonates in liquid and solid phase of wastewater and environmental samples by IC-ESI-MS/MS. *Analytical and Bioanalytical Chemistry*, **412**(20), 4807–4825.

Ashekuzzaman, S. M. and Jiang, J.-Q. 2017 Improving the removal of phosphate in secondary effluent of domestic wastewater treatment plant. In: *CEST2017 Proceedings*.

Bachus, H. 2003 Komplexbildner in Abbautests und in der Realität (Complexing agents in degradation tests and in reality). *Melliand Textilberichte/International Textile Reports*, **84**(3), 202–204.

BADSR 1976 *Bayer AG Data short Report*. Cited by OECD SIDS 1996.

BADSR 1989 *Bayer AG Data short Report*. Cited by OECD SIDS 1996.

Baeyer, H. von and Hofmann, K. A. 1897 Acetodiphosphorige Säure (Etidronic acid). *Berichte der Deutschen Chemischen Gesellschaft,* **30**(2), 1973–1978.

Baraka-Lokmane, S., Sorbie, K., Poisson, N. and Kohler, N. 2009 Can Green Scale Inhibitors Replace Phosphonate Scale Inhibitors?: Carbonate Coreflooding Experiments. *Petroleum Science and Technology*, **27**(4), 427–441.

Barja, B. C., Tejedor-Tejedor, M. I. and Anderson, M. A. 1999 Complexation of Methylphosphonic Acid with the Surface of Goethite Particles in Aqueous Solution. *Langmuir*, **15**(7), 2316–2321.

Bartels, T., Schuthof, J. and Arends, J. 1979 The adsorption of two polyphosphonates on hydroxyapatite and their influence on the acid solubility of whole bovine enamel. *Journal of Dentistry*, **7**(3), 221–229.

BfG 2021a Ethylendiamintetraessigsäure (EDTA). Langjährige Entwicklung im Rheineinzugsgebiet (Ethylenediaminetetraacetic acid (EDTA). Long-term development in the Rhine catchment area.). https://undine.bafg.de/rhein/guetemessstellen/img/EDTA_Gerloff_29112021.pdf (accessed 06 February 2022).

BfG 2021b Nährstoffe. Langjährige Entwicklung im Rheineinzugsgebiet (Nutrients. Long-term development in the Rhine catchment area.). https://undine.bafg.de/rhein/guetemessstellen/img/Naehrstoffe_Gerloff_25112021.pdf (accessed 06 February 2022).

Bisson, C., Adams, N. B. P., Stevenson, B., Brindley, A. A., Polyviou, D., Bibby, T. S., Baker, P. J., Hunter, C. N. and Hitchcock, A. 2017 The molecular basis of phosphite and hypophosphite recognition by ABC-transporters. *Nature Communications*, **8**(1), 1746.

Black, J. R. 2016 Complexes. In: *Encyclopedia of Geochemistry: A Comprehensive Reference Source on the Chemistry of the Earth*, W. M. White (ed.), Springer International Publishing, Cham, pp. 1–4.

Black, S. N., Bromley, L. A., Cottier, D., Davey, R. J., Dobbs, B. and Rout, J. E. 1991 Interactions at the organic/inorganic interface: Binding motifs for phosphonates at the surface of barite crystals. *Journal of the Chemical Society, Faraday Transactions*, **87**(20), 3409–3414.

Boels, L. 2012 *Removal and Recovery of Phosphonate Antiscalants*. Dissertation, Delft University of Technology, Delft.

Boels, L., Keesman, K. J. and Witkamp, G.-J. 2012 Adsorption of phosphonate antiscalant from reverse osmosis membrane concentrate onto granular ferric hydroxide. *Environmental Science and Technology*, **46**(17), 9638–9645.

Boels, L., Tervahauta, T. and Witkamp, G. J. 2010 Adsorptive removal of nitrilotris(methylenephosphonic acid) antiscalant from membrane concentrates by iron-coated waste filtration sand. *Journal of Hazardous Materials*, **182**(1-3), 855–862.

Boels, L. and Witkamp, G.-J. 2011 Carboxymethyl Inulin Biopolymers: A Green Alternative for Phosphonate Calcium Carbonate Growth Inhibitors. *Crystal Growth and Design*, **11**(9), 4155–4165.

Bonilla-Petriciolet, A., Mendoza-Castillo, D. I. and Reynel-Ávila, H. E. 2017 *Adsorption Processes for Water Treatment and Purification.* Springer International Publishing, Cham.

Bordas, F. and Bourg, A. C. M. 1998 Effect of Complexing Agents (EDTA and ATMP) on the Remobilization of Heavy Metals from a Polluted River Sediment. *Aquatic Geochemistry*, **4**(2), 201–214.

Borggaard, O. K., Raben-Lange, B., Gimsing, A. L. and Strobel, B. W. 2005 Influence of humic substances on phosphate adsorption by aluminium and iron oxides. *Geoderma*, **127**(3-4), 270–279.

Botta, F., Lavison, G., Couturier, G., Alliot, F., Moreau-Guigon, E., Fauchon, N., Guery, B., Chevreuil, M. and Blanchoud, H. 2009 Transfer of glyphosate and its degradate AMPA to surface waters through urban sewerage systems. *Chemosphere*, **77**(1), 133–139.

Boujelben, N., Bouzid, J., Elouear, Z., Feki, M., Jamoussi, F. and Montiel, A. 2008 Phosphorus removal from aqueous solution using iron coated natural and engineered sorbents. *Journal of Hazardous Materials*, **151**(1), 103–110.

Boyd, C. E. 2015 Phosphorus. In: *Water Quality*, C. E. Boyd (ed.), Springer International Publishing, Cham, pp. 243–261.

Brezonik, P. L. and Arnold, W. A. 2011 *Water chemistry*: *An introduction to the chemistry of natural and engineered aquatic systems.* Oxford University Press, Oxford.

Browning, F. H. and Fogler, H. S. 1995 Effect of Synthesis Parameters on the Properties of Calcium Phosphonate Precipitates. *Langmuir*, **11**(10), 4143–4152.

Browning, F. H. and Fogler, H. S. 1996 Effect of Precipitating Conditions on the Formation of Calcium−HEDP Precipitates. *Langmuir*, **12**(21), 5231–5238.

Bryant, D. 2004 The chemistry of phosphorus. In: *Phosphorus in environmental technologies*. *Principles and applications*, E. Valsami-Jones (ed.). Integrated environmental technology series, IWA Publishing, London, pp. 1–19.

Bucheli-Witschel, M. and Egli, T. 2001 Environmental fate and microbial degradation of aminopolycarboxylic acids. *FEMS Microbiology Reviews*, **25**(1), 69–106.

Cabrera, F., Arambarri, P. de, Madrid, L. and Toga, C. G. 1981 Desorption of phosphate from iron oxides in relation to equilibrium pH and porosity. *Geoderma*, **26**(3), 203–216.

Catherine, Q., Susanna, W., Isidora, E.-S., Mark, H., Aurélie, V. and Jean-François, H. 2013 A review of current knowledge on toxic benthic freshwater cyanobacteria – ecology, toxin production and risk management. *Water Research*, **47**(15), 5464–5479.

Cegarra, J., Gacén, J., Cayuela, D. and Riva, M. C. 1994 Comparison of stabilisers for wool bleaching with hydrogen peroxide. *Journal of the Society of Dyers and Colourists*, **110**(9), 308–310. Cited by HERA 2004.

Charlet, L., Dise, N. and Stumm, W. 1993 Sulfate adsorption on a variable charge soil and on reference minerals. *Agriculture, Ecosystems and Environment*, **47**(2), 87–102.

Chaussemier, M., Pourmohtasham, E., Gelus, D., Pécoul, N., Perrot, H., Lédion, J., Cheap-Charpentier, H. and Horner, O. 2015 State of art of natural inhibitors of calcium carbonate scaling. A review article. *Desalination*, **356**, 47–55.

ChemAxon Ltd. 2017 Database of https://chemicalize.com (accessed 09 December 2017).

Chen, J., Xu, L., Han, J., Su, M. and Wu, Q. 2015 Synthesis of modified polyaspartic acid and evaluation of its scale inhibition and dispersion capacity. *Desalination*, **358**, 42–48.

Chen, Y., Baygents, J. C. and Farrell, J. 2017 Removing phosphonate antiscalants from membrane concentrate solutions using granular ferric hydroxide. *Journal of Water Process Engineering*, **19**, 18–25.

Chen, Y., Wu, F., Lin, Y., Deng, N., Bazhin, N. and Glebov, E. 2007 Photodegradation of glyphosate in the ferrioxalate system. *Journal of Hazardous Materials*, **148**(1-2), 360–365.

Chhim, N., Haddad, E., Neveux, T., Bouteleux, C., Teychené, S. and Biscans, B. 2020 Performance of green antiscalants and their mixtures in controlled calcium carbonate precipitation conditions reproducing industrial cooling circuits. *Water Research*, **186**, 116334.

Chirby, D., Franck, S. and Troutner, D. E. 1988 Adsorption of 153Sm-EDTMP on calcium hydroxyapatite. *International Journal of Radiation Applications and Instrumentation. Part A. Applied Radiation and Isotopes*, **39**(6), 495–499.

Chitrakar, R., Tezuka, S., Sonoda, A., Sakane, K., Ooi, K. and Hirotsu, T. 2006 Phosphate adsorption on synthetic goethite and akaganeite. *Journal of Colloid and Interface Science*, **298**(2), 602–608.

Chorus, I., Köhler, A., Beulker, C., Fastner, J., van de Weyer, K., Hegewald, T. and Hupfer, M. 2020 Decades needed for ecosystem components to respond to a sharp and drastic phosphorus load reduction. *Hydrobiologia*, **847**(21), 4621–4651.

Connect Chemicals 2018 *Material Safety Data Sheet - Hydroxy Phosphono Acetic Acid 50%*.

Cook, A. M., Daughton, C. G. and Alexander, M. 1978 Phosphonate utilization by bacteria. *Journal of Bacteriology*, **133**(1), 85–90.

Corbridge, D. E. C. 2013 *Phosphorus*: *Chemistry, biochemistry and technology,* 6th ed. CRC Press, Boca Raton.

Cornel, P. 1991 Abtrennung und Rückgewinnung von Stoffen durch Adsorption und Ionenaustausch (Separation and recovery of substances by adsorption and ion exchange). *Chemie Ingenieur Technik*, **63**(10), 969–976.

Cornel, P. and Schaum, C. 2009 Phosphorus recovery from wastewater: needs, technologies and costs. *Water Science and Technology*, **59**(6), 1069–1076.

Correll, D. L. 1999 Phosphorus: a rate limiting nutrient in surface waters. *Poultry Science*, **78**(5), 674–682.

Cui, G., Liu, M., Chen, Y., Zhang, W. and Zhao, J. 2016 Synthesis of a ferric hydroxide-coated cellulose nanofiber hybrid for effective removal of phosphate from wastewater. *Carbohydrate Polymers*, **154**, 40–47.

Dąbrowski, A. 2001 Adsorption — from theory to practice. *Advances in Colloid and Interface Science*, **93**(1), 135–224.

Daughton, C. G., Cook, A. M. and Alexander, M. 1979 Bacterial conversion of alkylphosphonates to natural products via carbon-phosphorus bond cleavage. *Journal of Agricultural and Food Chemistry*, **27**(6), 1375–1382.

Davenport, B., DeBoo, A., Dubois, F. and Kishi, A. 2000 *CEH Report: Chelating Agents*. Cited by Nowack 2004.

Day, G. M., Hart, B. T., McKelvie, I. D. and Beckett, R. 1997 Influence of Natural Organic Matter on the Sorption of Biocides onto Goethite, II. Glyphosate. *Environmental Technology*, **18**(8), 781–794.

Deliyanni, E., Peleka, E. and Lazaridis, N. 2007 Comparative study of phosphates removal from aqueous solutions by nanocrystalline akaganéite and hybrid surfactant-akaganéite. *Separation and Purification Technology*, **52**(3), 478–486.

Denison, F. H., Haygarth, P. M., House, W. A. and Bristow, A. W. 1998 The Measurement of Dissolved Phosphorus Compounds: Evidence for Hydrolysis During Storage and Implications for Analytical Definitions in Environmental Analysis. *International Journal of Environmental Analytical Chemistry*, **69**(2), 111–123.

DIN 38406-3 *German standard methods for the examination of water, waste water and sludge - Cations (group E) - Part 3: Determination of calcium and magnesium, complexometric method (E 3).* Beuth Verlag GmbH, Berlin.

DIN 38409 *German standard methods for the examination of water, waste water and sludge - Parameters characterizing effects and substances (group H) - Part 7: Determination of acid and base-neutralizing capacities (H 7) (DIN 38409-7:2005-12).* Beuth Verlag GmbH, Berlin.

DIN 66131 *Determination of specific surface area of solids by gas adsorption using the method of Brunauer, Emmett and Teller (BET).* Beuth Verlag GmbH, Berlin.

Dodds, W. K., Bouska, W. W., Eitzmann, J. L., Pilger, T. J., Pitts, K. L., Riley, A. J., Schloesser, J. T. and Thornbrugh, D. J. 2009 Eutrophication of U.S. freshwaters: analysis of potential economic damages. *Environmental Science and Technology*, **43**(1), 12–19.

Dodds, W. K., Jones, J. R. and Welch, E. B. 1998 Suggested classification of stream trophic state: distributions of temperate stream types by chlorophyll, total nitrogen, and phosphorus. *Water Research*, **32**(5), 1455–1462.

Dollinger, J., Dagès, C. and Voltz, M. 2015 Glyphosate sorption to soils and sediments predicted by pedotransfer functions. *Environmental Chemistry Letters*, **13**(3), 293–307.

Dongmei, L., Hui, H., Tingjin, Y., Mingzhu, H., Yi, R., Chunliu, L. and Na, H. 2011 Study on the Optimum Preparation Process Conditions of Iron Oxide Coated Sand. In: *2011 International Conference on Computer Distributed Control and Intelligent Environmental Monitoring (CDCIEM)*, pp. 1823–1826.

Drenkova-Tuhtan, A., Schneider, M., Franzreb, M., Meyer, C., Gellermann, C., Sextl, G., Mandel, K. and Steinmetz, H. 2017 Pilot-scale removal and recovery of dissolved phosphate from secondary wastewater effluents with reusable ZnFeZr adsorbent @ Fe_3O_4/SiO_2 particles with magnetic harvesting. *Water Research*, 77–87.

Drenkova-Tuhtan, A., Sheeleigh, E. K., Rott, E., Meyer, C. and Sedlak, D. L. 2021 Sorption of recalcitrant phosphonates in reverse osmosis concentrates and wastewater effluents - influence of metal ions. *Water Science and Technology*, **83**(4), 934–947.

Eisenreich, S. J., Bannerman, R. T. and Armstrong, D. E. 1975 A simplified phosphorus analysis technique. *Environmental Letters*, **9**(1), 43–53.

EPA 2013 *European Phosphonate Association – Phosphonates in Detergents*: *EPA Detergent Phosphonates Dossier*.

Ernst, M., Sperlich, A., Zheng, X., Gan, Y., Hu, J., Zhao, X., Wang, J. and Jekel, M. 2007 An integrated wastewater treatment and reuse concept for the Olympic Park 2008, Beijing. *Desalination*, **202**(1-3), 293–301.

EU 1991 *Council Directive 91/271/EEC of 21 May 1991 concerning urban waste-water treatment*: *European Union*.

EU 1993 *Council Regulation (EEC) 793/93 of 23 March 1993 on the evaluation and control of the risks of existing substances: European Union*.

EU 1994 *Commission Regulation (EC) 1179/94 of 25 May 1994 concerning the first list of priority substances as foreseen under Council Regulation (EEC) No 793/93: European Union*.

EU 1998 *Commission Directive 98/15/EC of 27 February 1998 amending Council Directive 91/271/EEC with respect to certain requirements established in Annex I thereof*: *European Union*.

EU 2000 *Directive 2000/60/EC of the European Parliament and of the Council of 23 October 2000 establishing a framework for Community action in the field of water policy*: *European Union*.

EU 2004 *Regulation (EC) No 648/2004 of the European Parliament and of the Council of 31 March 2004 on detergents*: *European Union*.

Fettig, J., Seydel, P. and Steinert, C. 2000 Removal of Phosphonates and Polyphosphates in the Coagulation Process. In: *Chemical Water and Wastewater Treatment VI*, H. H. Hahn, E. Hoffmann and H. Ødegaard (eds.), Springer Berlin Heidelberg, Berlin, Heidelberg, pp. 279–288.

Fischer, K. 1991 Sorption of chelating agents (HEDP and NTA) onto mineral phases and sediments in aquatic model systems. *Chemosphere*, **22**(1-2), 15–27.

Fischer, K. 1992 Sorption of chelating agents (HEDP and NTA) onto mineral phases and sediments in aquatic model systems. *Chemosphere*, **24**(1), 51–62.

Fischer, K. 1993 Distribution and elimination of HEDP in aquatic test systems. *Water Research*, **27**(3), 485–493.

Ford, R. 2006 Structural Dynamics of Metal Partitioning to Mineral Surfaces. In: *Natural Attenuation of Trace Element Availability in Soils*, R. Hamon (ed.), CRC Press, pp. 73–88.

Fox, E. M. and Mendz, G. L. 2006 Phosphonate degradation in microorganisms. *Enzyme and Microbial Technology*, **40**(1), 145–150.

Friedfeld, S. J., He, S. and Tomson, M. B. 1998 The Temperature and Ionic Strength Dependence of the Solubility Product Constant of Ferrous Phosphonate. *Langmuir*, **14**(13), 3698–3703.

Froelich, P. N. 1988 Kinetic control of dissolved phosphate in natural rivers and estuaries: A primer on the phosphate buffer mechanism. *Limnology and Oceanography*, **33**, 649–668.

Fu, Z., Wu, F., Song, K., Lin, Y., Bai, Y., Zhu, Y. and Giesy, J. P. 2013 Competitive interaction between soil-derived humic acid and phosphate on goethite. *Applied Geochemistry*, **36**, 125–131.

G.Ternan, N., Mc Grath, J. W., Mc Mullan, G. and Quinn, J. P. 1998 Review: Organophosphonates: occurrence, synthesis and biodegradation by microorganisms. *World Journal of Microbiology and Biotechnology*, **14**(5), 635–647.

Gales, M. E., Julian, E. C. and Kroner, R. C. 1966 Method for Quantitative Determination of Total Phosphorus in Water. *Journal - American Water Works Association*, **58**(10), 1363–1368.

Gao, Y. and Mucci, A. 2003 Individual and competitive adsorption of phosphate and arsenate on goethite in artificial seawater. *Chemical Geology*, **199**(1–2), 91–109.

Garcia, C., Courbin, G., Ropital, F. and Fiaud, C. 2001 Study of the scale inhibition by HEDP in a channel flow cell using a quartz crystal microbalance. *Electrochimica Acta*, **46**(7), 973–985.

Gartiser, S. and Urich, E. 2002 *Einsatz umweltverträglicher Chemikalien in der Kühlwasserkonditionierung (Use of environment-friendly chemicals in cooling water conditioning),* Texte 70/02, Umweltbundesamt, Berlin, Germany. https://www.umweltbundesamt.de/sites/default/files/medien/publikation/long/2218.pdf (accessed 10 July 2021).

Geelhoed, J. S., Hiemstra, T. and van Riemsdijk, W. H. 1997 Phosphate and sulfate adsorption on goethite: Single anion and competitive adsorption. *Geochimica et Cosmochimica Acta*, **61**(12), 2389–2396.

Geelhoed, J. S., Hiemstra, T. and van Riemsdijk, W. H. 1998 Competitive Interaction between Phosphate and Citrate on Goethite. *Environmental Science and Technology*, **32**(14), 2119–2123.

Genz, A. 2005 *Entwicklung einer neuen Adsorptionstechnik zur Entfernung natürlicher Organika mit granuliertem Eisenhydroxid (Development of a new adsorption technique for the removal of natural organics with granulated ferric hydroxide)*. Dissertation, TU Berlin, Berlin.

Genz, A., Baumgarten, B., Goernitz, M. and Jekel, M. 2008 NOM removal by adsorption onto granular ferric hydroxide: Equilibrium, kinetics, filter and regeneration studies. *Water Research*, **42**(1-2), 238–248.

Genz, A., Kornmuller, A. and Jekel, M. 2004 Advanced phosphorus removal from membrane filtrates by adsorption on activated aluminium oxide and granulated ferric hydroxide. *Water Research*, **38**(16), 3523–3530.

Gerbino, A. J. 1996 *Quantifying the retention and release of polyphosphonates in oil and gas producing formations using surface complexation and precipitation theory*. Dissertation, Rice University, Houston, Texas.

Gledhill, W. E. and Feijtel, T. C. J. 1992 Environmental Properties and Safety Assessment of Organic Phosphonates Used for Detergent and Water Treatment Applications. In: *Detergents*, N. T. de Oude (ed.), Springer Berlin Heidelberg, Berlin, Heidelberg, pp. 261–285.

Goldberg, S. and Sposito, G. 1985 On the mechanism of specific phosphate adsorption by hydroxylated mineral surfaces: A review. *Communications in Soil Science and Plant Analysis*, **16**(8), 801–821.

Greenlee, L. F., Freeman, B. D. and Lawler, D. F. 2014 Ozonation of phosphonate antiscalants used for reverse osmosis desalination: Parameter effects on the extent of oxidation. *Chemical Engineering Journal*, **244**, 505–513.

Greenlee, L. F., Lawler, D. F., Freeman, B. D., Marrot, B. and Moulin, P. 2009 Reverse osmosis desalination: Water sources, technology, and today's challenges. *Water Research*, **43**(9), 2317–2348.

Grohmann, A. and Horstmann, B. 1989 *Der Einsatz von Phosphonaten unter umwelttechnischen Gesichtspunkten*: *Forschungsbericht 102 063 22 UFA-B 89-018 (The use of phosphonates from an environmental point of view: Research Report 102 063 22 UFA-B 89-018*.)

Groß, R., Bunke, D., Moch, K. and Leisewitz, A. 2012 *Untersuchung der Einsatzmengen von schwer abbaubaren organischen Inhaltsstoffen in Wasch- und Reinigungsmitteln im Vergleich zum Einsatz dieser Stoffe in anderen Branchen im Hin-*

blick auf den Nutzen einer Substitution (Investigation of the use of poorly degradable organic ingredients in detergents and cleaning agents in comparison with the use of these substances in other industries with regard to the benefits of substitution), UBA-FB 3709 65 430. https://www.bmu.de/fileadmin/Daten_BMU/Pools/Forschungsdatenbank/fkz_3709_65_430_wasch_und_reinigungsmittel_bf.pdf (accessed 08 July 2021).

Gross, R. A. and Kalra, B. 2002 Biodegradable polymers for the environment. *Science*, **297**(5582), 803–807.

Günther, K., Henze, W. and Umland, F. 1987 Mobilisationsverhalten von Thallium und Cadmium in einem Flußsediment (Mobilization behavior of thallium and cadmium in a river sediment). *Zeitschrift fur Analytische Chemie*, **327**(3-4), 301–303.

Halliwell, D. J., McKelvie, I. D., Hart, B. T. and Dunhill, R. H. 2001 Hydrolysis of triphosphate from detergents in a rural waste water system. *Water Research*, **35**(2), 448–454.

Han, C., Lalley, J., Iyanna, N. and Nadagouda, M. N. 2017 Removal of phosphate using calcium and magnesium-modified iron-based adsorbents. *Materials Chemistry and Physics*, **198**, 115–124.

Hanke, I., Wittmer, I., Bischofberger, S., Stamm, C. and Singer, H. 2010 Relevance of urban glyphosate use for surface water quality. *Chemosphere*, **81**(3), 422–429.

Hasson, D., Shemer, H. and Sher, A. 2011 State of the Art of Friendly “Green” Scale Control Inhibitors: A Review Article. *Industrial and Engineering Chemistry Research*, **50**(12), 7601–7607.

Held, S. 1989 Zum Umweltverhalten von Komplexbildnern auf Phosphonsäurebasis (On the environmental behavior of phosphonic acid-based complexing agents). *Textilveredlung*, **24**(11), 394–398.

Helfferich, F. 1962 Ligand Exchange. I. Equilibria. *Journal of the American Chemical Society*, **84**(17), 3237–3242.

Hendriks, A. T. W. M. and Langeveld, J. G. 2017 Rethinking Wastewater Treatment Plant Effluent Standards: Nutrient Reduction or Nutrient Control? *Environmental Science and Technology*, **51**(9), 4735–4737.

HERA 2004 *Human & Environmental Risk Assessment on ingredients of European household cleaning products*. https://www.heraproject.com/files/30-F-04-%20HERA%20Phosphonates%20Full%20web%20wd.pdf (accessed 08 July 2021).

Hilbrandt, I., Lehmann, V., Zietzschmann, F., Ruhl, A. S. and Jekel, M. 2019a Quantification and isotherm modelling of competitive phosphate and silicate adsorption onto micro-sized granular ferric hydroxide. *RSC Advances*, **9**(41), 23642–23651.

Hilbrandt, I., Ruhl, A. and Jekel, M. 2018 Conditioning Fixed-Bed Filters with Fine Fractions of Granulated Iron Hydroxide (µGFH). *Water*, **10**(10), 1324.

Hilbrandt, I., Shemer, H., Ruhl, A. S., Semiat, R. and Jekel, M. 2019b Comparing fine particulate iron hydroxide adsorbents for the removal of phosphate in a hybrid adsorption/ultrafiltration system. *Separation and Purification Technology.*, **221**, 23–28.

Ho, Y. and Mckay, G. 1999 Pseudo-second order model for sorption processes. *Process Biochemistry*, **34**(5), 451–465.

Ho, Y. S., Porter, J. F. and Mckay, G. 2002 Equilibrium Isotherm Studies for the Sorption of Divalent Metal Ions onto Peat: Copper, Nickel and Lead Single Component Systems. *Water, Air, and Soil Pollution*, **141**(1), 1–33.

Ho, Y.-S. 2006 Second-order kinetic model for the sorption of cadmium onto tree fern: a comparison of linear and non-linear methods. *Water Research*, **40**(1), 119–125.

Hoelger, C., Held-Beller, S. and Palmtag, J. 2008 Phosphonate als ökologisch sinnvolle Alternative zur DTPA – Ergebnisse einer Studie bei MD Albbruck (Phosphonates as an ecologically sound alternative to DTPA - Results of a study at MD Albbruck). *Wochenblatt für Papierfabrikation*, **11-12**, 666–669.

Horiguchi, M. and Kandatsu, M. 1959 Isolation of 2-aminoethane phosphonic acid from rumen protozoa. *Nature*, **184**, 901–902.

Horsman, G. P. and Zechel, D. L. 2017 Phosphonate Biochemistry. *Chemical Reviews*, **117**(8), 5704–5783.

Horstmann, B. and Grohmann, A. 1988 Untersuchungen zur biologischen Abbaubarkeit von Phosphonaten (Investigations into the Biodegradability of Phosphonates). *Vom Wasser*, **70**, 163–178.

Huang, N., Wang, W.-L., Xu, Z.-B., Wu, Q.-Y. and Hu, H.-Y. 2019 UV/chlorine oxidation of the phosphonate antiscalant 1-Hydroxyethane-1, 1-diphosphonic acid (HEDP) used for reverse osmosis processes: Organic phosphorus removal and scale inhibition properties changes. *Journal of Environmental Management*, **237**, 180–186.

Huber, L. 1975 Untersuchungen über die biologische Abbaufähigkeit und Fischtoxizität von 2 organischen Komplexbildnern auf Phosphonsäurebasis (ATMP und HEDP) (Studies on the biodegradability and fish toxicity of 2 organic phosphonic acid-based complexing agents (ATMP and HEDP)). *Tenside Detergents*, **12**(6), 316–322.

IKSR 2012 *Auswertungsbericht Komplexbildner (Evaluation report complexing agents).* https://www.iksr.org/fileadmin/user_upload/DKDM/Dokumente/Fachberichte/DE/rp_De_0196.pdf *(*accessed 06 February 2022).

IKW 2007 *Nachhaltigkeitsbericht für das Berichtsjahr 2006 für die Wasch- und Reinigungsmittelbranche (Sustainability Report for the Detergents and Cleaning Products Sector for the 2006 Reporting Year)*. https://www.ikw.org/fileadmin/ikw/downloads/IKW-Allgemein/IKW_Nachhaltigkeitsbericht-2006.pdf (accessed 07 July 2021).

IKW 2011 *Nachhaltigkeit in der Wasch-, Pflege- und Reinigungsmittelbranche in Deutschland*: *2009 – 2010 (Sustainability in the detergents, cleaning agents and maintenance products industry in Germany: 2009 – 2010)*. https://www.ikw.org/fileadmin/ikw/downloads/Haushaltspflege/HP_Nachhaltigkeitsbericht09-10.pdf (accessed 07 July 2021).

detergents, cleaning agents and maintenance products

IKW 2017 *Nachhaltigkeit in der Wasch-, Pflege- und Reinigungsmittelbranche in Deutschland*: *2015 – 2016 (Sustainability in the detergents, cleaning agents and maintenance products industry in Germany: 2015 – 2016)*. https://www.ikw.org/fileadmin/ikw/downloads/Haushaltspflege/HP_Nachhaltigkeitsbericht__15_16.pdf (accessed 07 July 2021).

IKW 2021 *Nachhaltigkeit in der Wasch-, Pflege- und Reinigungsmittelbranche in Deutschland*: *Ausgabe 2021 (Sustainability in the detergents, cleaning agents and maintenance products industry in Germany: Edition 2021)*. https://www.ikw.org/fileadmin/ikw/downloads/Haushaltspflege/2021_IKW_Nachhaltigkeitsbericht.pdf (accessed 07 July 2021).

ISO 10707 *DIN EN ISO 10707:1998-03*: *Water quality - Evaluation in an aqueous medium of the "ultimate" aerobic biodegradability of organic compounds - Method by analysis of biochemical oxygen demand (closed bottle test).* Beuth Verlag GmbH, Berlin.

ISO 6878 *DIN EN ISO 6878:2004-09*: *Water quality-Determination of phosphorus-Ammonium molybdate spectrometric method.* Beuth Verlag GmbH, Berlin.

ISO 7827 *DIN EN ISO 7827:2013-03*: *Water quality - Evaluation of the "ready", "ultimate" aerobic biodegradability of organic compounds in an aqueous medium - Method by analysis of dissolved organic carbon (DOC).* Beuth Verlag GmbH, Berlin.

ISO 9408 *DIN EN ISO 9408:1999-12*: *Water quality - Evaluation of ultimate aerobic biodegradability of organic compounds in aqueous medium by determination of oxygen demand in a closed respirometer.* Beuth Verlag GmbH, Berlin.

ISO 9439 *DIN EN ISO 9439:2000-10*: *Water quality - Evaluation of ultimate aerobic biodegradability of organic compounds in aqueous medium - Carbon dioxide evolution test.* Beuth Verlag GmbH, Berlin.

ISO 9887 *DIN EN ISO 9887:1994-12*: *Water quality - Evaluation of the aerobic biodegradability of organic compounds in an aqueous medium - Semi-continuous activated sludge method (SCAS).* Beuth Verlag GmbH, Berlin.

ISO 9888 *DIN EN ISO 9888:1999-11*: *Water quality - Evaluation of ultimate aerobic biodegradability of organic compounds in aqueous medium - Static test (Zahn-Wellens method).* Beuth Verlag GmbH, Berlin.

Italmatch Chemicals 2015 *DEQUEST® 2040, 2050 and 2060 product series*. https://www.italmatch.com/wp-content/uploads/2015/06/ITAL000002_Water-treatment-DQ2040-2050-2060.pdf (accessed 04 July 2021).

Jäger, H.-U. and Schul, W. 2001 Alternativen zu EDTA (Alternatives to EDTA). Münchner Beiträge zur Abwasser-, Fisch- und Flußbiologie, **54**, 207–226. Cited by Schmidt et al. 2004.

Jarrahian, K., Singleton, M., Boak, L. and Sorbie, K. S. 2020 Surface Chemistry of Phosphonate Scale Inhibitor Retention Mechanisms in Carbonate Reservoirs. *Crystal Growth and Design*, **20**(8), 5356–5372.

Jaworska, J., van Genderen-Takken, H., Hanstveit, A., van de Plassche, E. and Feijtel, T. 2002 Environmental risk assessment of phosphonates, used in domestic laundry and cleaning agents in the Netherlands. *Chemosphere*, **47**(6), 655–665.

Jenkins, D., Ferguson, J. F. and Menar, A. B. 1971 Chemical processes for phosphate removal. *Water Research*, **5**(7), 369–389.

Jianbo, L., Liping, S., Xinhua, Z., Bin, L., Yinlei, L. and Lei, Z. 2009 Removal of Phosphate from Aqueous Solution Using Iron-Oxide-Coated Sand Filter Media: Batch Studies. In: *2009 International Conference on Environmental Science and Information Application Technology, ESIAT*, pp. 639–644.

Jonasson, R. G., Rispler, K., Wiwchar, B. and Gunter, W. D. 1996 Effect of phosphonate inhibitors on calcite nucleation kinetics as a function of temperature using light scattering in an autoclave. *Chemical Geology*, **132**(1-4), 215–225.

Jung, A., Bisaz, S. and Fleisch, H. 1973 The binding of pyrophosphate and two diphosphonates by hydroxyapatite crystals. *Calcified Tissue Research*, **11**(4), 269–280.

Kalaitzidou, K., Mitrakas, M., Raptopoulou, C., Tolkou, A., Palasantza, P.-A. and Zouboulis, A. 2016 Pilot-Scale Phosphate Recovery from Secondary Wastewater Effluents. *Environmental Processes*, **3**, 5–22.

Kamat, S. S. and Raushel, F. M. 2013 The enzymatic conversion of phosphonates to phosphate by bacteria. *Current Opinion in Chemical Biology*, **17**(4), 589–596.

Kan, A. T., Fu, G. and Tomson, M. B. 2005 Adsorption and precipitation of an aminoalkylphosphonate onto calcite. *Journal of Colloid and Interface Science*, **281**(2), 275–284.

Kan, A. T., Oddo, J. E. and Tomson, M. B. 1994 Formation of Two Calcium Diethylenetriaminepentakis(methylene phosphonic acid) Precipitates and Their Physical Chemical Properties. *Langmuir*, **10**(5), 1450–1455.

Kanematsu, M., Young, T. M., Fukushi, K., Sverjensky, D. A., Green, P. G. and Darby, J. L. 2011 Quantification of the effects of organic and carbonate buffers on arsenate and phosphate adsorption on a goethite-based granular porous adsorbent. *Environmental Science and Technology*, **45**(2), 561–568.

Karaca, S., Gürses, A., Ejder, M. and Açikyildiz, M. 2006 Adsorptive removal of phosphate from aqueous solutions using raw and calcinated dolomite. *Journal of Hazardous Materials*, **128**(2-3), 273–279.

Karl, D. M. 2014 Microbially Mediated Transformations of Phosphorus in the Sea: New Views of an Old Cycle. *Annual Review of Marine Science*, **6**(1), 279–337.

Kartashevsky, M., Semiat, R. and Dosoretz, C. G. 2015 Phosphate adsorption on granular ferric hydroxide to increase product water recovery in reverse osmosis-desalination of secondary effluents. *Desalination*, **364**, 53–61.

Kästner, W. and Gode, P. 1983 Methoden und Ergebnisse bei der toxikologischen und ökologischen Prüfung von Wasserbehandlungsmitteln (Methods and results in toxicological and ecological evaluation of water treatment agents). *Zeitschrift für Wasser- und Abwasser-Forschung*, **16**, 39–47.

Ketrane, R., Saidani, B., Gil, O., Leleyter, L. and Baraud, F. 2009 Efficiency of five scale inhibitors on calcium carbonate precipitation from hard water: Effect of temperature and concentration. *Desalination*, **249**(3), 1397–1404.

Ketsetzi, A., Stathoulopoulou, A. and Demadis, K. D. 2008 Being “green” in chemical water treatment technologies: issues, challenges and developments. *Desalination*, **223**(1-3), 487–493.

Kırboga, S. and Oner, M. 2012 The inhibitory effects of carboxymethyl inulin on the seeded growth of calcium carbonate. *Colloids and Surfaces B: Biointerfaces*, **91**, 18–25.

Kittredge, J. S. and Roberts, E. 1969 A carbon-phosphorus bond in nature. *Science*, **164**(3875), 37–42.

Klimeski, A., Chardon, W. J., Turtola, E. and Uusitalo, R. 2012 Potential and limitations of phosphate retention media in water protection: A process-based review of laboratory and field-scale tests. *Agricultural and Food Science*, **21**(3), 206–223.

Klinger, J., Sacher, F., Brauch, H.-J., Maier, D. and Worch, E. 1998 Verhalten organischer Phosphonsäuren bei der Trinkwasseraufbereitung (Behavior of Phosphonic Acids During Drinking Water Treatment). *Vom Wasser*, **91**, 15–27.

Knepper, T. P. and Weil, H. 2001 Studie zum Eintrag synthetischer Komplexbildner und Substanzen mit komplexbildenden Eigenschaften in die Gewässer (Study on the discharge of synthetic complexing agents and substances with complex-forming properties into the aquatic environment). *Vom Wasser*, **97**, 193–232.

Kononova, S. V. and Nesmeyanova, M. A. 2002 Phosphonates and their degradation by microorganisms. *Biochemistry (Moscow)*, **67**(2), 184–195.

Kuhn, R., Bryant, I. M., Jensch, R., Liebsch, S. and Martienssen, M. 2020 Photolysis of hexamethylenediaminetetra(methylenephosphonic acid) (HDTMP) using manganese and hydrogen peroxide. *Emerging Contaminants*, **6**, 10–19.

Kuhn, R., Bryant, I. M. and Martienssen, M. 2019 Unreactive Phosphorus - Organophosphonates (mini review). In: *Organic Compounds*, 1. Edition.

Kuhn, R., Jensch, R., Bryant, I. M., Fischer, T., Liebsch, S. and Martienssen, M. 2018 The influence of selected bivalent metal ions on the photolysis of diethylenetriamine penta(methylenephosphonic acid). *Chemosphere*, **210**, 726–733.

Kuhn, R., Tóth, E., Geppert, H., Fischer, T., Liebsch, S. and Martienssen, M. 2017 Identification of the Complete Photodegradation Pathway of Ethylenediaminetetra(methylenephosphonic acid) in Aqueous Solution. *Clean Soil Air Water*, **45**(5), 1500774.

Kumar, E., Bhatnagar, A., Hogland, W., Marques, M. and Sillanpää, M. 2014 Interaction of inorganic anions with iron-mineral adsorbents in aqueous media – a review. *Advances in Colloid and Interface Science*, **203**, 11–21.

Kumar, P. S. 2018 *Phosphate recovery from wastewater via reversible adsorption.* Dissertation, Delft University of Technology, Delft.

Kumar, P. S., Ejerssa, W. W., Wegener, C. C., Korving, L., Dugulan, A. I., Temmink, H., van Loosdrecht, M. C. M. and Witkamp, G.-J. 2018 Understanding and improving the reusability of phosphate adsorbents for wastewater effluent polishing. *Water Research*, **145**, 365–374.

Kumar, P. S., Korving, L., van Loosdrecht, M. C. M. and Witkamp, G.-J. 2019 Adsorption as a technology to achieve ultra-low concentrations of phosphate: Research gaps and economic analysis. *Water Research X*, **4**, 100029.

Kumar, R. A., Velayudhan, K. T., Ramachandran, V., Bhai, R. S., Unnikrishnan, G. and Vasu, K. 2010 Adsorption and removal kinetics of phosphonate from water using natural adsorbents. *Water Environment Research*, **82**(1), 62–68.

Kunaschk, M., Schmalz, V., Dietrich, N., Dittmar, T. and Worch, E. 2015 Novel regeneration method for phosphate loaded granular ferric (hydr)oxide—a contribution to phosphorus recycling. *Water Research*, **71**, 219–226.

Kuys, K. J. and Roberts, N. K. 1987 In situ investigation of the adsorption of styrene phosphonic acid on cassiterite by FTIR-ATR spectroscopy. *Colloids and Surfaces*, **24**(1), 1–17.

Kuzawa, K., Jung, Y.-J., Kiso, Y., Yamada, T., Nagai, M. and Lee, T.-G. 2006 Phosphate removal and recovery with a synthetic hydrotalcite as an adsorbent. *Chemosphere*, 45–52.

La Nauze, J. M., Rosenberg, H. and Shaw, D. C. 1970 The enzymic cleavage of the carbon-phosphorus bond: Purification and properties of phosphonatase. *Biochimica et Biophysica Acta (BBA) - Enzymology*, **212**(2), 332–350.

Lagergren, S. Y. 1898 *Zur Theorie der sogenannten Adsorption gelöster Stoffe (On the theory of the so-called adsorption of solutes),* Kungliga Svenska Vetenskapsakad. Stockholm: Handlingar. Bihang.

Laiti, E. and Öhman, L.-O. 1996 Acid/Base Properties and Phenylphosphonic Acid Complexation at the Boehmite/Water Interface. *Journal of Colloid and Interface Science*, **183**(2), 441–452.

Laiti, E., Öhman, L.-O., Nordin, J. and Sjöberg, S. 1995 Acid/Base Properties and Phenylphosphonic Acid Complexation at the Aged γ-Al_2O_3/Water Interface. *Journal of Colloid and Interface Science*, **175**(1), 230–238.

Le Moal, M., Gascuel-Odoux, C., Ménesguen, A., Souchon, Y., Étrillard, C., Levain, A., Moatar, F., Pannard, A., Souchu, P., Lefebvre, A. and Pinay, G. 2019 Eutrophication: A new wine in an old bottle? *Science of The Total Environment*, **651**(Pt 1), 1–11.

Lerbs, W., Stock, M. and Parthier, B. 1990 Physiological aspects of glyphosate degradation in Alcaligenes spec. strain GL. *Archives of Microbiology*, **153**(2), 146–150.

Lesueur, C., Pfeffer, M. and Fuerhacker, M. 2005 Photodegradation of phosphonates in water. *Chemosphere*, **59**(5), 685–691.

Levlin, E. 2010 Conductivity measurements for controlling municipal waste-water treatment. In: *Research and application of new technologies in wastewater treatment and municipal solid waste disposal in Ukraine, Sweden and Poland*, Research and application of new technologies in wastewater treatment and municipal solid waste disposal in Ukraine, Sweden and Poland, pp. 51–62.

Li, C., Yang, Q., Lu, S. and Liu, Y. 2021 Adsorption and mechanism study for phosphonate antiscalant HEDP removal from reverse osmosis concentrates by magnetic La/Zn/Fe_3O_4@PAC composite. *Colloids and Surfaces A: Physicochemical and Engineering Aspects*, **613**, 126056.

Li, L. and Stanforth, R. 2000 Distinguishing Adsorption and Surface Precipitation of Phosphate on Goethite (alpha-FeOOH). *Journal of Colloid and Interface Science*, **230**(1), 12–21.

Li, M., Liu, J., Xu, Y. and Qian, G. 2016 Phosphate adsorption on metal oxides and metal hydroxides: A comparative review. *Environmental Reviews*, **24**(3), 319–332.

Lin, J., He, S., Wang, X., Zhang, H. and Zhan, Y. 2019 Removal of phosphate from aqueous solution by a novel $Mg(OH)_2$/ZrO_2 composite: Adsorption behavior and

mechanism. *Colloids and Surfaces A: Physicochemical and Engineering Aspects*, **561**, 301–314.

Lin, J., Zhao, Y., Zhan, Y. and Wang, Y. 2020 Influence of coexisting calcium and magnesium ions on phosphate adsorption onto hydrous iron oxide. *Environmental Science and Pollution Research International*, **27**(10), 11303–11319.

Lin, L., Lei, Z., Wang, L., Liu, X., Zhang, Y., Wan, C., Lee, D.-J. and Tay, J. H. 2013 Adsorption mechanisms of high-levels of ammonium onto natural and NaCl-modified zeolites. *Separation and Purification Technology*, **103**, 15–20.

Liu, Y., Gao, L., Yu, L. and Guo, J. 2000 Adsorption of PBTCA on Alumina Surfaces and Its Influence on the Fractal Characteristics of Sediments. *Journal of Colloid and Interface Science*, **227**(1), 164–170.

Liu, R., Chi, L., Wang, X., Sui, Y., Wang, Y. and Arandiyan, H. 2018 Review of metal (hydr)oxide and other adsorptive materials for phosphate removal from water. *Journal of Environmental Chemical Engineering*, **6**(4), 5269–5286.

Liu, X. and Millero, F. J. 1999 The solubility of iron hydroxide in sodium chloride solutions. *Geochimica et Cosmochimica Acta*, **63**(19), 3487–3497.

Liu, Y. and Chen, J. 2014 Phosphorus Cycle. In: *Encyclopedia of Ecology*, Elsevier, pp. 181–191.

Liu, Y. and Liu, Y.-J. 2008 Biosorption isotherms, kinetics and thermodynamics. *Separation and Purification Technology*, **61**(3), 229–242.

Loganathan, P., Vigneswaran, S., Kandasamy, J. and Bolan, N. S. 2014 Removal and Recovery of Phosphate From Water Using Sorption. *Critical Reviews in Environmental Science and Technology*, **44**(8), 847–907.

LUBW 2015 Modellierung der Nährstoffeinträge in die Fließgewässer Baden-Württembergs für die Aktualisierung der Bewirtschaftungspläne nach WRRL. Modellbeschreibung und Ergebnisse der MONERIS-BW Version "März 2015" (Modeling of nutrient inputs into the flowing waters of Baden-Württemberg for the update of the management plans according to WFD. Model description and results of the MONERIS-BW version "March 2015".). https://pudi.lubw.de/detailseite/-/publication/44676 (accessed 06 February 2022).

Ludwig, Axel 2001 *Das Nährstoffelement Phosphor in limnischen Sedimenten verschiedener Herkunft: Konzentration und Bindungsformen (The nutrient element phosphorus in limnic sediments of different origins: concentration and binding forms)*. Dissertation, Heidelberg University Library, Heidelberg.

Lützenkirchen, J. 1997 Ionic Strength Effects on Cation Sorption to Oxides: Macroscopic Observations and Their Significance in Microscopic Interpretation. *Journal of Colloid and Interface Science*, **195**(1), 149–155.

Maise, H. 1984 Substanzen mit “threshold effect” und deren Verwendung in Reinigungsmitteln (Phosphonsäureverbindungen) (Substances with "threshold effect" and their use in cleaning agents (phosphonic acid compounds)). *Seifen - Öle - Fette - Wachse*, **110**(9 and 11/12), 267-269 and 332-334.

Martí, V., Jubany, I., Ribas, D., Benito, J. A. and Ferrer, B. 2021 Improvement of Phosphate Adsorption Kinetics onto Ferric Hydroxide by Size Reduction. *Water*, **13**(11), 1558.

Martinez, A., Tyson, G. W. and Delong, E. F. 2010 Widespread known and novel phosphonate utilization pathways in marine bacteria revealed by functional screening and metagenomic analyses. *Environmental Microbiology*, **12**(1), 222–238.

Martínez, R. J. and Farrell, J. 2017 Understanding Nitrilotris(methylenephosphonic acid) reactions with ferric hydroxide. *Chemosphere*, **175**, 490–496.

Martinod, A., Euvrard, M., Foissy, A. and Neville, A. 2008 Progressing the understanding of chemical inhibition of mineral scale by green inhibitors. *Desalination*, **220**(1-3), 345–352.

Matthijs, E., Oude, N. T. de, Bolte, M. and Lemaire, J. 1989 Photodegradation of ferric ethylenediaminetetra(methylenephosphonic acid) (EDTMP) in aqueous solution. *Water Research*, **23**(7), 845–851.

McGrath, J. M., Spargo, J. and Penn, C. J. 2014 Soil Fertility and Plant Nutrition. In: *Encyclopedia of Agriculture and Food Systems*, N. K. van Alfen (ed.), Academic Press, Oxford, pp. 166–184.

McGrath, J. W., Chin, J. P. and Quinn, J. P. 2013 Organophosphonates revealed: new insights into the microbial metabolism of ancient molecules. *Nature Reviews. Microbiology*, **11**(6), 412–419.

McGrath, J. W., Hammerschmidt, F. and Quinn, J. P. 1998 Biodegradation of phosphonomycin by Rhizobium huakuii PMY1. *Applied and Environmental Microbiology*, **64**(1), 356–358.

McMullan, G., Harrington, F. and Quinn, J. P. 1992 Metabolism of phosphonoacetate as the sole carbon and phosphorus source by an environmental bacterial isolate. *Applied and Environmental Microbiology*, **58**(4), 1364–1366.

McMullan, G. and Quinn, J. P. 1993 The utilization of aminoalkylphosphonic acids as sole nitrogen source by an environmental bacterial isolate. *Letters in Applied Microbiology*, **17**(3), 135–138.

Means, J. L. and Alexander, C. A. 1981 The environmental biogeochemistry of chelating agents and recommendations for the disposal of chelated radioactive wastes. *Nuclear and Chemical Waste Management*, **2**(3), 183–196.

Mendez, J. C. and Hiemstra, T. 2019 Carbonate Adsorption to Ferrihydrite: Competitive Interaction with Phosphate for Use in Soil Systems. *ACS Earth and Space Chemistry*, **3**(1), 129–141.

Menzel, D. W. and Corwin, N. 1965 The Measurement of Total Phosphorus in Seawater Based on the Liberation of Organically Bound Fractions by Persulfate Oxidation. *Limnology and Oceanography*, **10**(2), 280–282.

Metcalf, J. S. and Souza, N. R. 2019 Cyanobacteria and Their Toxins. In: *Evaluating Water Quality to Prevent Future Disasters*, vol. 11. Separation Science and Technology, Elsevier, pp. 125–148.

Metzner, G. and Nägerl, H.-D. 1982 Umweltverhalten zweier Wasserkonditionierungsmittel auf Phosphonat- und Polyacrylatbasis (Environmental behavior of two phosphonate- and polyacrylate-based water conditioners). *Tenside Surfactants Detergents*, **19**(1), 23–29.

Milonjic, S. 2007 A consideration of the correct calculation of thermodynamic parameters of adsorption. *Journal of the Serbian Chemical Society*, **72**(12), 1363–1367.

Moore, J. K., Braymer, H. D. and Larson, A. D. 1983 Isolation of a Pseudomonas sp. Which Utilizes the Phosphonate Herbicide Glyphosate. *Applied and Environmental Microbiology*, **46**(2), 316–320.

Morillo, E., Undabeytia, T. and Maqueda, C. 1997 Adsorption of Glyphosate on the Clay Mineral Montmorillonite: Effect of Cu(II) in Solution and Adsorbed on the Mineral. *Environmental Science and Technology*, **31**(12), 3588–3592.

Müller, G., Steber, J. and Waldhoff, H. 1984 Zum Einfluss von Hydroxyethandiphosphonsäure auf die Phosphatelimination mit $FeCl_3$ und die Remobilisierung von Schwermetallen: Ergebnisse von Labor-und Feldversuchen (On the influence of 1-hydroxyethylidene-(1,1-diphosphonic acid) on phosphate elimination with $FeCl_3$ and remobilization of heavy metals: Results of laboratory and field experiments). *Vom Wasser*, **63**, 63–78.

Müller, U. and Sacher, F. 2016 *Auswirkung von Konzentraten der Trinkwasserenthärtung in Fließgewässern (Effect of concentrates of drinking water softening in flowing waters),* TZW-Schriftenreihe, **71**.

MUNLV 2004 *Untersuchungen zum Eintrag und zur Elimination von gefährlichen Stoffen in kommunalen Kläranlagen (Investigations on the input and elimination of hazardous substances in municipal wastewater treatment plants)*. https://docplayer.org/25495397-Umwelt-untersuchungen-zum-eintrag-und-zur-elimination-von-gefaehrlichen-stoffen-in-kommunalen-klaeranlagen.html (accessed 06 February 2022).

Murphy, J. and Riley, J. P. 1962 A modified single solution method for the determination of phosphate in natural waters. *Analytica Chimica Acta*, **27**, 31–36.

Nagul, E. A., McKelvie, I. D., Worsfold, P. and Kolev, S. D. 2015 The molybdenum blue reaction for the determination of orthophosphate revisited: Opening the black box. *Analytica Chimica Acta*, **890**, 60–82.

Nederlof, M. M. and Hoogendoorn, J. H. 2005 Desalination of brackish groundwater: the concentrate dilemma. *Desalination*, **182**(1-3), 441–447.

Neft, A., Claus, M. B., Schmidt, S., Minke, R. and Steinmetz, H. 2010 Looking closer on phosphorus fractions in WWTP effluents: Implications on the optimisation of phosphorus removal. In: *Proceedings of the 1st IWA Austrian Young Water Professionals Conference*, IWA (ed.), IWA-4306.

Nowack, B. 1998 The behavior of phosphonates in wastewater treatment plants of Switzerland. *Water Research*, **32**(4), 1271–1279.

Nowack, B. 2002a Aminopolyphosphonate removal during wastewater treatment. *Water Research*, **36**(18), 4636–4642.

Nowack, B. 2002b Determination of phosphonic acid breakdown products by high-performance liquid chromatography after derivatization. *Journal of Chromatography A*, **942**(1-2), 185–190.

Nowack, B. 2003 Environmental chemistry of phosphonates. *Water Research*, **37**(11), 2533–2546.

Nowack, B. 2004 Environmental chemistry of phosphonic acids. In: *Phosphorus in environmental technologies*. *Principles and applications*, E. Valsami-Jones (ed.). Integrated environmental technology series, IWA Publishing, London, pp. 147–173.

Nowack, B. and Baumann, U. 1998 Biologischer Abbau der Photolyseprodukte von Fe^{III}EDTA (Biodegradation of the photolysis products of Fe^{III}EDTA). *Acta Hydrochimica et Hydrobiologica*, **26**(2), 104–108.

Nowack, B. and Stone, A. T. 1999a Adsorption of Phosphonates onto the Goethite-Water Interface. *Journal of Colloid and Interface Science*, **214**(1), 20–30.

Nowack, B. and Stone, A. T. 1999b The Influence of Metal Ions on the Adsorption of Phosphonates onto Goethite. *Environmental Science and Technology*, **33**(20), 3627–3633.

Nowack, B. and Stone, A. T. 2000 Degradation of Nitrilotris(methylenephosphonic Acid) and Related (Amino)Phosphonate Chelating Agents in the Presence of Manganese and Molecular Oxygen. *Environmental Science and Technology*, **34**(22), 4759–4765.

Nowack, B. and Stone, A. T. 2002 Homogeneous and Heterogeneous Oxidation of Nitrilotrismethylenephosphonic Acid (NTMP) in the Presence of Manganese(II, III) and Molecular Oxygen. *Journal of Physical Chemistry B*, **106**(24), 6227–6233.

Nowack, B. and Stone, A. T. 2003 Manganese-catalyzed degradation of phosphonic acids. *Environmental Chemistry Letters*, **1**(1), 24–31.

Nowack, B. and Stone, A. T. 2006 Competitive adsorption of phosphate and phosphonates onto goethite. *Water Research*, **40**(11), 2201–2209.

Obojska, A., Lejczak, B. and Kubrak, M. 1999 Degradation of phosphonates by streptomycete isolates. *Applied Microbiology and Biotechnology*, **51**(6), 872–876.

Oddo, J. E. and Tomson, M. B. 1990 The solubility and stoichiometry of calcium-diethylenetriaminepenta(methylene phosphonate) at 70° in brine solutions at 4.7 and 5.0 pH. *Applied Geochemistry*, **5**(4), 527–532.

OECD SIDS 1996 *PBTC CAS N°: 37971-36-1*.

OECD 2006 *OECD Guidelines for the Testing of Chemicals: Revised Introduction to the OECD Guidelines for Testing of Chemicals, Section 3.* OECD Publishing, Paris.

Pairat, R., Sumeath, C., Browning, F. H. and Fogler, H. S. 1997 Precipitation and Dissolution of Calcium−ATMP Precipitates for the Inhibition of Scale Formation in Porous Media. *Langmuir*, **13**(6), 1791–1798.

Parfitt, R. L. 1979 Anion Adsorption by Soils and Soil Materials. *Advances in Agronomy*, **30**, 1–50.

Parfitt, R. L. and Russell, J. D. 1977 Adsorption on hydrous oxides. IV. Mechanisms of adsorption of various ions on goethite. *Journal of Soil Science*, **28**(2), 297–305.

Patel, H. 2019 Fixed-bed column adsorption study: a comprehensive review. *Applied Water Science*, **9**(3).

Petrone, L. 2013 Molecular surface chemistry in marine bioadhesion. *Advances in Colloid and Interface Science*, **195-196**, 1–18.

Pilgrim, C. D. 2018 Chelation. In: *Encyclopedia of Engineering Geology*, P. Bobrowsky and B. Marker (eds.). Encyclopedia of Earth Sciences Series, Springer International Publishing, Cham, pp. 1–2.

Pipke, R., Amrhein, N., Jacob, G. S., Schaefer, J. and Kishore, G. M. 1987 Metabolism of glyphosate in an Arthrobacter sp. GLP-1. *European Journal of Biochemistry*, **165**(2), 267–273.

Popov, K., Rönkkömäki, H. and Lajunen, L. H. J. 2002 Critical evaluation of stability constants of phosphonic acids (IUPAC Technical Report). *Pure and Applied Chemistry*, **74**(11).

Preisner, M., Neverova-Dziopak, E. and Kowalewski, Z. 2020 An Analytical Review of Different Approaches to Wastewater Discharge Standards with Particular Emphasis on Nutrients. *Environmental Management*, **66**(4), 694–708.

Quinn, J. P., Kulakova, A. N., Cooley, N. A. and McGrath, J. W. 2007 New ways to break an old bond: the bacterial carbon-phosphorus hydrolases and their role in biogeochemical phosphorus cycling. *Environmental Microbiology*, **9**(10), 2392–2400.

Rahimi, T., Vaezi, N., Khazaei, M., Vakili, B. and Izanloo, H. 2016 Application of Granular Ferric Hydroxide in Removal of Nitrate from Aqueous Solutions. *Journal of Safety, Environment, and Health Research*, **1**(1), 31–35.

Raschke, H., Rast, H.-G., Kleinstück, R., Sicius, H. and Wischer, D. 1994 Utilization of 2-phosphonobutane-1,2,4-tricarboxylic acid as source of phosphorus by environmental bacterial isolates. *Chemosphere*, **29**(1), 81–88.

Rawls, H. R., Bartels, T. and Arends, J. 1982 Binding of polyphosphonates at the water/hydroxyapatite interface. *Journal of Colloid and Interface Science*, **87**(2), 339–345.

Ray, S. S., Gusain, R. and Kumar, N. 2020 Chapter four – Adsorption in the context of water purification. In: *Carbon Nanomaterial-Based Adsorbents for Water Purification: Micro and Nano Technologies*, S. S. Ray, R. Gusain and N. Kumar (eds.), Elsevier, pp. 67–100.

Reichert, J. K. 1996 *Organophosphonsäuren*: *Bewertung der Leistungsfähigkeit biologischer Abwasserbehandlungsaıılagen zu ihrer Eliminierung und Beurteilung ihres Umweltgefährdungspotentials (Organophosphonic acids: evaluation of the performance of biological wastewater treatment plants for their elimination and assessment of their environmental hazard potential),* Deutsche Bundesstiftung Umwelt, Roetgen.

Reinhardt, T., Gómez Elordi, M., Minke, R., Schönberger, H. and Rott, E. 2020a Batch studies of phosphonate adsorption on granular ferric hydroxides. *Water Science and Technology*, **81**(1), 10–20.

Reinhardt, T., Veizaga Campero, A. N., Minke, R., Schönberger, H. and Rott, E. 2020b Batch Studies of Phosphonate and Phosphate Adsorption on Granular Ferric Hydroxide (GFH) with Membrane Concentrate and Its Synthetic Replicas. *Molecules*, **25**(21).

Rietra, Hiemstra and van Riemsdijk, W. H. 1999 Sulfate Adsorption on Goethite. *Journal of Colloid and Interface Science*, **218**(2), 511–521.

Rietra, R. P., Hiemstra, T. and van Riemsdijk, W. H. 2001 Interaction between calcium and phosphate adsorption on goethite. *Environmental Science and Technology*, **35**(16), 3369–3374.

Rosenberg, H. and La Nauze, J. M. 1967 The metabolism of phosphanates by microorganisms. The transport of aminoethylphosphonic acid in Basillus cereus. *Biochimica et Biophysica Acta (BBA) - General Subjects*, **141**(1), 79–90.

Rott, E. 2016 *Untersuchungen zur Elimination von Phosphor aus phosphonathaltigen Industrieabwässern (Investigations on the removal of phosphorus from phosphonate-containing industrial wastewaters)*. Dissertation, Institut für Siedlungswasserbau, Wassergüte- und Abfallwirtschaft, Universität Stuttgart, Stuttgart.

Rott, E. 2018 *Organophosphonates: Environmental problems related to them and possible solutions for their elimination from industrial wastewater,* 4th International Conference on Pollution Control & Sustainable Environment and 6th Edition of International Conference on Water Pollution & Sewage Management, 27 July 2018, Rome, Italy.

Rott, E., Happel, O., Armbruster, D. and Minke, R. 2020a Behavior of PBTC, HEDP, and Aminophosphonates in the Process of Wastewater Treatment. *Water*, **12**(1).

Rott, E., Happel, O., Armbruster, D. and Minke, R. 2020b Influence of Wastewater Discharge on the Occurrence of PBTC, HEDP, and Aminophosphonates in Sediment, Suspended Matter, and the Aqueous Phase of Rivers. *Water*, **12**(3), 803.

Rott, E., Minke, R., Bali, U. and Steinmetz, H. 2017a Removal of phosphonates from industrial wastewater with UV/Fe^{II}, Fenton and UV/Fenton treatment. *Water Research*, **122**, 345–354.

Rott, E., Minke, R. and Steinmetz, H. 2017b Removal of phosphorus from phosphonate-loaded industrial wastewaters via precipitation/flocculation. *Journal of Water Process Engineering*, **17**, 188–196.

Rott, E., Nouri, M., Meyer, C., Minke, R., Schneider, M., Mandel, K. and Drenkova-Tuhtan, A. 2018a Removal of phosphonates from synthetic and industrial wastewater with reusable magnetic adsorbent particles. *Water Research*, **145**, 608–617.

Rott, E., Reinhardt, T. and Minke, R. 2019 *Untersuchungen zur Elimination von Phosphonaten und ortho-Phosphat aus Abwasser mithilfe metallhaltiger Filtermaterialien*: *Abschlussbericht an die Willy-Hager-Stiftung (Investigations on the removal of phosphonates and orthophosphate from wastewater using metal-containing filter materials: final report to the Willy Hager Foundation).*

Rott, E., Reinhardt, T., Wasielewski, S., Raith-Bausch, E. and Minke, R. 2018b Optimized Procedure for Determining the Adsorption of Phosphonates onto Granular Ferric Hydroxide using a Miniaturized Phosphorus Determination Method. *Journal of Visualized Experiments* 135, e57618.

Rott, E., Steinmetz, H. and Metzger, J. W. 2018c Organophosphonates: A review on environmental relevance, biodegradability and removal in wastewater treatment plants. *Science of the Total Environment*, **615**, 1176–1191.

Rout, P. R., Bhunia, P. and Dash, R. R. 2014 A mechanistic approach to evaluate the effectiveness of red soil as a natural adsorbent for phosphate removal from wastewater. *Desalination and Water Treatment*, **54**(2), 358–373.

Rout, P. R., Bhunia, P. and Dash, R. R. 2015 Effective utilization of a sponge iron industry by-product for phosphate removal from aqueous solution: A statistical and kinetic modelling approach. *Journal of the Taiwan Institute of Chemical Engineers*, **46**, 98–108.

Sabin, F., Türk, T. and Vogler, A. 1992 Photo-oxidation of organic compound in the presence of titanium dioxide: determination of the efficiency. *Journal of Photochemistry and Photobiology A: Chemistry*, **63**(1), 99–106.

Saeger, V. W., Tucker, E. S., Frazier, T., Renaudette, W. J., Yepez, H. and Mieure, J. P. *Environmental Fate testing of Dequest Phosphonates* Monsanto unpublished report AC-77-SS-13. Cited by HERA 2004.

Saha, B., Griffin, L. and Blunden, H. 2010 Adsorptive separation of phosphate oxyanion from aqueous solution using an inorganic adsorbent. *Environmental Geochemistry and Health*, **32**(4), 341–347.

Schaum, C. 2018 Wastewater treatment of the future: Health, water and resource protection. In: *Phosphorus*. *Polluter and resource of the future : removal and recovery from wastewater*, C. Schaum (ed.). Integrated environmental technology series, IWA Publishing, London, pp. 537–554.

Schindler, D. W., Carpenter, S. R., Chapra, S. C., Hecky, R. E. and Orihel, D. M. 2016 Reducing Phosphorus to Curb Lake Eutrophication is a Success. *Environmental Science and Technology*, **50**(17), 8923–8929.

Schindler, P. W. 1990 Co-adsorption of metal ions and organicligands: Formation of ternary surface complexes. In: *Mineral-Water Interface Geochemistry*, M. F. Hochella and A. F. White (eds.), De Gruyter, Berlin, Boston, pp. 281–308.

Schmidt, C. K., Fleig, M., Sacher, F. and Brauch, H.-J. 2004 Occurrence of aminopolycarboxylates in the aquatic environment of Germany. *Environmental Pollution*, **131**(1), 107–124.

Schmidt, C. K., Raue, B., Brauch, H.-J. and Sacher, F. 2014 Trace-level analysis of phosphonates in environmental waters by ion chromatography and inductively coupled plasma mass spectrometry. *International Journal of Environmental Analytical Chemistry*, **94**(4), 385–398.

Schöberl, P. and Huber, L. 1988 Ökologisch relevante Daten von nichttensidischen Inhaltsstoffen in Wasch- und Reinigungsmitteln (Ecologically relevant data of non-surfactant ingredients in detergents and cleaning agents). *Tenside Surfactants Detergents*, **25**(2), 99–107.

Schönberger, H. 1991 Zur biologischen Abbaubarkeit im Abwasserbereich: Ist der Zahn-Wellens-Abbautest der richtige Test? (On the biodegredability in the waste water management. Is the Zahn-Wellens-Test the suitable test?). *Zeitschrift für Wasser- und Abwasserforschung*, **24**, 118–128.

Schöpke, R. 2013 *Entwicklung eines Verfahrens zur Adsorption von Phosphor an körnigem Eisenhydroxid und Regeneration des Adsorptionsmittels zur Phosphorrückgewinnung (Development of a process for adsorption of phosphorus on granular ferric hydroxide and regeneration of the adsorbent for phosphorus recovery),* Dissertation, Schriftenreihe Siedlungswasserwirtschaft und Umwelt, Eigenverlag des Lehrstuhls Wassertechnik und Siedlungswasserbau der Brandenburgischen Technischen Universität, Cottbus-Senftenberg.

Schowanek, D. and Verstraete, W. 1990a Phosphonate utilization by bacteria in the presence of alternative phosphorus sources. *Biodegradation*, **1**(1), 43–53.

Schowanek, D. and Verstraete, W. 1990b Phosphonate utilization by bacterial cultures and enrichments from environmental samples. *Applied and Environmental Microbiology*, **56**(4), 895–903.

Schowanek, D. and Verstraete, W. 1991 Hydrolysis and Free Radial Mediated Degradation of Phosphonates. *Journal of Environmental Quality*, **20**(4), 769–776.

Sigg, L. and Stumm, W. 1981 The interaction of anions and weak acids with the hydrous goethite (α-FeOOH) surface. *Colloids and Surfaces*, **2**(2), 101–117.

Song, S., Peng, W. and Li, H. 2021 Surface Chemistry of Mineral Adsorbents. In: *Adsorption at Natural Minerals/Water Interfaces*, S. Song and B. Li (eds.), Springer International Publishing, Cham, pp. 55–91.

Sperlich, A. 2010 *Phosphate adsorption onto granular ferric hydroxide (GFH) for wastewater reuse,* First Edition, ITU-Schriftenreihe, **14.** Papierflieger, Clausthal-Zellerfeld.

Sperlich, A., Schimmelpfennig, S., Baumgarten, B., Genz, A., Amy, G., Worch, E. and Jekel, M. 2008 Predicting anion breakthrough in granular ferric hydroxide (GFH) adsorption filters. *Water Research*, **42**(8-9), 2073–2082.

Sperlich, A., Warschke, D., Wegmann, C., Ernst, M. and Jekel, M. 2010 Treatment of membrane concentrates: Phosphate removal and reduction of scaling potential. *Water Science and Technology*, **61**(2), 301–306.

Sperlich, A., Werner, A., Genz, A., Amy, G., Worch, E. and Jekel, M. 2005 Breakthrough behavior of granular ferric hydroxide (GFH) fixed-bed adsorption filters: modeling and experimental approaches. *Water Research*, **39**(6), 1190–1198.

Squire, D. 2000 Reverse osmosis concentrate disposal in the UK. *Desalination*, **132**(1-3), 47–54.

Stasi, R., Neves, H. I. and Spira, B. 2019 Phosphate uptake by the phosphonate transport system PhnCDE. *BMC Microbiology*, **19**(1), 79.

Steber, J. and Wierich, P. 1986 Properties of hydroxyethane diphosphonate affecting its environmental fate: Degradability, sludge adsorption, mobility in soils, and bioconcentration. *Chemosphere*, **15**(7), 929–945.

Steber, J. and Wierich, P. 1987 Properties of aminotris (methylenephosphonate) affecting its environmental fate: Degradability, sludge adsorption, mobility in soils, and bioconcentration. *Chemosphere*, **16**(6), 1323–1337.

Stone, A. T., Knight, M. A. and Nowack, B. 2002 Speciation and Chemical Reactions of Phosphonate Chelating Agents in Aqueous Media. In: *Chemicals in the environment*. *Fate, impacts, and remediation*, R. L. Lipnick (ed.), vol. 806. ACS Symposium Series 806, American Chemical Society; Distributed by Oxford University Press, Washington, DC, pp. 59–94.

Stone, B. L. and White, A. K. 2012 Most probable number quantification of hypophosphite and phosphite oxidizing bacteria in natural aquatic and terrestrial environments. *Archives of Microbiology*, **194**(3), 223–228.

Studnik, H., Liebsch, S., Forlani, G., Wieczorek, D., Kafarski, P. and Lipok, J. 2015 Amino polyphosphonates - chemical features and practical uses, environmental durability and biodegradation. *New Biotechnology*, **32**(1), 1–6.

Stumm, W. 1995 The Inner-Sphere Surface Complex. In: *Aquatic Chemistry*, vol. 244. Advances in Chemistry 244, American Chemical Society, pp. 1–32.

Stumm, W., Wehrli, B. and Wieland, E. 1987 Surface Complexation and Its Impact on Geochemical Kinetics. *Croatica Chemica Acta*, **60**, 429–456.

Su, C. and Suarez, D. L. 1997 In Situ Infrared Speciation of Adsorbed Carbonate on Aluminum and Iron Oxides. *Clays and Clay Minerals*, **45**(6), 814–825.

Sun, S., Wang, S., Ye, Y. and Pan, B. 2019 Highly efficient removal of phosphonates from water by a combined Fe(III)/UV/co-precipitation process. *Water Research*, **153**, 21–28.

Talebi Atouei, M., Rahnemaie, R., Goli Kalanpa, E. and Davoodi, M. H. 2016 Competitive adsorption of magnesium and calcium with phosphate at the goethite water interface: Kinetics, equilibrium and CD-MUSIC modeling. *Chemical Geology*, **437**, 19–29.

Tan, K. L. and Hameed, B. H. 2017 Insight into the adsorption kinetics models for the removal of contaminants from aqueous solutions. *Journal of the Taiwan Institute of Chemical Engineers*, **74**, 25–48.

Tang, Y., Yang, W., Yin, X., Liu, Y., Yin, P. and Wang, J. 2008 Investigation of $CaCO_3$ scale inhibition by PAA, ATMP and PAPEMP. *Desalination*, **228**(1-3), 55–60.

Trivedi, P., Axe, L. and Dyer, J. 2001 Adsorption of metal ions onto goethite: single-adsorbate and competitive systems. *Colloids and Surfaces A: Physicochemical and Engineering Aspects*, **191**(1-2), 107–121.

Tschäbunin, G., Schwedt, G. and Fischer, P. 1989 Zur Analytik von Polymethylenphosphonsäuren (On the analysis of polymethylenephosphonic acids). *Zeitschrift fur Analytische Chemie*, **333**(2), 123–128.

UBA 2003 Informationen rund um Wasch- und Reinigungsmittel (Information about detergents and cleaning agents). http://web.archive.org/web/20040404120236/http://umweltbundesamt.de/uba-info-daten/daten/wasch/trends.htm (accessed 08 July 2021).

UBA 2017 Gewässer in Deutschland. Zustand und Bewertung (Water bodies in Germany. Status and assessment). https://www.umweltbundesamt.de/publikationen/gewaesser-in-deutschland (accessed 06 February 2022).

US EPA 2007 *Advanced Wastewater Treatment to Achieve Low Concentration of Phosphorus* EPA 910-R-07-002. https://nepis.epa.gov/Exe/ZyPURL.cgi?Dockey=P1004JC4.TXT (accessed 21 June 2021).

US EPA 2009 *Nutrient Control Design Manual*: *State of Technology Review Report* EPA/600/R-09/012, Washington, DC.

US EPA 2016 *Status of Nutrient Requirements for NPDES-Permitted Facilities*. https://www.epa.gov/sites/production/files/2017-06/documents/potw_nutrient_lim_and_mon_as_of_2_5_2016._2.08.17.pdf (accessed 21 June 2021).

US EPA 2017 *Estimation Programs Interface Suite™ for Microsoft® Windows, v 4.11.* United States Environmental Protection Agency, Washington, DC, USA.

Valsami-Jones, E. 2004 The geochemistry and mineralogy of phosphorus. In: *Phosphorus in environmental technologies*. *Principles and applications*, E. Valsami-Jones (ed.). Integrated environmental technology series, IWA Publishing, London, pp. 20–50.

Villalobos, M. and Leckie, J. O. 2001 Surface Complexation Modeling and FTIR Study of Carbonate Adsorption to Goethite. *Journal of Colloid and Interface Science*, **235**(1), 15–32.

Villarreal-Chiu, J. F., Quinn, J. P. and McGrath, J. W. 2012 The genes and enzymes of phosphonate metabolism by bacteria, and their distribution in the marine environment. *Frontiers in Microbiology*, **3**, 19.

Violante, A., Pigna, M., Ricciardella, M. and Gianfreda, L. 2002 Adsorption of phosphate on variable charge minerals and soils as affected by organic and inorganic ligands. In: *Soil Mineral-Organic Matter-Microorganism Interactions and Ecosystem Health, Dynamics, Mobility and Transformation of Pollutants and Nutrients*, vol. 28. Developments in Soil Science, Elsevier, pp. 279–295.

Voigt, A., Kleffmann, M. and Durth, A. 2013 Verbesserung der Phosphorelimination auf Kläranlagen vor dem Hintergrund steigender Anforderungen (Improvement of phosphorus removal at wastewater treatment plants against the background of increasing requirements). In: *14. Kölner Kanal und Kläranlagen Kolloquium*. *9. und 10. September 2013 im Maternushaus, Köln*, J. Pinnekamp and V. Kölling (eds.). Aachener Schriften zur Stadtentwässerung 17, Gesellschaft zur Förderung der Siedlungswasserwirtschaft an der RWTH Aachen e.V, Aachen.

Vuorio, K., Järvinen, M. and Kotamäki, N. 2020 Phosphorus thresholds for bloom-forming cyanobacterial taxa in boreal lakes. *Hydrobiologia*, **847**(21), 4389–4400.

Wang, H., Zhu, J., FU, Q.-L., XIONG, J.-W., Hong, C., HU, H.-Q. and Violante, A. 2015 Adsorption of Phosphate onto Ferrihydrite and Ferrihydrite-Humic Acid Complexes. *Pedosphere*, **25**(3), 405–414.

Wang, Shu, Sun, Shuhui, Shan, Chao and Pan, Bingcai 2019 Analysis of trace phosphonates in authentic water samples by pre-methylation and LC-Orbitrap MS/MS. *Water Research*, **161**, 78–88.

Wang, Zhi, Chen, Gongde, Patton, Samuel, Ren, Changxu, Liu, Jinyong and Liu, Haizhou 2019 Degradation of nitrilotris-methylenephosphonic acid (NTMP) antiscalant via persulfate photolysis: Implications on desalination concentrate treatment. *Water Research*, **159**, 30–37.

Wang, Z., Shi, M., Li, J. and Zheng, Z. 2014 Influence of moderate pre-oxidation treatment on the physical, chemical and phosphate adsorption properties of iron-containing activated carbon. *Journal of Environmental Sciences*, **26**(3), 519–528.

Wasielewski, S., Rott, E., Minke, R. and Steinmetz, H. 2018 Evaluation of Different Clinoptilolite Zeolites as Adsorbent for Ammonium Removal from Highly Concentrated Synthetic Wastewater. *Water*, **10**(5), 584.

Weiner, E. R. 2013 *Applications of environmental aquatic chemistry*: *A practical guide,* 3. ed. CRC Press, Boca Raton, Fla.

Weng, L., van Riemsdijk, W. H. and Hiemstra, T. 2012 Factors controlling phosphate interaction with iron oxides. *Journal of Environmental Quality*, **41**(3), 628–635.

White, A. K. and Metcalf, W. W. 2007 Microbial metabolism of reduced phosphorus compounds. *Annual Review of Microbiology*, **61**, 379–400.

White, P. J. and Hammond, J. P. 2009 The sources of phosphorus in the waters of Great Britain. *Journal of Environmental Quality*, **38**(1), 13–26.

WHO 2020 *The WHO recommended classification of pesticides by hazard and guidelines to classification*: *2019 edition,* Geneva.

Wijnja and Schulthess 2000 Vibrational Spectroscopy Study of Selenate and Sulfate Adsorption Mechanisms on Fe and Al (Hydr)oxide Surfaces. *Journal of Colloid and Interface Science*, **229**(1), 286–297.

Worch, E. 2012 *Adsorption Technology in Water Treatment*: *Fundamentals, Processes, and Modeling.* De Gruyter, Berlin.

Worsfold, P., McKelvie, I. and Monbet, P. 2016 Determination of phosphorus in natural waters: A historical review. *Analytica Chimica Acta*, **918**, 8–20.

Xie, J., Wang, Z., Lu, S., Wu, D., Zhang, Z. and Kong, H. 2014 Removal and recovery of phosphate from water by lanthanum hydroxide materials. *Chemical Engineering Journal*, **254**, 163–170.

Xing, B. and Pignatello, J. J. 2005 SORPTION | Organic Chemicals. In: *Encyclopedia of Soils in the Environment*, D. Hillel (ed.), Elsevier, Oxford, pp. 537–548.

Xu, N., Chen, M., Zhou, K., Wang, Y., Yin, H. and Chen, Z. 2014 Retention of phosphorus on calcite and dolomite: speciation and modeling. *RSC Advances*, **4**(66), 35205.

Xu, Z.-B., Wang, W.-L., Huang, N., Wu, Q.-Y., Lee, M.-Y. and Hu, H.-Y. 2019 2-Phosphonobutane-1,2,4-tricarboxylic acid (PBTCA) degradation by ozonation: Kinetics, phosphorus transformation, anti-precipitation property changes and phosphorus removal. *Water Research*, **148**, 334–343.

Xyla, A. G., Mikroyannidis, J. and Koutsoukos, P. G. 1992 The inhibition of calcium carbonate precipitation in aqueous media by organophosphorus compounds. *Journal of Colloid and Interface Science*, **153**(2), 537–551.

Yan, Fei, Zhang, Fangfu, Bhandari, Narayan, Wang, Lu, Dai, Zhaoyi, Zhang, Zhang, Liu, Ya, Ruan, Gedeng, Kan, Amy and Tomson, Mason 2015 Adsorption and precipitation of scale inhibitors on shale formations. *Journal of Petroleum Science and Engineering*, **136**, 32–40.

Yan, L., Xu, Y., Yu, H., Xin, X., Wei, Q. and Du, B. 2010 Adsorption of phosphate from aqueous solution by hydroxy-aluminum, hydroxy-iron and hydroxy-iron-aluminum pillared bentonites. *Journal of Hazardous Materials*, **179**(1-3), 244–250.

Yan, Liang-guo, Yang, Kun, Shan, Ran-ran, Yan, Tao, Wei, Jing, Yu, Shu-jun, Yu, Hai-qin and Du, Bin 2015 Kinetic, isotherm and thermodynamic investigations of phosphate adsorption onto core-shell Fe_3O_4@LDHs composites with easy magnetic separation assistance. *Journal of Colloid and Interface Science*, **448**, 508–516.

Yang, Q., Liu, Y., Gu, A., Ding, J. and Shen, Z. 2001 Investigation of Calcium Carbonate Scaling Inhibition and Scale Morphology by AFM. *Journal of Colloid and Interface Science*, **240**(2), 608–621.

Yates, D. and Healy, T. 1975 Mechanism of anion adsorption at the ferric and chromic oxide/water interfaces. *Journal of Colloid and Interface Science*, **52**(2), 222–228.

Yeoman, S., Stephenson, T., Lester, J. and Perry, R. 1988 The removal of phosphorus during wastewater treatment: A review. *Environmental Pollution*, **49**(3), 183–233.

Yousefi, M., Nabizadeh, R., Alimohammadi, M., Mohammadi, A. A. and Mahvi, A. H. 2019 Removal of phosphate from aqueous solutions using granular ferric hydroxide process optimization by response surface methodology. *Desalination and Water Treatment*, **158**, 290–300.

Yu, W., Di Song, Chen, W. and Yang, H. 2020 Antiscalants in RO membrane scaling control. *Water Research*, **183**, 115985.

Zach-Maor, A., Semiat, R. and Shemer, H. 2011a Adsorption-desorption mechanism of phosphate by immobilized nano-sized magnetite layer: Interface and bulk interactions. *Journal of Colloid and Interface Science*, **363**(2), 608–614.

Zach-Maor, A., Semiat, R. and Shemer, H. 2011b Synthesis, performance, and modeling of immobilized nano-sized magnetite layer for phosphate removal. *Journal of Colloid and Interface Science*, **357**(2), 440–446.

Zeleznick, L. D., Myers, T. C. and Titchener, E. B. 1963 Growth of Escherichia coli on methyl- and ethylphosphonic acids. *Biochimica et Biophysica Acta*, **78**(3), 546–547.

Zelmanov, G. and Semiat, R. 2015 The influence of competitive inorganic ions on phosphate removal from water by adsorption on iron (Fe^{+3}) oxide/hydroxide nanoparticles-based agglomerates. *Journal of Water Process Engineering*, **5**, 143–152.

Zhang, B., Zhang, L., Li, F., Hu, W. and Hannam, P. M. 2010 Testing the formation of Ca–phosphonate precipitates and evaluating the anionic polymers as Ca–phosphonate precipitates and $CaCO_3$ scale inhibitor in simulated cooling water. *Corrosion Science*, **52**(12), 3883–3890.

Zhang, Y., Yin, H., Zhang, Q., Li, Y. and Yao, P. 2016 Synthesis and characterization of novel polyaspartic acid/urea graft copolymer with acylamino group and its scale inhibition performance. *Desalination*, **395**, 92–98.

Zhao, B., Zhang, Y., Dou, X., Yuan, H. and Yang, M. 2015 Granular ferric hydroxide adsorbent for phosphate removal: demonstration preparation and field study. *Water Science and Technology*, **72**(12), 2179–2186.

Zheng, S. K., Chen, J. J., Jiang, X. M. and Li, X. F. 2011 A comprehensive assessment on commercially available standard anion resins for tertiary treatment of municipal wastewater. *Chemical Engineering Journal*, **169**(1-3), 194–199.

Zholnin, A. V., Zudov, V. G., Leitsin, V. A., Nosova, R. L. and Smirnov, E. M. 1990 Preparation of the iron complexes of nitrilotrimethylenephosphonic acid from zinc-production waste. *Journal of Applied Chemistry of the USSR*, **63**, 803–807. Cited by Nowack 2004.

Zhou, J., Xu, Z. P., Qiao, S., Liu, Q., Xu, Y. and Qian, G. 2011 Enhanced removal of triphosphate by MgCaFe-Cl-LDH: synergism of precipitation with intercalation and surface uptake. *Journal of Hazardous Materials*, **189**(1-2), 586–594.

Verzeichnis der in der Schriftenreihe „Stuttgarter Berichte zur Siedlungswasserwirtschaft“ seit 2008 erschienenen Veröffentlichungen

Band 192	Siedlungswasserwirtschaftliches Kolloquium an der Universität Stuttgart	Zukunftsfähige Wasserversorgung – Von der lokalen zur globalen Herausforderung 22. Trinkwasserkolloquium am 14.02.2008 (2008) 116 S., 29 Abb., 4 Tab. (34,80 €)
Band 193	Hassan H. Shawly	Urban Water – Integrated Resource Planning to Meet Future Demand in Jeddah – Saudi Arabia (2008) 182 S., 38 Abb., 30 Tab. (34,80 €)
Band 194	Holger Kauffmann	Arsenelimination aus Grundwasser (2008) 151 S., 55 Abb., 22 Tab. (34,80 €)
Band 195	Siedlungswasserwirtschaftliches Kolloquium an der Universität Stuttgart	Betrieb und Sanierung von Entwässerungssystemen 83. Siedlungswasserwirtschaftliches Kolloquium am 09.10.2008 (2008) 160 S., 45 Abb. 7 Tab. (34,80 €)
Band 196	Siedlungswasserwirtschaftliches Kolloquium an der Universität Stuttgart	Von der Ressource bis zum Lebensmittel höchster Qualität 23. Trinkwasserkolloquium am 12.02.2009 (2009) 151 S., 59 Abb., 17 Tab. (34,80 €)
Band 197	Khaja Zillur Rahman	Treatment of arsenic containing artificial wastewater in different laboratory-scale constructed wetlands (2009) 184 S., 36 Abb., 10 Tab. (34,80 €)
Band 198	Juliane Gasse	Quantifizierung der Emissionen aus Abwasseranlagen und deren Auswirkungen auf die hygienische Qualität von Fließgewässern (2009) 220 S., 66 Abb., 77 Tab. (34,80 €)
Band 199	Siedlungswasserwirtschaftliches Kolloquium an der Universität Stuttgart	Abwasserbewirtschaftung im Spannungsfeld politischer, klimatischer und technischer Entwicklungen 84. Siedlungswasserwirtschaftliches Kolloquium am 08.10.2009 (2009) 213 S., 56 Abb., 24 Tab. (34,80 €)
Band 200	Darla Nickel	Erfassung und Bewertung des Einflusses von gebietsstrukturellen Eigenschaften auf Trinkwasserpreise (2009) 174 S., 27 Abb., 43 Tab. (34,80 €)

Band 201	Siedlungswasserwirtschaftliches Kolloquium an der Universität Stuttgart	Grundwasser und Grundwasserleiter – Nutzungskonflikte und Lösungsansätze 24. Trinkwasserkolloquium am 25.02.2010 (2010) 168 S., 81 Abb., 12 Tab. (34,80 €)
Band 202	Alexander Weidelener	Phosphorrückgewinnung aus kommunalem Klärschlamm als Magnesium-Ammonium-Phosphat (MAP) (2010) 165 S., 69 Abb., 15 Tab. (34,80 €)
Band 203	Siedlungswasserwirtschaftliches Kolloquium an der Universität Stuttgart	Kanalsanierung – Werterhalt durch Wissensvorsprung 1. Stuttgarter Runde am 15.04.2010 (2010) 70 S., 26 Abb., 16 Tab. (24,80 €)
Band 204	Siedlungswasserwirtschaftliches Kolloquium an der Universität Stuttgart	Regenwasserbehandlung in Abwasseranlagen – Prozesse und Lösungsansätze 85. Siedlungswasserwirtschaftliches Kolloquium am 14.10.2010 (2010) 213 S., 73 Abb., 11 Tab. (34,80 €)
Band 205	Fabio Chui Pressinotti	Anpassung der Tropfkörpertechnologie an heiße Klimazonen (2010) 196 S., 82 Abb., 22 Tab. (34,80 €)
Band 206	Siedlungswasserwirtschaftliches Kolloquium an der Universität Stuttgart	Herausforderungen und Lösungen für die Wasserversorgung - Wettbewerb, Versorgungssicherheit, Innovation, Effizienzsteigerung 25. Trinkwasserkolloquium am 24.02.2011 (2011) 160 S., 47 Abb., 1 Tab. (34,80 €)
Band 207	Siedlungswasserwirtschaftliches Kolloquium an der Universität Stuttgart	Kanalsanierung – Werterhalt durch Wissensvorsprung 2. Stuttgarter Runde am 14.04.2011 (2011) 80 S., 27 Abb., 1 Tab. (24,80 €)
Band 208	Siedlungswasserwirtschaftliches Kolloquium an der Universität Stuttgart	Neue Verfahren und Betriebsstrategien in der Abwasserbehandlung 86. Siedlungswasserwirtschaftliches Kolloquium am 13.10.2011 (2011) 172 S., 71 Abb., 25 Tab. (34,80 €)
Band 209	Siedlungswasserwirtschaftliches Kolloquium an der Universität Stuttgart	Wasserversorgung und Energie – Nutzungskonflikte; Management und Technik zur Optimierung der Energieeffizienz 26. Trinkwasserkolloquium am 16.02.2012 (2012) 156 S., 81 Abb., 15 Tab. (34,80 €)

Band 210	Geremew Sahilu Gebrie	Integrated Decision Support Tools for Rural Water Supply based on Ethiopian Case-Studies (2012) 310 S., 101 Abb., 110 Tab. (34,80 €)
Band 211	Siedlungswasserwirtschaftliches Kolloquium an der Universität Stuttgart	Mikroschadstoffe und Nährstoffrückgewinnung – Praxiserfahrungen und Umsetzungspotenzial in der Abwasserreinigung 87. Siedlungswasserwirtschaftliches Kolloquium am 11.10.2012 (2012) 102 S., 44 Abb., 19 Tab. (34,80 €)
Band 212	Christian Johannes Locher	Anaerobe Behandlung von Abwasserkonzentraten aus der Halbstofferzeugung von Papierfabriken (2012), 206 S., 67 Abb., 40 Tab. (34,80 €)
Band 213	Siedlungswasserwirtschaftliches Kolloquium an der Universität Stuttgart	Trinkwasserqualität und Gewässerschutz – Trinkwasserverordnung, Gewässerschutzkonzepte, Spurenstoffe 27. Trinkwasserkolloquium am 21.02.2013 (2013) 134 S., 77 Abb., 10 Tab. (34,80 €)
Band 214	Olaf Jerzy Kujawski	Entwicklung eines anlagenweiten Steuerungs- und Regelungskonzeptes für Biogasanlagen (2013) 238 S., 78 Abb., 35 Tab. (34,80 €)
Band 215	Siedlungswasserwirtschaftliches Kolloquium an der Universität Stuttgart	Kanalsanierung – Werterhalt durch Wissensvorsprung 3. Stuttgarter Runde am 18.04.2013 (2013) 84 S., 109 Abb., 2 Tab. (24,80 €)
Band 216	Iosif Mariakakis	A two stage process for hydrogen and methane production by the fermentation of molasses (2013) 202S., 33 Abb., 34 Tab. (34,80 €)
Band 217	Siedlungswasserwirtschaftliches Kolloquium an der Universität Stuttgart	Management des urbanen Wasserhaushalts – mehr als nur Kanalnetzplanung 88. Siedlungswasserwirtschaftliches Kolloquium am 10.10.2013 (2013) 178 S., 74 Abb., 18 Tab. (34,80 €)
Band 218	Özgül Demet Antakyali	An Evaluation of Integrated Wastewater and Solid Waste Management in Large Tourist Resorts (2013) 185 S., 71 Abb., 59 Tab. (34,80 €)
Band 219	Siedlungswasserwirtschaftliches Kolloquium an der Universität Stuttgart	Zukünftige Herausforderungen für die Wasserversorgung – Vom Klimawandel über die Demografie bis hin zur Organisation 28. Trinkwasserkolloquium am 13.02.2014 (2014) 150 S., 45 Abb., 7 Tab. (34,80 €)

Band 220	Siedlungswasserwirtschaftliches Kolloquium an der Universität Stuttgart	Kanalsanierung – Werterhalt durch Wissensvorsprung / Grundlagen, Konzepte und Innovation 4. Stuttgarter Runde am 10.04.2014 (2014) 108 S., 90 Abb. (24,80 €)
Band 221	Siedlungswasserwirtschaftliches Kolloquium an der Universität Stuttgart	Energiepotenziale kommunaler Kläranlagen erkennen, nutzen und kritisch bewerten 89. Siedlungswasserwirtschaftliches Kolloquium am 09.10.2014 (2014) 146 S. 58 Abb., 11 Tab. (34,80 €)
Band 222	Kristy Peña Muñoz	Integrated sludge management concepts for green energy production in wastewater treatment plants in Heujotzingo City, Mexico (2014) 268 S., 34 Abb., 79 Tab. (34,80 €)
Band 223	Siedlungswasserwirtschaftliches Kolloquium an der Universität Stuttgart	Zukunftsfähigkeit und Sicherheit der Wasserversorgung – Ressourcen / Tarife / Neue Technologien 29. Trinkwasserkolloquium am 26.02.2015 (2015) 132 S., 76 Abb., 32 Tab. (34,80 €)
Band 224	Timo Pittmann	Herstellung von Biokunststoffen aus Stoffströmen einer kommunalen Kläranlage (2015) 244 S., 54 Abb., 53 Tab. (34,80 €)
Band 225	Siedlungswasserwirtschaftliches Kolloquium an der Universität Stuttgart	Wasser Schutz Mensch 5. Aqua Urbanica und 90. Siedlungswasserwirtschaftliches Kolloquium am 07. und 08.10.2015 (2015) 338 S., 147 Abb., 28 Tab. (34,80 €)
Band 226	Sebastian Tews	Aerob-biologische und oxidative Verfahren zur Behandlung von Membrankonzentraten aus der Holzstoff- und Altpapieraufbereitung (2015) 245 S., 62 Abb., 31 Tab. (34,80 €)
Band 227	Peace Korshiwor Amoatey	Leakage Management in the Urban Water Supply System of Ghana: Estimation and Detection Modeling (2015) 245 S.,67 Abb., 62 Tab. (34,80 €)
Band 228	Sebastian Platz	Charakterisierung, Abtrennung und Nachweis von Pulveraktivkohle in der Abwasserreinigung (2015) 256 S., 74 Abb., 51 Tab. (34,80 €)
Band 229	Siedlungswasserwirtschaftliches Kolloquium an der Universität Stuttgart	3 Jahrzehnte Trinkwasserkolloquium 3 Jahrzehnte Entwicklung in Wasserversorgung und Gewässerschutz 30. Trinkwasserkolloquium am 18.02.2016 (2016) 160 S., 78 Abb., 3 Tab. (34,80 €)

Band 230	Siedlungswasserwirtschaftliches Kolloquium an der Universität Stuttgart	Stickstoffelimination auf kommunalen Kläranlagen im Spannungsfeld von Gewässerschutz, Energieeffizienzsteigerung und Industrieeinleitungen 91. Siedlungswasserwirtschaftliches Kolloquium am 13.10.2016 (2016) 132 S., 38 Abb., 15 Tab. (34,80 €)
Band 231	Siedlungswasserwirtschaftliches Kolloquium an der Universität Stuttgart	Stand des Umwelt- und Arbeitsschutzes bei der Verchromung von Metall und Kunststoff Kolloquium zum integrierten industriellen Umwelt- und Arbeitsschutz am 30.11.2016 (2016) 126 S., 54 Abb., 9 Tab. (34,80 €)
Band 232	Mehari Goitom Haile	Accounting for Uncertainties in the Modelling of Emissions from Combined Sewer Overflow Structures (2016) 197 S., 93 Abb., 22 Tab. (34,80 €)
Band 233	Eduard Rott	Untersuchungen zur Elimination von Phosphor aus phosphonathaltigen Industrieabwässern (2016) 258 S., 57 Abb., 26 Tab. (34,80 €)
Band 234	Kenan Güney	Investigating Water Reusability in Cotton Processing Textile Dye-house by Applying Membrane Filtration (2017) 219 S., 64 Abb., 57 Tab. (34,80 €)
Band 235	Siedlungswasserwirtschaftliches Kolloquium an der Universität Stuttgart	Risiken in der Wasserversorgung Vorsorge/Management/Minimierung/Kommunikation 31. Trinkwasserkolloquium am 06.04.2017 (2017) 132 S., 79 Abb., 6 Tab. (34,80 €)
Band 236	Pengfei Wang	Phosphorus recovery from wastewater via struvite crystallization in a fluidized bed reactor: Influence of operating parameters and reactor design on efficiency and product quality (2017) 202 S., 72 Abb., 20 Tab. (34,80 €)
Band 237	Siedlungswasserwirtschaftliches Kolloquium an der Universität Stuttgart	Chemikalienmanagement und Umweltschutz in der textilen Kette Kolloquium zur nachhaltigen Textilproduktion am 21.09.2017 (2017) 174 S.,48 Abb., 9 Tab. (34,80 €)
Band 238	Siedlungswasserwirtschaftliches Kolloquium an der Universität Stuttgart	Spurenstoffe im Regen- und Mischwasserabfluss Abwasserkolloquium 2017 am 26.10.2017 (2017) 130 S., 48 Abb., 13 Tab. (34,80 €)

Band 239	Marie Alexandra Launay	Organic micropollutants in urban wastewater systems during dry and wet weather – Occurence, spatio-temporal distribution and emissions to surface waters (2018) 240 S., 65 Abb., 38 Tab. (34,80 €)
Band 240	Asya Drenkova-Tuhtan	Phosphorus Elimination and Recovery from Wastewater with Reusable Nanocomposite Magnetic Particles (2018) 259 S., 78 Abb., 25 Tab. (34,80 €)
Band 241	Siedlungswasserwirtschaftliches Kolloquium an der Universität Stuttgart	Integrated Best Available Wastewater Management in the Textile Industry Colloquium on Textile Wastewater Management 2018-09-19 (2018) 182 S., 99 Abb., 14 Tab. (34,80 €)
Band 242	Siedlungswasserwirtschaftliches Kolloquium an der Universität Stuttgart	Spurenstoffe und antibiotikaresistente Bakterien – Schnittstelle Abwasserent- und Wasserversorgung Abwasserkolloquium 2018 am 08.11.2018 (2018) 118 S., 26 Abb., 8 Tab. (34,80 €)
Band 243	Karen Mouarkech	Combined energy and phosphorus recovery from black water, co-substrates and urine (2019) 296 S., 69 Abb., 107 Tab. (34,80 €)
Band 244	Siedlungswasserwirtschaftliches Kolloquium an der Universität Stuttgart	Minimisation of Wastewater Emission from Textile Finishing Industries Colloquium on Textile Wastewater Management 2019-09-19 (2019) 148 S., 60 Abb., 20 Tab. (34,80 €)
Band 245	Siedlungswasserwirtschaftliches Kolloquium an der Universität Stuttgart	Ansprüche an die Siedlungswasserwirtschaft – Kernaufgaben versus weitergehende Anforderungen Abwasserkolloquium 2019 am 10.10.2019 (2019) 143 S., 43 Abb., 2 Tab. (34,80 €)
Band 246	Siedlungswasserwirtschaftliches Kolloquium an der Universität Stuttgart	Sichere Trinkwasserversorgung trotz Klimawandel - wie resilient sind unsere Systeme und wo besteht Handlungsbedarf? 32. Trinkwasserkolloquium am 20.02.2020 (2020) 107 S., 52 Abb. http://dx.doi.org/10.18419/opus-10799
Band 247	Michael Seeger	Entwicklung und Validierung eines CSB-basierten und temperatursensitiven Bemessungsansatzes für Tropfkörper – Untersuchungen an technischen und halbtechnischen Tropfkörpern in warmen Klimazonen (2020) 308 S., 63 Abb., 46 Tab. http://dx.doi.org/10.18419/opus-10942

Band 248	Stephan Wasielewski	Ammoniumrückgewinnung aus Schlammwasser mittels Ionenaustausch an Klinoptilolith (2021) 273 S., 40 Abb., 52 Tab. http://dx.doi.org/10.18419/opus-11464
Band 249	Jovana Husemann	Development of a Decision Support Tool for Integrated Wastewater and Organic Material Flows Management in the Scope of Circular Economy (2021) 216 S., 52 Abb., 30 Tab. http://dx.doi.org/10.18419/opus-11891
Band 250	Tobias Reinhardt	Adsorptive Removal of Phosphonates and Ortho-phosphate From Membrane Concentrate Using Granular Ferric Hydroxide (2022) 214 S., 43 Abb., 18 Tab.

Forschungs- und Entwicklungsinstitut für
Industrie- und Siedlungswasserwirtschaft
sowie Abfallwirtschaft e.V. (FEI)